

# NONLINEAR GAUSSIAN FILTERING WITH MISSING AND DELAYED MEASUREMENTS

Ph.D. Thesis

*by*

AMIT KUMAR NAIK



DEPARTMENT OF ELECTRICAL ENGINEERING  
INDIAN INSTITUTE OF TECHNOLOGY  
INDORE  
MAY, 2025



# NONLINEAR GAUSSIAN FILTERING WITH MISSING AND DELAYED MEASUREMENTS

## A THESIS

*Submitted in partial fulfillment of the  
requirements for the award of the degree*

*of*

## DOCTOR OF PHILOSOPHY

*by*

AMIT KUMAR NAIK



DEPARTMENT OF ELECTRICAL ENGINEERING  
INDIAN INSTITUTE OF TECHNOLOGY

INDORE

MAY, 2025



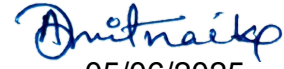


## INDIAN INSTITUTE OF TECHNOLOGY INDORE

### CANDIDATE'S DECLARATION

I hereby certify that the work which is being presented in the thesis entitled **“NONLINEAR GAUSSIAN FILTERING WITH MISSING AND DELAYED MEASUREMENTS”** in the partial fulfillment of the requirements for the award of the degree of DOCTOR OF PHILOSOPHY and submitted in the DEPARTMENT OF ELECTRICAL ENGINEERING, Indian Institute of Technology Indore, is an authentic record of my own work carried out during the time period from July 2019 to July 2024 under the supervision of Prof. Prabhat Kumar Upadhyay, Indian Institute of Technology Indore, India and Dr. Abhinoy Kumar Singh, Indian Institute of Technology Patna, India.

The matter presented in this thesis has not been submitted for the award of any other degree of this or any other institute.

  
05/06/2025

Signature of the student with date  
(Amit Kumar Naik)

-----

This is to certify that the above statement made by the candidate is correct to the best of my knowledge.



5/6/2025

Signature of Thesis Supervisor(s) with date  
Prof. Prabhat Kumar Upadhyay



24/06/2025

Signature of Thesis Supervisor(s) with date  
Dr. Abhinoy Kumar Singh

-----

**Amit Kumar Naik** has successfully given his Ph.D. Oral Examination held on May 6, 2025



5/6/2025

Signature of Thesis Supervisor(s) with date  
Prof. Prabhat Kumar Upadhyay



24/06/2025

Signature of Thesis Supervisor(s) with date  
Dr. Abhinoy Kumar Singh

-----



## ACKNOWLEDGEMENTS

Throughout my doctoral journey, I have received great supervision, encouragement, and support. I would like to express my deepest gratitude to all those who have contributed throughout the completion of this thesis.

First and foremost, I am immensely grateful to my supervisors, Prof. Prabhat Kumar Upadhyay and Dr. Abhinoy Kumar Singh (IIT Patna), for their excellent guidance, constant support, and encouragement over the years. I am truly thankful to them for spending their valuable time, shaping the thesis through expertise.

Furthermore, I am grateful to PSPC committee members Prof. Amod C. Umarikar and Prof. Abhishek Srivastava for their fruitful discussions and suggestions towards my research. I am also thankful to Dr. Maurizio Magarini (Politecnico di Milano, Milan, Italy); Dr. Paresh Date (Brunel University Uxbridge, London, U.K.); Dr. Amit Kumar Verma (IIT Patna); and Dr. Rajeeb Dey (NIT Silchar) for their insightful comments on research works. I also appreciate the research resources provided by IIT Indore, which provided an ambient environment for carrying out research work.

I am also thankful to my fellow researchers, Dr. Sumanta Kumar Nanda, Dr. Guddu Kumar, Mr. Yamalakonda Venu Gopal, and Mr. Neelanshu Garg and colleagues Mr. Suvamit Chakraborty, Dr. Adnan Iqbal, Dr. Anas Ullah Khan, and Dr. Suhel Khan. They have been extending their unwavering supports throughout my Ph.D. duration.

I would like to sincerely thank my friends Hemant Naik, Laukesh Jaiswal, Manish Meena, Sanjay Kushwaha, Yuvraj Soni for their unwavering support throughout my Ph.D. journey. Their encouragement and companionship have been invaluable.

Finally just as importantly, I dedicate this thesis to my family; particularly special and sincere thanks to my parents for their continuous and unconditional support and love throughout my life.

AMIT KUMAR NAIK

*Dedicated*  
*My <sup>to</sup> Family*



# ABSTRACT

The state variables are a set of variables that completely describe a system's behavior, *i.e.*, their temporal evolution results from the system dynamics. Thus, the knowledge of the state variables is crucial to study the behavior of any dynamic system. These variables are generally referred to as hidden (latent) states due to the unavailability of any direct information. Mostly, the latent states are inferred from the measurements (data) which are typically acquired from surveys, sensors, *etc.* The received measurements inherently involve some degree of uncertainty (due to imperfect sensors, mishandled data in surveys, or unknown measuring environments), giving an erroneous and unreliable knowledge of states. Such scenarios oblige one to settle for the best feasible estimate, in some sense (*e.g.*, minimum mean square error), of the states. Estimation, or more broadly filtering (a recursive process of estimation), facilitates a tool to determine the latent states of a dynamical system from the available system information and noisy measurements. It finds applications in numerous real-life problems—target tracking, biomedical, financial prediction, weather forecasting, industrial diagnosis *etc.*

For linear filtering problems, the Kalman filter (KF) provides an optimal solution. However, its performance deteriorates for nonlinear filtering problems. Subsequently, several nonlinear variants of the KF were reported in literature, referred to as nonlinear Gaussian filters; these filters approximate all the probability density functions (PDFs) as Gaussian during the filtering process. They involve intractable integrals which are numerically approximated during the filtering. Apart from Gaussian filtering, there is another class of nonlinear filters, named particle filtering, which is mostly beyond the scope of the contributions of this thesis.

Designing Gaussian filters is typically based on the assumption that the measurements involve no irregularities other than the additive white Gaussian noises. The practical measurements, however, can involve various irregularities. The focus of this thesis is on maintaining filtering accuracy in the presence of measurement irregularities. The thesis mainly focuses on two measurement irregularities: randomly delayed measurements and intermittent measurement losses, while the range of the measurement irregularities is relatively larger. In the case of random delays, measurements received at any given time may contain information from previous states. Conversely, intermittent measurement losses mean measurements are not received at regular intervals. These irregularities are not addressed in the design of the traditional Gaussian filters, leading to significant performance deterioration or even complete failure when these issues are present individually or jointly.

In the context of the above discussions, the primary focus of this thesis involves: i) redesigning the traditional Gaussian filters to handle the missing and delayed measurements and ii) performing stochastic stability analysis for the developed filter. In addition, this thesis also aims to improve the filtering accuracy by improving the numerical approximation accuracy of the intractable integrals.

In the first contribution, this thesis introduces a modified version of the extended Kalman filter to handle the missing measurements in systems that require fast and easy implementation. Its performance is verified explicitly with individual sinusoids identification problem.

Further, this thesis presents a new Gaussian filtering technique designed to manage large delays with fewer prerequisite probabilities. This method further eliminates

---

the necessity of setting an upper limit on delays, a requirement in current Gaussian filtering extensions for delayed measurements. As a result, this approach enhances filtering accuracy.

In another contribution, this thesis addresses a new kind of measurement irregularity and subsequently, develops a Gaussian filter to handle it. Under this irregularity, the actually received measurement contains the measurement from current and past instants. Such an irregularity is likely to appear in systems wherein different fractions of a measurement are acquired through individual sensors and are superimposed subsequently to form a complete measurement.

To analyze the temporal behavior, the thesis analyzes the stochastic stability of all the Gaussian filter evolved in the above discussed contributions. Subsequently, it identifies the conditions for which the developed filters remain exponentially bounded.

Finally, the thesis proposes an advanced version of Gaussian filtering that improves the filtering accuracy by utilizing a more precise numerical approximation technique.

The thesis validates the improved performance of all contributions, as discussed above, in comparison to the existing Gaussian filtering counterparts. The comparative analysis is based on root mean square error (RMSE) and computational time.

# Contents

<b>ABSTRACT</b>	<b>i</b>
<b>LIST OF FIGURES</b>	<b>vi</b>
<b>LIST OF TABLES</b>	<b>ix</b>
<b>LIST OF ABBREVIATIONS/ACRONYMS</b>	<b>xi</b>
<b>List of Symbols</b>	<b>xiv</b>
<b>1 Introduction</b>	<b>3</b>
1.1 Background . . . . .	3
1.1.1 Bayesian Filtering Framework: A Probabilistic Solution . . . .	5
1.1.2 Gaussian Filter: An Approximate Solution to Bayesian Filtering	7
1.1.3 Stochastic Stability Analysis of Gaussian Filters . . . . .	11
1.2 Motivation . . . . .	14
1.3 Objective . . . . .	16
1.4 Approaches and Methods . . . . .	16
1.5 Contribution . . . . .	17
1.6 Thesis Organization . . . . .	19
<b>2 Literature Review</b>	<b>22</b>
2.1 Evolution of Gaussian Filters . . . . .	22
2.1.1 Linearization-based Gaussian Filters . . . . .	23
2.1.2 Sigma Point-based Gaussian Filters . . . . .	25
2.2 Nonlinear Filtering in the Presence of Various Measurement Irregu-	
larities . . . . .	30
2.2.1 Missing Measurements . . . . .	30
2.2.2 Delayed Measurements . . . . .	32
2.3 Summary . . . . .	35
<b>3 Kalman-Based Multiple Sinusoids Identification from Intermittently</b>	
<b>Missing Measurements of the Superimposed Signal</b>	<b>37</b>
3.1 Introduction . . . . .	37
3.2 Problem Formulation . . . . .	39
3.3 Modified EKF for Missing Measurements and Sinusoids Identification	42
3.3.1 Modified EKF for Missing Measurements . . . . .	43
3.3.2 Identification of the Sinusoids Using the Modified EKF . . . .	48
3.4 Simulation and Results . . . . .	48

3.4.1	True Data Simulation . . . . .	50
3.4.2	RMSE Analysis of the EKF_M and Competitive Filters . . . . .	50
3.4.3	Sinusoids Identification from the Estimated States . . . . .	52
3.4.4	Performance Analysis with Different Time Series . . . . .	52
3.4.5	Performance Analysis with Varying Missing Measurements Probability . . . . .	53
3.4.6	Computational Time Analysis . . . . .	54
3.4.7	EKF_M for General Estimation and Filtering Problems . . . . .	56
3.5	Summary . . . . .	57
<b>4</b>	<b>Generalized Gaussian Filtering with Sporadically Missing Measurements</b>	<b>61</b>
4.1	Introduction . . . . .	61
4.2	Problem Formulation . . . . .	62
4.3	Gaussian Filtering for Missing Measurements . . . . .	63
4.4	Simulation Results . . . . .	66
4.4.1	Problem 1: Individual Signal Identification . . . . .	66
4.4.2	Problem 2: Sinusoidal Growth Model . . . . .	67
4.5	Summary . . . . .	69
<b>5</b>	<b>Poisson-Gaussian Filtering for Randomly Delayed Measurements</b>	<b>73</b>
5.1	Introduction . . . . .	73
5.2	Problem formulation . . . . .	75
5.3	Modified Gaussian filter for randomly delayed measurements . . . . .	77
5.4	Simulation and results . . . . .	81
5.4.1	Problem 1 . . . . .	82
5.4.2	Problem 2 . . . . .	83
5.4.3	Extended comparison for varying delay probabilities and mismatched model . . . . .	84
5.5	Summary . . . . .	86
<b>6</b>	<b>Gaussian Filtering with Stochastically Composed Current and Past Measurements</b>	<b>89</b>
6.1	Introduction . . . . .	89
6.1.1	The Proposed Measurement Irregularity . . . . .	90
6.1.2	An Overview of the Proposed Method . . . . .	91
6.2	Problem formulation . . . . .	92
6.3	Filtering with stochastically composed current and past measurements	93
6.3.1	Problem 1: Individual Sinusoids Identification . . . . .	98
6.3.2	Problem 2: Compartmental Population Estimation for COVID-19 Pandemic Model from Real Data . . . . .	101
6.3.3	Performance Analysis Against Varying Measurement Delays .	102
6.3.4	Computational Time Analysis . . . . .	103
6.4	Summary . . . . .	104
<b>7</b>	<b>Gaussian Filtering for Simultaneously Occurring Delayed and Missing Measurements</b>	<b>107</b>
7.1	Introduction . . . . .	107
7.2	Problem Formulation . . . . .	110

7.3	Modified Gaussian Filtering for Delayed and Missing Measurements . . . . .	112
7.4	Simulation Results . . . . .	118
7.4.1	Problem 1: Individual Sinusoids Identification . . . . .	119
7.4.2	Problem 2: Sinusoidal Growth Model . . . . .	121
7.4.3	Performance Validation for Other Gaussian Filters . . . . .	124
7.5	Summary . . . . .	125
<b>8</b>	<b>Stochastic Stability Analysis of Gaussian Filters with Measurement Irregularities</b>	<b>127</b>
8.1	Introduction . . . . .	127
8.1.1	Preparatory Operations . . . . .	129
8.1.2	Stochastic modeling of the estimation error of EKF_S . . . . .	131
8.1.3	Stability results . . . . .	133
8.2	Summary . . . . .	139
<b>9</b>	<b>Gaussian Kernel Quadrature Kalman Filter</b>	<b>143</b>
9.1	Introduction . . . . .	143
9.2	Gaussian Kernel Quadrature Kalman Filter . . . . .	146
9.2.1	Univariate Gauss-Hermite Quadrature Rule for Approximating $I_0^1(g(x))$ . . . . .	148
9.2.2	Univariate Gaussian Kernel Quadrature Rule for Approximating $I_0^1(g(x))$ . . . . .	149
9.2.3	Multivariate Extension of Gaussian Kernel Quadrature Rule . . . . .	155
9.3	Simulation and Results . . . . .	160
9.3.1	Problem 1: Numerical Approximation of Intractable Integral . . . . .	160
9.3.2	Problem 2: Sinusoidal Growth Model . . . . .	161
9.4	Summary . . . . .	162
<b>10</b>	<b>Conclusions and Future Works</b>	<b>167</b>
10.1	Performance gain of the proposed methods in terms of accuracy and computational demand . . . . .	167
10.2	Conclusions . . . . .	168
10.3	Future Works . . . . .	171

# List of Figures

2.1	Different types of delays inherently existing in a wireless sensor networks. . . . .	34
3.1	Block diagram of multiple sinusoids identification problem from intermittently missing measurements of superimposed signal. The block diagram is presented for network/communication channel as the cause for missing measurements. . . . .	40
3.2	Ideal measurements and actually received measurements with intermittent missing measurements possibility for the real part of the superimposed signal. . . . .	49
3.3	RMSE plots of the proposed EKF_M and the competitive filters for missing measurements probability of 0.1 ( $\rho = 0.9$ ). . . . .	49
3.4	RMSE plots of the proposed EKF_M and the competitive filters for missing measurements probability of 0.2 ( $\rho = 0.8$ ). . . . .	51
3.5	Plots of the true sinusoids forming the superimposed signal and the sinusoids identified from the measurements of the superimposed signal using the proposed EKF_M and the ordinary Gaussian filters for missing measurements probability of 0.2. . . . .	53
3.6	Case-1: Sinusoids identified by all filters at missing measurement probability of 0.2. . . . .	54
3.7	Case-2: Sinusoids identified by all filters at missing measurement probability of 0.2. . . . .	55
3.8	Plots of mean RMSEs against varying missing measurements probability. . . . .	56
4.1	Problem 2: CRMSE comparison for different Gaussian filters and their respective extensions under the proposed Gaussian filtering framework for missing measurements probabilities of 0.1 and 0.2. . . . .	68
4.2	Problem 2: RMSE comparison for different Gaussian filters and their respective extensions under the proposed Gaussian filtering framework for missing measurements probabilities of 0.1 and 0.2. . . . .	69
5.1	Schematic diagram of the delay occurrences considering that the average delay information is known. As the average delay information is known, Poisson distribution features the delay characteristics. . . .	76
5.2	Problem 1, Scenario-1: Mean RMSEs obtained for the proposed and the existing filters for varying average delay ( $\lambda$ ). . . . .	83
5.3	Problem 1, Scenario-2: Mean RMSEs obtained for the proposed and the existing filters for varying average delay ( $\lambda$ ). . . . .	83

5.4	Problem 2: Mean RMSEs obtained for the proposed and the existing filters for varying average delay ( $\lambda$ ). . . . .	84
5.5	Problem 1, Scenario-1: Performance analysis with mismatched delay model. . . . .	86
6.1	Block diagram for receiving the irregular measurement $\mathbf{y}_k$ as stochastic combination of the current and past hypothetical true measurements. This block diagram considers the following: i) three sources are used for observing the measurements into three independent pieces and ii) a propagation channel (PC) can be maximum of one-step delayed, <i>i.e.</i> , the delay simply means to one-step delay. . . . .	93
6.2	Problem 1: Mean RMSE comparison between the proposed and traditional Gaussian filters at different noisy environments considering $\mathbf{z}_{k-1}$ and $\mathbf{z}_{k-2}$ collectively compose 20% of $\mathbf{y}_k$ . . . . .	99
6.3	Sinusoids identification by different filters considering $\mathbf{z}_{k-1}$ and $\mathbf{z}_{k-2}$ collectively compose 20% of $\mathbf{y}_k$ and the noise environment as Case-1. . . . .	100
6.4	Problem 2: Mean RMSEs of the proposed and traditional Gaussian filters at different noisy environments considering $\mathbf{z}_{k-1}$ and $\mathbf{z}_{k-2}$ collectively compose 20% of $\mathbf{y}_k$ . . . . .	102
6.5	Problem 1, Case-1: Mean RMSEs comparison between the proposed and competitive Gaussian filters at different delay scenarios. The hypothetical true measurements $\mathbf{z}_{k-N_d}$ with $N_d = (1, 3, 5)$ are assumed to compose 20% of $\mathbf{y}_k$ . . . . .	103
6.6	Problem 2, Case-1: Mean RMSEs comparison between the proposed and competitive Gaussian filters at different delay scenarios. The hypothetical true measurements $\mathbf{z}_{k-N_d}$ with $N_d = (1, 3, 5)$ are assumed to compose 20% of $\mathbf{y}_k$ . . . . .	104
7.1	Pictorial diagram representing the sequence to be followed to obtain the received measurement $\mathbf{y}_k$ from the ideal $\mathbf{z}_1, \mathbf{z}_2, \dots, \mathbf{z}_k$ that would have been received in the lenient environment. . . . .	112
7.2	Problem 1, 1-delay scenario: Mean RMSE plots of all filters for varying delay probabilities, considering the missing measurement probability $\rho_m$ as 0.1 and 0.2. . . . .	120
7.3	Problem 1, 2-delay scenario: Mean RMSE plots of all filters for varying delay probabilities, considering the missing measurement probability $\rho_m$ as 0.1 and 0.2. . . . .	121
7.4	Problem 2, 1-delay scenario: Mean RMSE plots of all filters for varying delay probabilities, considering the missing measurement probability $\rho_m$ as 0.1 and 0.2. . . . .	122
7.5	Problem 2, 2-delay scenario: Mean RMSE plots of all filters for varying delay probabilities, considering the missing measurement probability $\rho_m$ as 0.1 and 0.2. . . . .	124
9.1	Problem 2: Comparison of RMSE plots of the proposed GKQKF with the UKF, CKF, CQKF, HDCKF, and QKF for Scenario 1. . . . .	163
9.2	Problem 2: Comparison of RMSE plots of the proposed GKQKF with the UKF, CKF, CQKF, HDCKF, and QKF for Scenario 2. . . . .	163





# List of Tables

3.1	Relative computational time comparison of the proposed and the competitive filters. . . . .	55
5.1	Average RMSEs obtained for the proposed method (CKF_RD_PD) and the existing delay filters (CKF_1D [121], CKF_RD [122], and MLCKF [123]) applied with varying delay probabilities ( $\rho_d$ ) for Problem 1 and Problem 2. The delay scenario is simulated for $\lambda = 1.5$ while Scenario 1 and Scenario 2 denoting the respective scenarios for Problem 1 and Problem 2. . . . .	85
7.1	Problem 1, 3-delay scenario: Average RMSEs obtained by MDCQKF, MDGHF, and their counterparts for different delay probabilities. . .	123
7.2	Problem 2, 3-delay scenario: Average RMSEs obtained by MDCQKF, MDGHF, and their counterparts for different delay probabilities. . .	123
7.3	Problem 1, three-delay scenario: Relative computational time comparison of MDCQKF, MDGHF, and their counterparts for 0.3 delay probability. . . . .	123
9.1	$I(f)$ with $n = \{4, 6\}$ : Numerically approximated values and % error obtained from different numerical approximation techniques used in the filtering literature. . . . .	162
10.1	<b>Chapter 3:</b> Relative accuracy and computational time comparison of the proposed method (EKF_M) and the competitive filters. The proposed EKF_M is considered as reference. . . . .	168
10.2	<b>Chapter 4:</b> Relative accuracy and computational time comparison between the traditional Gaussian filters and their extensions under the proposed method. The CKF-based extension of the proposed method <i>i.e.</i> , CKFS is considered as the reference. . . . .	168
10.3	<b>Chapter 5:</b> Relative accuracy and computational time comparison between the proposed CKF_RD_PD and competitive filters CKF_1D, CKF_RD, and MLCKF. The proposed method CKF_RD_PD is considered as the reference. . . . .	168
10.4	<b>Chapter 6:</b> Relative accuracy and computational time comparison between the traditional Gaussian filters CKF, CQKF, and GHF and their extensions under the proposed methodology. The CKF-based extension of the proposed method <i>i.e.</i> , CKF_S is considered as the reference. . . . .	169

10.5	<b>Chapter 7:</b> Relative accuracy and computational time comparison between the proposed MDCKF and competitive filters CKF, MEKF, CKF_RD, and MLCKF. The proposed method MDCKF is considered as the reference. . . . .	169
10.6	<b>Chapter 9:</b> Relative accuracy and computational time comparison between the existing Gaussian filters and proposed Gaussian filter GKQKF. The GKQKF is considered as reference. . . . .	169



# List of Abbreviations/Acronyms

**ASGHF** Adaptive sparse-grid Gauss-Hermite filter.

**ASQKF** Adaptive sparse-grid quadrature Kalman filter.

**BRV** Bernoulli random variable.

**CKF** Cubature Kalman filter.

**CQKF** Cubature quadrature Kalman filter.

**DTNS** Discrete-time nonlinear system.

**EKF** Extended Kalman filter.

**GHF** Gauss-Hermite filter.

**GKQKF** Gaussian kernel quadrature Kalman filter.

**HDCKF** High-degree cubature Kalman filter.

**HDCQKF** High-degree cubature-quadrature Kalman filter.

**HEKF** High-order extended Kalman filter.

**IEKF** Iterated extended Kalman filter.

**InEKF** Invariant extended Kalman filter.

**IUKF** Iterated unscented Kalman filter.

**KF** Kalman filter.

**MCKF** Maximum correntropy Kalman filter.

**MEEKF** Minimum error entropy Kalman filter.

**MMSE** Minimum mean square error.

**NCS** Network control system.

**PDF** Probability density function.

**QKF** Quadrature Kalman filter.

**RMSE** Root mean square error.

**SEKF** Second-order extended Kalman filter.

**SGHF** Sparse-grid Gauss-Hermite filter.

**SQKF** Sparse-grid quadrature Kalman filter.

**SQUKF** Square-root unscented Kalman filter.

**TUKF** Transformed unscented Kalman filter.

**UKF** Unscented Kalman filter.

**WSN** Wireless sensor network.

## List of Symbols

Notation	Definition
$n$	dimension of state
$q$	dimension of measurement
$t_k$	time at $k^{th}$ instant
$\mathbf{x}_k$	state vector at $t_k$
$\mathbf{z}_k$	ideal measurement vector at $t_k$
$T_s$	total number of sampling intervals
$f(\cdot), h(\cdot)$	known nonlinear functions
$\boldsymbol{\eta}_k$	process noise at $t_k$
$\boldsymbol{\nu}_k$	measurement noise at $t_k$
$\mathbf{x}_{1:k}$	set of all state vectors up to $t_k$ $\{\mathbf{x}_1, \mathbf{x}_2, \dots, \mathbf{x}_k\}$
$\mathbf{z}_{1:k}$	set of all true measurement vectors up to $t_k$ $\{\mathbf{z}_1, \mathbf{z}_2, \dots, \mathbf{z}_k\}$
$\hat{\mathbf{x}}_{k k-1}$	predicted state at $t_k$
$\mathbf{P}_{k k-1}$	predicted error covariance at $t_k$
$\hat{\mathbf{z}}_{k k-1}$	predicted true measurement at $t_k$
$\mathbf{P}_{k k-1}^{\mathbf{zz}}$	true measurement error covariance at $t_k$
$\mathbf{P}_{k k-1}^{\mathbf{xz}}$	state-true measurement cross-covariance at $t_k$
$\hat{\mathbf{x}}_{k k}$	estimated state at $t_k$
$\mathbf{P}_{k k}$	estimated error covariance at $t_k$
$\mathbf{Q}_k$	process noise covariance matrix at $t_k$
$\mathbf{R}_k$	measurement noise covariance matrix at $t_k$
$\mathbf{K}$	Kalman gain
$g(\cdot)$	arbitrary nonlinear function
$w(\mathbf{x})$	known weighting function
$\boldsymbol{\xi}_i$	sample points
$\boldsymbol{\omega}_i$	weights
$N_c$	number of sample points
$\mathbf{I}_n$	$n$ -dimensional identity matrix
$\mathbf{0}_{n \times 1}$	an array of $n$ -zeros
$\mathbb{V}$	Lyapunov function
$\dot{\mathbb{V}}(\cdot)$	time derivative of $\mathbb{V}$
$\zeta_k$	an arbitrary stochastic process at $t_k$
$\kappa', \sigma', \theta, \tau_1, \tau_2, \phi, \eta, \nu,$ $c_1, c_2, a, c, \rho_1, \rho_2, \epsilon',$ $h, q, q', r, r', \hat{\alpha}_j$	positive real numbers
$\bar{\Theta}$	Poisson random variable
$\lambda$	average delay
$\boldsymbol{\alpha}$	$k$ -dimensional array containing 0 and 1
$i, j, m, d, u, s$	indices
$\hat{\mathbf{y}}_{k k-1}$	predicted actual measurement at $t_k$
$\mathbf{P}_{k k-1}^{\mathbf{yy}}$	actual measurement error covariance at $t_k$
$\mathbf{P}_{k k-1}^{\mathbf{xy}}$	state-actual measurement cross-covariance at $t_k$
$\rho_d$	delay probability
$\Phi_j$	fraction of the original measurements acquired by the $j^{th}$ source
$N_d$	maximum delay

Notation	Definition
$\alpha_{k,j}$	portion of $\mathbf{z}_{k-j}$ ( $j \in \{0, 1, \dots, N_d\}$ ) in $\mathbf{y}_k$
$\hat{\alpha}_j$	mean of $\alpha_{k,j}$
$P_{a,j}$	variance of $\alpha_{k,j}$
$\mathcal{S}_k$	susceptible compartment
$\mathcal{I}_k$	infected compartment
$\mathcal{R}_k$	recovered compartment
$\kappa_{si}$	susceptible-to-infected rate
$\kappa_{ir}$	infected-to-recovered rate
$\kappa_{rs}$	recovered-to-susceptible rate
$\mathbf{z}(t)$	continuous time-domain measurement
$i$	imaginary number
$N_s$	number of sinusoids
$a_j$	amplitude of the $j^{th}$ sinusoid
$f_j$	frequency of the $j^{th}$ sinusoid
$T$	sampling interval
$\beta_k^i, \Theta_k^i$	$i^{th}$ Bernoulli random variables
$\boldsymbol{\rho}_k$ & $\phi_d$	expected value of $\beta_k$ and $\Theta_k^i$ , respectively
$\mathbf{F}_k$	Jacobian of $f(\mathbf{x}_k)$ around $\hat{\mathbf{x}}_{k k}$
$\mathbf{H}_k$	Jacobian of $h(\mathbf{x}_k)$ around $\hat{\mathbf{x}}_{k k-1}$
$\mathbf{e}_{k k}$	estimation error at $t_k$
$\mathbf{e}_{k k-1}$	prediction error $t_k$
$\bar{Q}^1(I_0^1)$	univariate quadrature rule
$\kappa(x, y)$	Gaussian kernel
$\sigma$	kernel bandwidth
$\boldsymbol{\xi}^{GK}$ & $\boldsymbol{\omega}^{GK}$	sample points and weights, respectively for GKQKF
$\boldsymbol{\xi}^{GH}$ & $\boldsymbol{\omega}^{GH}$	sample points and weights, respectively for GHF
$H_i(x)$	$i^{th}$ -order probabilistic Hermite polynomials
$\varphi_i^\alpha(x)$	eigenfunctions of $\kappa(x, y)$
$l$	integer
$\varphi_{2l}^\alpha(x)$	even order eigenfunction
$\varphi_{2l+1}^\alpha(x)$	odd order eigenfunction
$N_{gk}$	number of multivariate quadrature points

- Calculus, probability & statistics, and linear algebra.

Notation	Definition
$\mathbb{R}^n$	set of all ordered $n$ -tuples of real numbers
$\mathbb{R}^q$	set of all ordered $q$ -tuples of real numbers
$\mathcal{D}$	domain of integration
$\mathbb{E}[\cdot]$	statistical expectation operator
$\mathcal{P}(\cdot)$	statistical probability operator
$\mathcal{P}(\mathcal{E} \mathcal{F})$	probability of event $\mathcal{E}$ conditioned on event $\mathcal{F}$
$\mathcal{N}(\mu, \Sigma)$	normal distribution with mean $\mu$ and variance $\Sigma$
$\min(\cdot)$	minimum operator
$\ \cdot\ $	spectral norm
$\text{Tr}(\cdot)$	trace operator
$\Omega^l(\cdot)$	largest singular value
$\Omega^s(\cdot)$	smallest singular value
$\lambda^s(\cdot)$	smallest eigenvalue







# Chapter 1

## Introduction

### 1.1 Background

The focus of this thesis is majorly on developing advanced estimation and filtering algorithms. To understand the estimation and filtering, let us consider a typical dynamical system. The dynamic behavior of a dynamical system is characterized by its internal states. Many practical applications (some examples are discussed later) require to characterize the dynamical behavior of the states, which requires determining the internal states. However, the straightaway knowledge of the internal states are often difficult in practical applications. In such cases, some related parameters, known as measurements, are measured. The measurements may be obtained from sensor data, experiment data, *etc.* However, in any such case, the measurement data is noisy. Consequently, the problem becomes determining the internal states of the dynamical system from noisy measurements. The estimation algorithm provides a computational tool for addressing this problem. Then, the filtering is simply a recursive process of state estimation. As filtering is simply a broader sense of estimation, hereafter, the thesis will commonly use the term ‘filtering’ to characterize the sense of ‘estimation and filtering’.

A typical example of filtering includes radar data-based target tracking [1, 2]. The target’s dynamics such as the trajectory can be characterized by the axial positions of the target in the earth frame (axial velocities and accelerations may also be considered as states to model the axial positions in time series), which may be considered as the desired state. The noisy measurements may be the range and

elevation angle in the radar's frame. Then, the tracking problem becomes a computational problem of determining the axial positions (states) of the target from the radar data (measurements). This is where we need the estimation algorithm. As trajectory tracking requires updating the estimated axial positions of the target regularly, we require implementing the estimation algorithm recursively. As discussed above, such a recursive process of estimation is called filtering. In the target tracking applications, the filtering algorithms are often known as tracking algorithms.

The practical applications of the estimation and filtering algorithms extend much beyond the above-discussed target-tracking application. These algorithms are widely used in crucial engineering applications, such as space technologies, biomedical diagnosis and monitoring [3], industrial diagnosis and prognosis [4], weather forecasting [5] *etc.* Interestingly, the applications of these algorithms further extend to non-engineering applications as well, which include financial modeling [6] and pandemic modeling [7].

The filtering algorithms are designed to be implemented over the dynamical state space model of the system. The dynamical state space model consists of the process model and measurement model, which are briefly discussed below.

- *Process model:* It describes the evolution of states through time and also includes a noise term incorporating the modeling errors.

$$\mathbf{x}_k = f(\mathbf{x}_{k-1}) + \boldsymbol{\eta}_k, \quad (1.1)$$

- *Measurement model:* It demonstrates the relationship between the measured states and the measurements received. The errors in the measuring devices are modeled using a noise process.

$$\mathbf{z}_k = h(\mathbf{x}_k) + \boldsymbol{\nu}_k, \quad (1.2)$$

where  $\mathbf{x}_k \in \mathbb{R}^n$  and  $\mathbf{z}_k \in \mathbb{R}^q$  are state and measurement vectors, respectively, at  $k^{th}$  sampling instant,  $k \in \{1, 2, \dots, T_s\}$ , with  $T_s$  representing the number of sampling intervals. Moreover,  $f(\cdot): \mathbf{x}_{k-1} \rightarrow \mathbf{x}_k$  and  $h(\cdot): \mathbf{x}_k \rightarrow \mathbf{z}_k$  are known functions. Since the objective of this thesis is to address the nonlinear filtering problems,  $f(\cdot)$  and

$h(\cdot)$  represent nonlinear functions. Finally,  $\boldsymbol{\eta}_k$  and  $\boldsymbol{\nu}_k$  represent the process and measurement noises, respectively. Please note that the state-space model represented through Eqs. (1.1) and (1.2) is considered to be input-free for the sake of simplicity and the same is adopted throughout the thesis.

For the last several decades, the Bayesian filtering framework has been widely used for the estimation and filtering problems. It provides a probabilistic solution, which is described in the subsequent discussions.

### 1.1.1 Bayesian Filtering Framework: A Probabilistic Solution

Let us consider that we receive the sequence of noisy measurements  $\mathbf{z}_{1:k} = \{\mathbf{z}_1, \mathbf{z}_2, \dots, \mathbf{z}_k\}$  corresponding to  $\mathbf{x}_{1:k} = \{\mathbf{x}_1, \mathbf{x}_2, \dots, \mathbf{x}_k\}$  (Eqs. (1.1) and (1.2)); subsequently, the problem of estimation is statistical inversion or to infer about  $\mathbf{x}_k$  based on the measurements up to  $k^{th}$  instant (*i.e.*,  $\mathbf{z}_{1:k}$ ). In Bayesian filtering, the problem is reduced to computing the joint posterior distribution of all the states (including the initial state  $\mathbf{x}_0$ ) conditioned on the available measurements [8], *i.e.*,

$$p(\mathbf{x}_{0:k} | \mathbf{z}_{1:k}) = \frac{p(\mathbf{z}_{1:k} | \mathbf{x}_{0:k}) p(\mathbf{x}_{0:k})}{p(\mathbf{z}_{1:k})}, \quad (1.3)$$

where  $p(\mathbf{z}_{1:k} | \mathbf{x}_{0:k})$  is the likelihood,  $p(\mathbf{x}_{0:k})$  is the *a priori* probability density function (PDF), and  $p(\mathbf{z}_{1:k})$  is given by

$$p(\mathbf{z}_{1:k}) = \int_{\mathcal{D}} p(\mathbf{z}_{1:k} | \mathbf{x}_{0:k}) p(\mathbf{x}_{0:k}) d\mathbf{x}_{0:k}, \quad (1.4)$$

with  $\mathcal{D}$  signifying the domain of integration. It is worthwhile to note that the *a posteriori* PDF computation in Eq. (1.3) becomes increasingly problematical as time progresses. This is because of the ever-growing dimensionality of the PDF, which causes increased computational burden; it becomes particularly challenging in real-time applications, where an estimation is required immediately after the measurement is received. This issue is circumvented by the following assumptions [8, 9]: i) the states follow the Markov sequence and ii) the measurement at any time step depends upon the state from the same time-step. Subsequently, one can

settle for computing the filtering distribution  $p(\mathbf{x}_k|\mathbf{z}_{1:k})$  because it encapsulates the information of  $\mathbf{x}_k$  conveyed through  $\mathbf{z}_{1:k}$ , and it can be obtained by marginalizing  $p(\mathbf{x}_{0:k}|\mathbf{z}_{1:k})$  (Eq. (1.3)). Hereafter, we use the terms “prior PDF” and “posterior PDF” to denote  $p(\mathbf{x}_k|\mathbf{z}_{1:k-1})$  and  $p(\mathbf{x}_k|\mathbf{z}_{1:k})$ , respectively.

Taking into account the above-mentioned assumptions, the Bayesian filtering framework computes the posterior PDF (new posterior PDF)  $p(\mathbf{x}_k|\mathbf{z}_{1:k})$  in two steps [1, 8, 10].

- *Prediction update:* This step describes the propagation of the state in time and presents the belief about the state  $\mathbf{x}_k$  before the arrival of the current measurements  $\mathbf{z}_k$ . Specifically, it computes the predictive distribution  $p(\mathbf{x}_k|\mathbf{z}_{1:k-1})$  by leveraging the evidence from  $t_{k-1}$  (*i.e.*, the previous posterior PDF  $p(\mathbf{x}_{k-1}|\mathbf{z}_{1:k-1})$ ) as

$$p(\mathbf{x}_k|\mathbf{z}_{1:k-1}) = \int_{\mathbb{R}^n} p(\mathbf{x}_k|\mathbf{x}_{k-1})p(\mathbf{x}_{k-1}|\mathbf{z}_{1:k-1})d\mathbf{x}_{k-1}. \quad (1.5)$$

- *Measurement update:* Once the current measurement  $\mathbf{z}_k$  arrives, the prior PDF  $p(\mathbf{x}_k|\mathbf{z}_{1:k-1})$  is updated as

$$p(\mathbf{x}_k|\mathbf{z}_{1:k}) = \frac{p(\mathbf{z}_k|\mathbf{x}_k)p(\mathbf{x}_k|\mathbf{z}_{1:k-1})}{p(\mathbf{z}_k|\mathbf{z}_{1:k-1})}, \quad (1.6)$$

where

$$p(\mathbf{z}_k|\mathbf{z}_{1:k-1}) = \int_{\mathbb{R}^n} p(\mathbf{z}_k|\mathbf{x}_k)p(\mathbf{x}_k|\mathbf{z}_{1:k-1})d\mathbf{x}_k. \quad (1.7)$$

Eqs. (1.5) and (1.6) together provide the fundamental structure of Bayesian estimation for the system governed by Eqs. (1.1) and (1.2) through recursive formula (*i.e.*,  $p(\mathbf{x}_k|\mathbf{z}_{1:k-1})$  in the form of  $p(\mathbf{x}_{k-1}|\mathbf{z}_{1:k-1})$ ). Clearly, the solution provided by the Bayesian filter is probabilistic in nature which aims to track the conditional PDF of  $\mathbf{x}_k$ , and it does not provide a point estimate providing the best description of the system’s state in some sense. Moreover, in general practical scenarios, the multidimensional integrals of Eqs. (1.5) and (1.7) are intractable in nature [9, 11]. An exception involves the system being linear and the noises appearing in the system follow zero mean Gaussian distribution; for such systems, an optimal solution is provided by the Kalman filter (KF) [12], which provides a single decisive solution (a point estimate). However, no such optimal solution exists for the nonlinear filtering

problem.

Fortunately, the Gaussian assumption of the conditional density functions renders tractability to the Bayesian filter. Subsequently, the solution is simplified to the calculation of the multidimensional integrals.

### 1.1.2 Gaussian Filter: An Approximate Solution to Bayesian Filtering

As mentioned above, an approximate solution can be obtained through analytical simplification of conditional PDFs; the conditional PDFs appearing in Eqs. (1.5) and (1.7), *i.e.*,  $p(\mathbf{x}_k|\mathbf{z}_{1:k-1})$  and  $p(\mathbf{z}_k|\mathbf{z}_{1:k-1})$ , respectively, are assumed to follow Gaussian distribution [8, 11]. More specifically,

$$\begin{cases} p(\mathbf{x}_k|\mathbf{z}_{1:k-1}) \approx \mathcal{N}(\hat{\mathbf{x}}_{k|k-1}, \mathbf{P}_{k|k-1}) \\ p(\mathbf{z}_k|\mathbf{z}_{1:k-1}) \approx \mathcal{N}(\hat{\mathbf{z}}_{k|k-1}, \mathbf{P}_{k|k-1}^{\mathbf{zz}}), \end{cases} \quad (1.8)$$

where  $\mathcal{N}(\cdot, \cdot)$  being the conventional representation for Gaussian density;  $\hat{\mathbf{x}}_{k|k-1}$  and  $\mathbf{P}_{k|k-1}$  representing respectively the estimate and covariance of the predictive density while  $\hat{\mathbf{z}}_{k|k-1}$  and  $\mathbf{P}_{k|k-1}^{\mathbf{zz}}$  being the corresponding parameters for the predictive measurement density. The assumptions (1.8) ensure the Gaussianity of posterior PDF  $p(\mathbf{x}_k|\mathbf{z}_{1:k})$  (Eq. (1.6)), *i.e.*,

$$p(\mathbf{x}_k|\mathbf{z}_{1:k}) \approx \mathcal{N}(\hat{\mathbf{x}}_{k|k}, \mathbf{P}_{k|k}), \quad (1.9)$$

with  $\hat{\mathbf{x}}_{k|k}$  and  $\mathbf{P}_{k|k}$  being the estimate and covariance, respectively of the posterior PDF.

The Gaussian distribution is one of the most popular density functions that are used in many problems; it is amenable and contains the following distinctive properties

- Many natural random phenomena can be approximated by Gaussian PDF by means of the central limit theorem [10].
- The Gaussianity remains unaltered after linear transformation.

Another main approximation in developing the Bayesian filter in the Gaussian domain is that the noises appearing in the system follow the zero-mean Gaussian distribution [10, 13]. Specifically,  $\boldsymbol{\eta}_k \sim \mathcal{N}(0, \mathbf{Q}_k)$  and  $\boldsymbol{\nu}_k \sim \mathcal{N}(0, \mathbf{R}_k)$ . Pursuing this, the Gaussian filter is developed under the *moment matching method* of estimation [9], and the functional recursion in the Bayesian filter is simplified to propagation of mean and covariance of associated densities through the following steps

### Time update

In this step, the filter makes a prediction about the state  $\mathbf{x}_k$  in time advance, *i.e.*, before the arrival of the current measurement  $\mathbf{z}_k$  and using the available evidence from  $t_{k-1}$  ( $\hat{\mathbf{x}}_{k-1|k-1}$ ). Specifically, it computes the mean of the predictive density  $\hat{\mathbf{x}}_{k|k-1}$  and its covariance  $\mathbf{P}_{k|k-1}$ . The computation of  $\hat{\mathbf{x}}_{k|k-1}$  is as follows [8]

$$\hat{\mathbf{x}}_{k|k-1} = \mathbb{E}[\mathbf{x}_k | \mathbf{z}_{1:k-1}] = \mathbb{E}[f(\mathbf{x}_{k-1}) + \boldsymbol{\eta}_{k-1} | \mathbf{z}_{1:k-1}], \quad (1.10)$$

with  $\mathbb{E}[\cdot]$  representing the statistical expectation operator. As  $\boldsymbol{\eta}_k$  has zero mean, using the linearity property of the expectation operator, we can write

$$\begin{aligned} \hat{\mathbf{x}}_{k|k-1} &= \mathbb{E}[f(\mathbf{x}_{k-1}) | \mathbf{z}_{1:k-1}] \\ &= \int_{\mathbb{R}^n} f(\mathbf{x}_{k-1}) p(\mathbf{x}_{k-1} | \mathbf{z}_{1:k-1}) d\mathbf{x}_{k-1} \\ &\approx \int_{\mathbb{R}^n} f(\mathbf{x}_{k-1}) \mathcal{N}(\hat{\mathbf{x}}_{k-1|k-1}, \mathbf{P}_{k-1|k-1}) d\mathbf{x}_{k-1}. \end{aligned} \quad (1.11)$$

Likewise, the covariance is obtained as [9]

$$\begin{aligned} \mathbf{P}_{k|k-1} &= \mathbb{E}[(\mathbf{x}_k - \hat{\mathbf{x}}_{k|k-1})(\mathbf{x}_k - \hat{\mathbf{x}}_{k|k-1})^T | \mathbf{z}_{1:k-1}] \\ &= \int_{\mathbb{R}^n} f(\mathbf{x}_{k-1}) (f(\mathbf{x}_{k-1}))^T p(\mathbf{x}_{k-1} | \mathbf{z}_{1:k-1}) d\mathbf{x}_{k-1} + \mathbf{Q}_{k-1} - \hat{\mathbf{x}}_{k|k-1} \hat{\mathbf{x}}_{k|k-1}^T \\ &\approx \int_{\mathbb{R}^n} f(\mathbf{x}_{k-1}) (f(\mathbf{x}_{k-1}))^T \mathcal{N}(\hat{\mathbf{x}}_{k-1|k-1}, \mathbf{P}_{k-1|k-1}) d\mathbf{x}_{k-1} + \mathbf{Q}_{k-1} - \hat{\mathbf{x}}_{k|k-1} \hat{\mathbf{x}}_{k|k-1}^T. \end{aligned} \quad (1.12)$$



### Measurement update

This step computes the mean of the posterior density and its error covariance, *i.e.*,  $\hat{\mathbf{x}}_{k|k}$  and  $\mathbf{P}_{k|k}$ , respectively, as [11, 14]

$$\begin{cases} \hat{\mathbf{x}}_{k|k} = \hat{\mathbf{x}}_{k|k-1} + \mathbf{K}(\mathbf{z}_k - \hat{\mathbf{z}}_{k|k-1}) \\ \mathbf{P}_{k|k} = \mathbf{P}_{k|k-1} - \mathbf{K}\mathbf{P}_{k|k-1}^{\mathbf{zz}}\mathbf{K}^T, \end{cases} \quad (1.13)$$

where

$$\begin{aligned} \hat{\mathbf{z}}_{k|k-1} &= \mathbb{E}[(h(\mathbf{x}_k) + \boldsymbol{\nu}_k) | \mathbf{z}_{1:k-1}] \\ &\approx \int_{\mathbb{R}^n} h(\mathbf{x}_k) \mathcal{N}(\hat{\mathbf{x}}_{k|k-1}, \mathbf{P}_{k|k-1}) d\mathbf{x}_k \end{aligned} \quad (1.14)$$

and  $\mathbf{K}$  is the Kalman gain, expressed as

$$\mathbf{K} = \mathbf{P}_{k|k-1}^{\mathbf{xz}} (\mathbf{P}_{k|k-1}^{\mathbf{zz}})^{-1}, \quad (1.15)$$

with  $\mathbf{P}_{k|k-1}^{\mathbf{xz}}$  and  $\mathbf{P}_{k|k-1}^{\mathbf{zz}}$  denoting the state-measurement cross-covariance and covariance, respectively, given as [15]

$$\begin{aligned} \mathbf{P}_{k|k-1}^{\mathbf{xz}} &= \mathbb{E}[(\mathbf{x}_k - \hat{\mathbf{x}}_{k|k-1})(\mathbf{z}_k - \hat{\mathbf{z}}_{k|k-1})^T | \mathbf{z}_{1:k-1}] \\ &\approx \int_{\mathbb{R}^n} \mathbf{x}_k (h(\mathbf{x}_k))^T \mathcal{N}(\hat{\mathbf{x}}_{k|k-1}, \mathbf{P}_{k|k-1}) d\mathbf{x}_k - \hat{\mathbf{x}}_{k|k-1} \hat{\mathbf{z}}_{k|k-1}^T \end{aligned} \quad (1.16)$$

$$\begin{aligned} \mathbf{P}_{k|k-1}^{\mathbf{zz}} &= \mathbb{E}[(\mathbf{z}_k - \hat{\mathbf{z}}_{k|k-1})(\mathbf{z}_k - \hat{\mathbf{z}}_{k|k-1})^T | \mathbf{z}_{1:k-1}] \\ &\approx \int_{\mathbb{R}^n} h(\mathbf{x}_k) (h(\mathbf{x}_k))^T \mathcal{N}(\hat{\mathbf{x}}_{k|k-1}, \mathbf{P}_{k|k-1}) d\mathbf{x}_k - \hat{\mathbf{z}}_{k|k-1} \hat{\mathbf{z}}_{k|k-1}^T + \mathbf{R}_k. \end{aligned} \quad (1.17)$$

It should be noted that the integrands appearing in Eqs. (1.11), (1.12), (1.14), (1.16), and (1.17) are in the form of *nonlinear function*  $\times$  *Gaussian weight*, and corresponding integrals lack an analytical solution [11]. As discussed earlier, however, an analytical solution is obtained by the KF if the functions are linear, alternatively the integrands follow the form *linear function*  $\times$  *Gaussian weight*. Motivated by this, the extended Kalman filter (EKF) was developed, which first linearizes the

nonlinear functions appearing in the system using a derivative-based approach [10], and subsequently, follows the KF structure for recursive estimation. The EKF and its extensions [16–18] are referred to as *derivative-based* approaches due to the involvement of linearization step, which is the very reason incurring several drawbacks, including inferior filtering accuracy and slow convergence, in these filters [11].

Thankfully, there exist some numerical integration methods that provide reasonable approximate to these integrals; thus, implementation of different approaches bring about different versions of Gaussian filters.

To discuss the numerical approximation approach, let us first consider the generalized expression of the above-discussed integrals as [9]

$$I^n(g(\mathbf{x})) = \int_{\mathcal{D}} g(\mathbf{x})w(\mathbf{x})d\mathbf{x}, \quad (1.18)$$

with  $g(\cdot)$  being an arbitrary nonlinear function and  $w(\mathbf{x})$  representing the known weighting function, with  $w(\mathbf{x}) \geq 0$  for  $\mathbf{x} \in \mathcal{D}$ . The fundamental objective when numerically approximating  $I(g)$  involves computing a collection of points  $\xi_i$ ,  $i = \{1, 2, \dots, N_c\}$  and associated weights  $w_i$  such that

$$I^n(g(\mathbf{x})) \approx \sum_{i=1}^{N_c} w_i g(\xi_i) \quad (1.19)$$

provides the approximated value. Please note that the numerical methods available in the literature are defined only for the weighting function as standard normal distribution, *i.e.*,  $w(\mathbf{x}) \sim \mathcal{N}(\mathbf{0}_{n \times 1}, \mathbf{I}_n)$ , where  $\mathbf{0}_{n \times 1}$  is an array of  $n$  zeros and  $\mathbf{I}_n$  being  $n$ -dimensional identity matrix. Let us denote the corresponding integral as  $I_0^n(g(\mathbf{x}))$ , *i.e.*,

$$I_0^n(g(\mathbf{x})) = \int_{\mathbb{R}^n} g(\mathbf{x})\mathcal{N}(\mathbf{0}_{n \times 1}, \mathbf{I}_n)d\mathbf{x} \quad (1.20)$$

and following Eq. (1.19), its approximated value can be given as

$$I_0^n(g(\mathbf{x})) \approx \sum_{i=1}^{N_c} w_i g(\xi_i). \quad (1.21)$$

It should be noted that the weighting functions appearing in Eqs. (1.11), (1.12), (1.14), (1.16), and (1.17) do not follow standard normal distribution. Subsequently,

we use the change of variable method to extend the numerical approximation technique for any arbitrary normally distributed weighting function  $w(\mathbf{x}) \sim \mathcal{N}(\boldsymbol{\mu}, \boldsymbol{\Sigma})$ , given as [9]

$$I^n(g(\mathbf{x})) = \int_{\mathbb{R}^n} g(\mathbf{x}) \mathcal{N}(\boldsymbol{\mu}, \boldsymbol{\Sigma}) d\mathbf{x} = \frac{1}{\sqrt{\pi^n}} \int_{\mathbb{R}^n} g(\sqrt{2}\boldsymbol{\Sigma}\mathbf{x} + \boldsymbol{\mu}) \mathcal{N}(\mathbf{0}_{n \times 1}, \mathbf{I}_n) d\mathbf{x}. \quad (1.22)$$

### 1.1.3 Stochastic Stability Analysis of Gaussian Filters

In 1892, Lyapunov introduced his famous direct method in the theory of stability, which laid the groundwork for understanding the behavior of dynamic systems. The concept of stability refers to the system's ability to maintain its state or trajectory in the presence of small perturbations or changes in initial conditions or system parameters. Specifically, Lyapunov's stability theory involves the analysis of trajectories or solutions of a dynamic system over time.

For many differential equations (difference in discrete time) representing the systems, the solutions can not be obtained easily, making the stability analysis difficult. For such a system, Lyapunov introduced a function, widely known as the Lyapunov's function, to infer the stability of the systems without requiring the knowledge of the solutions [19, 20]. The Lyapunov function was originally introduced for the deterministic systems.

#### Exponential boundeness

Let  $\mathbb{V} : \mathbb{R}^n \rightarrow \mathbb{R}$  represents the Lyapunov function, then it holds the following properties [21]

- It is strictly positive.
- The time derivative is non-positive, *i.e.*,  $\dot{\mathbb{V}}(.) \leq 0$ .

However, the treatment of stochastic processes can not be done in same the way as that of the deterministic ones. The reason is that, while extending the Lyapunov stability theory from the deterministic to stochastic systems, the following questions arise

- How to come up with a suitable definition of stochastic stability?

- What criteria must a Lyapunov function meet?
- What should replace the inequality  $\dot{\mathbb{V}}(.) \leq 0$  to obtain the stability assertion?

For stochastic processes, mainly three types of stability can be performed: stability in probability, moment stability, and almost sure stability [21]. In 1965, Bucy identified that a stochastic Lyapunov function should possess the supermartingale property. He also provided remarkably straightforward conditions for both stability in probability and moment stability. Later, Has'minskii [22] explored almost sure stability in the context of linear stochastic processes.

However, we consider the notion of *moment stability* to perform the stochastic stability of the Gaussian filter. Specifically, we consider the concept of exponential boundedness in mean square, which can be described through the following definition [23]

**Definition 1.1.** *Let us consider that  $\zeta_k$  denotes a stochastic process and  $\kappa' > 0$ ,  $\sigma' > 0$ , and  $0 < \theta < 1$  are real numbers. Then,  $\zeta_k$  is said to be exponentially bounded in mean square if it satisfies*

$$\mathbb{E} [\|\zeta_k\|^2] \leq \kappa' \mathbb{E} [\|\zeta_0\|^2] \theta^k + \sigma' \quad \forall k \in \{1, 2, \dots\}, \quad (1.23)$$

where  $\|\cdot\|$  represents the spectral norm for matrices and Euclidean norm for vectors.

In our stability analysis, we approach Eq. (1.23) in a different way. In this regard, please refer to the subsequent discussion.

**Remark 1.1.** *Let us consider that  $\tau_1 > 0$ ,  $\tau_2 > 0$ ,  $\gamma' > 0$ , and  $0 < \phi < 1$  denote real numbers, and  $\mathbb{V}(\zeta_k)$  represents a scalar-valued stochastic process (stochastic Lyapunov function), which satisfies*

$$\tau_1 \|\zeta_k\|^2 \leq \mathbb{V}(\zeta_k) \leq \tau_2 \|\zeta_k\|^2 \quad (1.24)$$

and

$$\mathbb{E} [\mathbb{V}(\zeta_k) | \zeta_{k-1}] - \mathbb{V}(\zeta_{k-1}) \leq \gamma' - \phi \mathbb{V}(\zeta_{k-1}) \leq 0. \quad (1.25)$$

Then, the stochastic process  $\zeta_k$  satisfies

$$\mathbb{E} [\|\zeta_k\|^2] \leq \frac{\tau_2}{\tau_1} \mathbb{E} [\|\zeta_0\|^2] (1 - \phi)^k + \frac{\gamma'}{\tau_1} \sum_{i=0}^{k-1} (1 - \phi)^i. \quad (1.26)$$

*Proof.* Let us consider Eq. (1.25), it implies that

$$\mathbb{E} [\mathbb{V}(\zeta_k) | \zeta_{k-1}] \leq \gamma' + (1 - \phi) \mathbb{V}(\zeta_{k-1}) \quad (1.27)$$

Using the law of total expectations, we can write

$$\mathbb{E} [\mathbb{V}(\zeta_k) | \zeta_{k-2}] = \mathbb{E} [\mathbb{E} [\mathbb{V}(\zeta_k) | \zeta_{k-1}] | \zeta_{k-2}]. \quad (1.28)$$

Applying Eq. (1.27), the above equation can be expressed as

$$\begin{aligned} \mathbb{E} [\mathbb{V}(\zeta_k) | \zeta_{k-2}] &= \gamma' + (1 - \phi) \mathbb{E} [\mathbb{V}(\zeta_{k-1}) | \zeta_{k-2}] \\ &\leq \gamma' + (1 - \phi) \gamma' + (1 - \phi)^2 \mathbb{V}(\zeta_{k-2}). \end{aligned} \quad (1.29)$$

Similarly, extending the above expression conditioned to  $\zeta_0$  and taking an expectation, we obtain

$$\mathbb{E} [\mathbb{V}(\zeta_k) | \zeta_0] \leq (1 - \phi)^k \mathbb{E} [\mathbb{V}(\zeta_0)] + \gamma' \sum_{i=0}^{k-1} (1 - \phi)^i. \quad (1.30)$$

Subsequently, applying Eq. (1.24) deduces Eq. (1.26).  $\square$

Let us recall Eq. (1.26), as  $\sum_{i=0}^{k-1} (1 - \phi)^i \leq \sum_{i=0}^{\infty} (1 - \phi)^i = 1/\phi$ , it can be rewritten as

$$\mathbb{E} [\|\zeta_k\|^2] \leq \frac{\tau_2}{\tau_1} \mathbb{E} [\|\zeta_0\|^2] (1 - \phi)^k + \frac{\gamma'}{\tau_1 \phi}. \quad (1.31)$$

We now compare the above expression with Eq. (1.23). We observe that with  $\tau_2/\tau_1 = \kappa'$ ,  $1 - \phi = \theta$ , and  $\gamma'/(\tau_1 \phi) = \sigma'$ , Eq. (1.31) is the same as Eq. (1.23). Thus, we can say that the stochastic process  $\zeta_k$  remains exponentially bounded in mean square.

**Remark 1.2.** *Definition 1.1 and Remark 1.1 collectively conclude that any stochastic process remains bounded with an exponential envelope (i.e., satisfies Eq. (1.23))*

*if it satisfies the two criteria given by Eqs. (1.24) and (1.25).*

### Stability of modified Gaussian filters

In this thesis, we introduce multiple modified versions of the Gaussian filter to address various measurement irregularities. We extend our analysis to investigate the stochastic stability of these filtering algorithms, a concept previously discussed for an arbitrary stochastic process denoted as  $\zeta_k$ . In the context of the filtering algorithm, this amounts to checking whether the estimation error exhibits exponential boundedness [24, 25]. In this thesis, we analyze the stochastic stability of different restructured Gaussian filters by considering only the respective EKF-based structures. The reason is that the local linearization step involved in the EKF enables us to perform the stability analysis conveniently. Conversely, other Gaussian filters such as the UKF [26], CKF [9], CQKF [27], and GHF [28] propagate the nonlinearities of the systems, and these filters currently lack a rigorous mathematical treatment in the existing literature. The following discussion provides a context of our strategy for stability analysis of the Gaussian filter, which is performed later in this thesis.

As discussed above, the stability of the EKF can be examined by analyzing the behavior of the estimation error. Since the estimation error fundamentally follows a stochastic process, we describe its dynamics through a stochastic difference equation; thereby, characterizing it as a stochastic system. Subsequently, we employ Remark 1.2 as our criterion to establish the exponential boundedness of the estimation error. This achievement, in turn, demonstrates the stochastic stability of the EKF, and hence of corresponding Gaussian filter. To be more specific, Remark 1.2 is used to identify conditions under which the estimation error of the EKF exhibits exponential boundedness.

## 1.2 Motivation

As has been indicated in the beginning, the aim of this thesis is to address nonlinear filtering, Gaussian filtering to be specific. The Gaussian filters are sub-optimal yet they provide reasonable performance for many real-life problems. The various

versions of the Gaussian filter enable us to make a trade-off between accuracy and computational complexity [11].

An aspect of designing the Gaussian filtering is the assumption of receiving clean measurements without irregularities, which is often violated in practice. The practical measurements, stemming from various reasons, may involve irregularities: random delays and frequent losses. In the former case, the measurement received at any time instant may contain information about any of the previous states, while the measurements are not received at intermittent intervals in the latter case. Since the irregularities are not considered in the structures of the Gaussian filters, their performance tend to deteriorate significantly or even fail completely in the individual or joint presence of these irregularities [29]. Following which, we summarize the motivations of the thesis as follows

- Gaussian filters require complete measurements for a smooth filtering performance. In practice, however, one or more elements of the measurements may be frequently missing [29]. The earlier developments in this directions are mostly filter-specific, and thus find difficulty in addressing a wide class of problems. The motivation of this thesis is to develop a generalized Gaussian filtering algorithm to handle the partially missing measurements.
- The earlier developments are mainly designed to handle only one irregularity at a time: either delayed measurements or missing measurements. In practice, however, the simultaneous occurrence of these irregularities is possible. This motivated us to develop an advanced Gaussian filter that can handle the jointly occurring delayed and missing measurements.
- The existing methods for handling the delay require knowledge of a set of delay probabilities, which are hardly available in practical systems. Moreover, the methods arbitrarily assign the upper bound of the delay. The motivation of this thesis is to develop an advanced Gaussian filter that serves as both reducing the number of delay probability requirement and precisely characterizing the maximum possible delay in the measurements.
- The existing Gaussian filters are sub-optimal, with the accuracy depending on the accuracy of the underlying numerical approximation methods. This

motivated the thesis to develop an advanced Gaussian filtering algorithm to further improve the filtering accuracy by employing a more accurate numerical approximation method.

- The literature witnesses a number of contributions to study the stability for the linear Kalman filter, while there are only few contributions addressing the stochastic stability of the Gaussian filters. This motivation of the thesis is to prove the stochastic stability of the restructured Gaussian filters handling the different irregularities.

## 1.3 Objective

Following the motivation discussed in the previous section, we sketch out the objectives of the thesis as follows

- Design an advanced Gaussian filter to handle the intermittently missing measurements.
- Modify the Gaussian filter to handle the simultaneous occurrence of delayed and missing measurements.
- Introduce an advanced Gaussian filter that not only reduces the number of delay probability requirements but also relaxes the ambiguous assignment of the upper bound of the delay.
- Design a modified Gaussian filter to deal with stochastically composed current and previous measurements.
- Introduce a more accurate version of the Gaussian filter.
- Prove the stochastic stability of different Gaussian filters proposed in this thesis.

## 1.4 Approaches and Methods

Let us reiterate that this thesis is concerned with nonlinear filtering problem in Gaussian domain, wherein we aim to develop new Gaussian filtering algorithms to



handle various measurement irregularities and intractable integrals. In this regard, we adopt the following strategies

- Inclusion of the measurement irregularity: The effect of the irregularity phenomenon is incorporated by introducing a mathematical model.
- Modified Gaussian filter design: The author re-derives a few relevant parameters in the Gaussian filter according to the mathematical formulation. In the case of new Gaussian filter design, the author employs a new numerical approximation technique to handle the intractable integrals.
- Stability analysis: The author uses the criteria of checking the stochastic stability of general stochastic systems, and subsequently, extends it to prove the stochastic stability of the different Gaussian filters for their EKF-based extensions.
- Simulation: The simulation results are generated in MatLab, over a personal computer configured with 32 GB RAM, i5-8400 processor with the clock speed of 2.80 GHz.
- Validation: The author adopts the well-known root mean square error (RMSE) as a metric to compare the performance of different developments.

## 1.5 Contribution

The main contributions of this thesis are provided below

- This thesis offers an extensive and advanced review of the Gaussian filtering and various measurement irregularities.
- The conventional Gaussian filter is restructured to handle the missing measurements.
- A modified Gaussian filter is proposed to handle the simultaneously occurring delayed and missing measurements.

- A novel nonlinear Gaussian filtering algorithm is formulated to manage delayed measurements while requiring minimal prior information about delay probabilities.
- The traditional Gaussian filter is modified to deal with stochastically superimposed current and past measurements.
- The stochastic stability is studied for each of the above-mentioned Gaussian filters.
- An advanced Gaussian filter is proposed to handle the intractable integrals appearing during the filtering.

## List of Publications

### Journals (accepted/published)

- **Amit Kumar Naik**, Sumanta Kumar Nanda, Prabhat Kumar Upadhyay, and Abhinoy Kumar Singh. “Kalman-Based Multiple Sinusoids Identification from Intermittently Missing Measurements of the Superimposed Signal”. *International Journal of Adaptive Control and Signal Processing*.
- **Amit Kumar Naik**, Prabhat Kumar Upadhyay, Maurizio Magarini, and Abhinoy Kumar Singh, “Nonlinear Filtering with Sporadically Missing Sensor Data,” *IEEE Sensors Letters*, vol. 7, no. 10, pp. 1-4, Oct. 2023
- **Amit Kumar Naik**, Prabhat Kumar Upadhyay, and Abhinoy Kumar Singh, “Gaussian Kernel Quadrature Kalman Filter.” *European Journal of Control* 71 (2023): 100805.
- **Amit Kumar Naik**, Guddu Kumar, Prabhat Kumar Upadhyay, Paresh Date, and Abhinoy Kumar Singh, “Gaussian Filtering for Simultaneously Occurring Delayed and Missing Measurements.” *IEEE Access* 10 (2022): 100746-100762.

## Journals (submitted/under review)

- **Amit Kumar Naik**, Neelanshu Garg, Prabhat Kumar Upadhyay, and Abhinoy Kumar Singh. “Gaussian Filtering with Stochastically Composed Current and Past Measurements”. *IEEE Transactions on Automation Science and Engineering* (Revision III).
- **Amit Kumar Naik**, Neelanshu Garg, Guddu Kumar, Prabhat Kumar Upadhyay, and Abhinoy Kumar Singh. “Poisson-Gaussian Filtering with Randomly Delayed Measurements”. *IEEE Transactions on Automation Science and Engineering*.

## 1.6 Thesis Organization

The remaining part of the thesis is organized as follows. Chapter 2 reviews variants of different Gaussian filters and discusses the missing and delayed measurements phenomena. In Chapter 3, the extended Kalman filter is modified to handle the missing measurements phenomenon, which is followed a generalized Gaussian filter for missing measurements in Chapter 4. Chapter 5 proposes a Gaussian filter to handle large delays by using single average delay information. In Chapter 6, a new kind of delay irregularity is addressed. The simultaneous presence of the delayed and missing measurements are handled using an advanced Gaussian filter in Chapter 7. The stochastic stability is analyzed in Chapter 8, followed by a new Gaussian filter development in Chapter 9. Finally, Chapter 10 draws important conclusions with the discussion on the possible future research directions.



# Chapter 2

## Literature Review

In the previous chapter, we established the motivation behind this thesis: to develop advanced filtering algorithms specifically tailored for discrete-time nonlinear systems (DTNSs). Prevalent in engineering and science, DTNSs exhibit complex behaviors that cannot be accurately modeled using linear techniques. The primary objective is to improve the accuracy of filtering methods for such systems. To be specific, the review mainly focuses on the computationally efficient Gaussian filtering, a widely-recognized filtering algorithm for DTNSs.

This chapter further discusses various measurement irregularities in the network control systems (NCSs) and the developments appearing in the literature to handle them. Some predominantly occurring measurement irregularities are delayed measurement, intermittently missing measurements, non-Gaussian noise, and cyber-attack. This thesis primarily emphasizes the challenges posed by delay and missing measurements, it acknowledges the important issues of non-Gaussian noise and cyber-attacks.

### 2.1 Evolution of Gaussian Filters

The Bayesian filtering solution provided by Eqs. (1.5) and (1.7) involve intractable integrals that arise due to the non-linearities in practical systems. However, there are some cases where these integrals tend to have analytical solutions. A few notable examples include:

- Linear dynamical systems with additive white-Gaussian noise (AWGN): The

state and state-to-measurement transitions are governed by linear relationships and the process and measurement noises can be modeled by AWGNs. The well-celebrated Kalman filter [12] provides an optimal solution for such a system.

- Benes type non-linearity: This type of non-linearity typically comprises an exponential function of the state of the system. The optimal solution for such filtering problems is given by the Benes filter [30].

Let us now reiterate that the practical systems mostly exhibit non-linear dynamics, and the popular filtering technique, *i.e.*, Kalman filter [12] has demonstrated incompetency to handle it. Subsequently, some reasonable assumptions are made to handle the non-linearities in the systems. These assumptions have led to the development of two major classes of Gaussian filters, adopting individual strategies to handle the non-linearities: one category employing approximant (linear) to approximate the non-linearities (derivative-based) while another approximates the intractable integrals using numerical integration techniques (sigma point-based). Due to the involvement of the approximation step, these filters are also referred to as *approximate filters*.

To be specific, the derivative-based Gaussian filtering techniques represent the system non-linearity as the linear combination of some terms. On the other hand, as discussed in the previous chapter, the sigma point-based Gaussian filters calculate the approximated values of the intractable integrals through a collection of sample points (sigma points) associated with corresponding weights. A range of sigma point-based Gaussian filters has been documented in the literature, each employing different numerical approximation techniques involving individual sigma points and weights. Compared to their derivative-based counterparts, these sigma point-based Gaussian filters surpass in terms of both accuracy and numerical stability.

The subsequent discussion reviews numerous methods developed under the aforementioned linearization-based and sigma point-based Gaussian filtering.

### 2.1.1 Linearization-based Gaussian Filters

The filters in this category, including the EKF and its variants, approximate the nonlinear function with a linear one. Apart from the linearization process, these

filters share the same structure as the Kalman filter. The author now provides a moderately detailed discussion on these filters.

### **The EKF and its subsequent versions**

Being developed in early 1960s, the EKF is arguably one of the earliest nonlinear Gaussian filters and is continuing to be remarkably applicable in industrial and theoretical developments. It linearizes the system nonlinearities by taking the first-order Jacobian around the latest estimates which are the previous and predicted estimates respectively for the process and measurement models. Thereupon, it follows the structure of the linear Kalman filter to calculate the estimate recursively. The EKF is probably one of the most preferred filters in real-life estimation problems. Operation and control in power systems [31], space exploration through low earth orbit satellites [32], modeling and studying the epidemic spread [33], fault detection in battery banks [34], and industrial process monitoring are a few noticeable practical examples employing the EKF.

The EKF is widely recognized as practical standard in nonlinear filtering theory for systems with comprehensible models, such as navigation systems. However, it also suffers from several drawbacks due to the involvement of linearization step. In the first instance, it may become divergent if the initial estimation is significantly mismatched from the true value or the model inaccurately imitates the actual system. In addition, the negligence of the approximation errors results into underestimated state-uncertainties, thrusting the EKF towards inconsistency. Moreover, the requirement of model continuity and small sampling instants become problematic, as the EKF involves the Jacobian calculation.

Despite its limitations, the EKF remains popular among practitioners due to its straightforward implementation and low computational requirements. Additionally, researchers have brought many technical advancements in the traditional EKF to overcome its drawbacks, and the following discussion explores some major variants.

- Second-order EKF (SEKF) [17, 18, 35] and high-order EKF (HEKF) [36]: As discussed earlier, the conventional EKF considers the Taylor series expansion only up to the first order in approximating the system non-linearity. The SEKF extends it by taking the second-order approximant and follows the

EKF structure of filtering. Motivated by this, the HEKF further includes the higher-order terms of the expansion for approximation. Consideration of the second and higher-order terms results in more accurate approximation. As a result, the EKF is surpassed in terms of accuracy by the SEKF and HEKF, with the latter being superior.

- Invariant EKF (InEKF) [37, 38]: Some practical nonlinear systems demonstrate symmetry or invariance and the EKF gives sub-optimal performance for such applications. The InEKF incorporates the strengths of the EKF and symmetry-preserving filters, extending the EKF to the Lie group (space resembling the Euclidean space locally). It uses the geometrically transformed state and output errors based on Lie group theory, reducing the dependency on the estimated state. Thus, the InEKF outperforms the EKF for nonlinear invariant systems.
- Iterated EKF (IEKF) [16, 39, 40]: In the update step of the EKF, the measurement model is linearized only one time. The IEKF improves the linearization accuracy by iteratively updating the center of the Taylor-series expansion, leading to an improved estimation accuracy. However, the iterative step increases the computational demand.

Despite the existence of multiple modified versions of the EKF, the derivative computation remains a major concern. It further worsens as the degree of non-linearity in the system increases. As previously discussed, the sigma points Gaussian filtering averts the Jacobean calculation, and can partially alleviate the limitations associated with the EKF and its advanced versions. In the subsequent discussion, the author examines notable advancements related to sigma points (derivative-free) Gaussian filtering.

### 2.1.2 Sigma Point-based Gaussian Filters

Unlike the EKF structure, the sigma point-based Gaussian filtering is free from the linearization step and directly propagates the non-linearity of system. Consequently, it faces intractable integrals during the filtering process, and requires numerical integration techniques to calculate the approximate value. As discussed earlier,



the numerical integration methods calculate a set of sample points (sigma points) and corresponding weights. Subsequently, the numerically approximated value of the integral is given as the weighted sum of the values of the nonlinear function calculated at sigma points.

The use of individual numerical integration techniques has induced different sigma point Gaussian filters. In the following discussion, the author reviews a range of these filters and their variants.

### **Unscented Kalman filter (UKF) and its versions**

The development of the UKF [26] was mainly motivated by the process of only approximation of nonlinear function in the EKF, while statistical information on states is also available. It offers an alternative to linearization. Unlike the EKF, which relies on analytical linearization to handle non-linearity, the UKF employs statistical linearization based on predefined rules. The driving intuition was that *a distribution represented by a small number of parameters can be more conveniently approximated than approximating the nonlinear function*. Following this, the pioneers sought a parameterization technique that could simultaneously capture the parameters of the original distribution while exactly propagating them through the nonlinear function. Thus, a discrete distribution is generated with the statistical parameters (mainly mean and covariance) remaining unchanged. The elements (points) of the discrete distribution are also referred to as the sigma points and can directly undergo nonlinear transformation. Subsequently, the desired statistical parameters are obtained by calculating the corresponding parameters of the transformed set. The complete exploitation of the nonlinearity immediately eliminates the need for linearization that is not possible for non-differentiable functions.

Recognizing the superior performance to the EKF, the UKF gained significant attention and was employed as an alternative to the EKF in many practical applications. These include grid integration and control [41], distant tracking of vessel [42], continuous monitoring of respiratory rate [43], manipulation of an unmanned aerial vehicle [44], and target tracking [45].

The filtering literature has witnessed several advancements in the UKF; the discussion below summarizes some important developments of them.

- Iterated UKF (IUKF) [46, 47]: As mentioned earlier, the inclusion of the iterative step improved the performance of the conventional EKF (IEKF), inspiring the inclusion of the same in the UKF. However, the iterative process in the UKF differs slightly from that of the IEKF: termination criterion and step length. Moreover, the most recent covariance matrix governs the generation of a new set of sigma points at each iteration, making the set closer to the true distribution at each step. As result, the IUKF outperforms the traditional UKF.
- Transformed UKF (TUKF) [48]: The higher-dimensional problems (usually greater than 3) become problematic for the UKF in term of numerical instability. This is because of the loss of positive definiteness of the covariance matrix which stems from the negative weight of the central sigma point (mean). To circumvent the problem, a new set of sigma points is generated and embedded into the traditional UKF leading to the development of the TUKF.
- Square-root UKF (SQUKF) [49]: The conventional UKF computes the square root of the covariance matrix by applying the Cholesky factorization. It is only possible when the covariance matrix is positive semi-definite, which is not always practically guaranteed and leads to implementation failure. The SQUKF efficiently deals with this problem as it replaces the Cholesky decomposition with QR decomposition technique, insuring the positive semi-definiteness of the state covariance matrix.

Apart from the above, various practical applications celebrate other important versions of the UKF. To name a few, [50] applies the scaled UKF for bearing-only target tracking while [51] employs the similar for fault diagnosing in a offshore windmill system. In other developments, the traffic flow monitoring and control was performed using an incremental-based UKF [52], and [53] used hybrid UKF for robotics manipulation.

### **Cubature Kalman filter (CKF) and its versions**

A popular iteration of the sigma point technique is the Cubature Kalman Filter (CKF) [9]. With slight variations from the UKF, the CKF selects sigma points

based on the cubature rule. The core of the cubature rule involves transformation of the state from Cartesian to spherical-radial coordinate. Subsequently, the resulting integral is factorized into spherical and radial integrals, with the former and latter being approximated by the third-degree spherical and first-order Gauss quadrature rules, respectively. Finally, the CKF combines these rules, resulting into spherical-radial rule and extends it for Gaussian weights. Due to the superior performance over the UKF, the CKF attracted various specialties, such as useful remaining life prediction of Lithium-ion battery [54], monitoring and orientations of a spacecraft [55], and dynamic state estimation in power systems [56].

This work was extended in [27] by considering the third-order Gauss-Laguerre quadrature rule to approximate the radial integral, developing a new filter termed as cubature-quadrature Kalman filter (CQKF). Taking the higher order gives an increased number of sigma points which more accurately approximate the integrals, however at slightly higher computational complexity. Although the higher-order radial rule was used by CQKF, the high degree of spherical rule remained unexplored until the developments in [57] and [58] exploited the high-degree spherical rules. The former restructured the CKF and the latter modified the CQKF and referred to them as higher-degree CKF (HDCKF) and higher-degree CQKF (HDCQKF), respectively. The discussed filters are widely applied in target tracking [59], space exploration[60], navigation [61] *etc.*

In addition, several modifications were incorporated in the CKF and CQKF, introducing modified versions of these filters and applied to different applications. Specifically, the square-root versions of the CKF [62], CQKF [63, 64], HDCKF [65], transformed CQKF [66], and iterated CKF [67] are some notable examples.

### **Gauss-Hermite filter (GHF) and its versions**

Gauss-Hermite quadrature rule is a suitable candidate for numerically approximating intractable integrals for a single dimension. In practice, however, dealing with multi-dimensional systems is common. The Gauss-Hermite filter [28] implements tensor product of single-dimensional sample points, which enables to approximate multi-dimensional integrals. It should be mentioned that the sample size and system dimension are exponentially related, becoming problematic in terms of compu-

tational complexity for high dimensional systems, (usually  $n > 5$ ).

Two popular versions of the GHF were proposed to ease the computational demand: sparse-grid GHF (SGHF) [68] and adaptive sparse-grid GHF (ASGHF) [69], with the former using the Smolyak rule and the latter employing adaptive-grid method to reduce the number of quadrature points. The SGHF and ASGHF peculiarly lessen the computational complexity without compromising the accuracy. Unfortunately, the computational burden of the SGHF and ASGHF are still high enough to restrict their applicability in high-dimensional system, despite the fact that GHFs hold high-rank among the accurate Gaussian filters.

The Gaussian filters and their extensions are associated with certain drawbacks, including: i) inconsistency in the set of nonlinear equations, ii) numerical solutions that often result in undesirable negative weights and complex roots, and iii) cubature points that may fall outside the support of the PDFs. These challenges make it difficult to formulate general cubature rules that can be applied across different dimensions and orders. Consequently, most cubature rules are specifically designed for a given dimension and order. Recognizing these limitations has provided valuable insights that have contributed to the development of new cubature rules with positive weights in [70], known as the conjugate unscented transformation (CUT).

The CUT identifies non-product sigma or cubature points with positive weights, capable of accurately integrating polynomial functions of a specified order with respect to Gaussian and Uniform probability density functions. Its objective is to achieve a rule with fewer points than the equivalent Gaussian quadrature product rules. This approach extends the unscented transformation, providing higher-order sigma points with positive weights for multivariate Gaussian. This method has been applied for estimating the probability of conjunction between two space objects [71]. The proposed approach leverages the CUT with the principle of maximum entropy to assess collision probability. The CUT points facilitate the efficient propagation of statistical moments associated with each object's orbital state, which are subsequently used to reconstruct the miss-distance probability density function through the principle of maximum entropy. Similarly [72] represented the PDFs with orthogonal polynomial and designed an estimation algorithm under maximum entropy framework.

## 2.2 Nonlinear Filtering in the Presence of Various Measurement Irregularities

The Gaussian filters discussed in the previous section are designed based on certain ideal assumptions about measurements. Specifically, the filters assume that measurements are received at each sampling instant and provide information about the states from the exactly same moment, apart from the being disturbed by Gaussian white noise. However, these assumptions are often not met in practical systems involving network control system (NCS) or more broadly wireless sensor networks (WSNs). The WSNs offer several advantages over the conventional wired systems: distant monitoring in real-time with quick response, highly scalable, and economical [73–75]. However, the complex structure of WSNs poses many challenges; the compromised data quality being among the major concerns which is considered in this thesis.

As mentioned in Chapter 1 of this thesis, the practical measurements are frequently corrupted by the some irregularities. These include missing measurements, where an estimator does not receive measurements at random sampling instants; delayed measurements, which contain information about the state from past instants; cyber-attacked measurements, intentionally altered or destroyed; and non-Gaussian noise, where measurement errors deviate from a Gaussian distribution. Please note that this thesis is specifically centered around the irregularities of delayed and missing measurements.

In what follows, the author presents a discussion on concerned measurement irregularities: their inducing factors, developments to handle these irregularities, *etc.*

### 2.2.1 Missing Measurements

During the filtering process in practical systems, there frequently arises a situation where the required *information* to produce an estimate is not available for many time instants, and referred to as missing measurement. The measurement might be lost during any phase of the filtering: acquisition, propagation, and storage.

Generally, the following two notions of missing measurements are widely recognized in a wireless sensor network (WSN) [76]

- **Damaged measurement:** The sensor nodes in WSNs, typically deployed in geographically distant and complex environments, are energy-constrained due to being powered by battery. The acquired measurements are compressed before propagation through wireless channels, which also involves eliminating the measurements from some samples to reduce the number of data [77–79]. Moreover, the data are truncated and rounded. Such measurements can be regarded as damaged with certain degree, and hence missing ones due to being incompetent in providing any knowledge about quantity (state).
- **Missing data entries:** Regarding the most widely accepted definition, missing data typically refers to incomplete data entries. Specifically, if the entries (data source) are null at one or multiple sampling instants, it is considered to be the case of missing measurements.

The prevalent cause of missing measurements is their loss or damage during any of the stages between acquisition to storage. Both human and non-human elements contribute to measurement loss or damage. Human factors mainly include deceptive business: sensor nodes are physically damaged [80] or their communication environment is compromised [81]. Moreover, the intentional use of compressive sensing by the operator [82, 83] also causes missing measurements, as it involves frequent elimination of data to extend both battery (energy) and sensor lifetimes. On the other hand, non-human factors involve sensor-, communication channel-, storage-, and associated hardware-related issues, causing the frequent loss of measurements. In the first instance, the sensors are mostly battery-driven with limited power; the sensors operating at low power may drift toward instability and results into data loss [76]. In other reasons, time-sharing of sensors [84] and sensor malfunctions or temporal failure [85, 86] are sensor-related problems causing the missing measurements.

The network-related problems also contribute to the missing measurement phenomenon. For instance, the incompetent network and communication channels tend to lose measurement data [87]. In addition, physical obstacles, radio interference, and harsh environments such as desert and underwater [88–91] irregularly interrupt

the propagation of measurements. Moreover, highly noisy and cluttered surroundings cause the actual measurements to be unidentifiable [92].

Extending the above-discussion, the problem of missing measurements is identified in many practical applications, including power systems [93, 94], biomedical [95], and space technology [96]. Subsequently, many developments appear in the filtering literature to handle the problem of missing measurements in various applications. For instance, researchers detected the phenomenon in a multi-sensor system [97] and modified the traditional Kalman filter to handle it. In another study, the phenomenon was addressed in a saturated system where only one sensor propagates measurements within a sensor network [98]. A distributed filtering strategy was subsequently proposed to minimize the upper bound of the estimation error covariance matrix. Additionally, a sub-optimal filtering algorithm was developed for a jump Markov system under the influence of missing measurements [99], utilizing the Kullback-Leibler average fusion scheme. Lost observations in a cyber-physical system were discussed, leading to the development of an observer-based controller [100] specifically designed to handle missing measurements. Similarly, researchers employed the Kalman filter to estimate missing video frames (observations) in a nuclear power plant [101]. In a subsequent development, multiple Kalman filters were designed to efficiently estimate the state-of-charge for frequently missing voltage signals [102]. Overall, the problem of missing measurements has been explored extensively across different applications, resulting in a variety of problem-specific methods [103–107].

### 2.2.2 Delayed Measurements

Delay in measurements is another wide-spread irregularity in NSC/WSN. Under this irregularity, the latest received measurement may belong to any of the previous time instants, depending on the maximum possible delay extent. In other terms, the measurement possibly contains the information about the past states, while the required information is about the current state. Thus, this misleading information severely affects the estimation accuracy. A WSN inherently involves a degree of time-lag between the acquisition of a measurement (at sensor node) and its arrival at the estimator. This delay, in general, is accumulation of individual delays at

various stages of the WSN: nodal processing, queuing, transmission, and propagation delays [108–110]. The system operators generally have the knowledge of these delays.

In addition to the above, there are other factors that introduce delay in measurements: bandwidth limitations, highly noisy communication channels, packet drop, and network topology [111, 112]. In numerous instances, the delay is identifiable, and a straightforward solution involves adjusting the timing. However, especially when lacking timestamps and clock access, the delay remains uncertain; this variable and time-dependent delay is commonly referred to as random delay, which is specifically addressed in this thesis.

Filtering with delayed measurement started getting attention in the last quarter of the twentieth century [113, 114] and heightened in the starting of the twenty-first century [115–117]. The Kalman filter-based methods were particularly proposed to handle the delay in linear systems [118–120]. Importantly, the EKF and UKF for one-step delayed measurements are extended in [121], which serves as the primary starting point for the nonlinear Gaussian filtering with delayed measurements. Subsequently, the UKF was modified for two-delay [122]. For the CKF and GHF, the same methodology is further expanded in [123] and [124], respectively. A delay of up to one sample interval is referred to as one-step delayed measurement in this context. Later on, Singh *et al.* [125] improved upon the Gaussian filtering technique to handle arbitrary delays. However, this approach requires the prior knowledge of a great deal of delay probabilities, the majority of which are unknown or arbitrarily assigned. In a different method, rather than ambiguously allocating the delay probabilities, Esmzad *et al.* [126] adopted a likelihood-based technique, followed by many Gaussian filter-based approaches to deal with estimation problem with delayed measurements [127–130].

The author now provides a context on another important measurement irregularity, *i.e.*, non-Gaussian noise, although it is beyond the scope of this thesis. The non-Gaussian measurement noise frequently appears in many practical systems [131, 132]. The traditional Gaussian filters are incapable of handling non-Gaussianity as these are designed under the minimum mean square error (MMSE) criterion. For such systems, [133] proposed maximum correntropy Kalman filter (MCKF) based maximum correntropy criterion, which was applied in fusion posi-



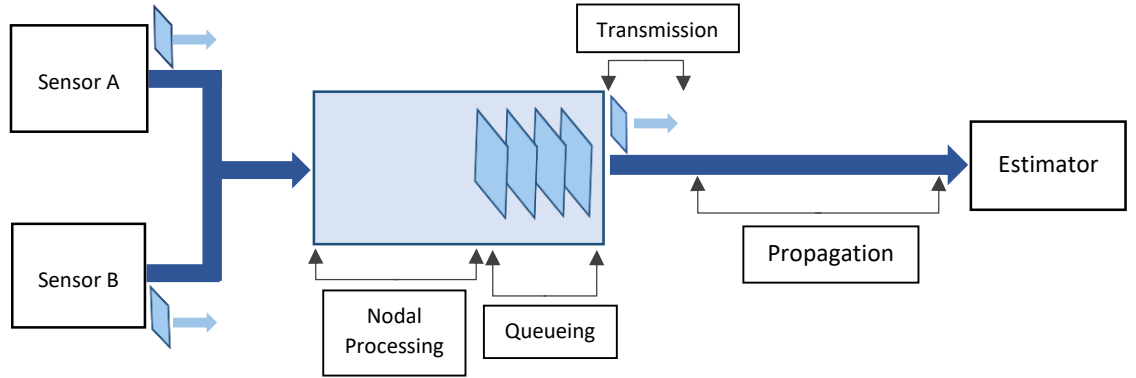


Figure 2.1: Different types of delays inherently existing in a wireless sensor networks.

tioning [134] and navigation [135]. Similarly, Reference [136] employed the minimum error entropy criterion and developed a minimum error entropy Kalman filter (MEEKF). The MEEKF handles non-Gaussianity more efficiently than the MCKF and finds applications in many problems, including cyber-attacks [137] and state-of-charge estimation [138]. In other developments, [139] and [140] tackle non-Gaussianity by representing the state PDFs as a finite sum of weighted Gaussian distribution, and propagating the uncertainty through nonlinear dynamics. The weights of these PDFs are updated by solving the convex optimization problem to satisfy the Chapman-Kolmogorov equation.

Based on the above discussion, the author now highlights the research gap in the filtering literature and resulting objectives of the thesis as follows

- To ensure optimal filtering performance, Gaussian filters depend on having complete measurements. However, in practical scenarios, it is common for one or more measurement elements to be unavailable. Previous advancements in this area primarily focused on specific filters, which limits their ability to tackle a broader range of issues. This motivated to introduce a generalized Gaussian filtering approach designed to address cases involving partially missing measurements.
- Earlier methods were primarily designed to address only one issue at a time *i.e.*, either delayed measurements or missing measurements. However, in practical scenarios, both challenges can arise simultaneously. This prompted the

development of an improved Gaussian filter capable of addressing delayed and missing measurements simultaneously.

- Existing approaches for managing delays often require knowledge of specific delay probabilities, which are rarely available in practical systems. Furthermore, these methods tend to arbitrarily assign an upper limit to the delay. This inspired to propose an advanced Gaussian filter that both reduces the dependency on delay probabilities and accurately defines the maximum possible delay in measurements.
- The existing Gaussian filters are suboptimal, as their accuracy is significantly influenced by the precision of the underlying numerical approximation methods. This thesis is therefore motivated to develop an advanced Gaussian filtering algorithm that enhances filtering accuracy through the adoption of a more precise numerical approximation technique.”

## 2.3 Summary

The following discussion highlights the summary of this chapter.

- The optimality is satisfied only for the linear system with additive Gaussian noise by the Kalman filter. In contrast, the nonlinear transformation of the PDF in the nonlinear Gaussian filters makes them sub-optimal, with the scope of accuracy improvement often involving increased computational burden.
- The employment of NCS/WSN in practical applications often introduces the phenomena of the delayed and missing measurements. The conventional Gaussian filters ignore the possibilities of these irregularities and degrade in their presence.
- The existing methods are mostly developed for particular system dynamics; the problem-specific nature precludes their applicability for other systems.
- The developments handling either delayed or missing measurements at a time are available in abundance. However, the simultaneous presence of these irregularities is also possible in practice.





## Chapter 3

# Kalman-Based Multiple Sinusoids Identification from Intermittently Missing Measurements of the Superimposed Signal

### 3.1 Introduction

The missing measurements phenomenon is a widespread measurement irregularity in wireless sensor networks (WSNs). In the previous chapters, the author presented a detailed discussion on the occurrence of this irregularity and the various causes triggering it. This chapter addresses the missing measurement phenomenon in the context of the sinusoidal identification problem, which can possibly arise in many practical applications.

Importance of sinusoids is well understood to practitioners working in almost every domain of science and technology. In many applications [141–146], a signal superimposed of several sinusoids is reported instead of a single sinusoid. Distorted signals and harmonically superimposed signals appearing in power systems [143, 144], communication systems [147], and sensor signals [148] are some notable practical examples. Analysis of distorted signals is crucial for fault detection [149] and performance monitoring of communication channels [150]. Similarly, harmonic analysis is important for power quality measurements [151], while the sensor signals are critical for

many of the electronics devices [152–154]. In most of these applications [144–146], the information is mostly available for the superimposed signal only. However, the knowledge of individual sinusoids is required for many applications, which illustrates the importance of identifying each sinusoid. Note that a sinusoid is fundamentally characterized by amplitude and frequency. Subsequently, the sinusoid identification problem reduces to amplitude and frequency estimation problem.

Earlier methods of amplitude and frequency estimation are based on maximum likelihood [155, 156] and Fourier analysis [157–160], which are computationally demanding and less accurate [161]. Some of the modified techniques [161–163] are suitable for offline estimation only. In the recent decades, the amplitude and frequency estimation is tackled as stochastic estimation problem, or more broadly, a stochastic filtering (recursive process of estimation) problem [143, 144]. The Kalman filter [1], involving time update and measurement update, is a popular stochastic filter, which is applicable to linear systems only. However, the superimposed signal (composed of multiple sinusoids) is inherently nonlinear with respect to the amplitude and frequency. Moreover, our problem essentially requires fast computation as the sampling interval is small to appropriately characterize the high-frequency sinusoids. For such a problem, the EKF [10] receives comparatively more attention due to simple and fast implementation.

As discussed earlier, the problem of individual sinusoids identification from the missing measurements of the superimposed signals is likely to be encountered in many real-life problems. The nature of considered problem demands the developed method to fulfill two criteria: i) it should be fast enough to tackle the presence of high frequencies in the measurement and ii) it should consider the non-linearity of the system. In our investigation, we found out the EKF to be a suitable candidate among the existing filters. Motivated by this, in this chapter, we redesign the traditional EKF to address the problem of frequency and amplitude estimation from intermittently missing measurements. In this regard, we reformulate the measurement model, based on Bernoulli random variables, to incorporate the possibility of missing measurements. Subsequently, we re-derive the traditional EKF for the modified measurement model. It is worth mentioning that the time update step (of estimation and filtering) [1] has no coherent relation with measurements (model).

Thus, this step remains unchanged even when the measurements are missing. The measurement update step [1], however, requires the estimate and error covariance of measurement and the state-measurement cross-covariance; we re-derive these expressions for the modified measurement model. Furthermore, we derive a Kalman gain expression to minimize the trace of the error covariance matrix for missing measurements. We also derive the resulting expression of the posterior error covariance. The simulation results reveal an improved performance of the modified EKF compared with the conventional Gaussian filters in identifying the multiple sinusoids from the intermittently missing measurements of the superimposed signal.

The main contributions of the chapter are as provided below.

- The chapter considers a widely appearing problem of individual sinusoids identification from intermittently missing measurements of the superimposed signal. The chapter attempts to solve this problem using nonlinear Kalman filtering technique (particularly, EKF-based). While this problem has been discussed in literature, the existing methodology fail under the environment of missing measurements.
- The chapter proposes a modified measurement model that can incorporate the possibility of missing measurements.
- The chapter introduces a new extension of EKF to handle the missing measurements. This extended version of EKF is then used for addressing the problem of individual sinusoids identification from intermittently missing measurements of the superimposed signal.
- The improved performance of the proposed extension of EKF for sinusoids identification is tested and compared with multiple ordinary Gaussian filters, including the EKF, UKF, CKF, and CQKF, as well as with recent extensions of Gaussian filters to handle missing measurements.

## 3.2 Problem Formulation

Consider Fig. 3.1 where multiple unknown sinusoids form a superimposed signal. A noisy measurement of the superimposed signal, denoted as  $\mathbf{z}_k$  ( $k \in \{1, 2, \dots, T_s\}$ )

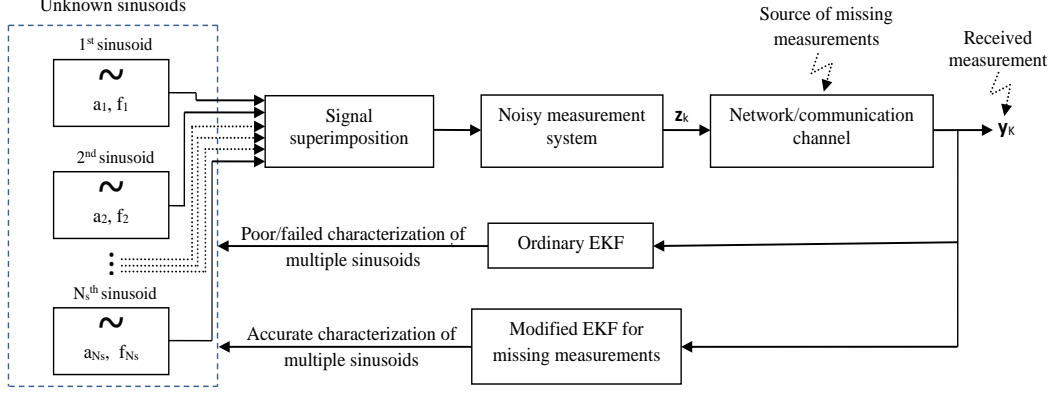


Figure 3.1: Block diagram of multiple sinusoids identification problem from intermittently missing measurements of superimposed signal. The block diagram is presented for network/communication channel as the cause for missing measurements.

at  $k^{th}$  sampling instant, is observed by the measurement system.  $\mathbf{z}_k$  is propagated through a network before it is available for estimation. During the propagation, some elements of  $\mathbf{z}_k$  are intermittently lost due to network fault, and a resulting measurement,  $\mathbf{y}_k$ , is received. Our objective is to identify the unknown sinusoids from the intermittently missing measurements of the superimposed signal, *i.e.*,  $\mathbf{y}_k$ . Alternatively, we aim to estimate the characterizing parameters, such as the amplitude and frequency, of each of the unknown sinusoids from  $\mathbf{y}_k$ . We choose the popularly known EKF for this purpose. However, the traditionally designed EKF is found to be inaccurate for missing measurements.

From the above discussion, our major goals are as follows:

- Redesign the traditional EKF for intermittently missing measurements.
- Apply the modified EKF to estimate the amplitude and frequency of each of the unknown sinusoids from  $\mathbf{y}_k$ .

Let us consider that the superimposed signal  $z(t)$  is composed of  $N_s$  sinusoids. Then, we can model  $z(t)$  as

$$z(t) = \sum_{j=1}^{N_s} a_j [\cos(2\pi f_j t) + i \sin(2\pi f_j t)], \quad (3.1)$$

where  $a_j$  and  $f_j$  ( $j \in \{1, 2, \dots, N_s\}$ ) are the amplitude and frequency, respectively, of the  $j^{th}$  sinusoid. As  $a_j$  and  $f_j$  are our desired quantities, we formulate the state



variable as  $\mathbf{x} = [f_1, f_2, \dots, f_{N_s}, a_1, a_2, \dots, a_{N_s}]^T$ . The amplitude and frequency do not change with time ideally. However, there may be slight variations in practical scenarios. Therefore, we model the state dynamics with an additive noise to incorporate such variations, *i.e.*,

$$\mathbf{x}_k = \mathbf{I}\mathbf{x}_{k-1} + \boldsymbol{\eta}_k. \quad (3.2)$$

where  $k \in \{1, 2, \dots, T_s\}$  denotes a sampling instant,  $\mathbf{I}$  is an identity matrix and  $\boldsymbol{\eta}_k \sim \mathcal{N}(0, \mathbf{Q}_k)$  is the process noise, with  $\mathcal{N}(\cdot, \cdot)$  is standard representation of Gaussian distribution.

Please note that Eq. (3.1) represents the continuous complex form of the superimposed sinusoids (measurements), which is complex power measured at different nodes in power systems. The phasor measurement unit captures the time-synchronized voltage and current phasor measurements and then calculates power components *i.e.*, active and reactive powers, based on these values. In filtering, however, it required to process the discrete measurement values. Alternatively, the power meters, *i.e.*, wattmeter and varmeter provide the samples (discrete values) of the real part (active power) and imaginary part (reactive power), respectively of the complex power for filtering. Thus, the discrete measurement  $\mathbf{z}_k$  is obtained by taking discrete-time samples of the real and imaginary parts individually of  $z(t)$  calculated at the time-instants  $kT$  ( $z_k = z(t)|_{t=kT}$ ), where  $k$  and  $T$  denote the time-instant and sampling interval, respectively. It is important that the selection of the sampling interval is based on the Nyquist criterion to avoid the aliasing effect. In practice, impacted by several factors such as instrumentation error, environmental conditions, and electromagnetic inference, the sensors give erroneous measurement (noisy measurement). The noisy measurement of  $z(t)$  at  $t_k$ , *i.e.*,  $\mathbf{z}_k$ , is modeled as

$$\mathbf{z}_k = \begin{bmatrix} \sum_{j=1}^{N_s} a_{j,k} \cos(2\pi f_{j,k}(k)T) \\ \sum_{j=1}^{N_s} a_{j,k} \sin(2\pi f_{j,k}(k)T) \end{bmatrix} + \boldsymbol{\nu}_k. \quad (3.3)$$

Furthermore, we model the intermittently missing measurement  $\mathbf{y}_k$  as

$$\mathbf{y}_k = \boldsymbol{\beta}_k \mathbf{z}_k = \boldsymbol{\beta}_k \left\{ \begin{bmatrix} \sum_{j=1}^{N_s} a_{j,k} \cos(2\pi f_{j,k}(k)T) \\ \sum_{j=1}^{N_s} a_{j,k} \sin(2\pi f_{j,k}(k)T) \end{bmatrix} + \boldsymbol{\nu}_k \right\}, \quad (3.4)$$

where  $\beta_k = \text{diag}([\alpha_k^1, \alpha_k^2, \dots, \alpha_k^q])$ , with  $\alpha_k^i (i \in \{1, 2, \dots, q\})$  being  $q$  Bernoulli random variables with a known probability  $\mathcal{P}(\alpha_k^i = 1) = \mathbb{E}[\alpha_k^i] = \rho_k^i$ .  $\alpha_k^i$  is independent in  $k$  as well as  $i$ .  $q$  is the number of measurement elements, which is equal to two in our case, and  $\mathbb{E}[\cdot]$  denotes the expectation and  $\mathcal{P}(\cdot)$  denotes the probability operator. Note that  $\beta_k$  is diagonal, *i.e.*,  $\beta_k = \beta_k^T$ . We will frequently use the notation  $\beta_k^2$  to denote  $\beta_k \beta_k^T$ , and similarly,  $\rho^2$  and  $(\beta_k - \rho)^2$ .

Following this, our simplified problem is to estimate  $\mathbf{x}_k$  from the intermittently missing measurements  $\mathbf{y}_k$  (Eq. (3.4)). The EKF, that we choose for this purpose, is designed for non-missing measurements (Eq. (3.3)). Thus, another problem is posed hereby as to modify the EKF for missing measurements.

### 3.3 Modified EKF for Missing Measurements and Sinusoids Identification

This section derives the modified EKF for handling the missing measurements. Subsequently, it applies the modified EKF for identifying the unknown sinusoids from intermittently missing measurements of the superimposed signal.

The derivation of the modified EKF is based on the modified measurement model (3.4), with no change in the state dynamics. As the measurement model is changed, the filter parameters corresponding to measurement, such as the measurement estimate, measurement error covariance, and state-measurement cross-covariance, need to be re-derived.

Before proceeding further, we represent Eqs. (3.2) and (3.3) in terms of standard state space model [10, 11], given as

$$\mathbf{x}_k = f(\mathbf{x}_{k-1}) + \boldsymbol{\eta}_k. \quad (3.5)$$

$$\mathbf{z}_k = h(\mathbf{x}_k) + \boldsymbol{\nu}_k. \quad (3.6)$$

Please refer to Chapter 1 for a detailed discussion on the relevant notations.

### 3.3.1 Modified EKF for Missing Measurements

The modified EKF involves two steps, time update and measurement update, which are discussed in the sequel.

#### Time update

This step computes the prior estimate and covariance, *i.e.*,  $\hat{\mathbf{x}}_{k|k-1}$  and  $\mathbf{P}_{k|k-1}$ , similar to the traditional EKF [1, 10]. Thus, we get

$$\begin{cases} \hat{\mathbf{x}}_{k|k-1} = f(\hat{\mathbf{x}}_{k-1|k-1}) \\ \mathbf{P}_{k|k-1} = \mathbf{F}_{k-1} \mathbf{P}_{k-1|k-1} \mathbf{F}_{k-1}^T + \mathbf{Q}_k, \end{cases} \quad (3.7)$$

where  $\mathbf{F}_{k-1} = \partial f(\mathbf{x}_{k-1}) / \partial \mathbf{x}_{k-1} |_{\mathbf{x}_{k-1} = \hat{\mathbf{x}}_{k-1|k-1}}$  represents the Jacobian matrix, while  $\hat{\mathbf{x}}_{k-1|k-1}$  and  $\mathbf{P}_{k-1|k-1}$  are posterior estimate and error covariance, respectively, at  $(k-1)^{th}$  instant.

#### Measurement update

This step computes the posterior update parameters,  $\hat{\mathbf{x}}_{k|k}$  and  $\mathbf{P}_{k|k}$ , which are based on a Kalman gain,  $\mathbf{K}$ , to minimize the trace of the error covariance  $\mathbf{P}_{k|k}$ . The computation of these quantities requires measurement estimate,  $\hat{\mathbf{y}}_{k|k-1}$ , measurement covariance,  $\mathbf{P}_{k|k-1}^{\mathbf{y}\mathbf{y}}$ , and state-measurement cross-covariance,  $\mathbf{P}_{k|k-1}^{\mathbf{x}\mathbf{y}}$ . In this section, we initially derive  $\hat{\mathbf{y}}_{k|k-1}$ ,  $\mathbf{P}_{k|k-1}^{\mathbf{y}\mathbf{y}}$ , and  $\mathbf{P}_{k|k-1}^{\mathbf{x}\mathbf{y}}$  for missing measurements, *i.e.*, with respect to Eq. (3.4). Then, we derive  $\mathbf{P}_{k|k}$  and  $\mathbf{K}$  (for missing measurements) so that the traditionally used relation [1, 10]

$$\hat{\mathbf{x}}_{k|k} = \hat{\mathbf{x}}_{k|k-1} + \mathbf{K}(\mathbf{y}_k - \hat{\mathbf{y}}_{k|k-1}) \quad (3.8)$$

gives an estimate of  $\mathbf{x}_k$  to minimize the square error.

We derive  $\hat{\mathbf{y}}_{k|k-1}$ ,  $\mathbf{P}_{k|k-1}^{\mathbf{y}\mathbf{y}}$ , and  $\mathbf{P}_{k|k-1}^{\mathbf{x}\mathbf{y}}$  for missing measurement  $\mathbf{y}_k$  (Eq. (3.4)) through the subsequent theorems.

**Theorem 3.1.** Measurement estimate for Eq. (3.4) is

$$\hat{\mathbf{y}}_{k|k-1} = \boldsymbol{\rho}_k h(\hat{\mathbf{x}}_{k|k-1}). \quad (3.9)$$

*Proof.* The measurement estimate is  $\hat{\mathbf{y}}_{k|k-1} = \mathbb{E}[\mathbf{y}_k] = \mathbb{E}[\boldsymbol{\beta}_k(h(\mathbf{x}_k) + \boldsymbol{\nu}_k)]$ . Here,  $\boldsymbol{\beta}_k$  represents the missing measurements status and is independent of  $\boldsymbol{\nu}_k$  and  $h(\mathbf{x}_k)$ . Thus,

$$\hat{\mathbf{y}}_{k|k-1} = \mathbb{E}[\boldsymbol{\beta}_k] \mathbb{E}[h(\mathbf{x}_k) + \boldsymbol{\nu}_k]. \quad (3.10)$$

The first-order Taylor series expansion of  $h(\mathbf{x}_k)$  around  $\hat{\mathbf{x}}_{k|k-1}$  gives

$$h(\mathbf{x}_k) = h(\hat{\mathbf{x}}_{k|k-1}) + \mathbf{H}_k \mathbf{e}_{k|k-1}, \quad (3.11)$$

where  $\mathbf{H}_k = \partial h(\mathbf{x}_k) / \partial \mathbf{x}_k|_{\mathbf{x}_k = \hat{\mathbf{x}}_{k|k-1}}$  is Jacobian matrix and  $\mathbf{e}_{k|k-1} = \mathbf{x}_k - \hat{\mathbf{x}}_{k|k-1}$ . Furthermore,  $\mathbb{E}[\boldsymbol{\beta}_k] = \boldsymbol{\rho}_k$ ,  $\mathbb{E}[\boldsymbol{\nu}_k] = 0$ , and  $\mathbb{E}[h(\mathbf{x}_k)] = h(\hat{\mathbf{x}}_{k|k-1})$  (as  $\mathbb{E}[\mathbf{e}_{k|k-1}] = 0$  in Eq. (3.11)). Subsequently, Eq. (3.10) simplifies to Eq. (3.9).  $\square$

**Theorem 3.2.** Measurement error covariance for Eq. (3.4) can be given as

$$\mathbf{P}_{k|k-1}^{\mathbf{y}\mathbf{y}} = \boldsymbol{\rho}_k \mathbf{H}_k \mathbf{P}_{k|k-1} \mathbf{H}_k^T + \boldsymbol{\rho}_k \mathbf{R}_k + (\boldsymbol{\rho}_k - \boldsymbol{\rho}_k^2) h(\hat{\mathbf{x}}_{k|k-1}) h(\hat{\mathbf{x}}_{k|k-1})^T. \quad (3.12)$$

*Proof.* The measurement error covariance is given as

$$\mathbf{P}_{k|k-1}^{\mathbf{y}\mathbf{y}} = \mathbb{E}[(\mathbf{y}_k - \hat{\mathbf{y}}_{k|k-1})(\mathbf{y}_k - \hat{\mathbf{y}}_{k|k-1})^T]. \quad (3.13)$$

For  $\mathbf{y}_k$  and  $\hat{\mathbf{y}}_{k|k-1}$  given in Eqs. (3.4) and (3.9), respectively, we get

$$\mathbf{y}_k - \hat{\mathbf{y}}_{k|k-1} = \boldsymbol{\beta}_k(h(\mathbf{x}_k) - h(\hat{\mathbf{x}}_{k|k-1})) + \boldsymbol{\beta}_k \boldsymbol{\nu}_k + (\boldsymbol{\beta}_k - \boldsymbol{\rho}_k) h(\hat{\mathbf{x}}_{k|k-1}).$$

Substituting  $h(\mathbf{x}_k) - h(\hat{\mathbf{x}}_{k|k-1})$  from Eq. (3.11), we obtain

$$\mathbf{y}_k - \hat{\mathbf{y}}_{k|k-1} = \underbrace{\boldsymbol{\beta}_k (\mathbf{H}_k \mathbf{e}_{k|k-1} + \boldsymbol{\nu}_k)}_{\mathbf{S}_1} + \underbrace{(\boldsymbol{\beta}_k - \boldsymbol{\rho}_k) h(\hat{\mathbf{x}}_{k|k-1})}_{\mathbf{S}_2}. \quad (3.14)$$

Substituting  $\mathbf{y}_k - \hat{\mathbf{y}}_{k|k-1}$  into Eq. (3.13), we can write

$$\mathbf{P}_{k|k-1}^{\mathbf{y}\mathbf{y}} = \sum_{i=1}^2 \sum_{j=1}^2 \mathbb{E}[\mathbf{S}_i \mathbf{S}_j^T]. \quad (3.15)$$

We now compute  $\mathbb{E}[\mathbf{S}_i \mathbf{S}_j^T] \forall (i, j) \in \{1, 2\}$ . In this regard, for  $\mathbf{S}_1$  given in Eq.

(3.14), we get

$$\begin{aligned} \mathbb{E}[\mathbf{S}_1 \mathbf{S}_1^T] = & \mathbb{E}[\beta_k^2] \left( \mathbf{H}_k \mathbb{E}[\mathbf{e}_{k|k-1} \mathbf{e}_{k|k-1}^T] \mathbf{H}_k^T + \mathbb{E}[\boldsymbol{\nu}_k \boldsymbol{\nu}_k^T] + \mathbf{H}_k \mathbb{E}[\mathbf{e}_{k|k-1}] \mathbb{E}[\boldsymbol{\nu}_k^T] \right. \\ & \left. + \mathbb{E}[\boldsymbol{\nu}_k] \mathbb{E}[\mathbf{e}_{k|k-1}^T] \mathbf{H}_k^T \right). \end{aligned}$$

Please note that  $\mathbb{E}[\beta_k^2] = \mathbb{E}[\beta_k] = \boldsymbol{\rho}_k$ ,  $\mathbb{E}[\mathbf{e}_{k|k-1} \mathbf{e}_{k|k-1}^T] = \mathbf{P}_{k|k-1}$ ,  $\mathbb{E}[\boldsymbol{\nu}_k] = 0$ , and  $\mathbb{E}[\boldsymbol{\nu}_k \boldsymbol{\nu}_k^T] = \mathbf{R}_k$ . Hence, we obtain

$$\mathbb{E}[\mathbf{S}_1 \mathbf{S}_1^T] = \boldsymbol{\rho}_k (\mathbf{H}_k \mathbf{P}_{k|k-1} \mathbf{H}_k^T + \mathbf{R}_k). \quad (3.16)$$

Similarly, for  $\mathbf{S}_1$  and  $\mathbf{S}_2$  given in Eq. (3.14), we can write

$$\mathbb{E}[\mathbf{S}_1 \mathbf{S}_2^T] = \mathbb{E}[\beta_k] (\mathbf{H}_k \mathbb{E}[\mathbf{e}_{k|k-1}] + \mathbb{E}[\boldsymbol{\nu}_k]) h(\hat{\mathbf{x}}_{k|k-1})^T \mathbb{E}[(\beta_k - \boldsymbol{\rho}_k)].$$

Substituting  $\mathbb{E}[\mathbf{e}_{k|k-1}] = 0$  and  $\mathbb{E}[\boldsymbol{\nu}_k] = 0$ , we get  $\mathbb{E}[\mathbf{S}_1 \mathbf{S}_2^T] = 0$ . Moreover, applying the joint estimation property, we obtain

$$\mathbb{E}[\mathbf{S}_2 \mathbf{S}_1^T] = \mathbb{E}[\mathbf{S}_1 \mathbf{S}_2^T] = 0. \quad (3.17)$$

Similarly, for  $\mathbf{S}_2$  given in Eq. (3.14), we obtain  $\mathbb{E}[\mathbf{S}_2 \mathbf{S}_2^T] = \mathbb{E}[(\beta_k - \boldsymbol{\rho}_k)^2] h(\hat{\mathbf{x}}_{k|k-1}) h(\hat{\mathbf{x}}_{k|k-1})^T$ . Subsequently, applying binomial expansion of  $(\beta_k - \boldsymbol{\rho}_k)^2$  and substituting  $\mathbb{E}[\beta_k^2] = \mathbb{E}[\beta_k] = \boldsymbol{\rho}_k$ , we get

$$\mathbb{E}[\mathbf{S}_2 \mathbf{S}_2^T] = (\boldsymbol{\rho}_k - \boldsymbol{\rho}_k^2) h(\hat{\mathbf{x}}_{k|k-1}) h(\hat{\mathbf{x}}_{k|k-1})^T. \quad (3.18)$$

Substituting  $\mathbb{E}[\mathbf{S}_i \mathbf{S}_j^T] \forall (i, j) \in \{1, 2\}$  (in sequence) from Eqs. (3.16), (3.17), and (3.18) into Eq. (3.15), we obtain Eq. (5.7).  $\square$

**Theorem 3.3.** The cross-covariance between the state  $\mathbf{x}_k$  and the modified measurement  $\mathbf{y}_k$  can be obtained as

$$\mathbf{P}_{k|k-1}^{\mathbf{xy}} = \mathbf{P}_{k|k-1} \mathbf{H}_k^T \boldsymbol{\rho}_k. \quad (3.19)$$

*Proof.* Please note that  $\mathbf{P}_{k|k-1}^{\mathbf{xy}} = \mathbb{E}[(\mathbf{x}_k - \hat{\mathbf{x}}_{k|k-1})(\mathbf{y}_k - \hat{\mathbf{y}}_{k|k-1})^T]$ . Substituting  $\mathbf{x}_k - \hat{\mathbf{x}}_{k|k-1} = \mathbf{e}_{k|k-1}$  and  $\mathbf{y}_k - \hat{\mathbf{y}}_{k|k-1}$  from Eq. (3.14), and simplifying further, we get

$$\begin{aligned} \mathbf{P}_{k|k-1}^{\mathbf{xy}} = & \mathbb{E}[(\mathbf{e}_{k|k-1})(\boldsymbol{\beta}_k \mathbf{H}_k \mathbf{e}_{k|k-1})^T] + \mathbb{E}[(\mathbf{e}_{k|k-1})(\boldsymbol{\beta}_k \boldsymbol{\nu}_k)^T] \\ & + \mathbb{E}[(\mathbf{e}_{k|k-1})((\boldsymbol{\beta}_k - \boldsymbol{\rho}_k)h(\hat{\mathbf{x}}_{k|k-1}))^T]. \end{aligned}$$

As  $\mathbb{E}[\mathbf{e}_{k|k-1}] = 0$ , the last two terms are zero. Subsequently, the independency of  $\boldsymbol{\beta}_k$  and  $\mathbf{e}_{k|k-1}$  gives

$$\mathbf{P}_{k|k-1}^{\mathbf{xy}} = \mathbb{E}[(\mathbf{e}_{k|k-1})(\mathbf{e}_{k|k-1})^T] \mathbf{H}_k^T \mathbb{E}[\boldsymbol{\beta}_k^T].$$

Substituting  $\mathbb{E}[(\mathbf{e}_{k|k-1})(\mathbf{e}_{k|k-1})^T] = \mathbf{P}_{k|k-1}$  and  $\mathbb{E}[\boldsymbol{\beta}_k^T] = \boldsymbol{\rho}_k$ ,  $\mathbf{P}_{k|k-1}^{\mathbf{xy}}$  is obtained in the form of Eq. (5.14).  $\square$

We now compute  $\mathbf{K}$  and  $\mathbf{P}_{k|k}$  for the modified measurement model (3.4). It should be mentioned that  $\mathbf{K}$  must minimize the trace of  $\mathbf{P}_{k|k}$  [1, 10].

**Theorem 3.4.**  $\mathbf{P}_{k|k}$  and  $\mathbf{K}$  for the modified measurement model, Eq. (3.4), can be given as

$$\mathbf{P}_{k|k} = (\mathbf{I} - \mathbf{K} \boldsymbol{\rho}_k \mathbf{H}_k) \mathbf{P}_{k|k-1}, \quad (3.20)$$

$$\mathbf{K} = \mathbf{P}_{k|k-1}^{\mathbf{xy}} \left( \mathbf{P}_{k|k-1}^{\mathbf{yy}} \right)^{-1}. \quad (3.21)$$

*Proof.* Please note that  $\mathbf{e}_{k|k} = \mathbf{x}_k - \hat{\mathbf{x}}_{k|k}$ . Substituting  $\hat{\mathbf{x}}_{k|k}$  from Eq. (3.8), we get

$$\mathbf{e}_{k|k} = \mathbf{x}_k - \hat{\mathbf{x}}_{k|k-1} - \mathbf{K}(\mathbf{y}_k - \hat{\mathbf{y}}_{k|k-1}). \quad (3.22)$$

Using Eq. (3.14), we get

$$\mathbf{e}_{k|k} = \underbrace{\mathbf{e}_{k|k-1} - \mathbf{K} \boldsymbol{\beta}_k \mathbf{H}_k \mathbf{e}_{k|k-1}}_{\mathbf{M}_1} - \underbrace{\mathbf{K} \boldsymbol{\beta}_k \boldsymbol{\nu}_k - \mathbf{K}(\boldsymbol{\beta}_k - \boldsymbol{\rho}_k)h(\hat{\mathbf{x}}_{k|k-1})}_{\mathbf{M}_2}. \quad (3.23)$$

As  $\mathbf{P}_{k|k} = \mathbb{E}[\mathbf{e}_{k|k} \mathbf{e}_{k|k}^T]$ , we can write

$$\mathbf{P}_{k|k} = \sum_{i=1}^2 \sum_{j=1}^2 \mathbb{E}[\mathbf{M}_i \mathbf{M}_j^T]. \quad (3.24)$$

We now compute  $\mathbb{E}[\mathbf{M}_i \mathbf{M}_j^T] \forall (i, j) \in \{1, 2\}$ . In this regard, expanding  $\mathbb{E}[\mathbf{M}_1 \mathbf{M}_1^T]$

after substituting  $\mathbf{M}_1$  from Eq. (3.23), and simplifying further, we get

$$\mathbb{E}[\mathbf{M}_1 \mathbf{M}_1^T] = \mathbf{P}_{k|k-1} - \mathbf{P}_{k|k-1} \mathbf{H}_k^T \boldsymbol{\rho}_k \mathbf{K}^T - \mathbf{K} \boldsymbol{\rho}_k \mathbf{H}_k \mathbf{P}_{k|k-1} + \mathbf{K} \boldsymbol{\rho}_k \mathbf{H}_k \mathbf{P}_{k|k-1} \mathbf{H}_k^T \mathbf{K}^T. \quad (3.25)$$

Similarly, for  $\mathbf{M}_1$  and  $\mathbf{M}_2$  given in Eq. (3.23), we can write

$$\mathbb{E}[\mathbf{M}_1 \mathbf{M}_2^T] = \mathbb{E}[(\mathbf{I} - \mathbf{K} \boldsymbol{\beta}_k \mathbf{H}_k)] \mathbb{E}[\mathbf{e}_{k|k-1}] \mathbb{E} \left[ \left( -\mathbf{K} \boldsymbol{\beta}_k \boldsymbol{\nu}_k - \mathbf{K}(\boldsymbol{\beta}_k - \boldsymbol{\rho}_k) h(\hat{\mathbf{x}}_{k|k-1}) \right)^T \right].$$

Please note that  $\mathbb{E}[\mathbf{e}_{k|k-1}] = 0$ , *i.e.*,  $\mathbb{E}[\mathbf{M}_1 \mathbf{M}_2^T] = 0$ , which also concludes

$$\mathbb{E}[\mathbf{M}_2 \mathbf{M}_1^T] = \mathbb{E}[\mathbf{M}_1 \mathbf{M}_2^T] = 0. \quad (3.26)$$

Furthermore, for  $\mathbf{M}_2$  given in Eq. (3.23), expanding  $\mathbb{E}[\mathbf{M}_2 \mathbf{M}_2^T]$  and substituting  $\mathbb{E}[\boldsymbol{\nu}_k^T] = 0$ , we get

$$\mathbb{E}[\mathbf{M}_2 \mathbf{M}_2^T] = \mathbf{K} \boldsymbol{\rho}_k \mathbf{R}_k \mathbf{K}^T + \mathbf{K}(\boldsymbol{\rho}_k - \boldsymbol{\rho}_k^2) h(\hat{\mathbf{x}}_{k|k-1}) h(\hat{\mathbf{x}}_{k|k-1})^T \mathbf{K}^T. \quad (3.27)$$

Let us now substitute  $\mathbb{E}[\mathbf{M}_i \mathbf{M}_j^T] \forall (i, j) \in \{1, 2\}$  from Eqs. (3.25), (3.26), and (3.27) into Eq. (3.24). Subsequently, we get

$$\begin{aligned} \mathbf{P}_{k|k} = & \mathbf{P}_{k|k-1} - \mathbf{K} \boldsymbol{\rho}_k \mathbf{H}_k \mathbf{P}_{k|k-1} - \mathbf{P}_{k|k-1} \mathbf{H}_k^T \boldsymbol{\rho}_k \mathbf{K}^T + \mathbf{K}(\boldsymbol{\rho}_k \mathbf{H}_k \mathbf{P}_{k|k-1} \mathbf{H}_k^T \\ & + \boldsymbol{\rho}_k \mathbf{R}_k + (\boldsymbol{\rho}_k - \boldsymbol{\rho}_k^2) h(\hat{\mathbf{x}}_{k|k-1}) h(\hat{\mathbf{x}}_{k|k-1})^T) \mathbf{K}^T. \end{aligned} \quad (3.28)$$

In terms of  $\mathbf{P}_{k|k-1}^{\mathbf{y}\mathbf{y}}$  and  $\mathbf{P}_{k|k-1}^{\mathbf{x}\mathbf{y}}$  expressions, derived through Theorems 3.2 and 3.3, respectively, we can write

$$\mathbf{P}_{k|k} = \mathbf{P}_{k|k-1} - \mathbf{K}(\mathbf{P}_{k|k-1}^{\mathbf{x}\mathbf{y}})^T - \mathbf{P}_{k|k-1}^{\mathbf{x}\mathbf{y}} \mathbf{K}^T + \mathbf{K} \mathbf{P}_{k|k-1}^{\mathbf{y}\mathbf{y}} \mathbf{K}^T. \quad (3.29)$$

As discussed previously, the Kalman gain  $\mathbf{K}$  minimizes the trace of  $\mathbf{P}_{k|k}$ , *i.e.*,  $\partial \text{Tr}[\mathbf{P}_{k|k}] / \partial \mathbf{K} = 0$ . Thus,

$$\frac{\partial \text{Tr}[\mathbf{P}_{k|k-1}]}{\partial \mathbf{K}} - \frac{\partial \text{Tr}[\mathbf{K}(\mathbf{P}_{k|k-1}^{\mathbf{x}\mathbf{y}})^T]}{\partial \mathbf{K}} - \frac{\partial \text{Tr}[\mathbf{P}_{k|k-1}^{\mathbf{x}\mathbf{y}} \mathbf{K}^T]}{\partial \mathbf{K}} + \frac{\partial \text{Tr}[\mathbf{K} \mathbf{P}_{k|k-1}^{\mathbf{y}\mathbf{y}} \mathbf{K}^T]}{\partial \mathbf{K}} = 0.$$

---

**Algorithm 3.1** Pseudo code for implementing the modified EKF
 

---

**Require:**  $\mathbf{Q}_k, \mathbf{R}_k, N, \boldsymbol{\rho}, T$ .

**Ensure:**  $\hat{\mathbf{x}}_{k|k} = [\hat{f}_1, \hat{f}_2, \dots, \hat{f}_{N_s}, \hat{a}_1, \hat{a}_2, \dots, \hat{a}_{N_s}]^T$ .

```

1: Initialisation:  $k = 1, \hat{\mathbf{x}}_{0|0}, \mathbf{P}_{0|0}$ .
2: while  $k \leq N$  do
3:   Compute the prior estimate,  $\hat{\mathbf{x}}_{k|k-1}$ , using Eq. (3.7)
4:   Compute the prior covariance,  $\mathbf{P}_{k|k-1}$ , using Eq. (3.7).
5:   Compute the measurement estimate,  $\hat{\mathbf{y}}_{k|k-1}$ , using Eq. (3.9).
6:   Compute the measurement error covariance,  $\mathbf{P}_{k|k-1}^{\mathbf{y}\mathbf{y}}$ , using Eq. (5.7).
7:   Compute the cross-covariance,  $\mathbf{P}_{k|k-1}^{\mathbf{x}\mathbf{y}}$ , using Eq. (5.14).
8:   Kalman gain:  $\mathbf{K} = \mathbf{P}_{k|k-1}^{\mathbf{x}\mathbf{y}} (\mathbf{P}_{k|k-1}^{\mathbf{y}\mathbf{y}})^{-1}$ .
9:   Updated estimate:  $\hat{\mathbf{x}}_{k|k} = \hat{\mathbf{x}}_{k|k-1} + \mathbf{K} (\mathbf{y}_k - \hat{\mathbf{y}}_{k|k-1})$ .
10:  Updated covariance:  $\mathbf{P}_{k|k} = (\mathbf{I} - \mathbf{K} \boldsymbol{\rho}_k \mathbf{H}_k) \mathbf{P}_{k|k-1}$ .
11:   $k = k + 1$ .
12: end while
13: return  $\hat{\mathbf{x}}_{k|k} (\forall k \in \{1, 2, \dots, N\})$ 
    
```

---

After solving this equation, we get  $\mathbf{K}$  (that minimizes the trace of  $\mathbf{P}_{k|k}$ ) same as Eq. (3.21). Substituting this  $\mathbf{K}$  into Eq. (3.29), we get  $\mathbf{P}_{k|k}$  in the form of Eq. (3.20).  $\square$

### 3.3.2 Identification of the Sinusoids Using the Modified EKF

In Section 3.2, we have reduced the identification problem of multiple sinusoids to a frequency and amplitude estimation problem. The state space model for this estimation problem is formulated through Eqs. (3.2) and (3.4), for the case of missing measurements. We can apply the modified EKF, derived in the previous section, for general state space model (Eqs. (3.5) and (3.6)), over Eqs. (3.2) and (3.4). The resulting posterior estimate, *i.e.*,  $\hat{\mathbf{x}}_{k|k} = [\hat{f}_{1,k}, \hat{f}_{2,k}, \dots, \hat{f}_{N_s,k}, \hat{a}_{1,k}, \hat{a}_{2,k}, \dots, \hat{a}_{N_s,k}]^T$ , gives the desired estimates of amplitude and frequency at time  $t_k$ . The estimated amplitude and frequency can be used to characterize the individual sinusoids. The pseudo code for implementing the modified EKF is provided in Algorithm 3.1.

## 3.4 Simulation and Results

In this section, we implement the modified EKF for identifying multiple sinusoids from intermittently missing noisy measurements of the superimposed signal. In this regard, we consider that the measurement signal is an electrical current signal,



CHAPTER 3. KALMAN-BASED MULTIPLE SINUSOIDS  
IDENTIFICATION FROM INTERMITTENTLY MISSING  
MEASUREMENTS OF THE SUPERIMPOSED SIGNAL

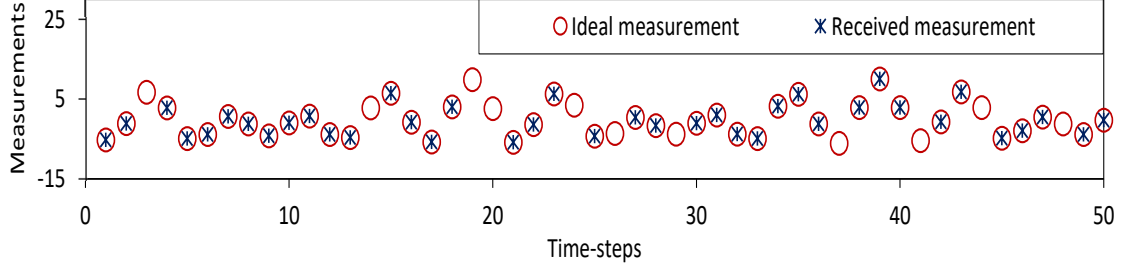


Figure 3.2: Ideal measurements and actually received measurements with intermittent missing measurements possibility for the real part of the superimposed signal.

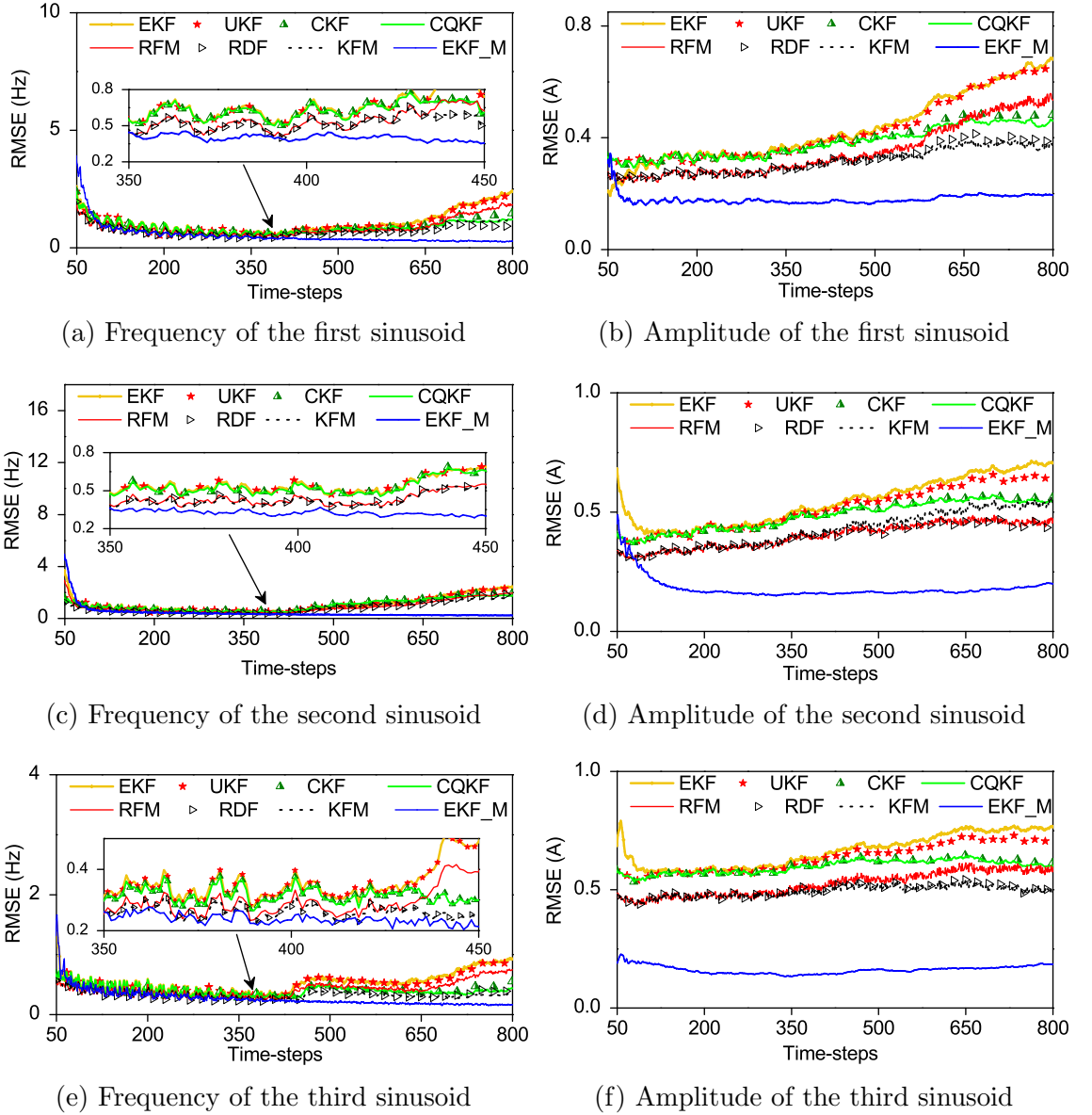


Figure 3.3: RMSE plots of the proposed EKF\_M and the competitive filters for missing measurements probability of 0.1 ( $\rho = 0.9$ ).

formed by the superposition of three different current signals. Throughout this section, we abbreviate the modified EKF as EKF\_M. The performance of the EKF\_M is

compared with ordinary Gaussian filters, i.e, EKF, UKF, CKF, and CQKF as well as with recent developments to handle missing measurements in different systems [97, 102, 106]. We abbreviate the methods in [97] as RDF, [102] as RFM, and [106] as KFM in this section. Our performance analysis will be restricted for missing measurements probability up to 0.6 ( $0.4 \leq \rho \leq 0.98$ ). Alternatively, we will consider that not more than 60% of the measurements are missing. The performance analysis is based on root mean square error (RMSE), which is broadly accepted in the literature [164].

### 3.4.1 True Data Simulation

We simulate the true data of frequency and amplitude of the three sinusoids using Eq. (3.2), which is represented by Eq. (3.5) in a generalized form. In this regard, we initialize the state (consisting of the frequencies and amplitudes) as  $\mathbf{x}_0 = [200 \ 800 \ 1000 \ 2 \ 3 \ 5]^T$  and use the process noise covariance as  $\mathbf{Q} = \text{diag}([\tau_f^2 \ \tau_f^2 \ \tau_f^2 \ \tau_a^2 \ \tau_a^2 \ \tau_a^2])$ , where  $\tau_f = 0.1$  and  $\tau_a = 0.0125$ . Similarly, the true measurement data is generated by propagating the true states through Eq. (3.3), which is represented by Eq. (3.6) in a generalized form. We assign the measurement noise covariance as  $\mathbf{R} = \text{diag}([0.09 \ 0.09])$  and consider different values for missing measurement probability ( $\rho_m = 1 - \rho$ ) for the analysis. Samples of the ideal measurement (expected to be received if no measurement is missing) and the corresponding missing measurements (with intermittent measurements missing) are shown in Fig. 3.2 over 50 time-steps, considering  $\rho = 0.8$  (missing measurements probability 0.2). For the filtering and analysis purpose, the true states and measurements are generated over 800 time-steps, considering a sampling interval of 0.25 *ms*.

### 3.4.2 RMSE Analysis of the EKF\_M and Competitive Filters

For the filtering purpose, the initial estimate and covariance of the state are taken as  $\hat{\mathbf{x}}_{0|0} = [205 \ 785 \ 990 \ 4 \ 2 \ 3]^T$  and  $\mathbf{P}_{0|0} = \text{diag}([25 \ 40 \ 20 \ 4 \ 1 \ 4])$ , respectively. We compute the RMSE at each time-step by implementing 500 Monte-Carlo runs. The RMSE plots of the EKF\_M and the ordinary Gaussian filters, such as the EKF, UKF,

CHAPTER 3. KALMAN-BASED MULTIPLE SINUSOIDS  
IDENTIFICATION FROM INTERMITTENTLY MISSING  
MEASUREMENTS OF THE SUPERIMPOSED SIGNAL

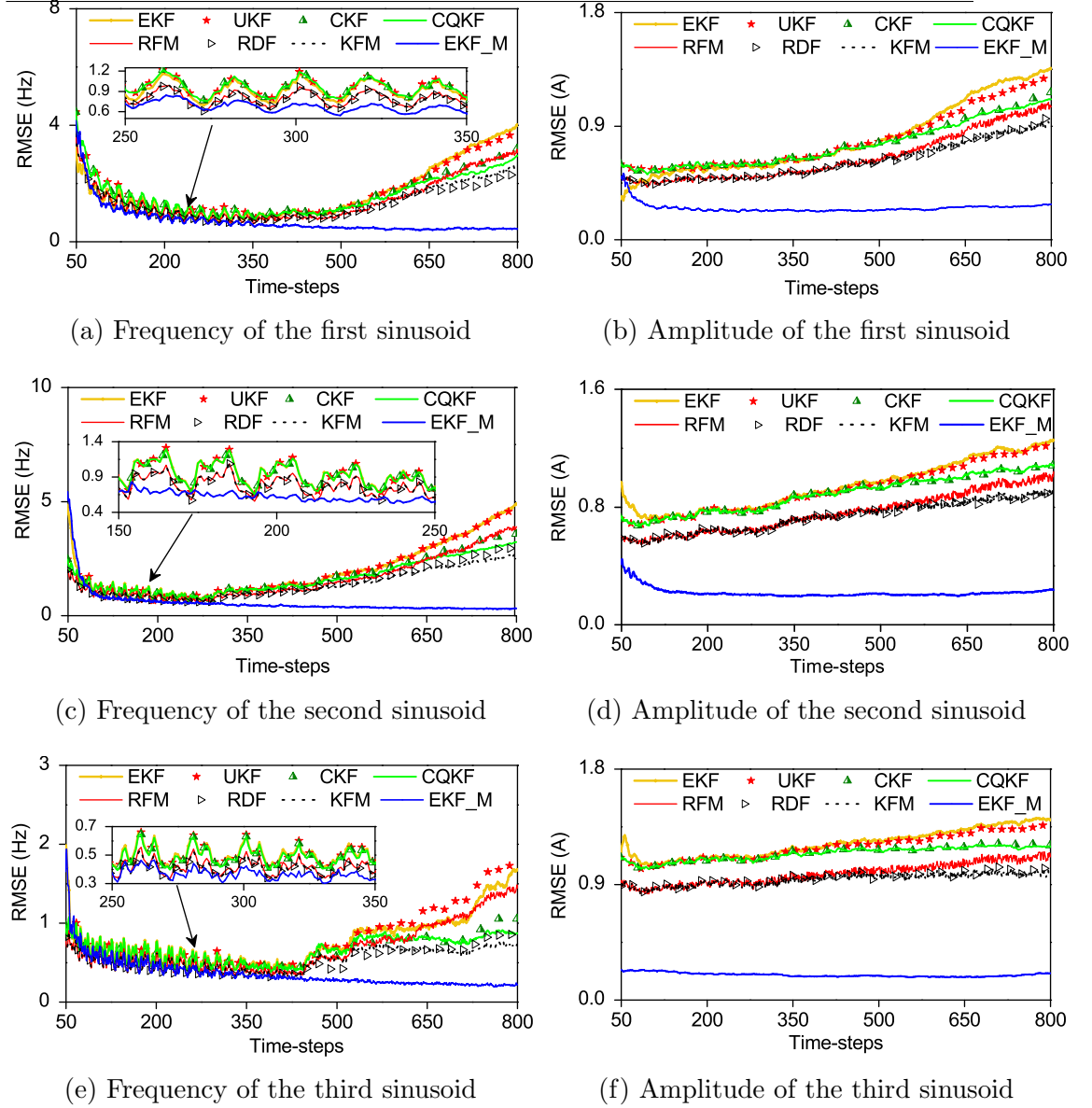


Figure 3.4: RMSE plots of the proposed EKF\_M and the competitive filters for missing measurements probability of 0.2 ( $\rho = 0.8$ ).

CKF, and CQKF are shown in Figs. 3.3 and 3.4 for missing measurements probabilities 0.1 and 0.2, respectively. The figures show a significantly reduced RMSE for the proposed EKF\_M compared with the competitive filters. It concludes a significantly improved estimation accuracy of the proposed EKF\_M compared with the competitive filters, in identifying the multiple sinusoids from missing measurements of the superimposed signal.

### 3.4.3 Sinusoids Identification from the Estimated States

As discussed earlier, a sinusoid is fundamentally characterized by its amplitude and frequency, and that is the reason why we formulated our multiple sinusoids identification problem as an amplitude and frequency estimation problem. In this subsection, we construct (identify) the unknown sinusoids from the estimated amplitude and frequency. In this regard, we obtain the amplitude and frequency of each sinusoid by averaging their respective estimates over the last 300 time-steps, which is expectedly the converged region. Subsequently, we plot the three sinusoids (forming the superimposed signal) in Fig. 3.5 for missing measurements probability of 0.2. We compare the identified sinusoids with the respective true sinusoids. The amplitude and frequency of the true sinusoids are obtained by averaging their respective true values over the last 300 time-steps. The figure illuminates that the sinusoids identified using the proposed EKF\_M closely characterize the true sinusoids. On the other hand, the sinusoids identified using the competitive filters are significantly mismatched with the true sinusoids.

### 3.4.4 Performance Analysis with Different Time Series

To further validate the performance, the proposed and other filters are tested with different time series as

- **Case-1:**  $\mathbf{x}_0 = [1000 \ 2500 \ 1500 \ 2 \ 1 \ 7]^T$ ,  $\mathbf{P}_0 = \text{diag}[5 \ 2 \ 5 \ 2 \ 12 \ 5]$ ,  $\hat{\mathbf{x}}_{0|0} \sim 0.9\mathcal{N}(\mathbf{x}_0, \mathbf{P}_0)$ ,  $\mathbf{Q}_k = \text{diag}[0.24 \ 0.24 \ 0.24 \ 0.015 \ 0.015 \ 0.015]$ , and  $\mathbf{R}_k = \text{diag}[0.9 \ 0.9]$ .
- **Case-2:**  $\mathbf{x}_0 = [50 \ 50 \ 50 \ 240 \ 240 \ 240]^T$ ,  $\mathbf{P}_0 = \text{diag}[2 \ 5 \ 2 \ 10 \ 8 \ 7]$ ,  $\hat{\mathbf{x}}_{0|0} \sim 0.8\mathcal{N}(\mathbf{x}_0, \mathbf{P}_0)$ ,  $\mathbf{Q}_k = \text{diag}[0.01 \ 0.01 \ 0.01 \ 0.16 \ 0.16 \ 0.16]$ , and  $\mathbf{R}_k = \text{diag}[2 \ 2]$ .

For the above-mentioned cases, the three sinusoids were identified using the proposed method and competitive methods considering the missing measurement probabilities of 0.2. Figs. 3.6 and 3.7 compare the sinusoids identified by different filters for Case-1 and Case-2, respectively. It can be observed the proposed method *i.e.*, identifies the sinusoids more closely compared to other filters.

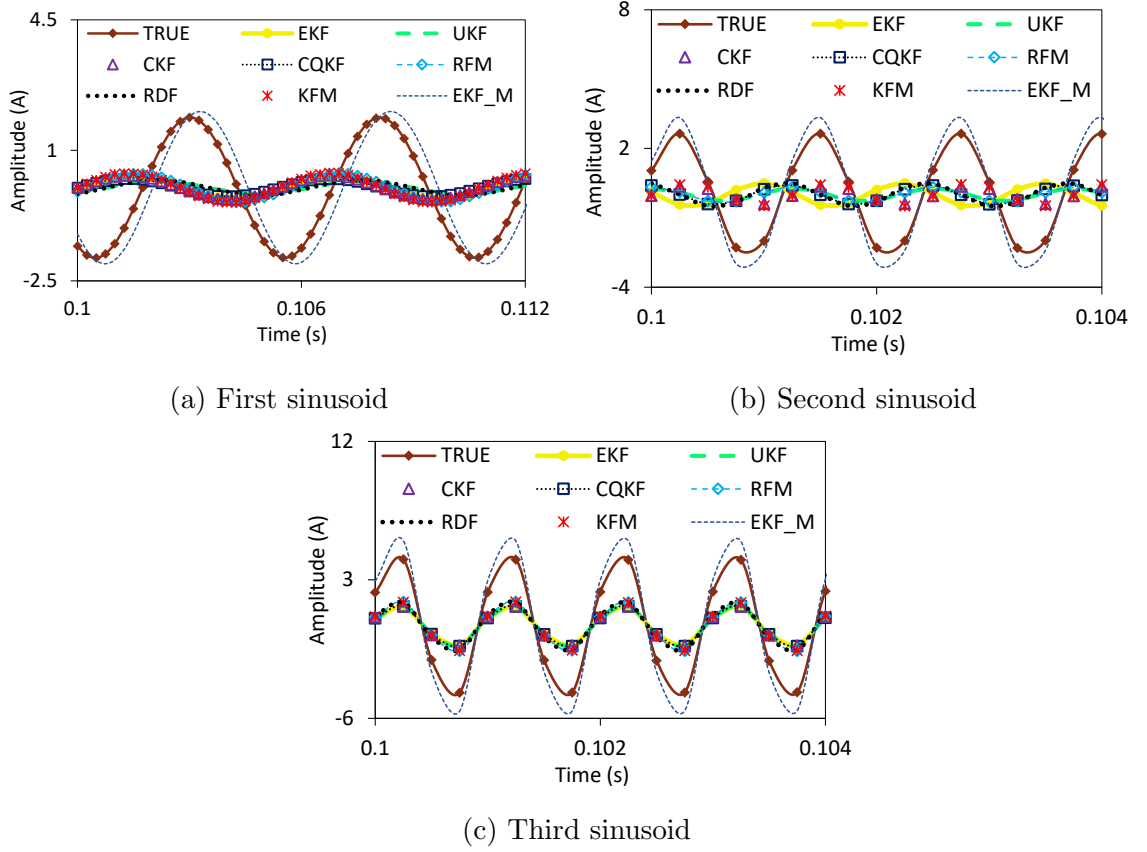


Figure 3.5: Plots of the true sinusoids forming the superimposed signal and the sinusoids identified from the measurements of the superimposed signal using the proposed EKF\_M and the ordinary Gaussian filters for missing measurements probability of 0.2.

### 3.4.5 Performance Analysis with Varying Missing Measurements Probability

To analyze the performance of the proposed EKF\_M and the competitive filters for varying missing measurements probability, the author plots the average RMSE (obtained over 800 time-steps) against the missing measurements probability in Fig. 3.8. We restrict our analysis for missing measurements probability up to 0.6. The figure demonstrates an increasing average RMSE as the missing measurements probability increases. Thus, we can conclude that the performance of the proposed EKF\_M and the ordinary Gaussian filters deteriorate as more measurements are missing, which is an expected response. However, the average RMSE obtained by the proposed EKF\_M is notably reduced compared with the ordinary Gaussian filters. This

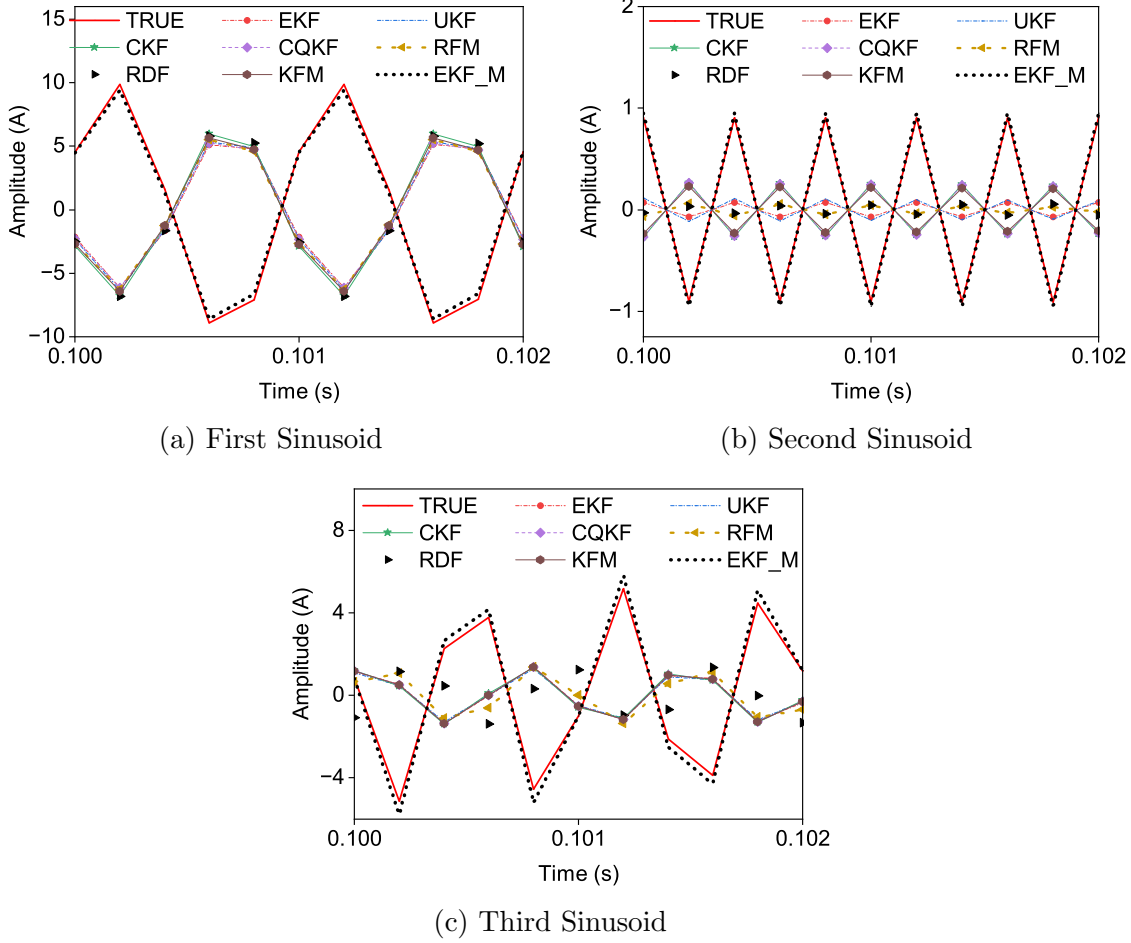


Figure 3.6: Case-1: Sinusoids identified by all filters at missing measurement probability of 0.2.

reflects that, although the accuracy deteriorates, the frequency and amplitude estimation using the EKF\_M is successful even if up to 60% of measurements are missing.

### 3.4.6 Computational Time Analysis

It should be mentioned that the practical applications of the superimposed signals (formed by the superimposition of multiple sinusoids) are usually on high frequency, *e.g.*, the telecommunication systems are commonly operated in the range of several kHz to MHz frequency. Therefore, the sampling interval should be sufficiently small to characterize the high-frequency signals, *e.g.*, sampling interval in our simulation environment is taken as 0.25 *ms*. Due to the small sampling interval, in general, the computational time of the filters become crucial. Thankfully, the ordinary EKF is considerably fast for practical applications. Table 3.1 compares the

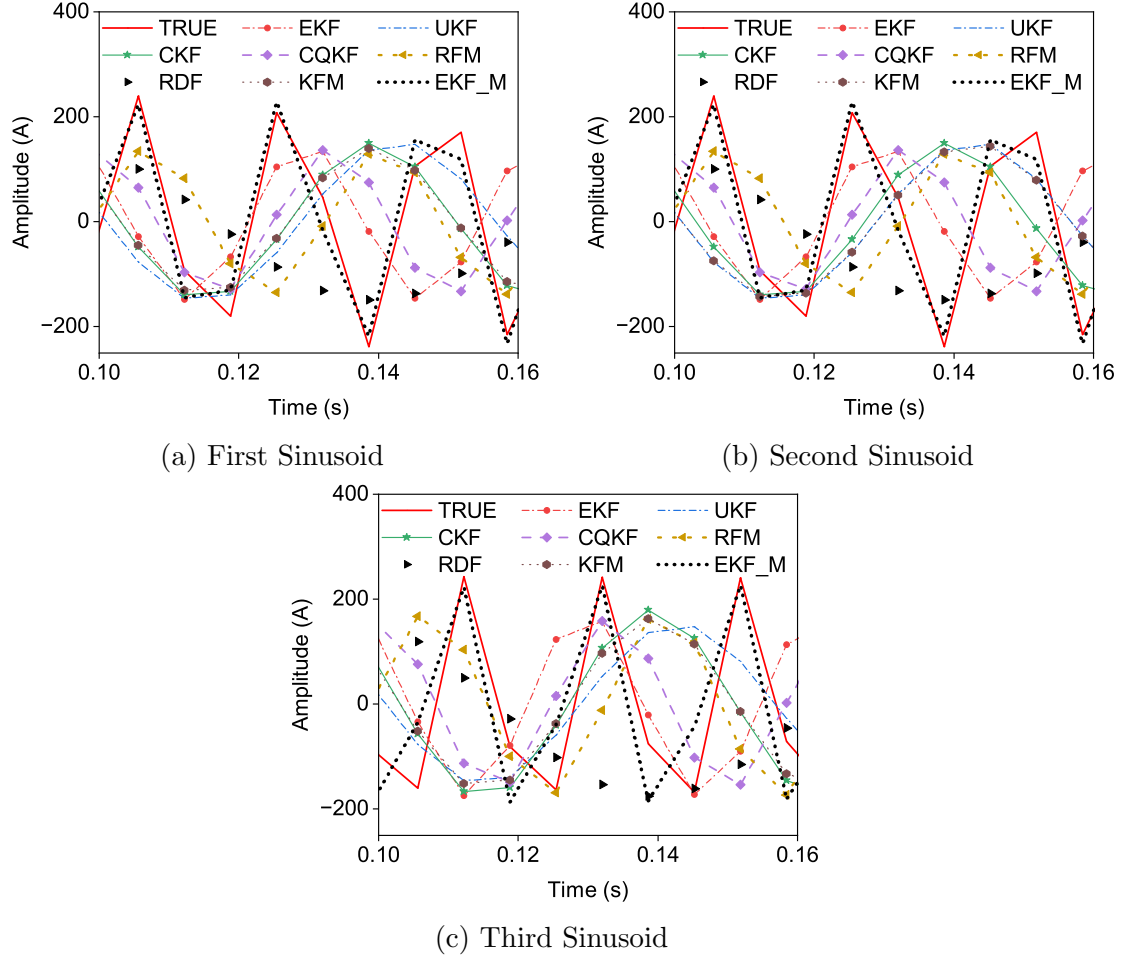


Figure 3.7: Case-2: Sinusoids identified by all filters at missing measurement probability of 0.2.

Table 3.1: Relative computational time comparison of the proposed and the competitive filters.

Filters	EKF	UKF	CKF	CQKF	RFM	RDF	KFM	EKF_M
Computational time	1	4.47	4.92	11.43	2.41	2.65	1.65	1.14

relative computational time of the proposed method and the competitive filters. It can be observed that the computational time of the EKF and EKF\_M are comparable, while the computational demands of other considered filters are considerably high. Thus, we expect that the computational time of the proposed EKF\_M is small enough for practical applications.

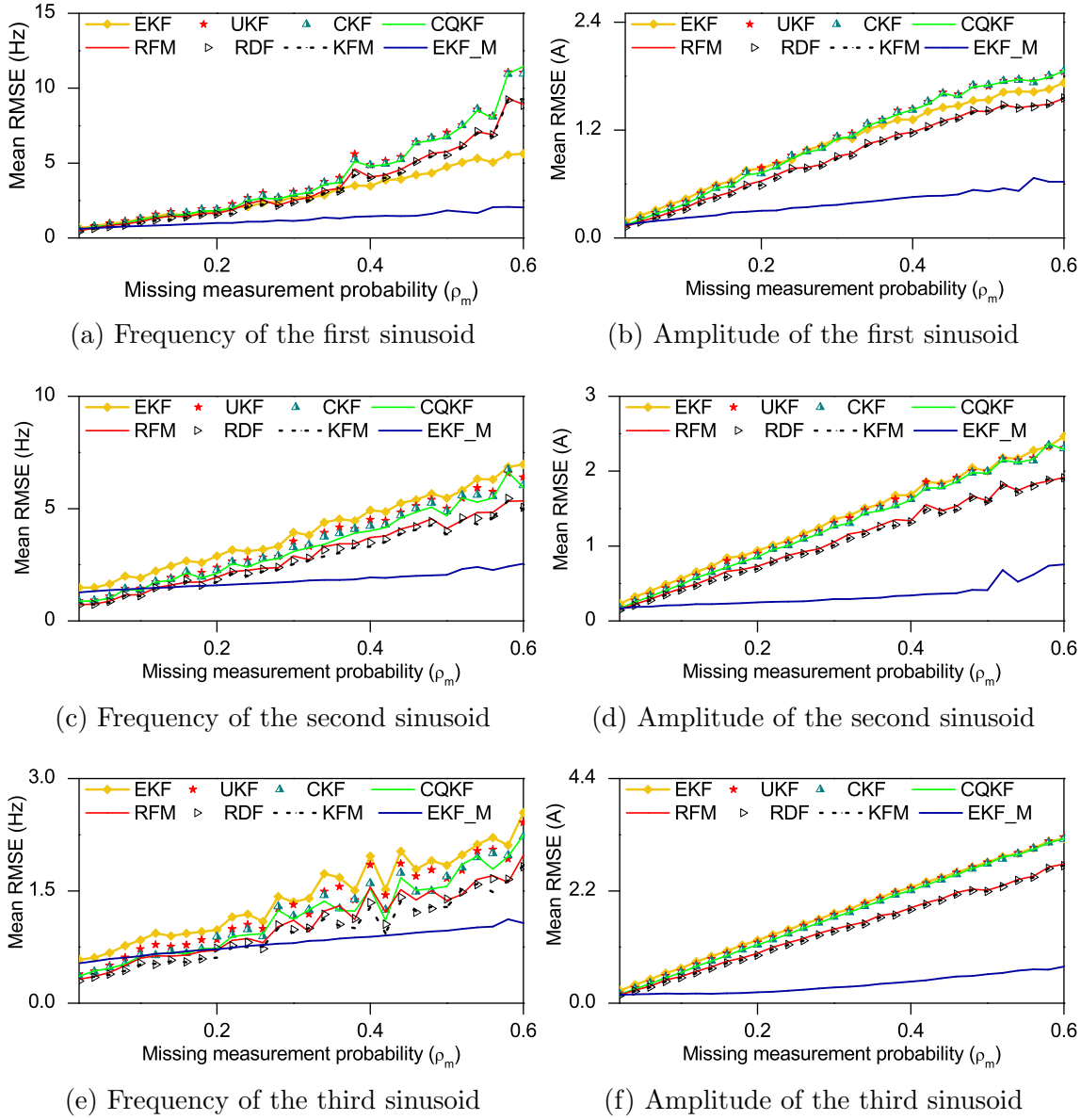


Figure 3.8: Plots of mean RMSEs against varying missing measurements probability.

### 3.4.7 EKF\_M for General Estimation and Filtering Problems

Although the core interest of this chapter is limited to the multiple sinusoids identification problem, the proposed EKF\_M is applicable to any practical estimation and filtering problem. It can potentially improve the accuracy of general estimation and filtering problems with missing measurements. Therefore, this development can be useful for various other domains, such as target tracking [2], industrial diagnosis and prognosis [4], and biomedical modeling [165], commonly witnessing the estimation



and filtering problems.

### 3.5 Summary

The signals appearing in real-life problems often witness the signals which are superimposed of multiple sinusoids, *e.g.*, distorted and harmonically superimposed signals appearing in power systems. In many of such cases, the succeeding analysis requires to identify the individual sinusoids from noisy measurements of the superimposed signal. For example, we can consider the harmonic power flow analysis problem in electrical power system [143, 144] and distortion analysis problem in communication signals [147]. The sinusoids are characterized by frequency and amplitude. Therefore, the sinusoids identification problem is simplified as frequency and amplitude estimation problem. The prominently used estimators for this purpose, such as the EKF, require the measurements to be available at every sampling instant. However, the measurements are frequently missing in practical sinusoids identification problems due to various reasons, such as network fault and high signal-to-noise ratio (please see the introduction section for a detailed discussion including other possible reasons). In this chapter, we designed a robust estimator, abbreviated as EKF-M, to deal with the missing measurements in the sinusoids identification problems. The simulation results reveal a significantly close identification of the unknown sinusoids using the proposed method in the presence of the missing measurements. It should be mentioned that the sinusoids identified by the ordinary Gaussian filters and the existing filters for the missing measurements (References [97, 102, 106]) are poorly matched with the true sinusoids in the same missing measurements environment. Further comparison of the modified and the ordinary Gaussian filters in terms of the RMSE reveals a significantly enhanced accuracy for the proposed method. Furthermore, the computational time of the modified EKF is merely 1.14 times the ordinary EKF, which should not be a worry for practical applications. Thus, the proposed method may be a recommended estimator for multiple sinusoids identification problems in the presence of missing measurements. On a different note, the modified EKF is a general estimation and filtering algorithm, not restricted to the sinusoids estimation problem only. Therefore, the contribution of this chapter can

benefit other domains as well, involving the estimation and filtering applications, such as target tracking and biomedical modeling.





## Chapter 4

# Generalized Gaussian Filtering with Sporadically Missing Measurements

### 4.1 Introduction

The work in this chapter is motivated from the last one which considered the problem of missing measurements and restructured the conventional EKF to handle it. It is well-known that the EKF suffers from the curse of dimensionality in terms of numerical instability and poor estimation accuracy due to involvement of Jacobean calculation [9, 11, 15]. Moreover, the performance may degrade as the system nonlinearities increase. These reasons may restrict the applicability of the EKF-based handling of the missing measurements (method proposed in the previous chapter) for complex systems. Therefore, with the aim to address the missing measurements phenomenon in a wide-range of practical applications, in this chapter, we propose a generalized Gaussian filtering algorithm to handle the missing measurements phenomenon. Unlike the EKF\_M (proposed in the last chapter), this method uses the last available measurement for the filtering if the measurement is lost at any time-step.

In this work, we propose an advanced Gaussian filter for handling missing measurements wherein one or more elements of the measurement vector may not be received by the estimator. We first introduce a stochastic measurement model that

incorporates the missing measurement possibility using the Bernoulli random variable (BRV). Following this, the measurement related parameters, *i.e.*, measurement estimate, covariance, and cross-covariance are rederived for the modified measurement model. For the simulation validation, we employed the CKF-, CQKF-, and GHF-based extensions of the proposed Gaussian filtering. The simulation results show the improved accuracy of the proposed Gaussian filter in the presence of the intermittently missing measurements.

Summarizing the discussion, the main contributions of this chapter can be described as follows:

- Formation of a modified measurement model that incorporates the missing possibility of individual measurement element;
- Adaptation of the Gaussian filtering for the modified measurement model;
- Validation of the improved performance for the proposed Gaussian filter for the CKF-, CQKF-, and GHF-based extensions of the proposed Gaussian filtering methodology.

## 4.2 Problem Formulation

Our first objective is to present a measurement model that incorporates the missing measurement possibilities. In this regard, let us recall the standard state-space model for nonlinear dynamical systems from Chapter 1 (with all notations being exactly the same)

$$\mathbf{x}_k = f(\mathbf{x}_{k-1}) + \boldsymbol{\eta}_k. \quad (4.1)$$

$$\mathbf{z}_k = h(\mathbf{x}_k) + \boldsymbol{\nu}_k. \quad (4.2)$$

To include the missing measurement possibility in the measurement model, we introduce a matrix with the main diagonal containing the BRVs, denoted by  $\beta_k^i$   $i \in \{1, 2, \dots, q\}$  ( $q$  denoting the dimension of the measurement vector). It should be noted that  $\beta_k^i$  attains either 0 or 1, with  $\beta_k^i = 1$  representing the corresponding element of the measurement is lost, while  $\beta_k^i = 0$  denotes that the measurement is received. Moreover, our modified measurement model propagates the last mea-

surement (*i.e.*,  $\mathbf{z}_{k-1}$ ) in case the measurement is received with the lost information. Following the discussion, we model the actual measurement (denoted as  $\mathbf{y}_k$ ) as

$$\mathbf{y}_k = \begin{bmatrix} 1 - \beta_k^1 & 0 & \cdots & 0 \\ 0 & 1 - \beta_k^2 & \cdots & 0 \\ \vdots & \vdots & \ddots & \vdots \\ 0 & 0 & \cdots & 1 - \beta_k^q \end{bmatrix} \mathbf{z}_k + \begin{bmatrix} \beta_k^1 & 0 & \cdots & 0 \\ 0 & \beta_k^2 & \cdots & 0 \\ \vdots & \vdots & \ddots & \vdots \\ 0 & 0 & \cdots & \beta_k^q \end{bmatrix} \mathbf{z}_{k-1}. \quad (4.3)$$

We consider the case where the missing measurement probability is known. Specifically,  $\mathcal{P}(\beta_k^i = 1) = \mathbb{E}[\beta_k^i] = \mu_k^i$ , with  $\mathcal{P}(\cdot)$  and  $\mathbb{E}[\cdot]$  respectively being the probability and expectation operators, denotes the missing measurement probability. It should be stressed that the traditional Gaussian filter is designed with respect to the state space model represented by Eqs. (4.1) and (4.2). Since the measurement model is modified now, the new problem is posed as designing the Gaussian filtering for the new state space model represented by Eqs. (4.1) and (4.3).

### 4.3 Gaussian Filtering for Missing Measurements

This section presents the restructured Gaussian filtering for missing measurements. The proposed method re-derives the measurement related parameters: measurement estimate, covariance, and cross-covariance. To this end, let us denote the measurement estimate, covariance, and cross-covariance for the hypothetical true measurement  $\mathbf{z}_k$  by  $\hat{\mathbf{z}}_{k|k-1}$ ,  $\mathbf{P}_{k|k-1}^{\mathbf{zz}}$ , and  $\mathbf{P}_{k|k-1}^{\mathbf{xz}}$ , respectively. Moreover,  $\hat{\mathbf{y}}_{k|k-1}$ ,  $\mathbf{P}_{k|k-1}^{\mathbf{yy}}$ , and  $\mathbf{P}_{k|k-1}^{\mathbf{xy}}$  are the corresponding parameters for the modified measurement model (Eq. (4.3)).

Before proceeding further, let us define  $\boldsymbol{\beta}_k = \text{diag}([\beta_k^1, \beta_k^2, \dots, \beta_k^q])$ ; thus, we can simplify Eq. (4.3) as

$$\mathbf{y}_k = (\mathbf{I} - \boldsymbol{\beta}_k)\mathbf{z}_k + \boldsymbol{\beta}_k\mathbf{z}_{k-1}. \quad (4.4)$$

with  $\mathbf{I}$  being an identity matrix of appropriate dimension.

**Remark 4.1.**  $\boldsymbol{\beta}_k$  and  $\mathbf{z}_k$  signify different physical events; thus,  $\boldsymbol{\beta}_k$  and  $\mathbf{z}_k$  will be statistically independent.

We now present three theorems that derive the relevant measurement parameters

for the modified measurement model (4.3).

**Theorem 4.1.** The measurement estimate for the modified measurement model (4.3) can be obtained as

$$\hat{\mathbf{y}}_{k|k-1} = (\mathbf{I} - \boldsymbol{\mu}_k)\hat{\mathbf{z}}_{k|k-1} + \boldsymbol{\mu}_k\hat{\mathbf{z}}_{k-1|k-1}, \quad (4.5)$$

with  $\boldsymbol{\mu}_k = \text{diag}([\mu_k^1, \mu_k^2, \dots, \mu_k^q])$ .

*Proof.* Let us use Eq. (4.4) to substitute  $\mathbf{y}_k$  in  $\hat{\mathbf{y}}_{k|k-1} = \mathbb{E}[\mathbf{y}_k]$ . Subsequently, applying Remark 4.1, we get

$$\hat{\mathbf{y}}_{k|k-1} = \mathbb{E}[(\mathbf{I} - \boldsymbol{\beta}_k)]\mathbb{E}[\mathbf{z}_k] + \mathbb{E}[\boldsymbol{\beta}_k]\mathbb{E}[\mathbf{z}_{k-1}]. \quad (4.6)$$

Substituting  $\mathbb{E}[\boldsymbol{\beta}_k] = \boldsymbol{\mu}_k$ ,  $\mathbb{E}[\mathbf{z}_k] = \hat{\mathbf{z}}_{k|k-1}$ , and  $\mathbb{E}[\mathbf{z}_{k-1}] = \hat{\mathbf{z}}_{k-1|k-1}$ , the above equation is reduced to Eq. (5.6).  $\square$

**Theorem 4.2.** The covariance  $\mathbf{P}_{k|k-1}^{\mathbf{y}\mathbf{y}}$  for the modified measurement model (4.4) is obtained as

$$\begin{aligned} \mathbf{P}_{k|k-1}^{\mathbf{y}\mathbf{y}} &= \sum_{j=0}^1 (\mathbf{I}(1-j) - \boldsymbol{\mu}_k) \mathbf{P}_{k-j|k-1}^{\mathbf{z}\mathbf{z}} \\ &\quad + \boldsymbol{\mu}_k(\mathbf{I} - \boldsymbol{\mu}_k)(\hat{\mathbf{z}}_{k|k-1} - \hat{\mathbf{z}}_{k-1|k-1})(\hat{\mathbf{z}}_{k|k-1} - \hat{\mathbf{z}}_{k-1|k-1})^T. \end{aligned} \quad (4.7)$$

*Proof.* From Eqs. (4.4) and (5.6), we obtain

$$\begin{aligned} \mathbf{y}_k - \hat{\mathbf{y}}_{k|k-1} &= \underbrace{(\mathbf{I} - \boldsymbol{\beta}_k)(\mathbf{z}_k - \hat{\mathbf{z}}_{k|k-1})}_{\boldsymbol{\Delta}_1} + \underbrace{\boldsymbol{\beta}_k(\mathbf{z}_{k-1} - \hat{\mathbf{z}}_{k-1|k-1})}_{\boldsymbol{\Delta}_2} \\ &\quad + \underbrace{(\boldsymbol{\mu}_k - \boldsymbol{\beta}_k)(\hat{\mathbf{z}}_{k|k-1} - \hat{\mathbf{z}}_{k-1|k-1})}_{\boldsymbol{\Delta}_3}. \end{aligned} \quad (4.8)$$

Substituting  $\mathbf{y}_k - \hat{\mathbf{y}}_{k|k-1}$  from above equation into  $\mathbf{P}_{k|k-1}^{\mathbf{y}\mathbf{y}} = \mathbb{E}[(\mathbf{y}_k - \hat{\mathbf{y}}_{k|k-1})(\mathbf{y}_k - \hat{\mathbf{y}}_{k|k-1})^T]$  gives

$$\mathbf{P}_{k|k-1}^{\mathbf{y}\mathbf{y}} = \sum_{i=1}^3 \sum_{j=1}^3 \mathbb{E}[\boldsymbol{\Delta}_i \boldsymbol{\Delta}_j^T]. \quad (4.9)$$

We now calculate  $\mathbb{E}[\boldsymbol{\Delta}_i \boldsymbol{\Delta}_j^T]$   $((i, j) \in \{1, 2\})$  individually.



**Remark 4.2.** For  $\mathbf{y}_k - \hat{\mathbf{y}}_{k|k-1}$  expressed in Eq. (4.8) and applying Remark 4.1, it can be easily concluded that  $\mathbb{E}[\Delta_i \Delta_j^T]_{i \neq j} = 0$ .

Following Remark 4.2, we calculate  $\mathbb{E}[\Delta_i \Delta_j^T]_{i=j}$  as follows

$$\begin{cases} \mathbb{E}[\Delta_1 \Delta_1^T] = \mathbb{E}[(\mathbf{I} - \beta_k)^2] \mathbb{E}[(\mathbf{z}_k - \hat{\mathbf{z}}_{k|k-1})(\mathbf{z}_k - \hat{\mathbf{z}}_{k|k-1})^T] \\ \mathbb{E}[\Delta_2 \Delta_2^T] = \mathbb{E}[\beta_k^2] \mathbb{E}[(\mathbf{z}_{k-1} - \hat{\mathbf{z}}_{k-1|k-1})(\mathbf{z}_{k-1} - \hat{\mathbf{z}}_{k-1|k-1})^T] \\ \mathbb{E}[\Delta_3 \Delta_3^T] = \mathbb{E}[(\boldsymbol{\mu}_k - \beta_k)^2] (\hat{\mathbf{z}}_{k|k-1} - \hat{\mathbf{z}}_{k-1|k-1})(\hat{\mathbf{z}}_{k|k-1} - \hat{\mathbf{z}}_{k-1|k-1})^T. \end{cases} \quad (4.10)$$

Let us now substitute  $\mathbb{E}[\beta_k^2] = \mathbb{E}[\beta_k] = \boldsymbol{\mu}_k$ ,  $\mathbb{E}[(\mathbf{z}_k - \hat{\mathbf{z}}_{k|k-1})(\mathbf{z}_k - \hat{\mathbf{z}}_{k|k-1})^T] = \mathbf{P}_{k|k-1}^{\mathbf{zz}}$ , and  $\mathbb{E}[(\beta_k - \boldsymbol{\mu}_k)^2] = \boldsymbol{\mu}_k(\mathbf{I} - \boldsymbol{\mu}_k)$ . Subsequently, substituting the resulting expression in Eq. (4.9) as well as applying Remark 4.2,  $\mathbf{P}_{k|k-1}^{\mathbf{yy}}$  can be expressed as given in Eq. (4.7).  $\square$

**Theorem 4.3.** The cross-covariance for  $\mathbf{y}_k$  can be obtained as

$$\mathbf{P}_{k|k-1}^{\mathbf{xy}} = (\mathbf{I} - \boldsymbol{\mu}_k) \mathbf{P}_{k|k-1}^{\mathbf{xz}} + \boldsymbol{\mu}_k \mathbf{P}_{k-1|k-1}^{\mathbf{xz}}. \quad (4.11)$$

*Proof.* Substituting  $\mathbf{y}_k - \hat{\mathbf{y}}_{k|k-1}$  from Eq. (4.8) into  $\mathbf{P}_{k|k-1}^{\mathbf{xy}} = \mathbb{E}[\mathbf{e}_{k|k-1}(\mathbf{y}_k - \hat{\mathbf{y}}_{k|k-1})^T]$  (where  $\mathbf{e}_{k|k-1} = \mathbf{x}_k - \hat{\mathbf{x}}_{k|k-1}$ ), we can write

$$\mathbf{P}_{k|k-1}^{\mathbf{xy}} = \mathbb{E}[\mathbf{e}_{k|k-1}(\Delta_1 + \Delta_2 + \Delta_3)^T]. \quad (4.12)$$

Substituting  $\Delta_1$  and  $\Delta_2$  from Eq. (4.8), we can write

$$\begin{cases} \mathbb{E}[\mathbf{e}_{k|k-1} \Delta_1^T] = \mathbb{E}[\mathbf{I} - \beta_k] \mathbb{E}[\mathbf{e}_{k|k-1}(\mathbf{z}_k - \hat{\mathbf{z}}_{k|k-1})^T] \\ \mathbb{E}[\mathbf{e}_{k|k-1} \Delta_2^T] = \mathbb{E}[\beta_k] \mathbb{E}[\mathbf{e}_{k|k-1}(\mathbf{z}_{k-1} - \hat{\mathbf{z}}_{k-1|k-1})^T]. \end{cases} \quad (4.13)$$

Let us first substitute  $\mathbb{E}[\mathbf{e}_{k|k-1}(\mathbf{z}_k - \hat{\mathbf{z}}_{k|k-1})^T] = \mathbf{P}_{k|k-1}^{\mathbf{xz}}$  and  $\mathbb{E}[\beta_k] = \boldsymbol{\mu}_k$  in above equation, and subsequently, substitute the resulting expression in Eq. (4.12). Moreover, Remark 4.1 concludes  $\mathbb{E}[\mathbf{e}_{k|k-1} \Delta_3^T] = 0$ . Following the discussion, Eq. (4.13) easily deduces Eq. (4.11).  $\square$

The unknown missing measurement probability is often closely approximated from the system's historic behavior, training data analysis, *etc.* Moreover, the true

value is usually small and thus, its deviation from the approximated value is also usually not very large. Consequently, the unknown missing measurement probability is concerning only in limited problems and the proposed method can efficiently handle a wide range of practical problems.

**Remark 4.3.** *The algorithm for the proposed Gaussian filter has steps similar to those of traditional Gaussian filter (see, e.g., [15]), except the parameters  $\hat{\mathbf{y}}_{k|k-1}$ ,  $\mathbf{P}_{k|k-1}^{yy}$ , and  $\mathbf{P}_{k|k-1}^{xy}$  replace  $\hat{\mathbf{z}}_{k|k-1}$ ,  $\mathbf{P}_{k|k-1}^{zz}$ , and  $\mathbf{P}_{k|k-1}^{xz}$ , respectively in the conventional Gaussian filtering algorithm.*

**Remark 4.4.** *It is apparent from Eqs. (5.6), (4.7), and (4.11) that the proposed Gaussian filtering algorithm requires to store the measurement vector, measurement estimate, covariance, and cross-covariance from time  $t_{k-1}$ . It leads to a marginally increased storage requirement compared to the traditional Gaussian filtering algorithm.*

## 4.4 Simulation Results

This section compares the performance of the proposed and conventional Gaussian filters in presence of the missing measurements. For this purpose, we choose the CKF, CQKF, and GHF and their extensions under the proposed Gaussian filtering framework represented by CKFS, CQKFS, and GHFS, respectively. It should be noted that the missing measurements possibility is not very large in general; thus, we restricted the analysis considering that not more than 20 measurements are missing (*i.e.*,  $\mu_k^i = 0.2$ ). The commonly accepted root mean square error (RMSE) criteria is selected as the performance metric. The simulation was carried out for 200 time-steps and validated with 200 Monte-Carlo runs.

### 4.4.1 Problem 1: Individual Signal Identification

Here, we consider the individual sinusoids identification problem from the missing measurements of the superimposed signal. As the amplitude and frequency are the characterizing parameters, the modified problem is to estimate the amplitude and frequency of the individual sinusoids. Assuming that the superimposed signal is

constructed by three sinusoids, the state dynamics follows [15]

$$\mathbf{x}_k = \mathbf{I}\mathbf{x}_{k-1} + \boldsymbol{\eta}_k. \quad (4.14)$$

$$\mathbf{z}_k = \begin{bmatrix} \sum_{j=1}^3 a_{j,k} \cos(2\pi f_{j,k}(k)T) \\ \sum_{j=1}^3 a_{j,k} \sin(2\pi f_{j,k}(k)T) \end{bmatrix} + \boldsymbol{\nu}_k, \quad (4.15)$$

where  $a_{j,k}$  and  $f_{j,k}$  denote the amplitude and frequency, respectively of the  $j^{th}$  sinusoid.

The dynamics of the states are generated considering  $\mathbf{x}_0 = [200 \ 800 \ 1000 \ 2 \ 2 \ 2]^T$ . The filter initialization is done by choosing  $\hat{\mathbf{x}}_{0|0} \sim \mathcal{N}(\mathbf{x}_0, \mathbf{P}_0)$ , where  $\mathbf{P}_0 = \text{diag}([10 \ 35 \ 25 \ 0.05 \ 0.05 \ 0.05])$ . Moreover, the noise covariances are chosen as  $\mathbf{Q}_k = \text{diag}([0.01 \ 0.01 \ 0.01 \ 0.04 \ 0.04 \ 0.04])$  and  $\mathbf{R}_k = \text{diag}([0.1 \ 0.1])$ . The results are generated considering sampling interval  $T = 0.25$  ms. We consider the performance metric as combined RMSE (CRMSE) [15]. The CRMSE for amplitude is obtained as

$$\text{ACRMSE}_k = \sqrt{\frac{\text{MSE}_k(a_1) + \text{MSE}_k(a_2) + \text{MSE}_k(a_3)}{3}}, \quad (4.16)$$

where  $\text{ACRMSE}_k$  represents the amplitude's CRMSE with  $\text{MSE}_k(a_j)$  ( $j = \{1, 2, 3\}$ ) being the MSE of the  $j^{th}$  amplitude. Similarly, we calculate the frequency's CRMSE (FCRMSE) as well. The CRMSEs are plotted for missing measurement probabilities of 0.1 and 0.2 in Fig. 4.1. The plots conclude reduced RMSEs for the CKFS, CQKFS, and GHFS compared with their conventional counterparts. It infers the superior performance of the proposed Gaussian filter in the presence of missing measurements phenomenon. Moreover, the relative computational times for the CKF, CQKF, GHF, CKFS, CQKFS, and GHFS are obtained as 1, 1.76, 1.49, 1.19, 1.96, and 1.67, respectively.

#### 4.4.2 Problem 2: Sinusoidal Growth Model

In this example, the author considers the problem of estimating the heading position of an autonomous robot. the state space model follows [29]

$$\mathbf{x}_k = 2 \cos(\mathbf{x}_{k-1}) + \boldsymbol{\eta}_k. \quad (4.17)$$

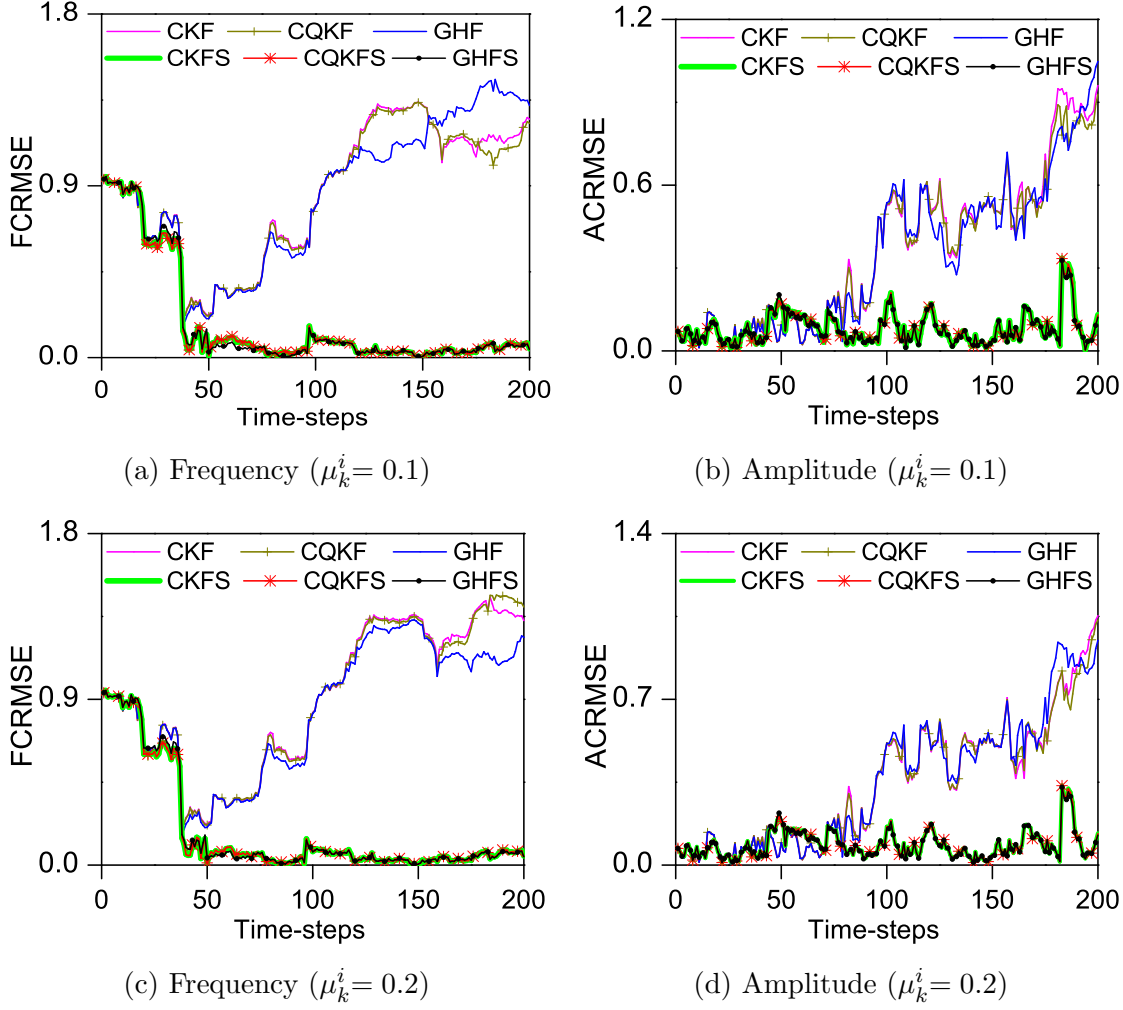


Figure 4.1: Problem 2: CRMSE comparison for different Gaussian filters and their respective extensions under the proposed Gaussian filtering framework for missing measurements probabilities of 0.1 and 0.2.

$$\mathbf{z}_k = \sqrt{1 + \mathbf{x}_k \mathbf{x}_k^T} + \boldsymbol{\nu}_k. \quad (4.18)$$

The different parameters are selected as follows.  $\mathbf{x}_0 = [1 \ 1]^T$ ,  $\mathbf{P}_0 = \mathbf{Q}_k = \mathbf{I}$ ,  $\hat{\mathbf{x}}_{0|0} \sim 0.8\mathcal{N}(\mathbf{x}_0, \mathbf{P}_0)$ , and  $\mathbf{R}_k = 0.25$ . Fig. 4.2 compares the RMSEs obtained by different filters with  $\mu_k^i$  chosen as 0.1 and 0.2. For this problem as well, reduced RMSEs are obtained by the proposed Gaussian filter. Thus, the improved filtering accuracy is achieved by implementing the proposed Gaussian filter in the presence of missing measurements. We observed the relative computational times for the CKF, CQKF, GHF, CKFS, CQKFS, and GHFS as 1, 2.29, 3.85, 1.04, 2.31, and 4.05, respectively.

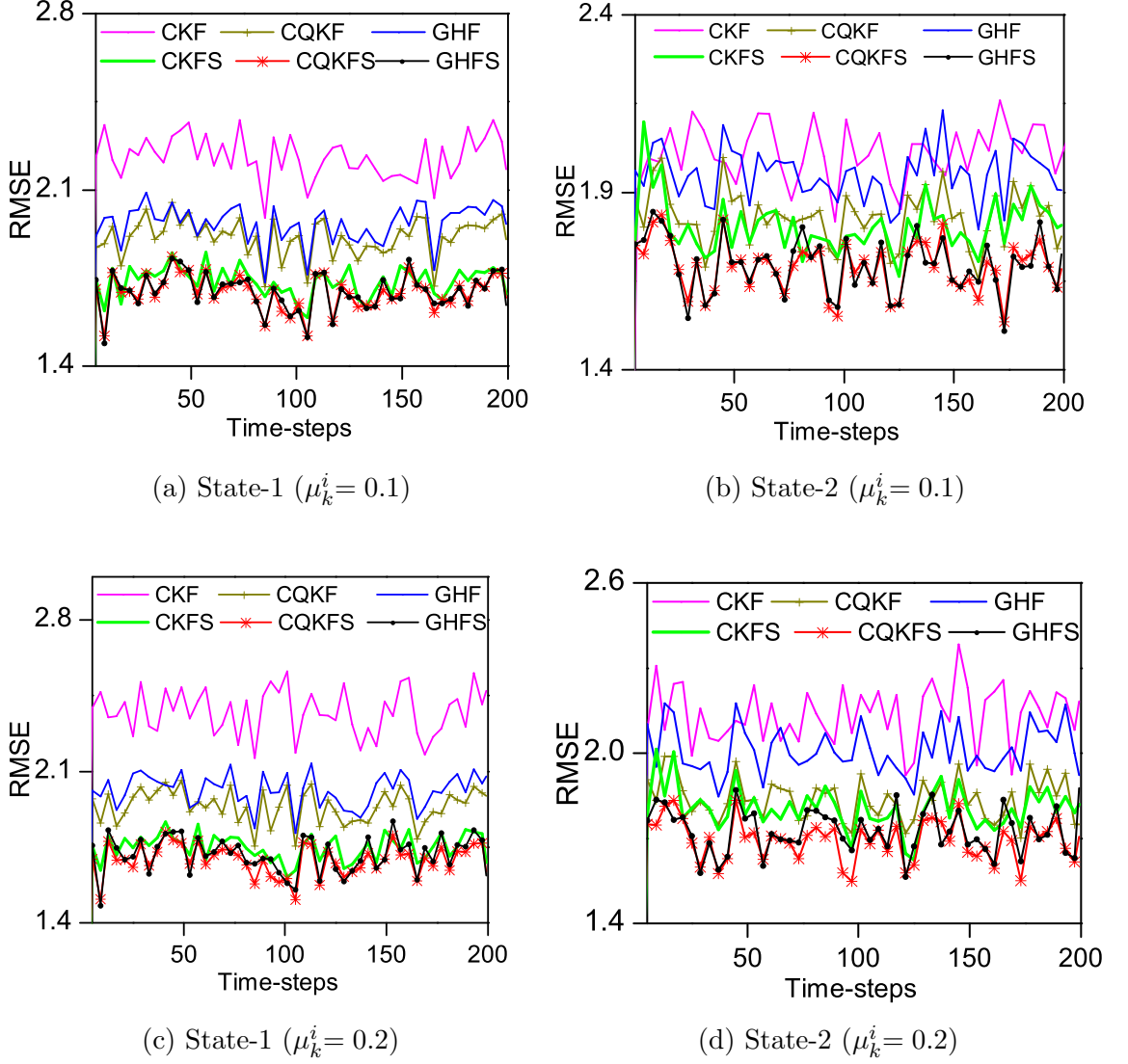


Figure 4.2: Problem 2: RMSE comparison for different Gaussian filters and their respective extensions under the proposed Gaussian filtering framework for missing measurements probabilities of 0.1 and 0.2.

## 4.5 Summary

The filtering accuracy largely depends upon the received measurements. The presence of unreliable communication channels and sensors in networked control systems often result in intermittently missing measurements. Ignoring the irregularity may lead to inferior filtering performance. In this chapter, we proposed an advanced Gaussian filtering methodology to handle the frequently missing measurements. In the first step, a modified measurement model is proposed, taking into account the possibility of partially missing measurements. Following this, the parameters pertinent to the measurement model are rederived; thus, the proposed Gaussian filter

is constituted. We considered the CKF-, CQKF-, and GHF-based extensions under the proposed methodology for simulation. The simulation results of two numerical examples illustrate that an improved filtering accuracy is achieved at slightly increased computational cost.

The impact of the sporadically missing measurements on the conventional filters may vary with problems. For example, the conventional filters diverge for the first simulation problem while they converge for the second simulation problem. However, in all cases, the extensions of the conventional filters under the proposed filtering methodology is expected to outperform their existing counterparts.







# Chapter 5

## Poisson-Gaussian Filtering for Randomly Delayed Measurements

### 5.1 Introduction

As discussed in the previous chapters, in conventional adjustment, Gaussian filters are tailored for non-delayed measurements. Specifically, an estimator receives a measurement at time  $t_k$  that must contain information about the state from the same time-step. This assumption is often violated in practical applications involving wireless sensor network (WSN), where network-induced delay causes the measurement from the past instant to be received at current  $t_k$ . In Chapter 2, the author comprehensively discussed factors responsible for delay induction in the system. the delayed measurements carry misleading information about the states and the Gaussian filtering, designed for non-delayed measurements, provides unreliable estimates.

The Gaussian filtering literature with delayed measurements mainly starts from [121], which extends the EKF and UKF for one-step delayed measurements. The same methodology is further extended for the CKF and GHF in [124] and [166], respectively. Here, one-step delayed measurement implies the delay of up to one sampling interval. Later, Singh *et al.* [125] redesigned the Gaussian filtering to handle arbitrary large delays conditioned to the assumption that the prior information about delay probabilities are known. In the subsequent development, Esmzad *et al.* [126] eased up this requirement by using a likelihood based method to calculate the delay probabilities. Developments in [125] and [126] ambiguously assign the

upper bound of delay if not exactly known. Such an ambiguous selection may pose adverse effect on filtering: an underestimated upper bound causes frequent measurement losses and ignore to assign a probability (weight) to some of the delayed measurements that are possible to arrive, severely harming the estimation accuracy; an overestimated upper bound assigns some probabilities (weights) to excessively delayed measurements at the cost of the probabilities of lesser delayed measurements that are possible to arrive, which again harms the accuracy. Nevertheless, an overestimated upper bound unnecessarily increases the computational demand as well.

The above discussion concludes that the existing delayed Gaussian filters [121, 124–126, 166] may be inappropriate selection for a wide class of practical systems mainly due to two reasons: i) improper selection of the unknown delay probabilities and ii) ambiguous selection of the upper bound of the delay.

In this chapter, we develop an advanced Gaussian filtering method to preclude the two major drawbacks of the existing delay filters, as mentioned above. Moreover, the proposed method is a suitable choice wherein it is difficult to achieve the time-stamping in measurements (*e.g.*, [167]). The proposed method requires the average delay information, which requires lesser assumption in delay probabilities. It should be noted that the Poisson distribution is the maximum entropy distribution for any arbitrary PDF subject to constraint as average value [168]. It also concludes that using the Poisson random variable results into more accurate system model. Thus, designed with a more accurate measurement model, the proposed filter demonstrates and improved accuracy as compared to [125] which uses a set of Bernoulli random variables to model the delay and other existing delay filters. It also requires lesser assumption about the delays than [125].

In designing of the proposed filter, we first reformulate the measurement model for incorporating delay possibilities using Poisson distribution. Subsequently, we re-derive the traditional Gaussian filtering method for the modified measurement model, which requires re-deriving the traditional expressions of the measurement estimate, measurement covariance, and the state-measurement cross-covariance. The proposed method is applicable to any of the existing Gaussian filters, such as the EKF, UKF, CKF, and GHF. We adopt the CKF-based design for validating the

improved accuracy of the proposed method.

## 5.2 Problem formulation

Let us recall the state-space model presented in Chapter 1, given as

$$\mathbf{x}_k = f(\mathbf{x}_{k-1}) + \boldsymbol{\eta}_k. \quad (5.1)$$

$$\mathbf{z}_k = h(\mathbf{x}_k) + \boldsymbol{\nu}_k. \quad (5.2)$$

For a detailed discussion on the notations, please refer to Chapter 1.

It should be mentioned that the above state-space model represents a non-delayed system. Thus, the non-delayed measurement  $\mathbf{z}_k$  misinforms about the state and can significantly deteriorate the filtering accuracy for the traditional Gaussian filters. As discussed earlier, the existing Gaussian filters for delay are limited by two major drawbacks [123, 125, 126]: requirement on a range of delay probabilities and ambiguous selection of the upper bound of delay. The identified limitations primarily stem from an inadequate delay modeling strategy. Specifically, these developments employ a number of Bernoulli random variables (BRVs) to incorporate the delay possibilities, with these number linearly increasing with the delay extent. Therefore, addressing these issues requires modifying the delay modeling approach and a corresponding redesign of the conventional filtering methodology. An important feature of the Poisson random variable is that it can model multiple delays with single statistical parameters. Moreover, it precludes the need of fixing the maximum delay.

Following the above discussion, our initial objective is to reformulate the measurement model (5.2) to incorporate the delay possibilities. As the average delay information is available, we choose Poisson distribution-based remodeling of (5.2). In this regard, let us denote  $\bar{\Theta}$  as Poisson random variable with its parameter  $\lambda$  being the average delay. Please note that the Poisson distribution is a discrete distribution function, taking values from  $\{0, 1, \dots\}$ . At any time  $t_k$ ,  $\bar{\Theta} = d$  represents a  $d$ -step delayed measurement. Moreover, if  $\mathcal{P}(\bar{\Theta})$  represents the probability mass

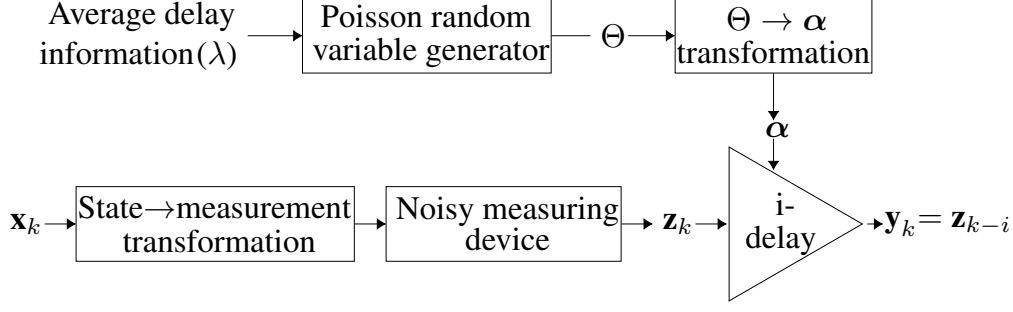


Figure 5.1: Schematic diagram of the delay occurrences considering that the average delay information is known. As the average delay information is known, Poisson distribution features the delay characteristics.

function of  $\bar{\Theta}$ , the probability of  $d$ -step delay follows

$$P(\bar{\Theta} = d) = \frac{e^{-\lambda} \lambda^d}{d!}. \quad (5.3)$$

To model the  $i^{th}$ -delayed measurement, we further introduce a  $k$ -dimensional array  $\alpha$  with its  $(i+1)^{th}$ -element being one and the remaining elements being zero. For example,  $i = 0$  (no-delay) gives  $\alpha = \{1, 0, 0, \dots, 0\}$  and  $i = 2$  (two-delay) gives  $\alpha = \{0, 0, 1, 0, \dots, 0\}$ . The array  $\alpha$  is governed by  $\bar{\Theta}$ . In particular,  $\bar{\Theta} = j$  infers that  $\alpha_{i+1} = 1$  for  $i = j$  and  $\alpha_{i+1} = 0 \forall i \neq j$ , which leads to  $j$ -step delay. Then, the delayed measurement at  $t_k$ , denoted as  $y_k$ , is modeled as

$$y_k = \sum_{i=0}^{k-1} \alpha_{i+1} z_{k-i}. \quad (5.4)$$

Please note that  $\bar{\Theta} = j$ , inferring  $\alpha_{i+1} = 1$  for  $i = j$  and  $\alpha_{i+1} = 0 \forall i \neq j$ , leads to  $j$ -step delay and gives  $y_k = z_{k-j}$ . In view of this, we also deduce

$$P(\alpha_{i+1} = 1) = \mathbb{E}[\alpha_{i+1}] = P(\bar{\Theta} = j) = \lambda_a^j = \frac{e^{-\lambda} \lambda^j}{j!}. \quad (5.5)$$

We refer to Fig. 5.1 for block diagram representing the process of receiving and modeling the delayed measurements.

**Remark 5.1.** In Eq. (5.3),  $\bar{\Theta}$  can be greater than  $k-1$ , particularly in first one or two steps for fairly large average delay (e.g.,  $\lambda \geq 1$ ). This situation theoretically demands measurements from negative time-steps, which is unfeasible. Therefore, to avoid this problem, we choose the delay as  $\min(\bar{\Theta}, k-1)$ , with  $\min(\cdot)$  representing

the minimum operator.

**Remark 5.2.** Remark 5.1 also concludes the increased probability of occurrence for  $k - 1$ . It is relatable to the truncated Poisson distribution for small values of  $\lambda$  in some measure. However, for large average values (e.g.,  $\lambda \geq 5$ ), the approximation no longer remains valid, obliging one to choose the truncated Poisson distribution. Thankfully, the range of average value considered for comparison (i.e.,  $0.5 \leq \lambda \leq 1.5$ ) is small enough that efficiently imitates the practical delays that include large ones; thus, it precludes the use of the truncated Poisson distribution in this case.

It is worth mentioning that the dynamical state space model of the delayed system is represented by Eqs. (5.1) and (5.4). Thus, our revised problem is to redesign the traditional Gaussian filtering method for the dynamical state space model represented by Eqs. (5.1) and (5.4).

### 5.3 Modified Gaussian filter for randomly delayed measurements

In this section, we introduce an advanced Gaussian filtering method for handling the delayed measurements. As conclusive from the traditional Gaussian filtering algorithm provided in [11, 15], any irregularity in the measurements influences only three expressions, including the measurement estimate  $\hat{\mathbf{z}}_{k|k-1}$ , measurement covariance  $\mathbf{P}_{k|k-1}^{\mathbf{zz}}$ , and the state-measurement cross-covariance  $\mathbf{P}_{k|k-1}^{\mathbf{xz}}$ . Thus, in order to develop the proposed filtering algorithm, we re-derive the three expressions for the delayed measurement  $\mathbf{y}_k$  through the three subsequent theorems.

**Theorem 5.1.** The measurement estimate  $\hat{\mathbf{y}}_{k|k-1}$ , for the delayed measurement  $\mathbf{y}_k$  is given as

$$\hat{\mathbf{y}}_{k|k-1} = \sum_{i=0}^{k-1} \lambda_a^i \hat{\mathbf{z}}_{k-i|k-1}. \quad (5.6)$$

*Proof.* For  $\mathbf{y}_k$  given in Eq. (5.4), we obtain

$$\hat{\mathbf{y}}_{k|k-1} = \mathbb{E}[\mathbf{y}_k] = \mathbb{E} \left[ \sum_{i=0}^{k-1} \alpha_{i+1} \mathbf{z}_{k-i} \right].$$

It is worth mentioning that  $\alpha_{i+1}$  governs the delay extent, while  $\mathbf{z}_{k-i}$  governs the measurement value, which are statistically independent. Thus, we can write

$$\hat{\mathbf{y}}_{k|k-1} = \sum_{i=0}^{k-1} \mathbb{E}[\alpha_{i+1}] \mathbb{E}[\mathbf{z}_{k-i}].$$

Substituting  $\mathbb{E}[\alpha_{i+1}]$  from Eq. (5.5), we obtain Eq. (5.6).  $\square$

**Theorem 5.2.** The measurement error covariance for the delayed measurement  $\mathbf{y}_k$  can be given as

$$\mathbf{P}_{k|k-1}^{\mathbf{y}\mathbf{y}} = \sum_{i=0}^{k-1} \lambda_a^i \mathbf{P}_{k-i|k-1}^{\mathbf{z}\mathbf{z}} + \sum_{i=0}^{k-1} \lambda_a^i (1 - \lambda_a^i) \hat{\mathbf{z}}_{k-i|k-1} \hat{\mathbf{z}}_{k-i|k-1}^T. \quad (5.7)$$

*Proof.* For  $\mathbf{y}_k$  and  $\hat{\mathbf{y}}_{k|k-1}$  given through Eqs. (5.4) and (5.6), respectively, we get

$$\mathbf{y}_k - \hat{\mathbf{y}}_{k|k-1} = \underbrace{\sum_{i=0}^{k-1} \alpha_{i+1} (\mathbf{z}_{k-i} - \hat{\mathbf{z}}_{k-i|k-1})}_{\mathbf{M}_1} + \underbrace{\sum_{i=0}^{k-1} (\alpha_{i+1} - \lambda_a^i) \hat{\mathbf{z}}_{k-i|k-1}}_{\mathbf{M}_2}. \quad (5.8)$$

Thus,  $\mathbf{P}_{k|k-1}^{\mathbf{y}\mathbf{y}} = \mathbb{E}[(\mathbf{y}_k - \hat{\mathbf{y}}_{k|k-1})(\mathbf{y}_k - \hat{\mathbf{y}}_{k|k-1})^T]$  can be expressed as

$$\mathbf{P}_{k|k-1}^{\mathbf{y}\mathbf{y}} = \mathbb{E}[\mathbf{M}_1 \mathbf{M}_1^T] + \mathbb{E}[\mathbf{M}_1 \mathbf{M}_2^T] + \mathbb{E}[\mathbf{M}_2 \mathbf{M}_1^T] + \mathbb{E}[\mathbf{M}_2 \mathbf{M}_2^T]. \quad (5.9)$$

As  $\alpha_{i+1}$  and  $\mathbf{z}_{k-i}$  are independent, for  $\mathbf{M}_1$  given in Eq. (5.8), we obtain

$$\mathbb{E}[\mathbf{M}_1 \mathbf{M}_1^T] = \sum_{i=0}^{k-1} \mathbb{E}[\alpha_{i+1}^2] \mathbb{E}[(\mathbf{z}_{k-i} - \hat{\mathbf{z}}_{k-i|k-1})(\mathbf{z}_{k-i} - \hat{\mathbf{z}}_{k-i|k-1})^T].$$

Please note that  $\mathbb{E}[(\mathbf{z}_{k-i} - \hat{\mathbf{z}}_{k-i|k-1})(\mathbf{z}_{k-i} - \hat{\mathbf{z}}_{k-i|k-1})^T] = \mathbf{P}_{k-i|k-1}^{\mathbf{z}\mathbf{z}}$ , with  $\mathbb{E}[\alpha_{i+1}^2] = \mathbb{E}[\alpha_{i+1}]$  from Eq. (5.5), we get

$$\mathbb{E}[\mathbf{M}_1 \mathbf{M}_1^T] = \sum_{i=0}^{k-1} \lambda_a^i \mathbf{P}_{k-i|k-1}^{\mathbf{z}\mathbf{z}}. \quad (5.10)$$

Similarly, for  $\mathbf{M}_1$  and  $\mathbf{M}_2$  defined in Eq. (5.8), we have

$$\mathbb{E}[\mathbf{M}_1 \mathbf{M}_2^T] = \mathbb{E}\left[\sum_{i=0}^{k-1} \alpha_{i+1} (\mathbf{z}_{k-i} - \hat{\mathbf{z}}_{k-i|k-1}) \sum_{i=0}^{k-1} (\alpha_{i+1} - \lambda_a^i) \hat{\mathbf{z}}_{k-i|k-1}^T\right].$$

This equation can be rewritten as

$$\mathbb{E} [\mathbf{M}_1 \mathbf{M}_2^T] = \sum_{s=0}^{k-1} \sum_{t=0}^{k-1} \mathbb{E} \left[ \boldsymbol{\alpha}_{s+1} (\boldsymbol{\alpha}_{t+1} - \lambda_a^t) \mathbf{z}_{k-s} \hat{\mathbf{z}}_{k-t|k-1}^T - \boldsymbol{\alpha}_{s+1} \times \right. \\ \left. (\boldsymbol{\alpha}_{t+1} - \lambda_a^t) \hat{\mathbf{z}}_{k-s|k-1} \hat{\mathbf{z}}_{k-t|k-1}^T \right].$$

As  $\mathbb{E}[\mathbf{z}_{k-s}] = \hat{\mathbf{z}}_{k-s|k-1}$ , we get

$$\mathbb{E} [\mathbf{M}_1 \mathbf{M}_2^T] = 0, \quad (5.11)$$

which also concludes that

$$\mathbb{E} [\mathbf{M}_2 \mathbf{M}_1^T] = 0. \quad (5.12)$$

Finally, for  $\mathbf{M}_2$  given in Eq. (5.8), we can write

$$\mathbb{E} [\mathbf{M}_2 \mathbf{M}_2^T] = \sum_{i=0}^{k-1} \mathbb{E} \left[ (\boldsymbol{\alpha}_{i+1} - \lambda_a^i)^2 \right] \hat{\mathbf{z}}_{k-i|k-1} \hat{\mathbf{z}}_{k-i|k-1}^T.$$

Taking Binomial expansion, and substituting  $\mathbb{E}[\boldsymbol{\alpha}_{i+1}^2] = \mathbb{E}[\boldsymbol{\alpha}_{i+1}]$  from Eq. (5.5), we obtain

$$\mathbb{E} [\mathbf{M}_2 \mathbf{M}_2^T] = \sum_{i=0}^{k-1} \lambda_a^i (1 - \lambda_a^i) \hat{\mathbf{z}}_{k-i|k-1} \hat{\mathbf{z}}_{k-i|k-1}^T. \quad (5.13)$$

Finally, substituting  $\mathbb{E}[\mathbf{M}_1 \mathbf{M}_1^T]$ ,  $\mathbb{E}[\mathbf{M}_1 \mathbf{M}_2^T]$ ,  $\mathbb{E}[\mathbf{M}_2 \mathbf{M}_1^T]$ , and  $\mathbb{E}[\mathbf{M}_2 \mathbf{M}_2^T]$  from Eqs. (5.10), (5.11), (5.12), and (5.13), respectively into Eq. (5.9), we obtain  $\mathbf{P}_{k|k-1}^{\mathbf{y}\mathbf{y}}$  as given in Eq. (5.7).  $\square$

**Theorem 5.3.** The state-measurement cross-covariance for the delayed measurement  $\mathbf{y}_k$  can be obtained as

$$\mathbf{P}_{k|k-1}^{\mathbf{x}\mathbf{y}} = \sum_{i=0}^{k-1} \lambda_a^i \mathbf{P}_{k-i|k-1}^{\mathbf{x}\mathbf{z}}. \quad (5.14)$$

*Proof.* Substituting  $\mathbf{y}_k - \hat{\mathbf{y}}_{k|k-1}$  from Eq. (5.8) in  $\mathbf{P}_{k|k-1}^{\mathbf{x}\mathbf{y}} = \mathbb{E}[(\mathbf{x}_k - \hat{\mathbf{x}}_{k|k-1})(\mathbf{y}_k - \hat{\mathbf{y}}_{k|k-1})^T]$ , we get

$$\mathbf{P}_{k|k-1}^{\mathbf{x}\mathbf{y}} = \mathbb{E}[(\mathbf{x}_k - \hat{\mathbf{x}}_{k|k-1})(\mathbf{M}_1 + \mathbf{M}_2)^T]. \quad (5.15)$$

For  $\mathbf{M}_1$  given in Eq. (5.8), we get

$$\mathbb{E}[(\mathbf{x}_k - \hat{\mathbf{x}}_{k|k-1})\mathbf{M}_1^T] = \mathbb{E}\left[(\mathbf{x}_k - \hat{\mathbf{x}}_{k|k-1}) \sum_{i=0}^{k-1} \boldsymbol{\alpha}_{i+1} (\mathbf{z}_{k-i} - \hat{\mathbf{z}}_{k-i|k-1})^T\right].$$

Following the previous discussion,  $\boldsymbol{\alpha}_{i+1}$  is independent of  $\mathbf{x}_k$  and  $\mathbf{z}_k$ . Thus, substituting  $\mathbb{E}[\boldsymbol{\alpha}_{i+1}]$  from Eq. (5.5), we get

$$\mathbb{E}[(\mathbf{x}_k - \hat{\mathbf{x}}_{k|k-1})\mathbf{M}_1^T] = \sum_{i=0}^{k-1} \lambda_a^i \mathbf{P}_{k-i|k-1}^{\mathbf{xz}}. \quad (5.16)$$

Similarly, for  $\mathbf{M}_2$  given in Eq. (5.8), we obtain

$$\mathbb{E}[(\mathbf{x}_k - \hat{\mathbf{x}}_{k|k-1})\mathbf{M}_2^T] = \mathbb{E}\left[(\mathbf{x}_k - \hat{\mathbf{x}}_{k|k-1}) \sum_{i=0}^{k-1} (\boldsymbol{\alpha}_{i+1} - \lambda_a^i) \hat{\mathbf{z}}_{k-i|k-1}^T\right].$$

Recalling that  $\boldsymbol{\alpha}_{i+1}$  and  $\mathbf{x}_k$  are statistically independent, we expand the above expression and substitute  $\mathbb{E}[\mathbf{x}_k] = \hat{\mathbf{x}}_{k|k-1}$  and the value of  $\mathbb{E}[\boldsymbol{\alpha}_{i+1}]$  from Eq. (5.5) in the resulting expression. Subsequently, we get

$$\mathbb{E}[(\mathbf{x}_k - \hat{\mathbf{x}}_{k|k-1})\mathbf{M}_2^T] = 0. \quad (5.17)$$

We now substitute  $\mathbb{E}[(\mathbf{x}_k - \hat{\mathbf{x}}_{k|k-1})\mathbf{M}_1^T]$  and  $\mathbb{E}[(\mathbf{x}_k - \hat{\mathbf{x}}_{k|k-1})\mathbf{M}_2^T]$  from Eqs. (5.16) and (5.17), respectively into Eq. (5.15) and obtain  $\mathbf{P}_{k|k-1}^{\mathbf{xy}}$  as expressed in Eq. (5.14).  $\square$

To this end, we reiterate that the proposed Gaussian filtering method re-derives the measurement parameters for delayed measurement  $\mathbf{y}_k$ . Subsequently, the traditional measurement parameters  $\hat{\mathbf{z}}_{k|k-1}$ ,  $\mathbf{P}_{k|k-1}^{\mathbf{zz}}$ , and  $\mathbf{P}_{k|k-1}^{\mathbf{xz}}$ , are replaced by the modified measurement parameters  $\hat{\mathbf{y}}_{k|k-1}$ ,  $\mathbf{P}_{k|k-1}^{\mathbf{yy}}$ , and  $\mathbf{P}_{k|k-1}^{\mathbf{xy}}$ , respectively for developing the proposed filtering algorithm. The pseudo code for implementing the proposed filtering algorithm for handling the delayed measurements is provided in Algorithm 5.1.



**Algorithm 5.1** Pseudo code for implementing the proposed Gaussian filtering algorithm

---

**Input:**  $\mathbf{Q}_k$ ,  $\mathbf{R}_k$ ,  $N_s$ ,  $\lambda$ , and filter-specific sigma points and weights.

**Output:**  $\hat{\mathbf{x}}_{k|k} \forall k \in \{1, 2, \dots, N_s\}$ .

- 1: *Initialisation:*  $\hat{\mathbf{x}}_{0|0}$ ,  $\mathbf{P}_{0|0}$ , and  $k = 1$ .
  - 2: **while**  $k \leq N_s$  **do**
  - 3:     Compute  $\hat{\mathbf{x}}_{k|k-1}$  and  $\mathbf{P}_{k|k}$  (References [11] and [15]).
  - 4:     Compute  $\hat{\mathbf{z}}_{k|k-1}$ ,  $\mathbf{P}_{k|k-1}^{zz}$ , and  $\mathbf{P}_{k|k-1}^{xz}$  (References [11] and [15]).
  - 5:     Compute  $\hat{\mathbf{y}}_{k|k-1}$ ,  $\mathbf{P}_{k|k-1}^{yy}$ , and  $\mathbf{P}_{k|k-1}^{xy}$  (Eqs. (5.6), (5.7), and (5.14), respectively).
  - 6:     Compute the Kalman gain as  $\mathbf{K} = \mathbf{P}_{k|k-1}^{xy} (\mathbf{P}_{k|k-1}^{yy})^{-1}$ .
  - 7:     Compute the desired posterior estimate as  $\hat{\mathbf{x}}_{k|k} = \hat{\mathbf{x}}_{k|k-1} + \mathbf{K}(\mathbf{y}_k - \hat{\mathbf{y}}_{k|k-1})$ .
  - 8:     Compute the posterior error covariance as  $\mathbf{P}_{k|k} = \mathbf{P}_{k|k-1} - \mathbf{K} \mathbf{P}_{k|k-1}^{yy} \mathbf{K}^T$ .
  - 9: **return**  $\hat{\mathbf{x}}_{k|k}$
  - 10:     $k = k + 1$
  - 11: **end while**
- 

## 5.4 Simulation and results

In this section, we implement the proposed filtering technique for the CKF-based formulation, which is abbreviated as CKF\_RD\_PD. We compare its performance with the traditional CKF [9] and three state-of-art delayed filtering algorithms abbreviated as CKF\_1D [124], CKF\_RD [125], and MLCKF [126] under the CKF-based formulations. Unless it is specified, we implement the CKF\_1D, CKF\_RD, and MLCKF by assigning their delay-probability parameter (presumed unknown delay probability) as 0.2. Moreover, we consider the maximum possible delay as four sampling intervals in implementing the CKF\_RD and MLCKF. As mentioned in [123, 124], the delays are usually not arbitrarily large. Therefore, we restrict the performance analysis for the average delay  $\lambda = 1.5$  (instantaneous delays may be significantly higher). We use Poisson random variable  $\bar{\Theta}$  and the non-delayed measurement  $\mathbf{z}_k$  (obtained through Eqs. (5.1) and (5.2))  $\forall k \in \{1, 2, \dots, N_s\}$  for generating the simulated dataset of the delayed measurements  $\mathbf{y}_k \forall k \in \{1, 2, \dots, N_s\}$  using Eq. (5.4). Our performance analysis is based on root mean square error (RMSE), obtained between the true and estimated states for various Monte-Carlo simulations. In this regard, we perform the simulation over 200 time-steps and implement 200 Monte-Carlo simulations for computing the RMSEs.

### 5.4.1 Problem 1

This problem is about identifying multiple sinusoids from noisy measurements of a signal formed by superimposition of all sinusoids [15, 125]. For the simulation, we particularly consider that three sinusoids are forming the superimposed signal. Please note that a sinusoid is fundamentally characterized by amplitude and frequency. Therefore, we characterize the three unknown sinusoids with the state variable  $\mathbf{x}_k = [f_{1,k} \ f_{2,k} \ f_{3,k} \ a_{1,k} \ a_{2,k} \ a_{3,k}]^T$ , where  $a_{i,k}$  and  $f_{i,k} \ \forall i \in \{1, 2, 3\}$  represent the amplitude and frequency, respectively of the  $i^{th}$  sinusoid. Subsequently, the state-space model follows Eqs. (4.14) and (4.15).

We define two different scenarios with different sets of initial frequencies and amplitudes, given as Scenario-1:  $\mathbf{x}_0 = [1000 \ 2500 \ 1500 \ 2 \ 1 \ 7]^T$  and Scenario-2:  $\mathbf{x}_0 = [200 \ 1000 \ 1200 \ 3 \ 4 \ 5]^T$ . Please note that the different sets of amplitudes and frequencies infer that different sets of sinusoids are forming the superimposed signal.

The initial estimate for filtering is taken as  $\hat{\mathbf{x}}_{0|0} \sim \mathcal{N}(\mathbf{x}_0, \mathbf{P}_0)$ , with  $\mathbf{P}_0 = \text{diag}([10 \ 2 \ 5 \ 0.2 \ 0.12 \ 0.5])$ . The noise covariances are  $\mathbf{Q}_k = \text{diag}([\tau_f^2 \ \tau_f^2 \ \tau_f^2 \ \tau_a^2 \ \tau_a^2 \ \tau_a^2])$  and  $\mathbf{R}_k = \text{diag}([0.09 \ 0.09])$ , with  $\tau_f = 0.14$  and  $\tau_a = 0.05$ . The RMSEs are computed by combining all amplitudes or frequencies together [15].

Figs. 5.2 and 5.3 show the mean RMSE plots of the amplitude and frequency for varying average delay. The figures conclude a reduced RMSE of the proposed CKF\_RD\_PD, which further concludes an improved accuracy of the proposed method. The figures also show that the RMSE increases with the increasing delay possibilities, which is well expected. Moreover, as the average delay increases, the RMSEs of the existing filters increase faster, which concludes that the accuracy of the existing filters deteriorates faster for the increasing delay. The relative computational times of CKF, CKF\_1D, CKF\_RD, MLCKF, CKF\_RD\_PD are observed as 1, 1.21, 1.19, 3.07, 1.512, respectively.

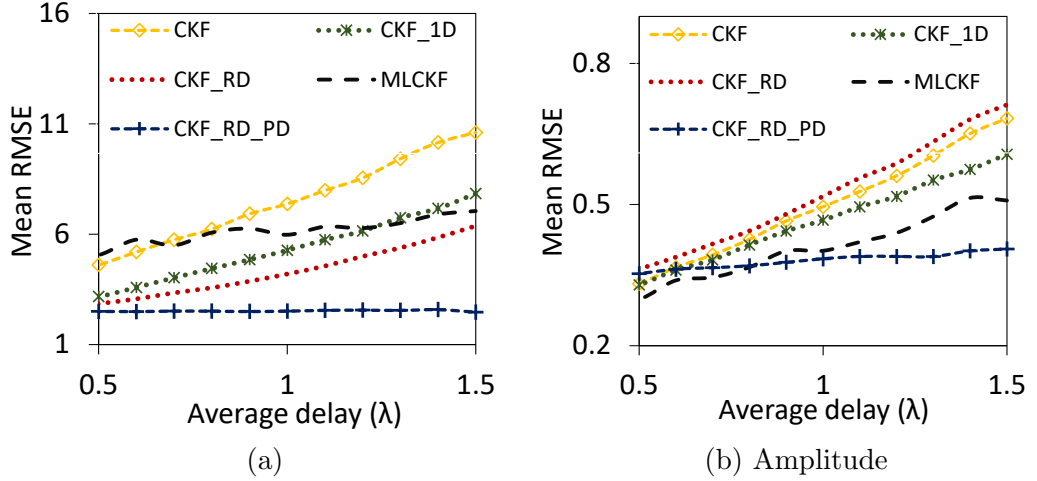


Figure 5.2: Problem 1, Scenario-1: Mean RMSEs obtained for the proposed and the existing filters for varying average delay ( $\lambda$ ).

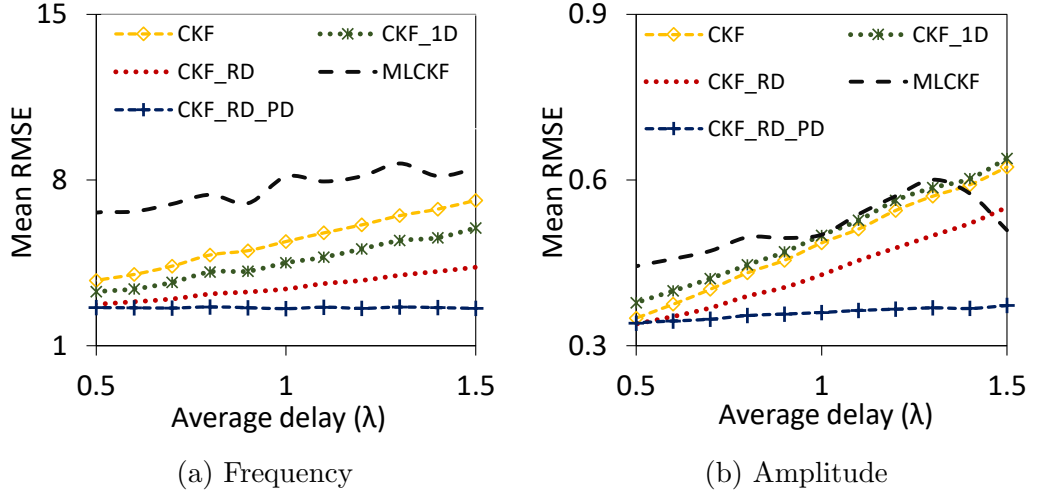


Figure 5.3: Problem 1, Scenario-2: Mean RMSEs obtained for the proposed and the existing filters for varying average delay ( $\lambda$ ).

### 5.4.2 Problem 2

We adopt the second problem from Reference [126], which follows the following state space model

$$\mathbf{x}_k = 0.5\mathbf{x}_{k-1} + \frac{25\mathbf{x}_{k-1}}{(1 + \mathbf{x}_{k-1}^2) + 8 \cos(1.2(k-1))} + \boldsymbol{\eta}_k. \quad (5.18)$$

$$\mathbf{z}_k = \frac{\mathbf{x}_k^2}{20} + \boldsymbol{\nu}_k. \quad (5.19)$$

We choose  $\mathbf{x}_0 = 2$ , and evaluate the performance for two scenarios of noise covariances, given as, Scenario-1:  $\mathbf{Q}_k = 5$  and  $\mathbf{R}_k = 1$  and Scenario-2:  $\mathbf{Q}_k = 2$  and

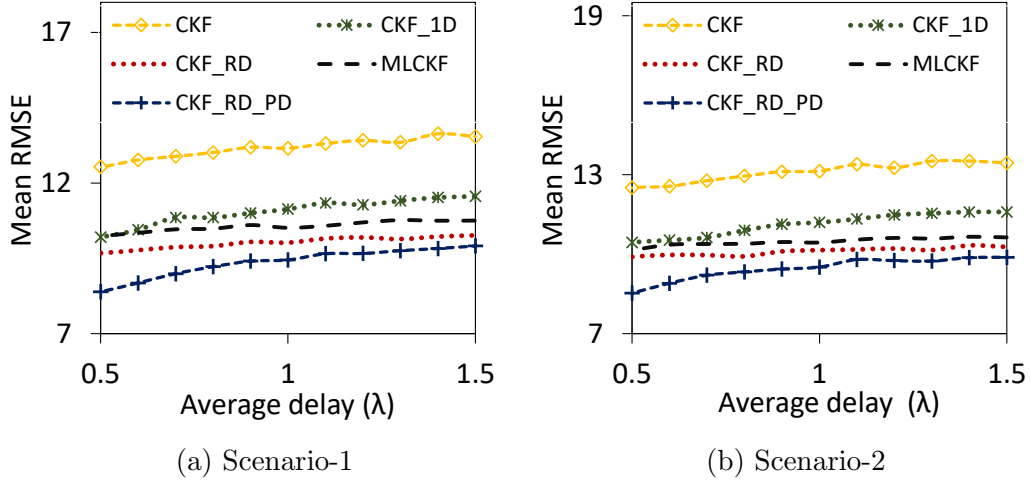


Figure 5.4: Problem 2: Mean RMSEs obtained for the proposed and the existing filters for varying average delay ( $\lambda$ ).

$\mathbf{R}_k = 0.5$ . The filter is initialized with  $\hat{\mathbf{x}}_{0|0} = 6$  and  $\mathbf{P}_{0|0} = 5$ .

The mean RMSEs of existing delay filters and the proposed CKF\_RD\_PD are compared in Fig. 5.4. It can be observed that the mean RMSEs for the CKF\_RD\_PD are notably reduced, which concludes the improved accuracy of the proposed method. The relative computational times are obtained similar to Problem 1.

### 5.4.3 Extended comparison for varying delay probabilities and mismatched model

The accuracy of the existing delay filters broadly depends on the preassigned delay probabilities. Thus, we further extend the comparative analysis for varying delay probabilities of the existing delay filters in Table 7.2 for Problems 1 and 2. The table concludes that the average RMSEs of the existing delay filters are consistently higher than the proposed CKF\_RD\_PD for all delay probabilities. It further concludes that the proposed filter outperforms the existing delay filters for all variations in the preassigned delay probabilities.

Table 5.1: Average RMSEs obtained for the proposed method (CKF\_RD\_PD) and the existing delay filters (CKF\_ID [121], CKF\_RD [122], and MLCKF [123]) applied with varying delay probabilities ( $\rho_d$ ) for Problem 1 and Problem 2. The delay scenario is simulated for  $\lambda = 1.5$  while Scenario 1 and Scenario 2 denoting the respective scenarios for Problem 1 and Problem 2.

States	$\rho_d$	Problem 1						Problem 2					
		Amplitude			Frequency			State 1			State 2		
		[121]	[122]	[123]	CKF_RD_PD	[121]	[122]	[123]	CKF_RD_PD	[121]	[122]	[123]	CKF_RD_PD
Scenario 1	0.2	0.522	1.049	0.456		5.352	2.862	7.109		11.592	10.274	10.632	
	0.5	0.571	0.578	0.466	0.4055	6.636	4.325	6.794	2.469	11.594	10.287	11.233	9.882
	0.8	0.607	0.712	0.509		7.840	6.375	7.051		11.761	10.686	11.713	
Scenario 2	0.2	0.505	1.199	0.601		3.598	2.744	8.497		11.411	9.836	11.063	
	0.5	0.592	0.496	0.511	0.372	5.314	3.571	7.928	2.578	11.292	10.043	11.409	9.385
	0.8	0.639	0.551	0.509		5.980	4.316	8.496		11.776	10.473	11.960	

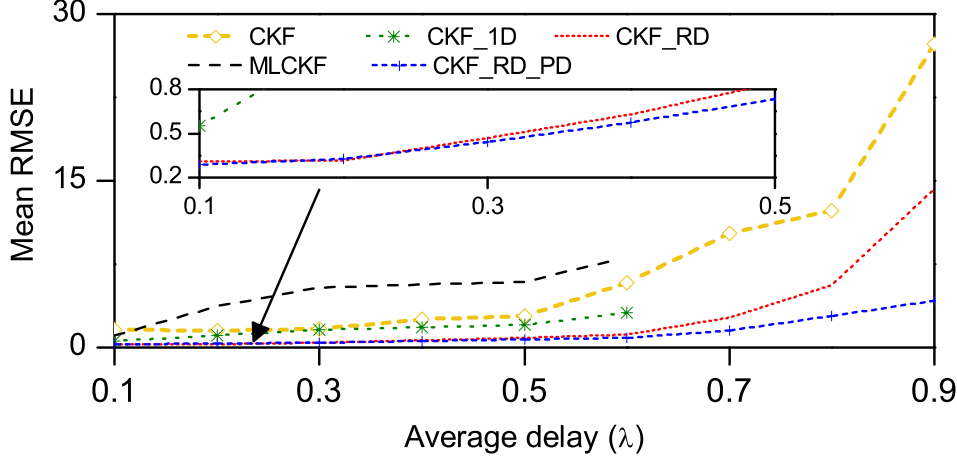


Figure 5.5: Problem 1, Scenario-1: Performance analysis with mismatched delay model.

We further extend the analysis to the scenario wherein the delay model mismatches with the proposed one (5.4). In this context, we generate the data  $\mathbf{y}_k$  through the model proposed in Reference [125] considering only Problem 1, Scenario-1 as the test system to keep it brief. Subsequently, we compare the mean RMSE for the amplitude in Fig. 5.5. The figure concludes an improved filtering performance of the proposed method even if the measurement model is mismatched. Please note that CKF\_1D and MLCKF completely fail for higher delay probabilities.

## 5.5 Summary

This chapter develops an advanced Gaussian filtering technique for handling delayed measurements. The proposed method reformulates the traditional measurement model using the Poisson distribution and considering that the average delay information is known. Subsequently, it re-derives the traditional expressions of the measurement estimate, measurement covariance, and the state-measurement cross-covariance, which are influenced by the delayed measurements.

The proposed method celebrates two major advantages over the existing delay filters: i) it requires the generally known average delay information instead of the usually unknown delay-probabilities and ii) it precludes the ambiguous selection of the upper bound of the delay. The proposed method is a general extension of the Gaussian filtering method, which is applicable to any of the existing Gaussian filters,

such as the EKF, UKF, and CKF. We use the CKF-based formulation for validating the improved accuracy of the proposed method for delayed measurements. The computational time of the proposed method is marginally increased in comparison to some of the existing filters.





# Chapter 6

## Gaussian Filtering with Stochastically Composed Current and Past Measurements

### 6.1 Introduction

As discussed in the previous chapter, the delayed measurements phenomenon inherently appears in many practical systems. The existing delay filters, such as [121–126], address the delay scenario with the measurements completely belonging to any of the previous time instants. Specifically, the complete measurement is received by a single sensor node. In many practical systems, however, the measurements are acquired in fractions at different geographical locations [169, 170]. Subsequently, these fractions are transmitted through individual communication channels to a data processing center and superimposed to form the complete measurement for filtering. The unreliable channels frequently cause one or more fractions of measurement to reach the estimator with delay. Consequently, the available measurement may contain some fractions from past instants. More specifically, the inaccurately received measurement is stochastically composed of the current and past hypothetically true measurements. To the best of the author’s knowledge, this irregularity is being addressed for the first time in the filtering literature.

### 6.1.1 The Proposed Measurement Irregularity

As discussed earlier, this chapter is concerned with a new kind of delayed measurement irregularity, which is, to the best of the authors' knowledge, yet not addressed in the filtering literature. Under this irregularity, the inaccurately received measurement  $\mathbf{y}_k$  (at  $t_k$ ) is stochastically composed of the current and past true measurements (hypothetical measurements that would have been received under the non-existence of the concerned irregularity), the hypothetical true measurement at  $t_k$  is denoted as  $\mathbf{z}_k$ .

The above mentioned irregularity appears when the measurement is generated and propagated through the following sequence of events: i)  $\mathbf{z}_k$  is observed into pieces using multiple sources (*e.g.*, with  $p$  number of sources, it may be observed  $\Phi_1\mathbf{z}_k, \Phi_2\mathbf{z}_k, \dots, \Phi_p\mathbf{z}_k$  with  $0 \leq \Phi_j \leq 1 \ \forall j \in \{1, 2, \dots, p\}$  and  $\sum_{j=0}^p \Phi_j = 1$ ), ii) the measurement pieces  $\Phi_1\mathbf{z}_k, \Phi_2\mathbf{z}_k, \dots, \Phi_p\mathbf{z}_k$  are independently propagated through asynchronously time-delayed channels, and iii) data received from all channels (measurement pieces) are superimposed to eventually obtain the measurement. Due to the asynchronously time-delayed propagations,  $\Phi_1\mathbf{z}_k, \Phi_2\mathbf{z}_k, \dots, \Phi_p\mathbf{z}_k$  get distributed over the current and future sampling instants. For example, if the maximum propagation delay is one sampling interval, then, each of  $\Phi_1\mathbf{z}_k, \Phi_2\mathbf{z}_k, \dots, \Phi_p\mathbf{z}_k$  reaches at either of  $t_k$  and  $t_{k+1}$ , depending on their respective propagation delays. In this case, at  $t_k$ , the estimator receives some measurement pieces from  $t_{k-1}$  (for delayed channels) and the remaining pieces from  $t_k$  (for non-delayed channels). Alternatively,  $\mathbf{y}_k$  is superimposed of  $\alpha_{k,1}\mathbf{z}_{k-1}$  and  $\alpha_{k,0}\mathbf{z}_k$ , with the constants  $\alpha_{k,1}$  and  $\alpha_{k,0}$  being unknown as the propagation delays of various channels are unknown and time-varying. Generalizing this discussion for larger propagation delays, it can be stated that  $\mathbf{y}_k$  is composed of  $\alpha_{k,N_d}\mathbf{z}_{k-N_d}, \alpha_{k,N_d-1}\mathbf{z}_{k-N_d+1}, \dots, \alpha_{k,0}\mathbf{z}_k$  with  $N_d$  representing the maximum delay in any propagation channel, and the coefficients  $\alpha_{k,N_d}, \alpha_{k,N_d-1}, \dots, \alpha_{k,0}$  remaining unknown. Summarily, the inaccurately received  $\mathbf{y}_k$  is stochastically composed of the current and past true measurements ( $\mathbf{z}_k, \mathbf{z}_{k-1}, \dots, \mathbf{z}_{k-N_d}$ ).

Let us discuss below two practical examples, where the measurements are observed into pieces, and different pieces are propagated with asynchronous delays, causing the concerned irregularity.

- Example 1 (from engineering domain): In power system state estimation [169], multiple power meters, located at peripheral branches, are installed to observe a power flow measurement into pieces. The power meter readings are independently transmitted through asynchronously delayed communication channels.
- Example 2 (from non-engineering domain): Let us consider the problem of estimating the model compartmental populations of COVID-19 pandemic model in a country [171, 172]. The measurements, in this case, may be the day-to-day infections, deaths, and vaccinations. Such data are generally revealed by the country's central agencies after superimposing the piece-wise received data from multiple local institutions. However, the local institutions' response times are asynchronous, resulting into asynchronous delays in receiving the pieces of the desired information.

### 6.1.2 An Overview of the Proposed Method

In this chapter, the author introduces an advanced Gaussian filtering technique to handle the concerned measurement irregularity, giving an inaccurate measurement that is stochastically composed of the current and past true measurements. In this regard, the author reformulates the measurement model to incorporate the possibility of the concerned irregularity. Subsequently, the author re-derives the traditional Gaussian filtering technique for the modified measurement model, resulting into the proposed filtering method. The proposed filtering method is named as Gaussian filtering with stochastically composed measurements (GFSCM). Interestingly, the proposed GFSCM is a general extension of Gaussian filtering, which is applicable to any of the existing Gaussian filters, such as the EKF, CKF, and GHF. The simulation validates the improved accuracy of GFSCM for two nonlinear filtering problems.

Let us now summarize the above discussion by highlighting the primary contributions of the chapter as follows

- Addressing a new kind of delayed measurement irregularity, with the actual measurement being stochastic composition of non-delayed and delayed measurements.

- Formation of a new measurement model incorporating the concerned irregularity.
- Designing a generalized Gaussian filter according to the newly formed measurement model.
- Validating an improved filtering performance of the proposed filter over the traditional Gaussian filters and popular existing works to handle the delayed measurements.

## 6.2 Problem formulation

Let us recall Eqs. (1.1) and (1.2) from Chapter 1 the nonlinear dynamical system with state space model given as

$$\mathbf{x}_k = f(\mathbf{x}_{k-1}) + \boldsymbol{\eta}_k. \quad (6.1)$$

$$\mathbf{z}_k = h(\mathbf{x}_k) + \boldsymbol{\nu}_k. \quad (6.2)$$

Please note that  $\mathbf{z}_k$  is the hypothetical true measurement, which would have been observed if there was no irregularity. Recalling the previous discussion, inaccurately received measurement is  $\mathbf{y}_k$ , which is stochastically composed of  $\mathbf{z}_k, \mathbf{z}_{k-1}, \dots, \mathbf{z}_{k-N_d}$ . Please note that  $N_d$  is practitioners' choice with freedom to choose any large value.

As discussed previously, the delays in propagation channels are unknown, which causes uncertainty in the measurement pieces being received at  $t_k$  from  $t_k, t_{k-1}, \dots, t_{k-N_d}$ . Therefore, the author randomly generates a set of coefficients as  $\alpha_{k,j} \sim \mathcal{N}(\hat{\alpha}_j, P_{a_j}) \forall j \in \{0, 1, \dots, N_d\}$ , characterizing the proportions of measurements contributed from the sampling instants  $t_{k-j} \forall j \in \{0, 1, \dots, N_d\}$ . Please note that the parameters  $\hat{\alpha}_j$  and  $P_{a_j}$  can be derived from the attributes and past records of the propagation channels, relating to the asynchronous delays.

Based on the stochastically generated coefficients  $\alpha_{k,j} (\forall j \in \{0, 1, \dots, N_d\})$ ,  $\mathbf{y}_k$  could be stochastically modeled as

$$\mathbf{y}_k = \sum_{j=0}^{N_d} \alpha_{k,j} \mathbf{z}_{k-j} = \sum_{j=0}^{N_d} \alpha_{k,j} (h(\mathbf{x}_{k-j}) + \boldsymbol{\nu}_{k-j}). \quad (6.3)$$

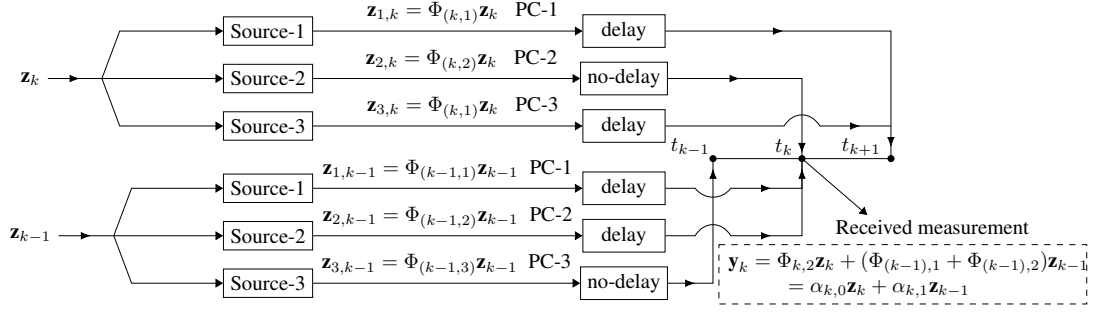


Figure 6.1: Block diagram for receiving the irregular measurement  $\mathbf{y}_k$  as stochastic combination of the current and past hypothetical true measurements. This block diagram considers the following: i) three sources are used for observing the measurements into three independent pieces and ii) a propagation channel (PC) can be maximum of one-step delayed, *i.e.*, the delay simply means to one-step delay.

Please refer to Fig. 6.1 for the process to generate and model the received measurement  $\mathbf{y}_k$ .

To this end, the objective is to estimate the unknown states  $\mathbf{x}_k \forall k \in \{1, 2, \dots\}$  as the inaccurate measurement  $\mathbf{y}_k$  is sequentially received  $\forall k \in \{1, 2, \dots\}$ . Please note that the actually received measurement  $\mathbf{y}_k$  is already modeled in terms of the hypothetical true measurements  $\mathbf{z}_{k-j} \forall j \in \{0, 1, \dots, N_d\}$  in Eq. (6.3). Therefore, accomplishing the objective requires re-deriving the traditional Gaussian filtering methodology for the state space model characterized by Eqs. (6.1) and (6.3).

**Remark 6.1.** Generalizing Fig. 6.1 for  $N_d$ -delay and  $p$  sources, the coefficients  $\alpha_{k,j} \forall j \in \{0, 1, \dots, N_d\}$  are obtained as the summation of random combinations of  $\Phi_j (j \in \{0, 1, \dots, p\})$ . Furthermore, the random combination at a particular instant results from the delay occurrences in different channels from the same instant. As the delay occurrences are considered to be independently and identically distributed, the resulting coefficients  $\alpha_{k,j}$  tend to be normally distributed following the central limit theorem [173].

### 6.3 Filtering with stochastically composed current and past measurements

In this section, the author derives the proposed GFSCM for the inaccurately received measurement that is stochastically composed of the current and past true measurements. Recalling the problem formulation, the proposed GFSCM can be

designed by re-deriving the traditional Gaussian filtering methodology for the modified measurement model, given in Eq. (6.3). Let us reiterate the inference that any variation in the measurements (*e.g.*, due to the concerned irregularity) influences only three expressions of the Gaussian filtering: the measurement estimate, measurement covariance, and state-measurement cross-covariance. Therefore, the re-derivation of traditional Gaussian filtering requires to re-derive only these three expressions.

To this end, let us denote as  $\hat{\mathbf{z}}_{k|k-1}$ ,  $\mathbf{P}_{k|k-1}^{\mathbf{zz}}$ , and  $\mathbf{P}_{k|k-1}^{\mathbf{xz}}$  the measurement estimate, measurement covariance, and state-measurement cross-covariance, respectively for the hypothetical true measurement  $\mathbf{z}_k$ . Let us similarly denote  $\hat{\mathbf{y}}_{k|k-1}$ ,  $\mathbf{P}_{k|k-1}^{\mathbf{yy}}$ , and  $\mathbf{P}_{k|k-1}^{\mathbf{xy}}$  as the corresponding parameters for the inaccurately received measurement  $\mathbf{y}_k$ . Please note that  $\hat{\mathbf{z}}_{k|k-1}$ ,  $\mathbf{P}_{k|k-1}^{\mathbf{zz}}$ , and  $\mathbf{P}_{k|k-1}^{\mathbf{xz}}$  are simply the corresponding expressions of the traditional Gaussian filtering. However, deriving the proposed GFSCM to derive  $\hat{\mathbf{y}}_{k|k-1}$ ,  $\mathbf{P}_{k|k-1}^{\mathbf{yy}}$ , and  $\mathbf{P}_{k|k-1}^{\mathbf{xy}}$ . Subsequently, the proposed GFSCM can be designed by replacing  $\hat{\mathbf{z}}_{k|k-1}$ ,  $\mathbf{P}_{k|k-1}^{\mathbf{zz}}$ , and  $\mathbf{P}_{k|k-1}^{\mathbf{xz}}$  with  $\hat{\mathbf{y}}_{k|k-1}$ ,  $\mathbf{P}_{k|k-1}^{\mathbf{yy}}$ , and  $\mathbf{P}_{k|k-1}^{\mathbf{xy}}$ , respectively in the traditional Gaussian filtering methodology. The subsequent theorems derive  $\hat{\mathbf{y}}_{k|k-1}$ ,  $\mathbf{P}_{k|k-1}^{\mathbf{yy}}$ , and  $\mathbf{P}_{k|k-1}^{\mathbf{xy}}$ .

**Theorem 6.1.** The measurement estimate  $\hat{\mathbf{y}}_{k|k-1}$  for the inaccurately received measurement  $\mathbf{y}_k$  (Eq. (6.3)) can be given as

$$\hat{\mathbf{y}}_{k|k-1} = \sum_{j=0}^{N_d} \hat{\alpha}_j \hat{\mathbf{z}}_{k-j|k-1}, \quad (6.4)$$

*Proof.* For  $\mathbf{y}_k$  given in Eq. (6.3), we get

$$\hat{\mathbf{y}}_{k|k-1} = \mathbb{E}[\mathbf{y}_k] = \mathbb{E} \left[ \sum_{j=0}^{N_d} \alpha_{k,j} \mathbf{z}_{k-j} \right].$$

Please note that  $\mathbf{z}_{k-j}$  and  $\alpha_{k,j}$  are statistically independent, as they depict measurement readings and propagation delays, respectively, which are independent events. Subsequently, we simplify the above equation as

$$\hat{\mathbf{y}}_{k|k-1} = \sum_{j=0}^{N_d} \mathbb{E}[\alpha_{k,j}] \mathbb{E}[\mathbf{z}_{k-j}].$$

As  $\mathbb{E}[\alpha_{k,j}] = \hat{\alpha}_j$ , this equation deduces to Eq. (6.4).  $\square$

**Theorem 6.2.** The measurement error covariance  $\mathbf{P}_{k|k-1}^{\mathbf{y}\mathbf{y}}$  for  $\mathbf{y}_k$  can be obtained as

$$\mathbf{P}_{k|k-1}^{\mathbf{y}\mathbf{y}} = \sum_{j=0}^{N_d} ((P_{\alpha_j} + \hat{\alpha}_j^2) \mathbf{P}_{k-j|k-1}^{\mathbf{z}\mathbf{z}} + P_{\alpha_j} \hat{\mathbf{z}}_{k-j|k-1} \hat{\mathbf{z}}_{k-j|k-1}^T). \quad (6.5)$$

*Proof.* For  $\mathbf{y}_k$  and  $\hat{\mathbf{y}}_{k|k-1}$  given by Eqs. (6.3) and (6.4), respectively, we get

$$\mathbf{y}_k - \hat{\mathbf{y}}_{k|k-1} = \underbrace{\sum_{j=0}^{N_d} \alpha_{k,j} (\mathbf{z}_{k-j} - \hat{\mathbf{z}}_{k-j|k-1})}_{\mathbf{\Delta}_1} + \underbrace{\sum_{j=0}^{N_d} (\alpha_{k,j} - \hat{\alpha}_j) \hat{\mathbf{z}}_{k-j|k-1}}_{\mathbf{\Delta}_2}. \quad (6.6)$$

Thus,  $\mathbf{P}_{k|k-1}^{\mathbf{y}\mathbf{y}} = \mathbb{E}[(\mathbf{y}_k - \hat{\mathbf{y}}_{k|k-1})(\mathbf{y}_k - \hat{\mathbf{y}}_{k|k-1})^T]$  can be expressed as

$$\mathbf{P}_{k|k-1}^{\mathbf{y}\mathbf{y}} = \mathbb{E}[\mathbf{\Delta}_1 \mathbf{\Delta}_1^T] + \mathbb{E}[\mathbf{\Delta}_1 \mathbf{\Delta}_2^T] + \mathbb{E}[\mathbf{\Delta}_2 \mathbf{\Delta}_1^T] + \mathbb{E}[\mathbf{\Delta}_2 \mathbf{\Delta}_2^T]. \quad (6.7)$$

In the following analysis, we calculate each term of the right side separately and aggregate them to obtain the expression of  $\mathbf{P}_{k|k-1}^{\mathbf{y}\mathbf{y}}$ .

As  $\alpha_{k,j}$  and  $\mathbf{z}_{k-j}$  are statistically independent, for  $\mathbf{\Delta}_1$  given in Eq. (6.6), we can write

$$\mathbb{E}[\mathbf{\Delta}_1 \mathbf{\Delta}_1^T] = \sum_{j=0}^{N_d} \mathbb{E}[\alpha_{k,j}^2] \mathbb{E}[(\mathbf{z}_{k-j} - \hat{\mathbf{z}}_{k-j|k-1})(\mathbf{z}_{k-j} - \hat{\mathbf{z}}_{k-j|k-1})^T].$$

Please note that  $\mathbb{E}[\alpha_{k,j}^2] = (P_{\alpha_j} + \hat{\alpha}_j^2)$  and  $\mathbb{E}[(\mathbf{z}_{k-j} - \hat{\mathbf{z}}_{k-j|k-1})(\mathbf{z}_{k-j} - \hat{\mathbf{z}}_{k-j|k-1})^T] = \mathbf{P}_{k-j|k-1}^{\mathbf{z}\mathbf{z}}$ . Thus, we get

$$\mathbb{E}[\mathbf{\Delta}_1 \mathbf{\Delta}_1^T] = \sum_{j=0}^{N_d} (P_{\alpha_j} + \hat{\alpha}_j^2) \mathbf{P}_{k-j|k-1}^{\mathbf{z}\mathbf{z}}. \quad (6.8)$$

Similarly, for  $\mathbf{\Delta}_1$  and  $\mathbf{\Delta}_2$  given in Eq. (6.6), we have

$$\mathbb{E}[\mathbf{\Delta}_1 \mathbf{\Delta}_2^T] = \mathbb{E}\left[\sum_{j=0}^{N_d} \alpha_{k,j} (\mathbf{z}_{k-j} - \hat{\mathbf{z}}_{k-j|k-1}) \sum_{j=0}^{N_d} (\alpha_{k,j} - \hat{\alpha}_j) \hat{\mathbf{z}}_{k-j|k-1}^T\right],$$

which can be rewritten as

$$\mathbb{E}[\Delta_1 \Delta_2^T] = \sum_{t=0}^{N_d} \sum_{u=0}^{N_d} \mathbb{E} \left[ \alpha_{k,t} (\alpha_{k,u} - \hat{\alpha}_u) \mathbf{z}_{k-t} \hat{\mathbf{z}}_{k-u|k-1}^T - \alpha_{k,t} (\alpha_{k,u} - \hat{\alpha}_u) \hat{\mathbf{z}}_{k-t|k-1} \hat{\mathbf{z}}_{k-u|k-1}^T \right].$$

As  $\mathbb{E}[\mathbf{z}_{k-t}] = \hat{\mathbf{z}}_{k-t|k-1}$ , we obtain

$$\mathbb{E}[\Delta_1 \Delta_2^T] = 0, \quad (6.9)$$

which further concludes

$$\mathbb{E}[\Delta_2 \Delta_1^T] = 0. \quad (6.10)$$

Finally, for  $\Delta_2$  given in Eq. (6.6), we can write

$$\mathbb{E}[\Delta_2 \Delta_2^T] = \sum_{j=0}^{N_d} \mathbb{E} [(\alpha_{k,j} - \hat{\alpha}_j)^2] \hat{\mathbf{z}}_{k-j|k-1} \hat{\mathbf{z}}_{k-j|k-1}^T.$$

Applying the Binomial expansion, and subsequently, substituting  $\mathbb{E}[\alpha_{k,j}^2] = (P_{\alpha_j} + \hat{\alpha}_j^2)$ , we get

$$\mathbb{E}[\Delta_2 \Delta_2^T] = \sum_{j=0}^{N_d} P_{\alpha_j} \hat{\mathbf{z}}_{k-j|k-1} \hat{\mathbf{z}}_{k-j|k-1}^T. \quad (6.11)$$

Substituting  $\mathbb{E}[\Delta_1 \Delta_1^T] = \sum_{j=0}^{N_d} (P_{\alpha_j} + \hat{\alpha}_j^2) \mathbf{P}_{k-j|k-1}^{zz}$ ,  $\mathbb{E}[\Delta_1 \Delta_2^T] = 0$ ,  $\mathbb{E}[\Delta_2 \Delta_1^T] = 0$ , and  $\mathbb{E}[\Delta_2 \Delta_2^T] = \sum_{j=0}^{N_d} P_{\alpha_j} \hat{\mathbf{z}}_{k-j|k-1} \hat{\mathbf{z}}_{k-j|k-1}^T$  from Eqs. (6.8), (6.9), (6.10), and (6.11), respectively into Eq. (6.7),  $\mathbf{P}_{k|k-1}^{yy}$  can be expressed in the form of Eq. (6.5).  $\square$

**Theorem 6.3.** The cross-covariance  $\mathbf{P}_{k|k-1}^{xy}$  for the inaccurately received measurement  $\mathbf{y}_k$  (Eq. (6.3)) is obtained as

$$\mathbf{P}_{k|k-1}^{xy} = \sum_{j=0}^{N_d} \hat{\alpha}_j \mathbf{P}_{k-j|k-1}^{xz}. \quad (6.12)$$

*Proof.* Note that  $\mathbf{P}_{k|k-1}^{xy} = \mathbb{E}[\mathbf{e}_{k|k-1}(\mathbf{y}_k - \hat{\mathbf{y}}_{k|k-1})^T]$ , with  $\mathbf{e}_{k|k-1} = \mathbf{x}_k - \hat{\mathbf{x}}_{k|k-1}$ . With  $\mathbf{y}_k - \hat{\mathbf{y}}_{k|k-1}$  given in Eq. (6.6), we get

$$\mathbf{P}_{k|k-1}^{xy} = \mathbb{E}[\mathbf{e}_{k|k-1} \Delta_1^T] + \mathbb{E}[\mathbf{e}_{k|k-1} \Delta_2^T]. \quad (6.13)$$



For  $\Delta_1$  defined in Eq. (6.6), we can express

$$\mathbb{E}[\mathbf{e}_{k|k-1}\Delta_1^T] = \mathbb{E}\left[\mathbf{e}_{k|k-1}\sum_{j=0}^{N_d}\alpha_{k,j}(\mathbf{z}_{k-j}-\hat{\mathbf{z}}_{k-j|k-1})^T\right].$$

As discussed previously,  $\alpha_{k,j}$  is independent of  $\mathbf{x}_k$  and  $\mathbf{z}_k$ . Thus, substituting  $\mathbb{E}[\alpha_{k,j}] = \hat{\alpha}_j$ , we conclude

$$\mathbb{E}[\mathbf{e}_{k|k-1}\Delta_1^T] = \sum_{j=0}^{N_d}\hat{\alpha}_j\mathbf{P}_{k-j|k-1}^{\mathbf{xz}}. \quad (6.14)$$

Similarly, for  $\Delta_2$  given in Eq. (6.6), we can write

$$\mathbb{E}[\mathbf{e}_{k|k-1}\Delta_2^T] = \mathbb{E}\left[\mathbf{e}_{k|k-1}\sum_{j=0}^{N_d}(\alpha_{k,j}-\hat{\alpha}_j)\hat{\mathbf{z}}_{k-j|k-1}^T\right].$$

Expanding the above equation and substituting  $\mathbb{E}[\alpha_{k,j}] = \hat{\alpha}_j$ , we get

$$\mathbb{E}[\mathbf{e}_{k|k-1}\Delta_2^T] = 0. \quad (6.15)$$

Substituting  $\mathbb{E}[\mathbf{e}_{k|k-1}\Delta_1^T] = \sum_{j=0}^{N_d}\hat{\alpha}_j\mathbf{P}_{k-j|k-1}^{\mathbf{xz}}$  and  $\mathbb{E}[\mathbf{e}_{k|k-1}\Delta_2^T] = 0$  from Eqs. (6.14) and (6.15), respectively into Eq. (6.13), we obtain  $\mathbf{P}_{k|k-1}^{\mathbf{xy}}$  in the form of Eq. (6.12).  $\square$

From the above derivations, we get  $\hat{\mathbf{y}}_{k|k-1}$ ,  $\mathbf{P}_{k|k-1}^{\mathbf{yy}}$ , and  $\mathbf{P}_{k|k-1}^{\mathbf{xy}}$ , corresponding to the inaccurately received measurement  $\mathbf{y}_k$ . Subsequently, the proposed GFSCM is designed by replacing  $\hat{\mathbf{z}}_{k|k-1}$ ,  $\mathbf{P}_{k|k-1}^{\mathbf{zz}}$ , and  $\mathbf{P}_{k|k-1}^{\mathbf{xz}}$  with  $\hat{\mathbf{y}}_{k|k-1}$ ,  $\mathbf{P}_{k|k-1}^{\mathbf{yy}}$  and  $\mathbf{P}_{k|k-1}^{\mathbf{xy}}$ , respectively in the traditional Gaussian filtering methodology. As the modeling of  $\mathbf{y}_k$  (Eq. (6.3)) considers the errors caused due to the concerned irregularity, the proposed GFSCM addresses the concerned irregularity during the filtering. We provide a pseudo code for implementing the proposed GFSCM in Algorithm 6.1.

In this section, the author validates the improved accuracy of the proposed GFSCM for two simulation problems. The abbreviations CKF\_S, CQKF\_S, and GHF\_S represent respectively the CKF-, CQKF-, and GHF-based formulations of the proposed GFSCM. The author also performs the comparison with the existing works MLCKF [126], CKF\_GD\_RD [174], CKF\_GD [175], and CKF\_DM [29]. As discussed

---

**Algorithm 6.1** Pseudo code for implementing the proposed GFSCM

---

**Input:**  $\mathbf{Q}_k$ ,  $\mathbf{R}_k$ ,  $N_s$ ,  $\hat{\alpha}_j$ ,  $P_{a_j}$ ,  $N_d$ , and filter-specific points and weights for approximating intractable integrals.

**Output:**  $\hat{\mathbf{x}}_{k|k} \forall k \in \{1, 2, \dots, N_s\}$ .

```

1: Initialisation:  $\hat{\mathbf{x}}_{0|0}$ ,  $\mathbf{P}_{0|0}$ , and  $k = 1$ .
2: while  $k \leq N_s$  do
3:   Compute the predicted estimate and covariance of  $\mathbf{x}_k$ :  $\hat{\mathbf{x}}_{k|k-1}$  and  $\mathbf{P}_{k|k-1}$ 
     (Reference [15]).
4:   Compute the estimate and covariance for the hypothetical true measurement
      $\mathbf{z}_k$ :  $\hat{\mathbf{z}}_{k|k-1}$  and  $\mathbf{P}_{k|k-1}^{\mathbf{zz}}$  (Reference [15]).
5:   Compute the state-measurement cross-covariance:  $\mathbf{P}_{k|k-1}^{\mathbf{xz}}$  (Reference [15]).
6:   Compute the estimate and covariance for the received measurement  $\mathbf{y}_k$ :
      $\hat{\mathbf{y}}_{k|k-1}$  and  $\mathbf{P}_{k|k-1}^{\mathbf{yy}}$  (Eqs. (6.4) and (6.5), respectively).
7:   Compute the cross-covariance between  $\mathbf{x}_k$  and  $\mathbf{y}_k$ :  $\mathbf{P}_{k|k-1}^{\mathbf{xy}}$  (Eq. (6.12)).
8:   Compute the Kalman gain as  $\mathbf{K} = \mathbf{P}_{k|k-1}^{\mathbf{xy}} (\mathbf{P}_{k|k-1}^{\mathbf{yy}})^{-1}$ .
9:   Compute the desired posterior estimate as  $\hat{\mathbf{x}}_{k|k} = \hat{\mathbf{x}}_{k|k-1} + \mathbf{K}(\mathbf{y}_k - \hat{\mathbf{y}}_{k|k-1})$ .
10:  Compute the posterior error covariance as  $\mathbf{P}_{k|k} = \mathbf{P}_{k|k-1} - \mathbf{K} \mathbf{P}_{k|k-1}^{\mathbf{yy}} \mathbf{K}^T$ .
11: return  $\hat{\mathbf{x}}_{k|k}$ 
12:    $k = k + 1$ 
13: end while

```

---

in [121, 124], the propagation delays are mostly small. Thus, the simulation considers that the propagation delay does not exceed five sampling intervals, ensuring that  $N_d \leq 5$ . The performance analysis is based on the widely accepted root mean square error (RMSE) [15]. Please note that the measurement  $\mathbf{y}_k$  contains the past information and it is available to the practitioner for filtering (instead of  $\mathbf{z}_k$ ); thus, all filters in the simulation section are compared considering the measurement being  $\mathbf{y}_k$ .

### 6.3.1 Problem 1: Individual Sinusoids Identification

This example considers individual sinusoids identification problem from the measurements of the superimposed signal [15, 125], considering that three sinusoids constitute the superimposed signal. The sinusoid identification is identical to estimation of corresponding amplitudes and frequencies. Please refer to the state-space model represented by Eqs. (4.14) and (4.15) for this problem.

The initial true state considered as  $\mathbf{x}_0 = [200 \ 1000 \ 2000 \ 5 \ 4 \ 3]^T$ , while the initial estimate is generated from  $0.9\mathcal{N}(\mathbf{x}_0, \mathbf{P}_0)$ , where  $\mathbf{P}_0 = \text{diag}([20 \ 20 \ 20 \ 0.5 \ 0.5 \ 0.5])$  being the initial covariance. The simulation is performed over 200 time-steps for 300

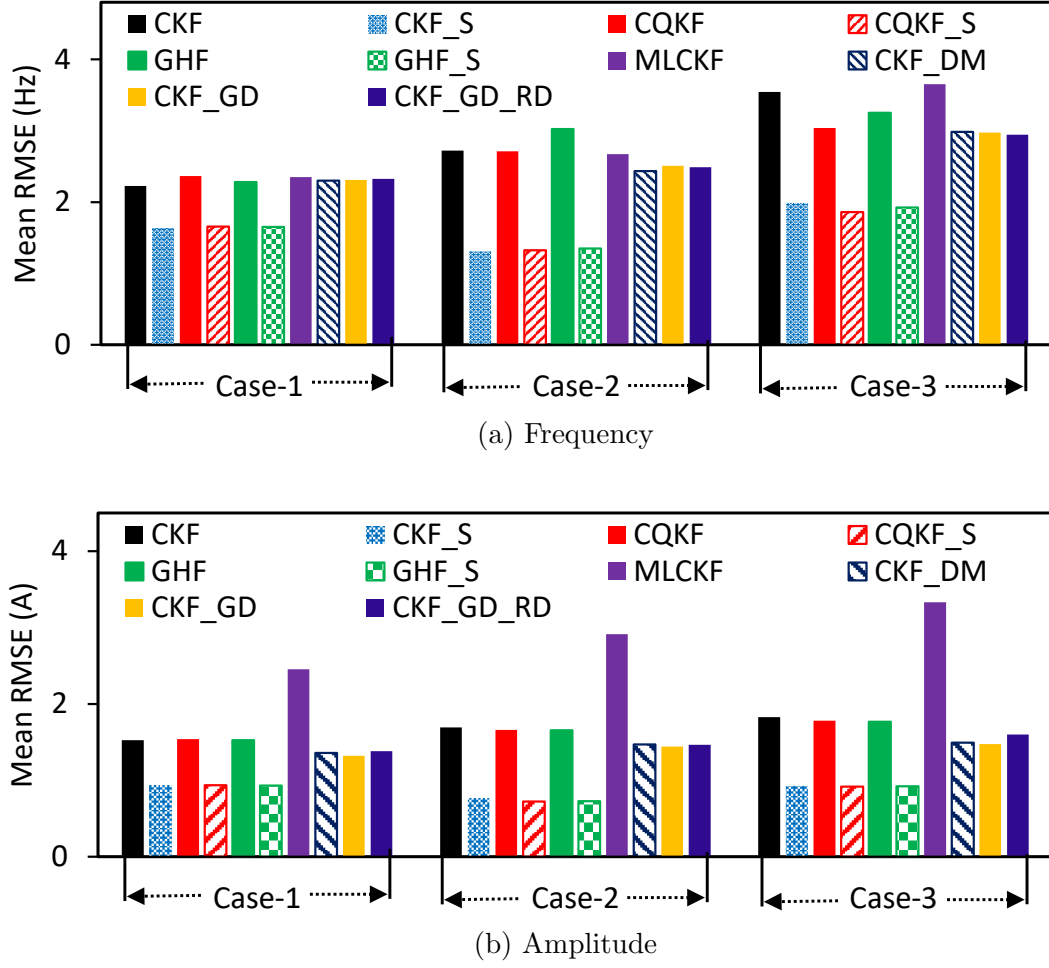
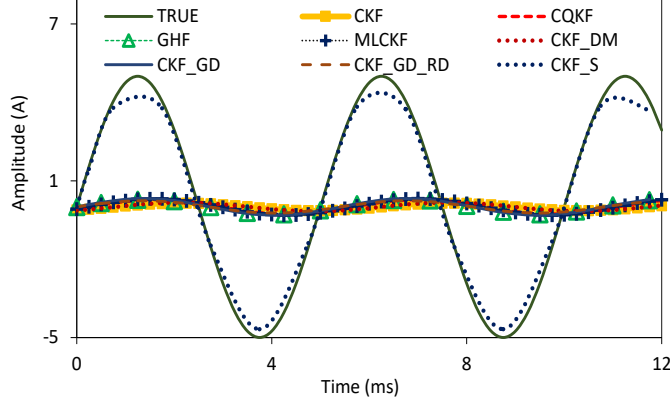


Figure 6.2: Problem 1: Mean RMSE comparison between the proposed and traditional Gaussian filters at different noisy environments considering  $\mathbf{z}_{k-1}$  and  $\mathbf{z}_{k-2}$  collectively compose 20% of  $\mathbf{y}_k$ .

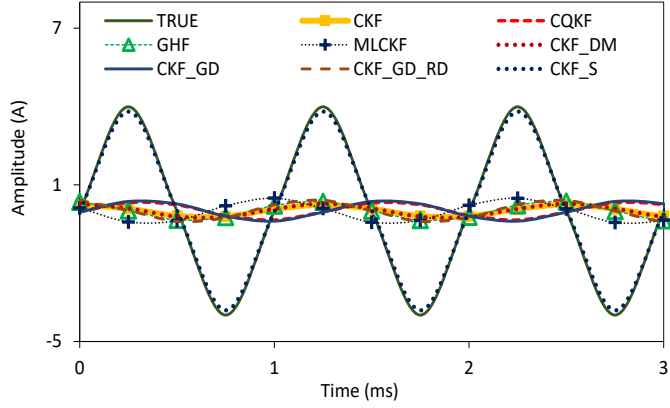
Monte-Carlo runs by selecting  $T = 0.25$  ms. The simulation is based on the assumption that  $\mathbf{y}_k$  is composed of  $\mathbf{z}_k$ ,  $\mathbf{z}_{k-1}$ , and  $\mathbf{z}_{k-2}$  with the corresponding coefficients  $\alpha_0 \sim \mathcal{N}(0.8, 0.01)$ ,  $\alpha_1 \sim \mathcal{N}(0.1, 0.0004)$ , and  $\alpha_2 \sim \mathcal{N}(0.1, 0.0004)$ .

### Performance analysis for varying noises

For the implementation purpose, we assign  $\mathbf{Q}_k = \text{diag}([s_f \ s_f \ s_f \ s_a \ s_a \ s_a])$  and  $\mathbf{R}_k = \text{diag}([\tau_r \ \tau_r])$  and form three different noise scenarios (with  $\boldsymbol{\eta}_k \sim \mathcal{N}(0, \mathbf{Q}_k)$  and  $\boldsymbol{\nu}_k \sim \mathcal{N}(0, \mathbf{R}_k)$ ) as: i) Case-1:  $s_f = 0.08$ ,  $s_a = 0.005$ , and  $\tau_r = 0.09$ , ii) Case-2:  $s_f = 0.16$ ,  $s_a = 0.01$ , and  $\tau_r = 0.18$ , and iii) Case-3:  $s_f = 0.24$ ,  $s_a = 0.015$ , and  $\tau_r = 0.27$ . We obtain the RMSEs of amplitude at every time-instant as the average of RMSEs of the three amplitudes (corresponding to three sinusoids). The same approach is followed for obtaining the RMSEs of frequency as well at every time-instant. Finally, we



(a) First sinusoid



(b) Second sinusoid

Figure 6.3: Sinusoids identification by different filters considering  $\mathbf{z}_{k-1}$  and  $\mathbf{z}_{k-2}$  collectively compose 20% of  $\mathbf{y}_k$  and the noise environment as Case-1.

determine the mean of RMSEs of frequencies and amplitudes across all time instants, which will be referred to as mean RMSEs. Fig. 6.2 compares the mean RMSEs of the CKF, CQKF, and GHF with their counterparts CKF\_S, CQKF\_S, and GHF\_S under the proposed filtering methodology and MLCKF, CKF\_GD, CKF\_GD\_RD, and CKF\_DM. It can be observed that, in all cases, the CKF\_S, CQKF\_S, and GHF\_S give reduced mean RMSEs in comparison to all competitive filters. Thus, it can be concluded that the proposed Gaussian filtering method outperforms the traditional Gaussian filtering method and the existing delay filters in the presence of stochastically linearly combined measurements.

### Sinusoid identification

We consider 2-delay scenario and the first noise scenario (*i.e.*,  $N_d = 2$  and Case-1) to analyze the performance based on identifying the unknown sinusoids. Fig. 6.3 illus-

trates the two sinusoids identified by the CKF\_S. Please note that the performance of the CQKF\_S and GHF\_S are qualitatively superior to the CKF\_S and therefore the sinusoids identified by these filters are eliminated for brevity. It is clear from Fig. 6.3 that the sinusoids identified by the CKF\_S closely match the respective true sinusoids while other filters failed. It further validates the satisfactory estimation using the proposed Gaussian filtering method.

### 6.3.2 Problem 2: Compartmental Population Estimation for COVID-19 Pandemic Model from Real Data

In this problem, we estimate the compartmental populations for the popularly known susceptible-infected-recovered (SIR) pandemic model [171] of Covid-19. The estimation is performed using the real-data (measurements) obtained between 17 January 2021 and 26 April 2021 for Delhi, the capital of India. The state equation for the SIR-based Covid-19 pandemic model is [171]

$$\begin{bmatrix} \mathcal{S}_k \\ \mathcal{I}_k \\ \mathcal{R}_k \end{bmatrix} = \begin{bmatrix} -\kappa_{si}\mathcal{S}_{k-1}\mathcal{I}_{k-1} + \kappa_{rs}\mathcal{R}_{k-1} \\ \kappa_{si}\mathcal{S}_{k-1}\mathcal{I}_{k-1} - \kappa_{ir}\mathcal{I}_{k-1} \\ \kappa_{ir}\mathcal{I}_{k-1} - \kappa_{si}\mathcal{R}_{k-1} \end{bmatrix} + \boldsymbol{\eta}_k, \quad (6.16)$$

where  $\mathcal{S}_k$ ,  $\mathcal{I}_k$ , and  $\mathcal{R}_k$  represent the populations of susceptible, infected, and recovered, respectively, while  $\kappa_{si}$ ,  $\kappa_{ir}$ , and  $\kappa_{rs}$  denote susceptible-to-infected, infected-to-recovered, and recovered-to-susceptible rates, respectively. Subsequently, for the state variable  $\mathbf{x}_k = [\mathcal{S}_k \ \mathcal{I}_k \ \mathcal{R}_k]^T$ , the measurement equation is given as [171]

$$\mathbf{z}_k = \begin{bmatrix} 0 & 1 & 0 \\ 0 & 0 & 1 \end{bmatrix} \mathbf{x}_k + \boldsymbol{\nu}_k. \quad (6.17)$$

The true states of the considered city having 32 million population (contemporaneous) is generated by assigning  $\mathbf{x}_0 = [\mathcal{S}_0 \ 200 \ 1]^T$ , where  $\mathcal{S}_0$  denotes the remaining population after excluding the infected and recovered ones. For simulation purpose, we assign  $\kappa_{si} = 1.5$ ,  $\kappa_{ir} = 0.16$ ,  $\kappa_{rs} = 0.001$  [176]. Moreover, the initial estimate is taken as  $\hat{\mathbf{x}}_{0|0} \sim 0.9\mathcal{N}(\mathbf{x}_0, \mathbf{P}_0)$ , with  $\mathbf{P}_0 = \text{diag}([1000 \ 1000 \ 100])$ . The simulation is performed over 100 days for 300 Monte-Carlo runs, with sampling interval

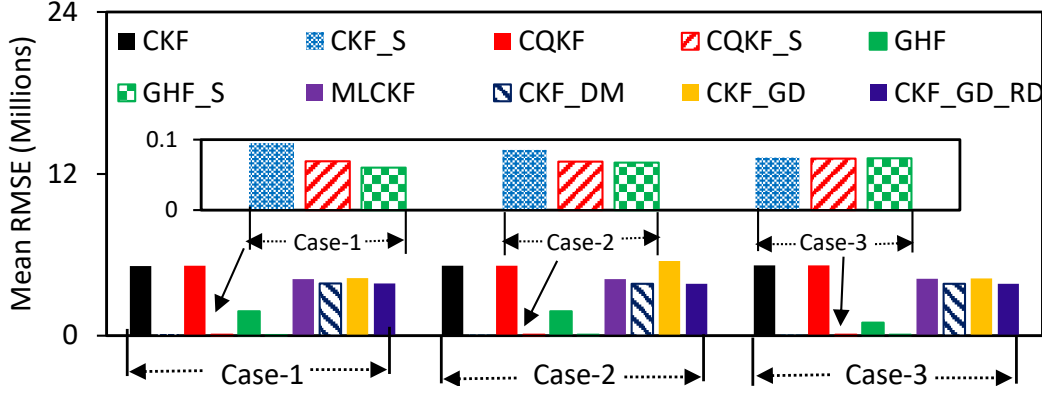


Figure 6.4: Problem 2: Mean RMSEs of the proposed and traditional Gaussian filters at different noisy environments considering  $\mathbf{z}_{k-1}$  and  $\mathbf{z}_{k-2}$  collectively compose 20% of  $\mathbf{y}_k$ .

of one day. Moreover, the coefficients  $\alpha_0$ ,  $\alpha_1$ , and  $\alpha_2$  are assumed to have the same statistics as described in Problem 1.

Please note that the primary objective of any pandemic model realization includes devising a plan for the susceptible population. Thus, we present the results only for susceptible compartment considering  $\mathbf{Q}_k = k_\eta \text{diag}([1000 \ 50 \ 5])$  and  $\mathbf{R}_k = k_\nu \text{diag}([1000 \ 80])$ , forming different noise environments (with  $\boldsymbol{\eta}_k \sim \mathcal{N}(0, \mathbf{Q}_k)$  and  $\boldsymbol{\nu}_k \sim \mathcal{N}(0, \mathbf{R}_k)$ ) as: i) Case-1:  $k_\eta = 1$ ,  $k_\nu = 1$ , ii) Case-2:  $k_\eta = 2$ ,  $k_\nu = 2$ , and iii) Case-3:  $k_\eta = 4$ ,  $k_\nu = 4$ .

Fig. 6.4 (scaled version shows the CKF\_S, CQKF\_S, and GHF\_S) compares the mean RMSEs of susceptible population estimated using the considered Gaussian filters (CKF, CQKF, and GHF) and their extensions under the proposed method (CKF\_S, CQKF\_S, and GHF\_S) for different noisy environments. The figure concludes that the CKF\_S, CQKF\_S, and GHF\_S give reduced mean RMSEs compared with the corresponding competitive filters. Conclusively, the proposed filtering method outperforms the traditional Gaussian filtering method.

### 6.3.3 Performance Analysis Against Varying Measurement Delays

We extend the performance analysis by varying the maximum delay (*i.e.*,  $N_d$ ) in measurements. As discussed in the beginning of this section, the practical delays are predominantly small. Therefore, we consider three delay scenarios, choosing  $N_d$  as

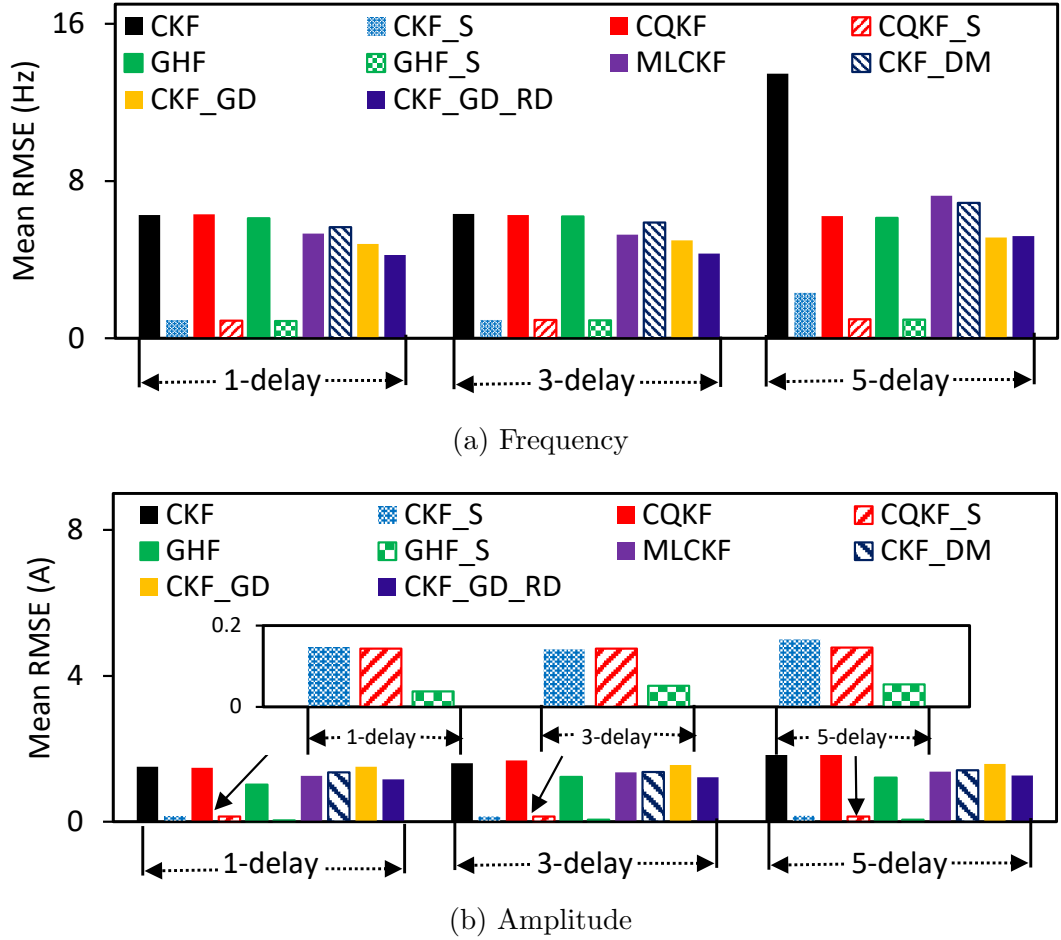


Figure 6.5: Problem 1, Case-1: Mean RMSEs comparison between the proposed and competitive Gaussian filters at different delay scenarios. The hypothetical true measurements  $\mathbf{z}_{k-N_d}$  with  $N_d = (1, 3, 5)$  are assumed to compose 20% of  $\mathbf{y}_k$ .

1, 3, and 5. Moreover, the coefficients are selected as  $\alpha_0 = 0.8$  and  $\alpha_j = (1 - \alpha_0)/N_d$ , where  $j = (1, 2, \dots, N_d)$ . We compare the mean RMSEs of different filters through Figs. 6.5 and 6.6 for the two problems. It is clear from the figures that, for all delay cases, the CKF\_S, CQKF\_S, and GHF\_S give reduced mean RMSEs compared with all considered filters. It infers the improved filtering accuracy of the proposed GFSCM when the actual measurement is received as a stochastic combination of the current and past true measurements.

### 6.3.4 Computational Time Analysis

We compared the relative computational times of all the filters for 2-delay, Case-1 scenario for Problem 1, considering the reference computational time of the CKF as 1 (ratio of computational time of the given filter to that of the CKF). We observed the

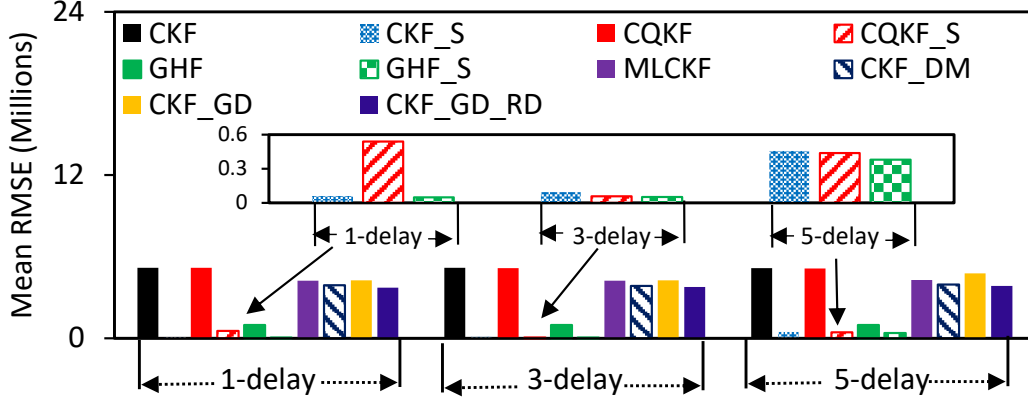


Figure 6.6: Problem 2, Case-1: Mean RMSEs comparison between the proposed and competitive Gaussian filters at different delay scenarios. The hypothetical true measurements  $\mathbf{z}_{k-N_d}$  with  $N_d = (1, 3, 5)$  are assumed to compose 20% of  $\mathbf{y}_k$ .

relative computational times of the CKF, CQKF, GHF, CKF\_S, CQKF\_S, GHF\_S, MLCKF, CKF\_DM, CKF\_GD, and CKF\_GD\_RD as 1, 1.625, 1.904, 1.031, 1.922, 2.167, 3.456, 1.103, 1.153, and 1.358, respectively. It is noteworthy to mention that the performance of all the filters are qualitatively similar for both other delay cases and Problem 2; we have omitted these comparison for brevity.

## 6.4 Summary

The practical measurements are often generated in pieces. The measurement pieces are commonly asynchronously propagated before their superimposition (to obtain the desired measurement). In such cases, the estimator receives an inaccurate measurement as stochastic composition of the current and past hypothetical true measurements. The practical examples include power system state estimation and Covid-19 pandemic model realizations (discussed in detail in the second section). This chapter re-derives the traditional Gaussian filtering method for filtering with the stochastically composed current and past true measurements. The resulting filtering method is named as GFSCM in its abbreviated form. In developing the proposed GFSCM, the author introduces a modified measurement model, considering that the inaccurately received measurement is stochastically composed of the current and past true measurements. Subsequently, the traditional Gaussian filtering method is re-derived for the modified measurement model. The improved accuracy



of the proposed GFSCM is validated for two simulation problems. Interestingly, the accuracy is increased without a significant deviation in the computational demand. The future work extension of this work may be to consider more irregularities in the measurement data and system models.



# Chapter 7

## Gaussian Filtering for Simultaneously Occurring Delayed and Missing Measurements

### 7.1 Introduction

The previous chapters have thoroughly examined the issues of delayed and missing measurements, including the factors causing these irregularities, their incorporation into the measurement model, and various solutions to handle them. To address the limitations of existing methods and narrow research gaps, the author has proposed several extensions of Gaussian filters to handle these irregularities individually (through Chapters 3 to 6). It is important to note that the techniques reviewed so far in the thesis (*e.g.*, [81]-[93] for missing measurements and [112]-[123] for delayed measurements) and the methods proposed in Chapters 3 to 6 are specifically designed to handle either delayed or missing measurements. However, as discussed in Chapter 2, these irregularities can occur simultaneously in wireless sensor networks (WSNs) since the factors triggering them may occur at different stages: from measurement acquisition at sensors to their arrival at the estimator [177, 178].

The literature [177–182] on filtering with simultaneously occurring delayed and missing measurements witnesses some developments for different classes of systems. For example, [177] considered this problem in coupled neural networks and developed an estimation method. Similarly, [179] develops a filtering algorithm for the

delayed and missing measurements. In this regard, it introduces separate stochastic models for incorporating the delay and missing measurements possibilities. Subsequently, it introduces a Ricatti-like equation for designing Kalman filtering method. However, [179] restricts the delay up to one sampling interval, wherein the practical delays can often be larger. Furthermore, [178] introduced unbiased finite impulse response-based filtering approach for finite-horizon case, considering the presence of delayed and missing measurements. However, it assumes that the delay is time-stamped, while delays without time-stamping are observed in many practical systems [167, 183]. Finally, [180] introduces three new designs of robust linear Kalman filtering for handling the simultaneously occurring delayed and missing measurements. However, in every design, it restricts the delay as one sampling interval, which can lead to poor accuracy if the real measurement delay is higher. Moreover, [179] and [180] rely on the augmented state-space approaches, which may increase the computational complexity significantly.

Although the above-discussed filtering methods [177–182] can handle the simultaneously occurring delayed and missing measurements, they have two broad limitations: i) they are designed for linear dynamical systems, ii) they fail to handle delays of more than one sampling interval without time-stamping. For the nonlinear dynamical systems, [126] is a popular development to handle the simultaneously occurring delays larger than one sampling instant and missing measurements. It integrates a likelihood-based technique with the nonlinear Gaussian filtering framework for handling the simultaneously occurring delayed and missing measurements. However, [126] uses an augmented state transition equation, with the size of the system growing by a factor of  $N_d$ , where  $N_d$  the maximum number of delays. Moreover, the use of Gaussian mixture with  $N_d$  components as a likelihood function causes computational issues with large number of components in the likelihood function. Indeed, the increased size of the covariance matrices itself can present significant computational issues in multidimensional integration involved.

In this chapter, we develop a new extension of Gaussian filtering to handle the simultaneously occurring delayed and missing measurements for nonlinear dynamical systems. In this regard, we reformulate the measurement model using a set of Bernoulli random variables to incorporate the possibilities of delayed and miss-

ing measurements. Subsequently, we re-derive the Gaussian filtering method for the modified measurement model. It should be mentioned that we modify only the measurement model. Consequently, in the redesigned Gaussian filtering, only the filtering parameters related to the measurements, such as the measurement estimate, the measurement covariance, and the state-measurement cross-covariance, are re-derived. It is worth mentioning that our contribution is on developing a generalized Gaussian filtering methodology for the problem of delayed as well as missing measurements. Thus, it can be used for extending any of the existing Gaussian filters, such as the EKF, the UKF, and the CKF, for handling the simultaneous occurrence of delayed and missing measurements. We test the performance of the proposed method under CKF-based formulation due to its popularity for high accuracy at a low computational cost. The performance analysis reveals an improved accuracy for the proposed method compared to the traditional Gaussian filtering method and its extensions in presence of delayed and missing measurements.

In view of the above discussion, we highlight the main contributions of the chapter as follows:

- We introduce a stochastically formulated measurement model that incorporates the possibility of simultaneously occurring delayed and missing measurements.
- We redesign the traditional Gaussian filtering for the modified measurement model to handle the simultaneous occurrences of the delayed and missing measurements.
- We consider arbitrarily large delays without time-stamping for nonlinear systems, whereas the existing filters such as those reported in [179, 180] (without time-stamping) and [178] (with time-stamping) address the delayed measurements only for linear systems. Moreover, our algorithm, in contrast to [126], avoids computationally expensive state augmentation and instead relies on analytical expressions for the necessary conditional moments (which are additive in the number of maximum delays).
- We validate the performance of the proposed Gaussian filtering methodology by two comprehensive simulation examples.

## 7.2 Problem Formulation

Our problem is to develop an advanced Gaussian filtering methodology to handle the simultaneous occurrence of delayed and missing measurements. The standard representation of the state-space model in a lenient environment (Eqs. (1.1) and (1.2) in Chapter 1) is as follows

$$\mathbf{x}_k = f(\mathbf{x}_{k-1}) + \boldsymbol{\eta}_k. \quad (7.1)$$

$$\mathbf{z}_k = h(\mathbf{x}_k) + \boldsymbol{\nu}_k. \quad (7.2)$$

Following our problem statement, we need to reformulate the measurement model (Eq. (7.2)) to address the simultaneous occurrence of randomly delayed and randomly missing measurements. Our reformulation of the measurement model is based on two sets of Bernoulli random variables, denoted by  $\beta$  and  $\Theta$ :  $\beta$  corresponds to the missing measurements and  $\Theta$  corresponds to the delayed measurements.

The measurements are generally received from multiple sources, and they all may not be missing at the same time. Thus, we consider that the measurement at any sampling instant may be partly missing, *i.e.*, specific elements of the measurement may be missing at any particular instant. Thus, we define a matrix of Bernoulli random variables,  $\boldsymbol{\beta}_k = \text{diag}[(\beta_k^1, \beta_k^2, \dots, \beta_k^q)]$  with  $\beta_k^i \forall i \in \{1, 2, \dots, q\}$  being  $q$  equiprobable Bernoulli random variables and  $\mathbb{E}[\boldsymbol{\beta}_k] = \boldsymbol{\rho}_k = \text{diag}[(\rho_k^1, \rho_k^2, \dots, \rho_k^q)]$ . It should be mentioned that  $\beta_k^i$  is either 0 or 1, with  $\beta_k^i = 0$  representing that the  $i^{th}$  element of the received measurement  $\mathbf{y}_k$ , denoted as  $\mathbf{y}_k(i)$ , is missing.

For modeling the delay portion, we restrict the maximum delay to  $N_d$ .  $N_d$  is the practitioner's choice and it can be assigned with a fairly large value if the expected delay is large. Therefore, our model and the proposed filtering technique should not be deemed to be restricted to small delays. We define  $N_d + 1$  equiprobable Bernoulli random variables: one for each of the current and the  $N_d$  possible delayed instants. At  $k^{th}$  instant, we denote them as  $\Theta_k^j \forall j \in \{1, 2, \dots, N_d + 1\}$  with  $P(\Theta_k^j = 1) = \mathbb{E}[\Theta_k^j] = \phi_d$ . Note that  $\Theta_k^{j+1}$  corresponds to  $j^{th}$  delayed instant. We assign  $\Theta_k^0 = 0$ ,

and model the actual measurement as

$$\mathbf{y}_k = \beta_k \left[ (1 - \Theta_k^0) \Theta_k^1 \mathbf{z}_k + (1 - \Theta_k^0)(1 - \Theta_k^1) \Theta_k^2 \mathbf{z}_{k-1} + \dots \right. \\ \left. + (1 - \Theta_k^0)(1 - \Theta_k^1) \dots (1 - \Theta_k^{N_d}) \Theta_k^{N_d+1} \mathbf{z}_{k-N_d} \right], \quad (7.3)$$

where  $\mathbf{y}_k$  is the actual received measurement due to the delay and missing possibilities. The coefficients of  $\mathbf{z}_{k-m} \forall m \in \{1, 2, \dots, N_d\}$  govern the delay extent. For example, if the measurement is one time-step delayed, *i.e.*,  $\mathbf{y}_k = \mathbf{z}_{k-1}$ , then coefficient of  $\mathbf{z}_{k-1}$ , *i.e.*,  $(1 - \Theta_k^0)(1 - \Theta_k^1) \Theta_k^2$  takes the value one, while the random variables associated with  $\mathbf{z}_{k-m} \forall m \neq 1$  remain zero. At the same time,  $\beta_k$  regulates the missing measurement possibility. The diagonal elements of  $\beta_k$  are Bernoulli random variables, which take the values zero or one. The value one ensures that the measurement is received, while the value zero indicates that the measurement is lost.

To this end, let us simplify the notation for the coefficients of  $\mathbf{z}_{k-m}$  as

$$\Lambda_k(m, j) = \left( \prod_{j=0}^m (1 - \Theta_k^j) \right) \Theta_k^{(m+1)}, \quad (7.4)$$

so that the received measurement is  $m$ -step delayed if  $\Lambda_k(m, j) = 1$ , which means  $\Theta_k^{m+1} = 1$  and  $\Theta_k^j = 0 \forall j \leq m$ . Subsequently, Eq. (7.3) can be represented as

$$\mathbf{y}_k = \beta_k [\Lambda_k(0, j) \mathbf{z}_k + \Lambda_k(1, j) \mathbf{z}_{k-1} + \dots + \Lambda_k(N_d, j) \mathbf{z}_{k-N_d}]. \quad (7.5)$$

Thus, the measurement model can be finally given as

$$\mathbf{y}_k = \beta_k \sum_{m=0}^{N_d} \Lambda_k(m, j) \mathbf{z}_{k-m}, \quad (7.6)$$

where  $\mathbf{y}_k$  is the actual received measurement due to delay and missing possibilities. At this end,  $\mathbf{z}_k$  may be considered as an ideal measurement that might have been received in the lenient environment. A pictorial diagram representing the sequence to be followed to get  $\mathbf{y}_k$  from  $\mathbf{z}_1, \mathbf{z}_2, \dots, \mathbf{z}_k$  is shown in Fig. 7.1.

It is assumed that  $\beta_k^i$  and  $\Theta_k^j$  are independent random variables  $\forall \{k, i, j\}$ . Furthermore,  $\beta_k^j$  and  $\Theta_k^j$  are independent of  $\beta_k^i$  and  $\Theta_k^i$ , respectively for  $j \neq i$ . Our

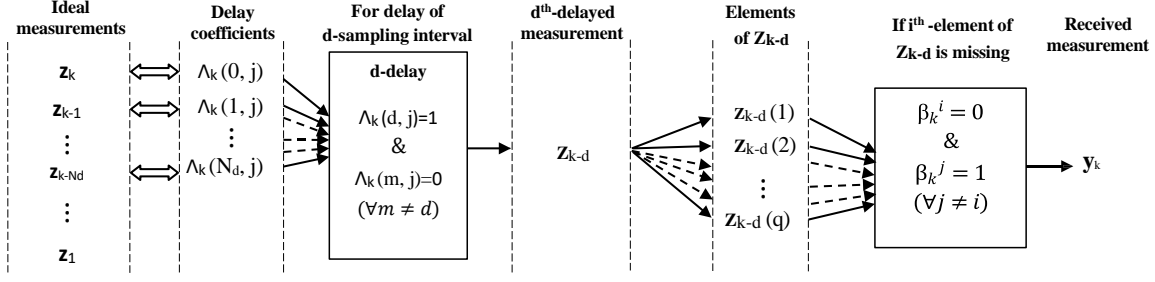


Figure 7.1: Pictorial diagram representing the sequence to be followed to obtain the received measurement  $y_k$  from the ideal  $z_1, z_2, \dots, z_k$  that would have been received in the lenient environment.

objective in the next section is to redesign the Gaussian filtering method for the state-space model represented by Eqs. (7.1) and (7.2) so that the possibilities of delayed and missing measurements are incorporated.

The above discussions emphasize the importance of the measurement model (7.6) for developing the proposed filtering algorithm. As mentioned in the previous section, some of the existing filters, such as [121, 123–125] and [184], also formulated similar measurement models. However, the models in [121, 123–125] characterize the delay possibilities only, while the same in [184] characterizes only the missing measurement possibility. Moreover, [121, 123, 124] characterize only limited and small delays. Thus, they fail to characterize the general practical scenarios of the simultaneously occurring delayed and missing measurements. Our measurement model in Eq. (7.6) efficiently characterizes the simultaneously occurring delayed and missing measurement possibilities. It considers any large delays and completely missing measurements unlike [121, 123–125] and [184], respectively.

## 7.3 Modified Gaussian Filtering for Delayed and Missing Measurements

The traditional Gaussian filtering is designed with respect to the measurement  $z$ , modeled in Eq. (7.2). In this section, we derive the necessary modifications to the algorithm to deal with the modified measurement  $y$ , modeled in Eq. (7.6). As the measurement model is changed, we re-derive all the related expressions in the traditional Gaussian filtering to propose the advanced Gaussian filtering for  $y$ . The



traditional Gaussian filtering uses only three such expressions, namely the measurement estimate  $\hat{\mathbf{z}}$ , measurement error covariance  $\mathbf{P}^{\mathbf{zz}}$ , and the cross covariance  $\mathbf{P}^{\mathbf{xz}}$ , derived for  $\mathbf{z}$ . We re-derive all the measurement related expressions in the Gaussian filtering algorithm for the modified measurement model above. On a different note, it should be mentioned that the state dynamics remains unaffected from the simultaneous occurrence of the delayed and missing measurements. Therefore, the time update step of the proposed filtering technique remains the same as the traditional Gaussian filtering [11, 15].

We now re-derive the measurement-related parameters through the subsequent discussions.

**Theorem 7.1.** For  $\mathbf{y}_k$  given in Eq. (7.6), the measurement estimate is

$$\hat{\mathbf{y}}_{k|k-1} = \sum_{m=0}^{N_d} \rho_k (1 - \phi_d)^m \phi_d \hat{\mathbf{z}}_{k-m|k-1}, \quad (7.7)$$

where  $\mathbb{E}[\mathbf{z}_{k-m}] = \hat{\mathbf{z}}_{k-m|k-1}$ .

*Proof.* Let us substitute the expression of  $\mathbf{y}_k$  from Eq. (7.6) in  $\hat{\mathbf{y}}_{k|k-1} = \mathbb{E}[\mathbf{y}_k]$ . Thus, we get

$$\hat{\mathbf{y}}_{k|k-1} = \mathbb{E}[\mathbf{y}_k] = \mathbb{E} \left[ \beta_k \left( \sum_{m=0}^{N_d} \Lambda_k(m, j) \mathbf{z}_{k-m} \right) \right]. \quad (7.8)$$

As the missing and delay occurrences are mutually independent events,  $\beta_k$  and  $\Lambda_k(m, j)$  are statistically independent. Moreover,  $\beta_k$  and  $\Lambda_k(m, j)$  are independent of the measurement value  $\mathbf{z}_k$  also. Thus, we simplify the above equation as

$$\hat{\mathbf{y}}_{k|k-1} = \mathbb{E}[\beta_k] \sum_{m=0}^{N_d} \mathbb{E}[\Lambda_k(m, j)] \mathbb{E}[\mathbf{z}_{k-m}]. \quad (7.9)$$

Following our previous notations  $\mathbb{E}[\mathbf{z}_{k-m}] = \hat{\mathbf{z}}_{k-m|k-1}$  and recalling the previous discussion, we get

$$\mathbb{E}[\Lambda_k(m, j)] = \mathbb{E} \left[ \left( \prod_{j=0}^m (1 - \Theta_k^j) \right) \Theta_k^{(m+1)} \right] = (1 - \phi_d)^m \phi_d. \quad (7.10)$$

Substituting  $\mathbb{E}[\mathbf{z}_{k-m}]$ ,  $\mathbb{E}[\beta_k]$ , and  $\mathbb{E}[\Lambda_k(m, j)]$  in Eq. (7.9), we get the expression of  $\hat{\mathbf{y}}_{k|k-1}$  as given in Eq. (7.7).  $\square$

**Theorem 7.2.** The covariance  $\mathbf{P}_{k|k-1}^{\mathbf{y}\mathbf{y}}$  for the modified measurement model  $\mathbf{y}_k$  is obtained as

$$\begin{aligned} \mathbf{P}_{k|k-1}^{\mathbf{y}\mathbf{y}} = & \sum_{m=0}^{N_d} \boldsymbol{\rho}_k (1 - \phi_d)^m \phi_d \mathbf{P}_{k-m|k-1}^{\mathbf{z}\mathbf{z}} + \sum_{m=0}^{N_d} (\boldsymbol{\rho}_k (1 - \phi_d)^m \phi_d \\ & - (\boldsymbol{\rho}_k (1 - \phi_d)^m \phi_d)^2) \hat{\mathbf{z}}_{k-m|k-1} \hat{\mathbf{z}}_{k-m|k-1}^T. \end{aligned} \quad (7.11)$$

*Proof.* The measurement error covariance is

$$\mathbf{P}_{k|k-1}^{\mathbf{y}\mathbf{y}} = \mathbb{E} \left[ (\mathbf{y}_k - \hat{\mathbf{y}}_{k|k-1}) (\mathbf{y}_k - \hat{\mathbf{y}}_{k|k-1})^T \right]. \quad (7.12)$$

From Eqs. (7.6) and (7.7), we get

$$\mathbf{y}_k - \hat{\mathbf{y}}_{k|k-1} = \sum_{m=0}^{N_d} \boldsymbol{\beta}_k \Lambda_k(m, j) \mathbf{z}_{k-m} - \sum_{m=0}^{N_d} \boldsymbol{\rho}_k (1 - \phi_d)^m \phi_d \hat{\mathbf{z}}_{k-m|k-1}, \quad (7.13)$$

which can be re-written as

$$\begin{aligned} \mathbf{y}_k - \hat{\mathbf{y}}_{k|k-1} = & \underbrace{\sum_{m=0}^{N_d} \boldsymbol{\beta}_k \Lambda_k(m, j) (\mathbf{z}_{k-m} - \hat{\mathbf{z}}_{k-m|k-1})}_{\boldsymbol{\Delta}_1} \\ & + \underbrace{\sum_{m=0}^{N_d} (\boldsymbol{\beta}_k \Lambda_k(m, j) - \boldsymbol{\rho}_k (1 - \phi_d)^m \phi_d) \hat{\mathbf{z}}_{k-m|k-1}}_{\boldsymbol{\Delta}_2}. \end{aligned} \quad (7.14)$$

From Eqs. (7.12) and (7.14), we can write

$$\mathbf{P}_{k|k-1}^{\mathbf{y}\mathbf{y}} = \mathbb{E}[\boldsymbol{\Delta}_1 \boldsymbol{\Delta}_1^T] + \mathbb{E}[\boldsymbol{\Delta}_1 \boldsymbol{\Delta}_2^T] + \mathbb{E}[\boldsymbol{\Delta}_2 \boldsymbol{\Delta}_1^T] + \mathbb{E}[\boldsymbol{\Delta}_2 \boldsymbol{\Delta}_2^T]. \quad (7.15)$$

We can now compute every expectation term individually for  $\boldsymbol{\Delta}_1$  and  $\boldsymbol{\Delta}_2$  defined in Eq. (7.14) and add them to obtain  $\mathbf{P}_{k|k-1}^{\mathbf{y}\mathbf{y}}$ . In this regard, for  $\boldsymbol{\Delta}_1$  given in Eq. (7.14), we get

$$\mathbb{E}[\boldsymbol{\Delta}_1 \boldsymbol{\Delta}_1^T] = \sum_{m=0}^{N_d} \mathbb{E}[\boldsymbol{\beta}_k^2] \mathbb{E}[\Lambda_k^2(m, j)] \mathbb{E}[(\mathbf{z}_{k-m} - \hat{\mathbf{z}}_{k-m|k-1})(\mathbf{z}_{k-m} - \hat{\mathbf{z}}_{k-m|k-1})^T].$$

Following previous discussions,  $\mathbb{E}[\boldsymbol{\beta}_k^2] = \mathbb{E}[\boldsymbol{\beta}_k] = \boldsymbol{\rho}_k$ ,  $\mathbb{E}[\Lambda_k^2(m, j)] = \mathbb{E}[(\Lambda_k(m, j))] =$

$(1 - \phi_d)^m \phi_d$ , and  $\mathbb{E}[(\mathbf{z}_{k-m} - \hat{\mathbf{z}}_{k-m|k-1})(\mathbf{z}_{k-m} - \hat{\mathbf{z}}_{k-m|k-1})^T] = \mathbf{P}_{k-m|k-1}^{\mathbf{zz}}$ , the above equation can be simplified as

$$\mathbb{E}[\Delta_1 \Delta_1^T] = \sum_{m=0}^{N_d} \rho_k (1 - \phi_d)^m \phi_d \mathbf{P}_{k-m|k-1}^{\mathbf{zz}}. \quad (7.16)$$

Similarly, for  $\Delta_1$  and  $\Delta_2$  given in Eq. (7.14), we can write

$$\begin{aligned} \mathbb{E}[\Delta_1 \Delta_2^T] = & \mathbb{E} \left[ \left( \sum_{s=0}^{N_d} \beta_k \Lambda_k(s, j) (\mathbf{z}_{k-s} - \hat{\mathbf{z}}_{k-s|k-1}) \right) \right. \\ & \times \left. \left( \sum_{u=0}^{N_d} (\beta_k \Lambda_k(u, j) - \rho_k (1 - \phi_d)^u \phi_d) \hat{\mathbf{z}}_{k-u|k-1} \right)^T \right]. \end{aligned}$$

After further simplification, we get

$$\begin{aligned} \mathbb{E}[\Delta_1 \Delta_2^T] = & \sum_{s=0}^{N_d} \sum_{u=0}^{N_d} \mathbb{E} \left[ \beta_k \Lambda_k(s, j) (\beta_k \Lambda_k(u, j) - \rho_k (1 - \phi_d)^u \phi_d)^T \mathbf{z}_{k-s} \hat{\mathbf{z}}_{k-u|k-1}^T \right. \\ & \left. - \beta_k \Lambda_k(s, j) (\beta_k \Lambda_k(u, j) - \rho_k (1 - \phi_d)^u \phi_d)^T \hat{\mathbf{z}}_{k-s|k-1} \hat{\mathbf{z}}_{k-u|k-1}^T \right]. \end{aligned}$$

After substituting all the expectation terms from previous discussions and considering that  $\mathbb{E}[\mathbf{z}_{k-s}] = \hat{\mathbf{z}}_{k-s|k-1}$ , we get

$$\mathbb{E}[\Delta_1 \Delta_2^T] = 0. \quad (7.17)$$

This also leads to

$$\mathbb{E}[\Delta_2 \Delta_1^T] = 0. \quad (7.18)$$

Finally, for  $\Delta_2$  given in Eq. (7.14), we have

$$\mathbb{E}[\Delta_2 \Delta_2^T] = \mathbb{E} \left[ \sum_{m=0}^{N_d} (\beta_k \Lambda_k(m, j) - \rho_k (1 - \phi_d)^m \phi_d)^2 \hat{\mathbf{z}}_{k-m|k-1} \hat{\mathbf{z}}_{k-m|k-1}^T \right].$$

Applying binomial expansion and simplifying further, we get

$$\begin{aligned} \mathbb{E}[\Delta_2 \Delta_2^T] = & \sum_{m=0}^{N_d} \left( \mathbb{E}[\beta_k^2] \mathbb{E}[\Lambda_k^2(m, j)] + (\rho_k \phi_d (1 - \phi_d)^m)^2 \right. \\ & \left. - 2 \mathbb{E}[\beta_k] \mathbb{E}[\Lambda_k(m, j)] \rho_k (1 - \phi_d)^m \phi_d \right) \hat{\mathbf{z}}_{k-m|k-1} \hat{\mathbf{z}}_{k-m|k-1}^T. \end{aligned}$$

Substituting  $\mathbb{E}[\beta_k^2] = \rho_k$  and  $\mathbb{E}[\Lambda_k^2(m, j)] = (1 - \phi_d)^m \phi_d$ , we obtain

$$\mathbb{E}[\Delta_2 \Delta_2^T] = \sum_{m=0}^{N_d} (\rho_k (1 - \phi_d)^m \phi_d - (\rho_k (1 - \phi_d)^m \phi_d)^2) \hat{\mathbf{z}}_{k-m|k-1} \hat{\mathbf{z}}_{k-m|k-1}^T. \quad (7.19)$$

We now substitute  $\mathbb{E}[\Delta_1 \Delta_1^T]$ ,  $\mathbb{E}[\Delta_1 \Delta_2^T]$ ,  $\mathbb{E}[\Delta_2 \Delta_1^T]$ , and  $\mathbb{E}[\Delta_2 \Delta_2^T]$  from Eqs. (7.16), (7.17), (7.18), and (7.19), respectively, in Eq. (7.15) to obtain  $\mathbf{P}_{k|k-1}^{\mathbf{y}\mathbf{y}}$  as expressed in Eq. (7.11).  $\square$

**Theorem 7.3.** The state-measurement cross-covariance  $\mathbf{P}_{k|k-1}^{\mathbf{x}\mathbf{y}}$  for  $\mathbf{y}_k$  can be given as

$$\mathbf{P}_{k|k-1}^{\mathbf{x}\mathbf{y}} = \sum_{m=0}^{N_d} \phi_d (1 - \phi_d)^m \mathbf{P}_{k-m|k-1}^{\mathbf{x}\mathbf{z}} \rho_k. \quad (7.20)$$

*Proof.* Substituting  $\mathbf{y}_k - \hat{\mathbf{y}}_{k|k-1}$  from Eq. (7.14) into expression  $\mathbf{P}_{k|k-1}^{\mathbf{x}\mathbf{y}} = \mathbb{E}[(\mathbf{x}_k - \hat{\mathbf{x}}_{k|k-1})(\mathbf{y}_k - \hat{\mathbf{y}}_{k|k-1})^T]$ , we get

$$\mathbf{P}_{k|k-1}^{\mathbf{x}\mathbf{y}} = \mathbb{E}[(\mathbf{x}_k - \hat{\mathbf{x}}_{k|k-1})\Delta_1^T] + \mathbb{E}[(\mathbf{x}_k - \hat{\mathbf{x}}_{k|k-1})\Delta_2^T]. \quad (7.21)$$

For  $\Delta_1$  given in Eq. (7.14), we can write

$$\mathbb{E}[(\mathbf{x}_k - \hat{\mathbf{x}}_{k|k-1})\Delta_1^T] = \sum_{m=0}^{N_d} (\mathbb{E}[\beta_k] \mathbb{E}[\Lambda_k(m, j)] \mathbb{E}[(\mathbf{x}_k - \hat{\mathbf{x}}_{k|k-1})(\mathbf{z}_{k-m} - \hat{\mathbf{z}}_{k-m|k-1})^T]). \quad (7.22)$$

Substituting  $\mathbb{E}[\beta_k]$  and  $\mathbb{E}[\Lambda_k(m, j)]$ , we obtain

$$\mathbb{E}[(\mathbf{x}_k - \hat{\mathbf{x}}_{k|k-1})\Delta_1^T] = \sum_{m=0}^{N_d} (1 - \phi_d)^m \phi_d \mathbf{P}_{k-m|k-1}^{\mathbf{x}\mathbf{z}} \rho_k. \quad (7.23)$$

Similarly, for  $\Delta_2$  given in Eq. (7.14), we get

$$\begin{aligned} \mathbb{E}[(\mathbf{x}_k - \hat{\mathbf{x}}_{k|k-1})\Delta_2^T] &= \sum_{m=0}^{N_d} \mathbb{E}[(\beta_k \Lambda_k(m, j) - \rho_k (1 - \phi_d)^m \phi_d)] \\ &\quad \times \mathbb{E}[(\mathbf{x}_k - \hat{\mathbf{x}}_{k|k-1})\hat{\mathbf{z}}_{k-m|k-1}^T]. \end{aligned} \quad (7.24)$$

As  $\beta_k$  and  $\Lambda_k(m, j)$  are independent,  $\mathbb{E}[\beta_k \Lambda_k(m, j)] = \mathbb{E}[\beta_k] \mathbb{E}[\Lambda_k(m, j)] = \rho_k (1 -$

$\phi_d)^m \phi_d$ . Thus, we can write

$$\mathbb{E}[(\boldsymbol{\beta}_k \Lambda_k(m, j) - \boldsymbol{\rho}_k (1 - \phi_d)^m \phi_d)] = 0. \quad (7.25)$$

Substituting this into Eq. (7.24), we get

$$\mathbb{E}[(\mathbf{x}_k - \hat{\mathbf{x}}_{k|k-1}) \boldsymbol{\Delta}_2^T] = 0. \quad (7.26)$$

Substituting  $\mathbb{E}[(\mathbf{x}_k - \hat{\mathbf{x}}_{k|k-1}) \boldsymbol{\Delta}_1^T]$  and  $\mathbb{E}[(\mathbf{x}_k - \hat{\mathbf{x}}_{k|k-1}) \boldsymbol{\Delta}_2^T]$  from Eqs. (7.23) and (7.26), respectively, into Eq. (7.21), it is deduced to Eq. (7.20).  $\square$

As discussed at the beginning of this section, the proposed filtering method modifies the traditional Gaussian filtering by re-deriving the expressions of measurement estimate, measurement covariance, and state-measurement cross-covariance (Eqs. (7.7), (7.11), and (7.20), respectively). Please follow [11, 15] for a detailed discussion on the traditional Gaussian filtering. The proposed filtering algorithm also follows the same filtering strategy by replacing the expressions of  $\hat{\mathbf{z}}_{k|k-1}$ ,  $\mathbf{P}_{k|k-1}^{\mathbf{zz}}$ , and  $\mathbf{P}_{k|k-1}^{\mathbf{xz}}$  with the re-derived expressions of  $\hat{\mathbf{y}}_{k|k-1}$ ,  $\mathbf{P}_{k|k-1}^{\mathbf{yy}}$ , and  $\mathbf{P}_{k|k-1}^{\mathbf{xy}}$ , respectively. We provide the pseudo-code for implementing the proposed filtering method in Algorithm 7.1.

In advancing the traditional Gaussian filtering for handling various measurement irregularities, such as the delayed and missing measurements, the major difficulty appears in incorporating those irregularities through mathematical models. The problem becomes yet more challenging if the irregularities are uncertain to appear at any particular sampling instant, as considered in this chapter. We handled this problem by mathematically characterizing such irregularities, particularly the delayed and missing measurements, by formulating a stochastic model, as in Eq. (7.6).

**Remark 7.1.** *Our measurement model utilizes a sequence of Bernoulli random variables to characterize the possibility of a measurement coming from various possible past instants. A future research problem may be to introduce a more convenient model by reducing the required number of random variables.*

**Remark 7.2.** *Our filter design strategy concludes that handling the measurement irregularities becomes convenient if an efficient mathematical model for characterizing*

**Algorithm 7.1** Pseudo-code for extending the sigma-point based Gaussian filters under the proposed filtering technique

---

**Input:**  $\mathbf{Q}_k, \mathbf{R}_k, T_s, \rho, \phi_d$ , filter-specific sigma points, and weights.

**Output:**  $\hat{\mathbf{x}}_{k|k}$ .

---

```

1: Initialisation:  $\hat{\mathbf{x}}_{0|0}, \hat{\mathbf{P}}_{0|0}, k = 1$ .
2: while  $k \leq T_s$  do
3:   Compute the predicted estimate and covariance of  $\mathbf{x}_k$ :  $\hat{\mathbf{x}}_{k|k-1}$  and  $\hat{\mathbf{P}}_{k|k-1}$  (see,
     e.g., References [11, 15]).
4:   Compute the estimate and covariance of the ideal measurement ( $\mathbf{z}_k$ ):  $\hat{\mathbf{z}}_{k|k-1}$ ,
      $\mathbf{P}_{k|k-1}^{\mathbf{zz}}$  (see, e.g., References [11, 15]).
5:   Compute the cross-covariance between state and ideal measurement  $\mathbf{z}_k$ :
      $\mathbf{P}_{k|k-1}^{\mathbf{xz}}$  (see, e.g., References [11, 15]).
6:   Compute the estimate and covariance of the received measurement  $\mathbf{y}_k$ :  $\hat{\mathbf{y}}_{k|k-1}$ 
     (Eq. (7.7)) and  $\mathbf{P}_{k|k-1}^{\mathbf{yy}}$  (Eq. (7.11)).
7:   Compute the cross-covariance between  $\mathbf{x}_k$  and received measurements  $\mathbf{y}_k$ :
      $\mathbf{P}_{k|k-1}^{\mathbf{xy}}$  (Eq. (7.20)).
8:   Kalman gain:  $\mathbf{K} = \mathbf{P}_{k|k-1}^{\mathbf{xy}} (\mathbf{P}_{k|k-1}^{\mathbf{yy}})^{-1}$ .
9:   Updated estimate:  $\hat{\mathbf{x}}_{k|k} = \hat{\mathbf{x}}_{k|k-1} + \mathbf{K}(\mathbf{y}_k - \hat{\mathbf{y}}_{k|k-1})$ .
10:  Updated covariance:  $\hat{\mathbf{P}}_{k|k} = \hat{\mathbf{P}}_{k|k-1} - \mathbf{K} \mathbf{P}_{k|k-1}^{\mathbf{yy}} \mathbf{K}^T$ .
11: return  $\hat{\mathbf{x}}_{k|k}$ 
12: end while

```

---

*the concerned irregularities is formulated.*

**Remark 7.3.** *The proposed method fetches some information, such as the measurement estimate, measurement covariance, and state-measurement cross-covariance, from past instants, which causes additional storage capacity requirement. Similar additional storage requirements also occur in existing delay filters, e.g., see [15].*

**Remark 7.4.** *The proposed filtering methodology simplifies to the traditional Gaussian filtering methodology for zero probabilities of delay and missing measurements ( $\rho^i = \phi_d = 1$ ) and  $N_d = 0$ , if we use the convention  $0^0 = 1$ .*

## 7.4 Simulation Results

In real-life problems, the measurement systems (including the measuring devices and the supplementary units) are usually designed to efficiently capture the measurements. Therefore, they may not be expected to miss many measurements. Subsequently, the missing measurement probability is usually small. Thus, we consider the missing measurement probability up to 0.2 for the simulation, which means

around 20% of the measurements are missing. On the other hand, the delay inherently appears in the measurements. Therefore, we consider a sufficiently large range of the delay probability ( $0.1 \leq 1 - \phi_d \leq 0.9$ ). Moreover, it should be mentioned that the practical measurement systems are designed for small delays. Hence, we restrict the maximum possible delay to one to three time-steps (denoted as 1-delay, 2-delay, and 3-delay scenarios, respectively). The simulation is performed for 500 time-steps and the RMSEs are obtained by implementing 300 Monte-Carlo simulations.

For the performance analysis, we considered three popular and advanced Gaussian filters, namely, the CKF [9], CQKF [27], and GHF [28]. With their extensions under the modified filtering method, which are abbreviated as MDCKF, MDCQKF, and MDGHF, respectively. We use the root mean square error (RMSE) as our performance metrics. Please note that we will frequently use the notation  $\rho_m = 1 - \rho$  to denote the missing measurements probability.

We compare the MDCKF with the following filters: i) traditional CKF [9], ii) the CKF-based formulation of [125], which extends the Gaussian filtering technique for arbitrary delays, iii) [184], wherein the EKF is modified for missing measurements, and iv) the CKF-based formulation of [126], which considers simultaneously occurring delay and missing measurements. We abbreviate the CKF-based formulations of [125], and [126] as CKF\_RD, and MLCKF, respectively, while the EKF-based formulation of [184] is abbreviated as MEKF. Please note that we use the EKF-based design of [184] unlike the CKF-based designs for other filters, as [184] is particularly designed for the EKF and becomes inapplicable to other filters.

#### 7.4.1 Problem 1: Individual Sinusoids Identification

In this simulation problem, we consider an identification problem of individual sinusoids from the measurements of multiple superimposed sinusoids [11, 15]. Sinusoids identification is equivalent to estimating their amplitudes and frequencies from the measurements of the superimposed signal. We consider that the superimposed signal consists of three sinusoids. Thus, the state vector is formed as  $\mathbf{x}_k = [f_{1,k} \ f_{2,k} \ f_{3,k} \ a_{1,k} \ a_{2,k} \ a_{3,k}]^T$ . Subsequently, the state-space model follows Eqs. (4.14) and (4.15) (please refer to Chapter 4 for a detailed discussion).

The initial true and estimated states are taken as  $\mathbf{x}_0 = [200 \ 800 \ 1000 \ 2 \ 3 \ 5]^T$

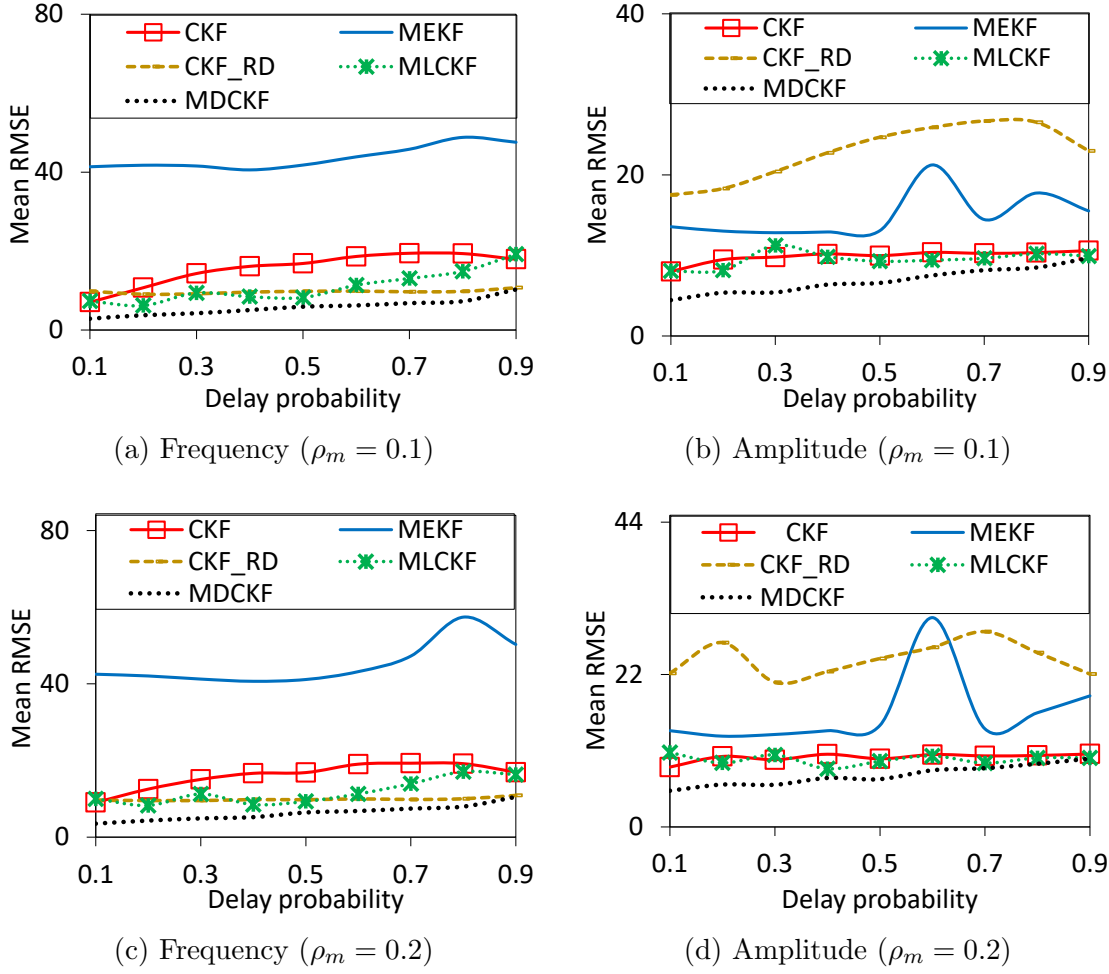


Figure 7.2: Problem 1, 1-delay scenario: Mean RMSE plots of all filters for varying delay probabilities, considering the missing measurement probability  $\rho_m$  as 0.1 and 0.2.

and  $\hat{\mathbf{x}}_{0|0} = [205 \ 785 \ 990 \ 4 \ 2 \ 3]^T$ , respectively, while the initial covariance is taken as  $\mathbf{P}_{0|0} = \text{diag}([25 \ 50 \ 20 \ 4 \ 1 \ 4])$ . The noise covariances are taken as  $\mathbf{Q}_k = \text{diag}([0.01 \ 0.01 \ 0.04 \ 0.25 \ 0.25 \ 0.25])$  and  $\mathbf{R}_k = \text{diag}([0.9 \ 0.9])$ . We obtain the RMSEs for the amplitude and frequency by taking the square root of the average of the mean square errors of the three amplitudes and frequencies, respectively, considering sampling interval as 0.25 ms. Please refer to Eq. (4.16) and associated discussion in Chapter 4.

We plot the mean RMSE (obtained over the time-steps) for varying delay probabilities in Figs. 7.2 and 7.3 for 1-delay and 2-delay, respectively. The mean RMSE plots show a reduced RMSE for the proposed MDCKF compared to the ordinary CKF and considered delay and missing filters. It concludes that the proposed filtering method has improved accuracy compared to these filters. The relative compu-



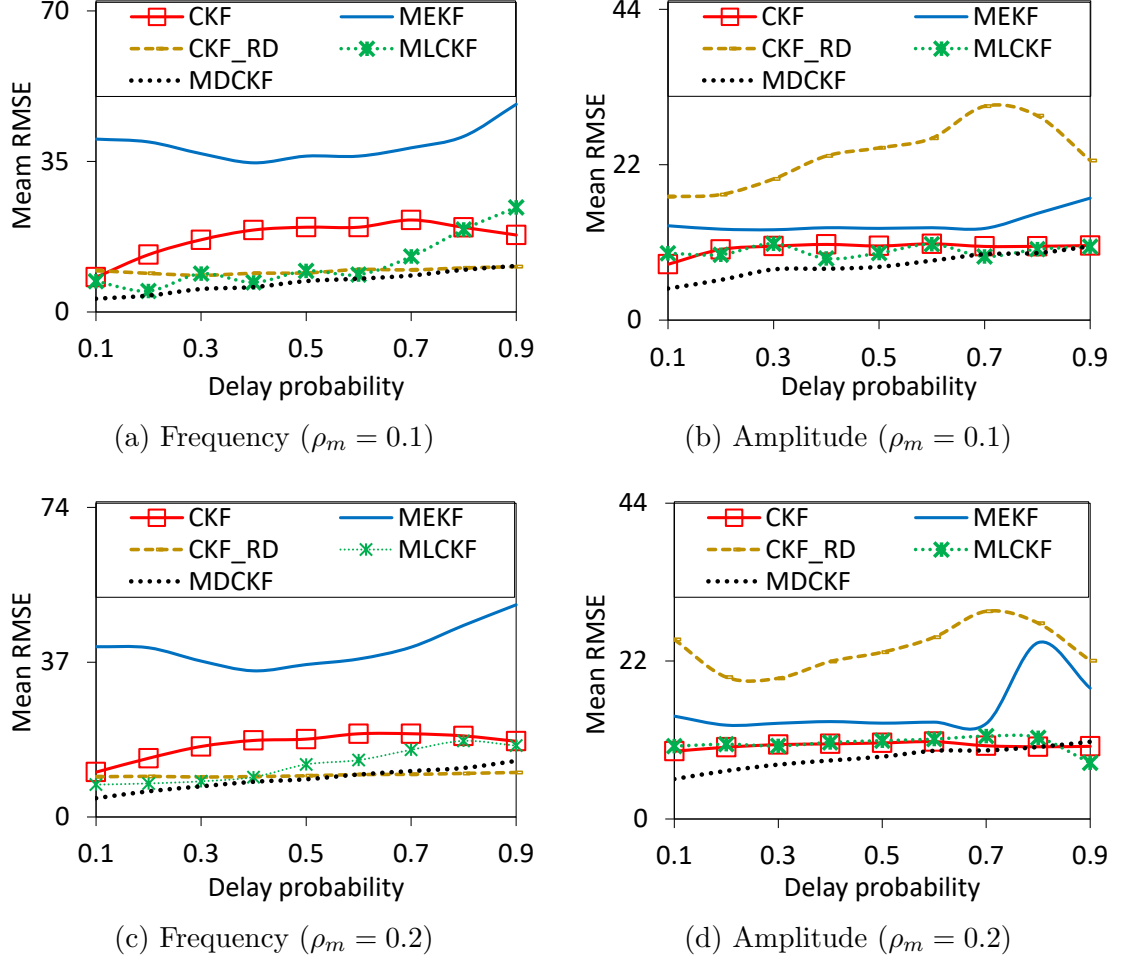


Figure 7.3: Problem 1, 2-delay scenario: Mean RMSE plots of all filters for varying delay probabilities, considering the missing measurement probability  $\rho_m$  as 0.1 and 0.2.

tational times for the MEKF, CKF, CKF\_RD, MLCKF, and MDCKF are observed as 1, 1.56, 1.69, 3.24, and 1.72, respectively.

### 7.4.2 Problem 2: Sinusoidal Growth Model

In this problem, we consider a two-dimensional system following sinusoidal dynamics [15, 29]. The author has already discussed the system in Section 4.4.2, Chapter 4, and the state-space model is given by Eqs. (4.17) and (4.18).

The true data of the state and measurement are generated by considering the initial state as  $\mathbf{x}_0 = [0.1 \ 0.1]^T$ . The filter is initialized with the initial estimate  $\hat{\mathbf{x}}_{0|0} = 0.9\mathbf{x}_0$  and  $\mathbf{P}_{0|0} = 7\mathbf{I}_2$ . The noise covariances are assigned as  $\mathbf{Q}_k = 0.1\mathbf{I}_2$  and  $\mathbf{R}_k = 0.1$ .

Figs. 7.4 and 7.5 show the mean RMSE plots for varying delay probability under

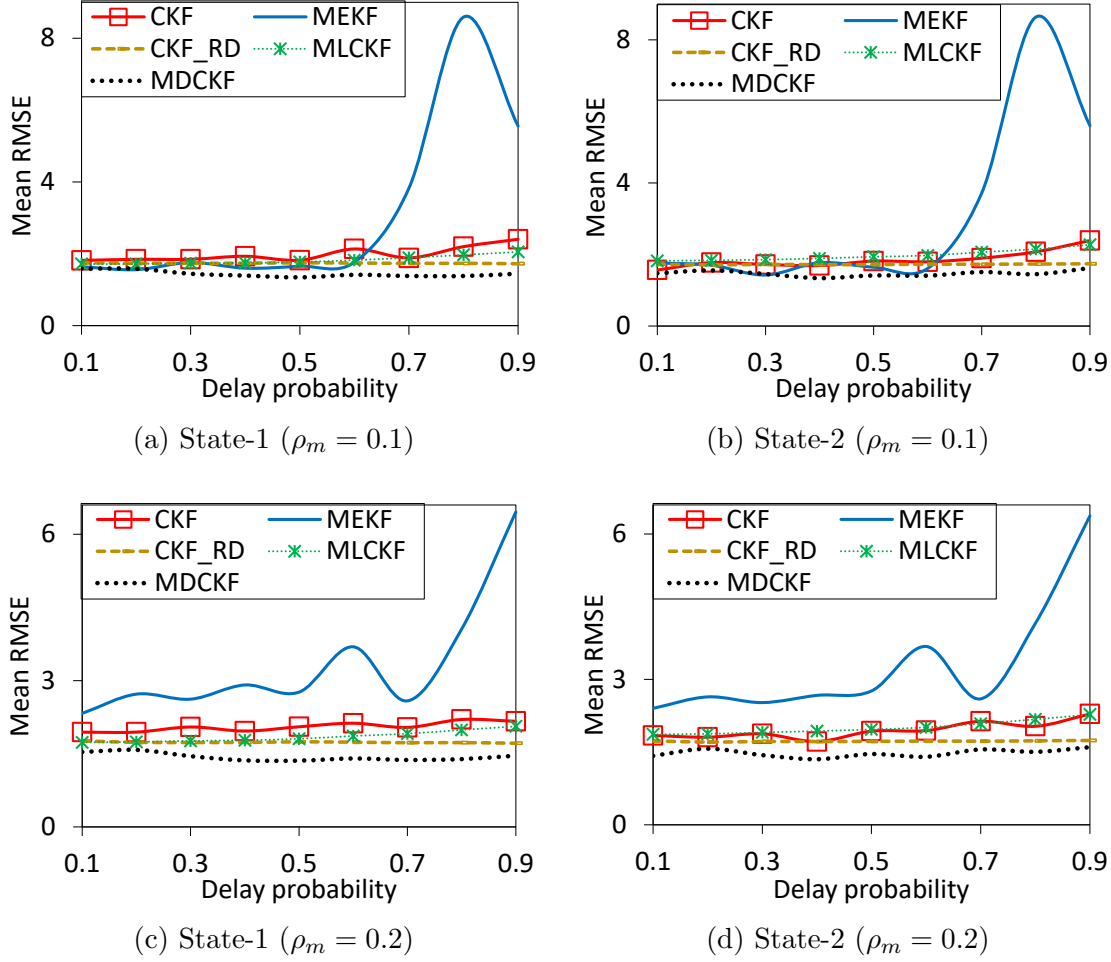


Figure 7.4: Problem 2, 1-delay scenario: Mean RMSE plots of all filters for varying delay probabilities, considering the missing measurement probability  $\rho_m$  as 0.1 and 0.2.

different scenarios formed by changing the maximum delay possibility and the missing measurements probability. The mean RMSE plots show a reduced RMSE for the MDCKF compared to the ordinary CKF, CKF\_RD, MEKF, and MLCKF, which concludes that the proposed filtering method outperforms the ordinary Gaussian filtering as well as the existing filters for handling the delay and missing measurements. The relative computational times of the CKF, MEKF, CKF\_RD, MLCKF, and MDCKF are obtained as 1, 2.86, 3.01, 5.78, and 3.04, respectively. It concludes that the computational time of the proposed method is marginally increased in comparison to some of the existing filters, while it remains marginally lower than others.

Table 7.1: Problem 1, 3-delay scenario: Average RMSEs obtained by MDCQKF, MDGHF, and their counterparts for different delay probabilities.

States	Filters	$\rho_m = 0.1$			$\rho_m = 0.2$		
		0.2	0.5	0.8	0.2	0.5	0.8
Amplitude	CQKF	8.78	10.24	10.54	9.52	10.33	10.51
	MDCQKF	5.55	7.36	8.70	6.10	7.61	9.10
	GHF	7.25	8.57	9.57	7.36	8.82	9.96
	MDGHF	5.01	5.48	6.79	4.15	5.06	6.62
Frequency	CQKF	11.70	17.10	18.55	13.89	18.34	18.09
	MDCQKF	3.78	5.92	8.71	4.40	6.61	9.02
	GHF	9.27	13.60	18.66	10.60	12.86	17.57
	MDGHF	3.46	5.89	8.20	4.49	6.69	8.41

Table 7.2: Problem 2, 3-delay scenario: Average RMSEs obtained by MDCQKF, MDGHF, and their counterparts for different delay probabilities.

States	Filters	$\rho_m = 0.1$			$\rho_m = 0.2$		
		0.2	0.5	0.8	0.2	0.5	0.8
State-1	CQKF	1.65	1.44	1.62	1.73	1.47	1.54
	MDCQKF	1.59	1.33	1.36	1.59	1.34	1.36
	GHF	1.74	1.67	2.17	1.89	1.69	2.24
	MDGHF	1.68	1.36	1.35	1.69	1.36	1.37
State-2	CQKF	1.56	1.50	1.47	1.58	1.52	1.46
	MDCQKF	1.56	1.43	1.33	1.56	1.43	1.33
	GHF	1.75	1.84	2.04	1.85	1.90	2.07
	MDGHF	1.67	1.49	1.33	1.65	1.48	1.34

Table 7.3: Problem 1, three-delay scenario: Relative computational time comparison of MDCQKF, MDGHF, and their counterparts for 0.3 delay probability.

$\rho_m$	Filters			
	CQKF	MDCQKF	GHF	MDGHF
0.1	1	1.091	0.812	1.083
0.2	1	1.1	0.813	0.908

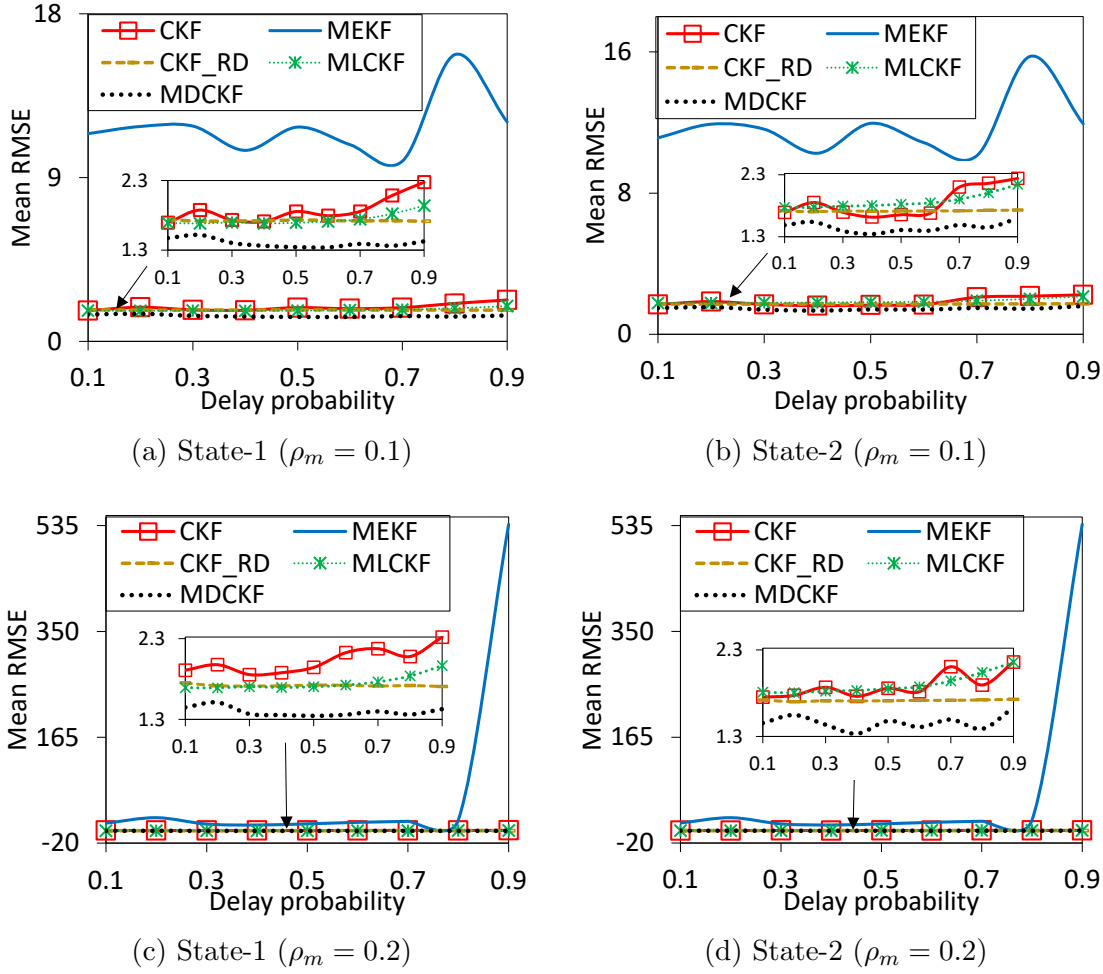


Figure 7.5: Problem 2, 2-delay scenario: Mean RMSE plots of all filters for varying delay probabilities, considering the missing measurement probability  $\rho_m$  as 0.1 and 0.2.

### 7.4.3 Performance Validation for Other Gaussian Filters

To compare the estimation accuracy of the proposed method and the ordinary Gaussian filtering method, we present the mean RMSEs of CKF-based plots only in Figs. 7.2 to 7.5. However, we further extend the comparative analysis for the other advanced and popular Gaussian filters, such as the CQKF [27] and GHF [28], in Tables 7.1 and 7.2. The tables present the mean RMSEs obtained using the CQKF, GHF, MDCQKF, and MDGHF for various delay and missing measurement probabilities. From the tables, we conclude that RMSE is reduced for the MDCQKF and MDGHF compared with their traditional counterparts CQKF and GHF, respectively. It is worth mentioning that the results for 2-delay scenarios are qualitatively very similar and are omitted for brevity. The computational times remain similar

for the proposed and the existing Gaussian filtering methods (Table 7.3).

## 7.5 Summary

The chapter introduces a new extension of Gaussian filtering to efficiently handle the simultaneously occurring delayed and missing measurements. The proposed method reformulates the measurement model stochastically to introduce the possibility of simultaneously occurring delayed and missing measurements. Subsequently, the proposed filtering method is designed by re-deriving the traditional Gaussian filtering method for the modified measurement model. We compare the proposed filter with the CKF and three well-known filters which handle the delay and missing measurements individually or simultaneously. The performance of the proposed method is validated for two simulation problems. We also studied the exponential stability of the proposed method for its EKF-based design. It is worth mentioning that the computational time of the proposed method remains similar to traditional Gaussian filtering.



# Chapter 8

## Stochastic Stability Analysis of Gaussian Filters with Measurement Irregularities

### 8.1 Introduction

The Gaussian filters [9, 10, 26, 27] have been applied in a range of practical applications due to improved performance over the traditional Kalman filter (KF), which is designed only for linear systems [12]. The extended Kalman filter (EKF) and unscented Kalman filter (UKF) have witnessed extensive use particularly in industries [34, 53, 185] due to their simpler implementation, lower computational cost, and reasonable accuracy.

However, implementing the Gaussian filters in real-time applications poses challenges in assessing its performance because the true state ( $\mathbf{x}_k$ ) is inaccessible. While offline simulations can offer some insights into filter performance, precise mathematical models are not always available. The Gaussian filters face two main sources of estimation error [11, 15, 186]: initialization error and stochastic errors from process and measurement noise. Initially, the dominant error is due to incorrect initialization, requiring time for the estimated state to approximately align with the true state. Once the initial error converges, noise-induced errors persist and contribute to the estimation error. Therefore, it is crucial to evaluate the Gaussian filter's performance online by measuring the convergence rate and persistent error

bounds in real systems. Such an analysis tool would be beneficial for many safety or performance-critical systems, including aircraft health management systems [187]. Other safety-critical applications includes autonomous vehicles and aerospace systems [188], wherein maintaining the stochastic stability of Gaussian filters can prevent catastrophic failures by providing reliable state estimates.

Reinforcing the discussion, the author further highlights below the importance of examining the stochastic stability of Gaussian filters.

- It helps understanding and managing estimation errors, ensuring they remain within acceptable bounds over time, which is vital for the filter’s reliability in real-world applications.
- It ensures the filter performs well under various noise conditions and uncertainties, which is crucial for designing robust systems.
- It advances the theoretical foundation of filtering techniques, facilitating the development of more advanced and efficient algorithms.

The literature witness some developments analyzing the error behavior for various Gaussian filters. For instance, [189–191] studied the stability properties for the EKF; they shown that the EKF remains bounded if the initial estimation error and noise covariances small enough. In other developments, [192] and [24] identified the conditions for the boundedness of the UKF and CKF, respectively. These studies [24, 189–192] are carried out considering the measurement model to be free of any measurement irregularities. It should be noted that the presence of irregularities, *e.g.*, delayed and missing measurements can significantly harm the estimation accuracy (error behavior), as discussed in the previous chapters. Therefore, the studies in [24, 189–192] may no longer be effective in their presence (irregularity). Probably, [193] and [194] are within very few studies, exploring the stability properties of the EKF and UKF, respectively, in the presence of missing measurements.

The scarce mathematical treatment of the Gaussian filters in the presence of irregularities has motivated the author to carry out stochastic stability analysis of various Gaussian filters handling delayed and missing measurements (discussed through Chapter 3 to Chapter 7). However, for simplicity reasons, in this chapter,



the author only presents the stability results for the modified Gaussian filter discussed in Chapter 6. Moreover, the author would like to mention that the approach (discussed in the later part of this chapter) applies to other Gaussian filters (for delay and missing measurements). Specifically, the same approach can be followed to study the stochastic stability for modified Gaussian filters, EKF\_M (Chapter 3), CKFM (Chapter 4), CKF\_RD\_PD (Chapter 5), and MDCKF (Chapter 7).

In this chapter, the author considers the Gaussian filter proposed in Chapter 6 (abbreviated as GFSCM) for stability analysis; the GFSCM is designed to handle the irregularity in which the received measurement is stochastically composed of both current and past measurements. The author studies the stochastic stability of the EKF-based formulation of the GFSCM, abbreviated as EKF\_S. Please note that stochastic stability of the GFSCM can also be studied through other Gaussian filters such as the CKF, CQKF, and GHF. However, these filters directly propagate the nonlinearities of the system, which poses severe challenges. On the other hand, the involvement of linearization step in the EKF simplifies the analysis to that of a linear system that can be performed more conveniently. The notion of stability is chosen as ‘exponentially bounded’, requiring that the estimation error is exponentially bounded in mean square if a set of presumptions are fulfilled.

### 8.1.1 Preparatory Operations

To establish the stochastic stability analysis for the GFSCM, the author recalls relevant models and parameters from previous chapters and performs some notation simplifications.

#### Retrieval of System Model and GFSCM Parameters

Let us first retrieve the following: i) standard state-space model (Eqs. (1.1) and (1.2)), ii) irregular measurement  $\mathbf{y}_k$  from Chapter 6 (Eq. (6.3)), and iii) parameters of the GFSCM derived through Theorems 6.1, 6.2, and 6.3, orderly given as follows

- State-space model:

$$\mathbf{x}_k = f(\mathbf{x}_{k-1}) + \boldsymbol{\eta}_k. \quad (8.1)$$

$$\mathbf{z}_k = h(\mathbf{x}_k) + \boldsymbol{\nu}_k. \quad (8.2)$$

- The GFSCM-related parameters:

$$\mathbf{y}_k = \sum_{j=0}^{N_d} \alpha_{k,j} \mathbf{z}_{k-j} = \sum_{j=0}^{N_d} \alpha_{k,j} (h(\mathbf{x}_{k-j}) + \boldsymbol{\nu}_{k-j}). \quad (8.3)$$

$$\hat{\mathbf{y}}_{k|k-1} = \sum_{j=0}^{N_d} \hat{\alpha}_j \hat{\mathbf{z}}_{k-j|k-1}, \quad (8.4)$$

$$\mathbf{P}_{k|k-1}^{\mathbf{y}\mathbf{y}} = \sum_{j=0}^{N_d} ((P_{\alpha_j} + \hat{\alpha}_j^2) \mathbf{P}_{k-j|k-1}^{\mathbf{z}\mathbf{z}} + P_{\alpha_j} \hat{\mathbf{z}}_{k-j|k-1} \hat{\mathbf{z}}_{k-j|k-1}^T). \quad (8.5)$$

$$\mathbf{P}_{k|k-1}^{\mathbf{x}\mathbf{y}} = \sum_{j=0}^{N_d} \hat{\alpha}_j \mathbf{P}_{k-j|k-1}^{\mathbf{x}\mathbf{z}}. \quad (8.6)$$

$$\mathbf{K} = \mathbf{P}_{k|k-1}^{\mathbf{x}\mathbf{y}} (\mathbf{P}_{k|k-1}^{\mathbf{y}\mathbf{y}})^{-1}. \quad (8.7)$$

$$\hat{\mathbf{x}}_{k|k} = \hat{\mathbf{x}}_{k|k-1} + \mathbf{K}(\mathbf{y}_k - \hat{\mathbf{y}}_{k|k-1}). \quad (8.8)$$

$$\mathbf{P}_{k|k} = \mathbf{P}_{k|k-1} - \mathbf{K} \mathbf{P}_{k|k-1}^{\mathbf{y}\mathbf{y}} \mathbf{K}^T. \quad (8.9)$$

### Retrieval of Stability-Related Definitions

Let us recall Definition 1.1 (Chapter 1) which defines exponential boundedness, as

$$\mathbb{E} [\|\boldsymbol{\zeta}_k\|^2] \leq \kappa' \mathbb{E} [\|\boldsymbol{\zeta}_0\|^2] \theta^k + \sigma' \quad \forall k \in \{1, 2, \dots\}. \quad (8.10)$$

Please refer to Chapter 1 for a detailed discussion on notations. Moreover, let us revisit the criteria given in Remark 1.1 (Chapter 1), which is the standard results available to infer the exponential stability in the mean square for a stochastic process (notations definitions are the same as given in Chapter 1).

$$\tau_1 \|\boldsymbol{\zeta}_k\|^2 \leq \mathbb{V}(\boldsymbol{\zeta}_k) \leq \tau_2 \|\boldsymbol{\zeta}_k\|^2 \quad (8.11)$$

$$\mathbb{E} [\mathbb{V}(\boldsymbol{\zeta}_k) | \boldsymbol{\zeta}_{k-1}] - \mathbb{V}(\boldsymbol{\zeta}_{k-1}) \leq \gamma' - \phi \mathbb{V}(\boldsymbol{\zeta}_{k-1}) \leq 0. \quad (8.12)$$

As discussed in Chapter 1, the stochastic process  $\boldsymbol{\zeta}_k$  satisfies exponential boundedness (Eq. (8.10)) if it fulfills Eqs. (8.11) and (8.12). The author uses the same approach to prove the stochastic stability of the GFSCM by considering the stochas-

tic process as the estimation error, which is expressed as

$$\mathbf{e}_{k|k} = \mathbf{x}_k - \hat{\mathbf{x}}_{k|k}. \quad (8.13)$$

Specifically, to prove the stability of the GFSCM, it is required to prove that  $\mathbf{e}_{k|k}$  remains exponentially bounded (follows Eq. (8.10)) by first satisfying Eqs. (8.11) and (8.12).

### Notations Simplification

For a convenient readability, let us simplify the notations  $\hat{\mathbf{x}}_{k|k-1}$ ,  $\mathbf{e}_{k|k-1}$ ,  $\mathbf{P}_{k|k-1}$ ,  $\hat{\mathbf{z}}_{k|k-1}$ ,  $\mathbf{P}_{k|k-1}^{\mathbf{zz}}$ ,  $\mathbf{P}_{k|k-1}^{\mathbf{xz}}$ ,  $\hat{\mathbf{y}}_{k|k-1}$ ,  $\mathbf{P}_{k|k-1}^{\mathbf{yy}}$ ,  $\mathbf{P}_{k|k-1}^{\mathbf{xy}}$ ,  $\hat{\mathbf{x}}_{k|k}$ ,  $\mathbf{e}_{k|k}$ , and  $\mathbf{P}_{k|k}$  as  $\tilde{\mathbf{x}}_k$ ,  $\tilde{\mathbf{e}}_k$ ,  $\tilde{\mathbf{P}}_k$ ,  $\tilde{\mathbf{z}}_k$ ,  $\tilde{\mathbf{P}}_k^{\mathbf{zz}}$ ,  $\tilde{\mathbf{P}}_k^{\mathbf{xz}}$ ,  $\tilde{\mathbf{y}}_k$ ,  $\tilde{\mathbf{P}}_k^{\mathbf{yy}}$ ,  $\tilde{\mathbf{P}}_k^{\mathbf{xy}}$ ,  $\hat{\mathbf{x}}_k$ ,  $\hat{\mathbf{e}}_k$ , and  $\hat{\mathbf{P}}_k$ , respectively.

### 8.1.2 Stochastic modeling of the estimation error of EKF\_S

Recalling the ordinary EKF parameters from [10],

$$\begin{cases} \tilde{\mathbf{x}}_k = f(\hat{\mathbf{x}}_{k-1}) \\ \tilde{\mathbf{P}}_k = \mathbf{F}_{k-1} \hat{\mathbf{P}}_{k-1} \mathbf{F}_{k-1}^T + \mathbf{Q}_k, \end{cases} \quad (8.14)$$

where  $\mathbf{F}_k$  represents the Jacobian of  $f(\mathbf{x}_k)$  computed for  $\mathbf{x}_k = \hat{\mathbf{x}}_k$ . Similarly [10],

$$\begin{cases} \tilde{\mathbf{z}}_k = h(\tilde{\mathbf{x}}_k), \tilde{\mathbf{P}}_k^{\mathbf{zz}} = \mathbf{H}_k \tilde{\mathbf{P}}_k \mathbf{H}_k^T + \mathbf{R}_k, \tilde{\mathbf{P}}_k^{\mathbf{xz}} = \tilde{\mathbf{P}}_k \mathbf{H}_k^T \\ \mathbf{K} = \tilde{\mathbf{P}}_k^{\mathbf{xz}} (\tilde{\mathbf{P}}_k^{\mathbf{zz}})^{-1} \\ \hat{\mathbf{x}}_k = \tilde{\mathbf{x}}_k + \mathbf{K} (\mathbf{z}_k - \tilde{\mathbf{z}}_k) \\ \hat{\mathbf{P}}_k = \tilde{\mathbf{P}}_k - \mathbf{K} \tilde{\mathbf{P}}_k^{\mathbf{zz}} \mathbf{K}^T, \end{cases} \quad (8.15)$$

where  $\mathbf{H}_k$  is the Jacobian matrix of  $h(\mathbf{x}_k)$  at  $\tilde{\mathbf{x}}_k$ , while  $\mathbf{K}$  represents the Kalman gain.

Before proceeding to the modeling of  $\hat{\mathbf{e}}_k$ , let us consider the following Taylor

series expansions

$$\begin{cases} f(\mathbf{x}_k) = f(\hat{\mathbf{x}}_k) + \mathbf{F}_k \hat{\mathbf{e}}_k + \Psi^f(\mathbf{x}_k, \hat{\mathbf{x}}_k) \\ h(\mathbf{x}_k) = h(\tilde{\mathbf{x}}_k) + \mathbf{H}_k \tilde{\mathbf{e}}_k + \Psi^h(\mathbf{x}_k, \tilde{\mathbf{x}}_k), \end{cases} \quad (8.16)$$

where  $\Psi^f(\mathbf{x}_k, \hat{\mathbf{x}}_k)$  and  $\Psi^h(\mathbf{x}_k, \tilde{\mathbf{x}}_k)$  represent the corresponding remainder terms.

To model  $\hat{\mathbf{e}}_k = \mathbf{x}_k - \hat{\mathbf{x}}_k$ , let us now substitute  $\mathbf{x}_k = f(\mathbf{x}_{k-1}) + \boldsymbol{\eta}_k$  and  $\tilde{\mathbf{x}}_k = f(\hat{\mathbf{x}}_{k-1})$  from Eqs. (8.1) and (8.14), respectively into  $\tilde{\mathbf{e}}_k = \mathbf{x}_k - \tilde{\mathbf{x}}_k$ . Subsequently, substituting  $f(\mathbf{x}_{k-1}) = f(\hat{\mathbf{x}}_{k-1}) + \mathbf{F}_{k-1} \hat{\mathbf{e}}_{k-1} + \Psi^f(\mathbf{x}_{k-1}, \hat{\mathbf{x}}_{k-1})$  using Eq. (8.16) in the resulting expression, we get

$$\tilde{\mathbf{e}}_k = \mathbf{F}_{k-1} \hat{\mathbf{e}}_{k-1} + \Psi^f(\mathbf{x}_{k-1}, \hat{\mathbf{x}}_{k-1}) + \boldsymbol{\eta}_k. \quad (8.17)$$

Similar to Eq. (8.15), we can express  $\hat{\mathbf{x}}_k$  in terms of  $\mathbf{y}_k$  giving  $\hat{\mathbf{e}}_k = \mathbf{x}_k - \tilde{\mathbf{x}}_k - \mathbf{K}(\mathbf{y}_k - \tilde{\mathbf{y}}_k)$ . Subsequently, substituting  $\mathbf{x}_k = f(\mathbf{x}_{k-1}) + \boldsymbol{\eta}_k$ ,  $\mathbf{y}_k = \sum_{j=0}^{N_d} \alpha_{k,j} \mathbf{z}_{k-j}$ ,  $\tilde{\mathbf{y}}_k = \sum_{j=0}^{N_d} \hat{\alpha}_j \hat{\mathbf{z}}_{k-j|k-1}$ , and  $\tilde{\mathbf{x}}_k = f(\hat{\mathbf{x}}_{k-1})$  from Eqs. (8.1), (8.3), (8.4), and (8.14), respectively, we get

$$\hat{\mathbf{e}}_k = f(\mathbf{x}_{k-1}) - f(\hat{\mathbf{x}}_{k-1}) + \boldsymbol{\eta}_k - \mathbf{K} \left( \sum_{j=0}^{N_d} (\alpha_{k,j} \mathbf{z}_{k-j} - \hat{\alpha}_j \tilde{\mathbf{z}}_{k-j}) \right). \quad (8.18)$$

We substitute  $\mathbf{z}_{k-j} = h(\mathbf{x}_{k-j}) + \boldsymbol{\nu}_{k-j}$  (extending Eq. (8.2)),  $\tilde{\mathbf{z}}_{k-j} = h(\tilde{\mathbf{x}}_{k-j})$  (extending Eq. (8.15)), and  $f(\mathbf{x}_{k-1}) - f(\hat{\mathbf{x}}_{k-1}) = \mathbf{F}_{k-1} \hat{\mathbf{e}}_{k-1} + \Psi^f(\mathbf{x}_{k-1}, \hat{\mathbf{x}}_{k-1})$  (extending Eq. (8.16)). Thus, we get

$$\hat{\mathbf{e}}_k = \mathbf{F}_{k-1} \hat{\mathbf{e}}_{k-1} + \Psi^f(\mathbf{x}_{k-1}, \hat{\mathbf{x}}_{k-1}) + \boldsymbol{\eta}_k - \mathbf{K} \sum_{j=0}^{N_d} [\alpha_{k,j} (h(\mathbf{x}_{k-j}) + \boldsymbol{\nu}_{k-j}) - \hat{\alpha}_j h(\tilde{\mathbf{x}}_{k-j})]. \quad (8.19)$$

Let now apply the following steps: i) add and subtract  $\sum_{j=0}^{N_d} \hat{\alpha}_j \mathbf{H}_{k-j} \tilde{\mathbf{e}}_{k-j}$  on the right side of the above equation and ii) expand  $h(\mathbf{x}_{k-j}) = h(\tilde{\mathbf{x}}_{k-j}) + \mathbf{H}_{k-j} \tilde{\mathbf{e}}_{k-j} + \Psi^h(\mathbf{x}_{k-j}, \tilde{\mathbf{x}}_{k-j})$  using Eq. (8.16). Subsequently, we obtain

$$\begin{aligned} \hat{\mathbf{e}}_k = & \mathbf{F}_{k-1} \hat{\mathbf{e}}_{k-1} + \Psi^f(\mathbf{x}_{k-1}, \hat{\mathbf{x}}_{k-1}) + \boldsymbol{\eta}_k - \mathbf{K} \sum_{j=0}^{N_d} \left[ (\alpha_{k,j} - \hat{\alpha}_j) (h(\tilde{\mathbf{x}}_{k-j}) \right. \\ & \left. + \mathbf{H}_{k-j} \tilde{\mathbf{e}}_{k-j}) + \alpha_{k,j} \Psi^h(\mathbf{x}_{k-j}, \tilde{\mathbf{x}}_{k-j}) + \hat{\alpha}_j \mathbf{H}_{k-j} \tilde{\mathbf{e}}_{k-j} + \alpha_{k,j} \boldsymbol{\nu}_{k-j} \right]. \end{aligned} \quad (8.20)$$

After expanding  $\tilde{\mathbf{e}}_{k-j} = \mathbf{F}_{k-j-1} \hat{\mathbf{e}}_{k-j-1} + \Psi^f(\mathbf{x}_{k-j-1}, \hat{\mathbf{x}}_{k-j-1}) + \boldsymbol{\eta}_{k-j}$  using Eq. (8.17), the above equation can be arranged as

$$\hat{\mathbf{e}}_k = \mathbf{j}_k \hat{\mathbf{e}}_{k-1} + \mathbf{i}_k + \mathbf{m}_k + \mathbf{n}_k, \quad (8.21)$$

where

$$\begin{cases} \mathbf{j}_k = (\mathbf{I} - \hat{\alpha}_0 \mathbf{K} \mathbf{H}_k) \mathbf{F}_{k-1} \\ \mathbf{i}_k = \boldsymbol{\eta}_k - \mathbf{K} \sum_{j=0}^{N_d} (\alpha_{k,j} \boldsymbol{\nu}_{k-j} + \hat{\alpha}_j \mathbf{H}_{k-j} \boldsymbol{\eta}_{k-j}) \\ \mathbf{m}_k = \Psi^f(\mathbf{x}_{k-1}, \hat{\mathbf{x}}_{k-1}) - \mathbf{K} \sum_{j=0}^{N_d} \left[ \alpha_{k,j} \Psi^h(\mathbf{x}_{k-j}, \tilde{\mathbf{x}}_{k-j}) + \hat{\alpha}_j \mathbf{H}_{k-j} \Psi^f(\mathbf{x}_{k-j-1}, \hat{\mathbf{x}}_{k-j-1}) \right] \\ \mathbf{n}_k = -\mathbf{K} \sum_{j=0}^{N_d} \left[ (\alpha_{k,j} - \hat{\alpha}_j) (h(\tilde{\mathbf{x}}_{k-j}) + \mathbf{H}_{k-j} \tilde{\mathbf{e}}_{k-j}) + \sum_{j=1}^{N_d} \hat{\alpha}_j \mathbf{H}_{k-j} \mathbf{F}_{k-j-1} \hat{\mathbf{e}}_{k-j-1} \right]. \end{cases} \quad (8.22)$$

### 8.1.3 Stability results

Recalling the previous discussion, to prove the stability of EKF<sub>S</sub>, we need to prove that there exists a scalar-valued stochastic process  $V(\hat{\mathbf{e}}_k)$  corresponding to  $\hat{\mathbf{e}}_k$  given in (8.21), which satisfies Eqs. (8.11) and (8.12). To derive the stochastic stability results, we consider the noise processes  $\boldsymbol{\eta}_k$  and  $\boldsymbol{\nu}_k$  to have an upper bound, instead of treating them as Gaussian random variables (the same as [189]). Subsequently, we adopt the following assumptions from the literature [189, 195]

- The system, noise, and filter parameters satisfy the following bounds:

$$\begin{aligned} \|\boldsymbol{\eta}_k\| &\leq \eta, \quad \|\boldsymbol{\nu}_k\| \leq \nu, \quad \|\mathbf{F}_k\| \leq a, \quad \|\mathbf{H}_k\| \leq c \\ \|\Psi^f(\mathbf{x}_{k-1}, \hat{\mathbf{x}}_{k-1})\| &\leq c_1 \|\hat{\mathbf{e}}_{k-1}\|^2 \\ \|\Psi^h(\mathbf{x}_k, \tilde{\mathbf{x}}_k)\| &\leq c_2 \|\tilde{\mathbf{e}}_k\|^2 \\ \rho_1 \mathbf{I} &\leq \hat{\mathbf{P}}_k \leq \tilde{\mathbf{P}}_k \leq \rho_2 \mathbf{I} \\ \|\hat{\mathbf{e}}_{k-1}\| &\leq \|\tilde{\mathbf{e}}_k\| \leq \epsilon, \quad \|h(\tilde{\mathbf{x}}_k)\| \leq h \\ q\mathbf{I} &\leq \mathbf{Q}_k \leq q'\mathbf{I} \quad \text{and} \quad r\mathbf{I} \leq \mathbf{R}_k \leq r'\mathbf{I}, \end{aligned} \quad (8.23)$$

with  $\eta, \nu, a, c, c_1, c_2, \rho_1, \rho_2, \epsilon, h, q, q', r$ , and  $r'$  representing positive real numbers.

- $\mathbf{F}_k$  is non-singular  $\forall k \geq 0$ .

Before proceeding further, we prove the following lemmas, which will be finally used in proving the stability.

**Lemma 8.1.** Let us assume that the bounds presented in Eq. (8.23) hold true, then the Kalman gain satisfies

$$\|\mathbf{K}\| \leq \frac{\Phi(P_{a_j}, \hat{\alpha}_j) \rho_2 c}{r}, \quad (8.24)$$

where  $\Phi(P_{a_j}, \hat{\alpha}_j) = \sum_{j=0}^{N_d} \hat{\alpha}_j / (\sum_{j=0}^{N_d} (P_{a_j} + \hat{\alpha}_j^2))$ .

*Proof.* Let us consider the expression of  $\mathbf{K}$  from Eq. (8.15) (given for  $\mathbf{z}_k$ ). Extending this expression for  $\mathbf{y}_k$ , we obtain  $\mathbf{K} = \tilde{\mathbf{P}}_k^{\mathbf{xy}} (\tilde{\mathbf{P}}_k^{\mathbf{yy}})^{-1}$ , with  $\tilde{\mathbf{P}}_k^{\mathbf{yy}}$  and  $\tilde{\mathbf{P}}_k^{\mathbf{xy}}$  given in Eqs. (8.5) and (8.6), respectively. Then, applying the norm operator and using its property[195], we get  $\|\mathbf{K}\| \leq \|\tilde{\mathbf{P}}_k^{\mathbf{xy}}\| \|(\tilde{\mathbf{P}}_k^{\mathbf{yy}})^{-1}\|$ . To this end, let us re-write  $\tilde{\mathbf{P}}_k^{\mathbf{yy}}$  and  $\tilde{\mathbf{P}}_k^{\mathbf{xy}}$  (in Eqs. (8.5) and (8.6), respectively) by substituting  $\tilde{\mathbf{z}}_{k-j} = h(\tilde{\mathbf{x}}_{k-j})$ ,  $\tilde{\mathbf{P}}_{k-j}^{\mathbf{zz}} = \mathbf{H}_{k-j} \tilde{\mathbf{P}}_{k-j} \mathbf{H}_{k-j}^T + \mathbf{R}_{k-j}$ , and  $\tilde{\mathbf{P}}_{k-j}^{\mathbf{zx}} = \tilde{\mathbf{P}}_{k-j} \mathbf{H}_{k-j}^T$  by extending Eq. (8.15). For the modified  $\tilde{\mathbf{P}}_k^{\mathbf{yy}}$  and  $\tilde{\mathbf{P}}_k^{\mathbf{xy}}$  expressions, the inequality  $\|\mathbf{K}\| \leq \|\tilde{\mathbf{P}}_k^{\mathbf{xy}}\| \|(\tilde{\mathbf{P}}_k^{\mathbf{yy}})^{-1}\|$  can be re-written as

$$\|\mathbf{K}\| \leq \left\| \sum_{j=0}^{N_d} \left( \hat{\alpha}_j \tilde{\mathbf{P}}_{k-j} \mathbf{H}_{k-j}^T \right) \right\| \times \|(\boldsymbol{\Sigma}_s)^{-1}\|, \quad (8.25)$$

where

$$\boldsymbol{\Sigma}_s = \sum_{j=0}^{N_d} (P_{a_j} + \hat{\alpha}_j^2) (\mathbf{H}_{k-j} \tilde{\mathbf{P}}_{k-j} \mathbf{H}_{k-j}^T + \mathbf{R}_{k-j}) + \sum_{j=0}^{N_d} P_{a_j} h(\tilde{\mathbf{x}}_{k-j}) h(\tilde{\mathbf{x}}_{k-j})^T. \quad (8.26)$$

Please note the following for the above equation: i)  $\tilde{\mathbf{P}}_{k-j}$  is positive definite (from Eq. (8.23)), concluding  $\mathbf{H}_{k-j} \tilde{\mathbf{P}}_{k-j} \mathbf{H}_{k-j}^T$  to be positive semidefinite, as  $\mathbf{H}_{k-j} \in \mathbb{R}^{q \times n}$  can be singular ( $q = n$ ) or have nontrivial null space ( $q \neq n$ ), ii) The resultant of  $h(\tilde{\mathbf{x}}_{k-j}) h(\tilde{\mathbf{x}}_{k-j})^T$  is positive semidefinite, as it represents the multiplication of a real vector with its conjugate transpose, and iii)  $\tilde{\mathbf{R}}_{k-j}$  is positive definite (from Eq. (8.23)). These observations collectively conclude that  $\boldsymbol{\Sigma}_s$  is also a positive definite. Please note that the spectral norm is given as the largest singular value for a matrix, *i.e.*,  $\|\cdot\| = \Omega^l(\cdot)$ , with  $\Omega^l(\cdot)$  representing the largest singular value. Being a

positive definite matrix,  $\Sigma_s$  further satisfies  $\|(\Sigma_s)^{-1}\| = \Omega^l((\Sigma_s)^{-1}) = (\Omega^s(\Sigma_s))^{-1} = (\lambda^s(\Sigma_s))^{-1}$ , where  $\Omega^s(\cdot)$  and  $\lambda^s(\cdot)$  represent the smallest singular value and the smallest eigenvalue, respectively. Following the discussion, we can now use the Rayleigh-Ritz characterization [196] for computing  $\lambda^s(\Sigma_s)$ , which follows the inequality given as

$$\begin{aligned} \lambda^s(\Sigma_s) \geq & \min_{\|\chi\|=1} \left( \chi^T \sum_{j=0}^{N_d} (P_{a_j} + \hat{\alpha}_j^2) \mathbf{H}_{k-j} \tilde{\mathbf{P}}_{k-j} \mathbf{H}_{k-j}^T \chi \right) + \min_{\|\chi\|=1} \left( \chi^T \sum_{j=0}^{N_d} (P_{a_j} + \hat{\alpha}_j^2) \mathbf{R}_{k-j} \chi \right) \\ & + \min_{\|\chi\|=1} \left( \chi^T \sum_{j=0}^{N_d} P_{a_j} h(\tilde{\mathbf{x}}_{k-j}) h(\tilde{\mathbf{x}}_{k-j})^T \chi \right), \end{aligned} \quad (8.27)$$

with  $\chi$  being a non-zero vector with an appropriate dimension and  $\min(\cdot)$  denoting the minimum function. The positive semi-definiteness of  $\mathbf{H}_{k-j} \tilde{\mathbf{P}}_{k-j} \mathbf{H}_{k-j}^T$  and  $h(\tilde{\mathbf{x}}_{k-j}) h(\tilde{\mathbf{x}}_{k-j})^T$  (as discussed earlier) conclude that the first and third terms of the above expression, representing a quadratic form, become zero. We calculate the second term by applying the bound  $r\mathbf{I} \leq \mathbf{R}_k$  (from Eq. (8.23)), which gives  $\lambda^s(\Sigma_s) \geq \sum_{j=0}^{N_d} (P_{a_j} + \hat{\alpha}_j^2) r$ . Subsequently, taking its inverse and from the previous discussion, we obtain

$$\Omega^l((\Sigma_s)^{-1}) = (\lambda^s(\Sigma_s))^{-1} \leq \frac{1}{\sum_{j=0}^{N_d} (P_{a_j} + \hat{\alpha}_j^2) r}. \quad (8.28)$$

Let us now recall Eq. (8.25) and do the following substitutions: i) apply the inequalities  $\mathbf{P}_k \leq \rho_2 \mathbf{I}$  and  $\|\mathbf{H}_k\| \leq c$  (Eq. (8.23)) to get  $\sum_{j=0}^{N_d} \|\hat{\alpha}_j \tilde{\mathbf{P}}_{k-j} \mathbf{H}_{k-j}^T\| \leq \sum_{j=0}^{N_d} \hat{\alpha}_j \rho_2 c$  and ii) As  $\|(\Sigma_s)^{-1}\| = \Omega^l((\Sigma_s)^{-1})$ , substitute the inequality of  $\Omega^l((\Sigma_s)^{-1})$  from Eq. (8.28). Subsequently, Eq. (8.25) deduces the bound of  $\mathbf{K}$  as given in Eq. (8.24).  $\square$

**Lemma 8.2.** For  $\mathbf{j}_k$  defined in Eq. (8.22), there exists  $0 < \gamma < 1$ , satisfying the inequality

$$\mathbf{j}_k \hat{\mathbf{P}}_k^{-1} \mathbf{j}_k \leq (1 - \gamma) \hat{\mathbf{P}}_{k-1}^{-1}. \quad (8.29)$$

*Proof.* Substituting  $\hat{\mathbf{e}}_k = \mathbf{x}_k - \tilde{\mathbf{x}}_k - \mathbf{K}(\mathbf{y}_k - \tilde{\mathbf{y}}_k)$  into  $\hat{\mathbf{P}}_k = \mathbb{E}[\hat{\mathbf{e}}_k \hat{\mathbf{e}}_k^T]$ , we get

$$\hat{\mathbf{P}}_k = \tilde{\mathbf{P}}_k - \tilde{\mathbf{P}}_k^{\mathbf{xy}} \mathbf{K}^T - \mathbf{K}(\tilde{\mathbf{P}}_k^{\mathbf{xy}})^T + \mathbf{K} \tilde{\mathbf{P}}_k^{\mathbf{yy}} \mathbf{K}^T. \quad (8.30)$$

Substituting  $\tilde{\mathbf{P}}_k^{\mathbf{y}\mathbf{y}}(\mathbf{P}_{k|k-1}^{\mathbf{y}\mathbf{y}}) = \sum_{j=0}^{N_d} ((P_{\alpha_j} + \hat{\alpha}_j^2) \tilde{\mathbf{P}}_{k-j}^{\mathbf{z}\mathbf{z}} + P_{\alpha_j} \tilde{\mathbf{z}}_{k-j} \tilde{\mathbf{z}}_{k-j}^T)$  and  $\tilde{\mathbf{P}}_k^{\mathbf{x}\mathbf{y}}(\mathbf{P}_{k|k-1}^{\mathbf{x}\mathbf{y}}) = \sum_{j=0}^{N_d} \hat{\alpha}_j \tilde{\mathbf{P}}_{k-j}^{\mathbf{x}\mathbf{z}}$  from Eqs. (8.5) and (8.6), respectively, we get

$$\begin{aligned} \hat{\mathbf{P}}_k = & \tilde{\mathbf{P}}_k - \sum_{j=0}^{N_d} \hat{\alpha}_j \tilde{\mathbf{P}}_{k-j}^{\mathbf{x}\mathbf{z}} \mathbf{K}^T - \mathbf{K} \sum_{j=0}^{N_d} \hat{\alpha}_j (\tilde{\mathbf{P}}_{k-j}^{\mathbf{x}\mathbf{z}})^T \\ & + \mathbf{K} \sum_{j=0}^{N_d} \left( (P_{\alpha_j} + \hat{\alpha}_j^2) \tilde{\mathbf{P}}_{k-j}^{\mathbf{z}\mathbf{z}} + P_{\alpha_j} \tilde{\mathbf{z}}_{k-j} \tilde{\mathbf{z}}_{k-j}^T \right) \mathbf{K}^T. \end{aligned} \quad (8.31)$$

Expanding  $\tilde{\mathbf{z}}_{k-j} = h(\tilde{\mathbf{x}}_{k-j})$ ,  $\tilde{\mathbf{P}}_{k-j}^{\mathbf{z}\mathbf{z}} = \mathbf{H}_{k-j} \tilde{\mathbf{P}}_{k-j} \mathbf{H}_{k-j}^T + \mathbf{R}_{k-j}$ , and  $\tilde{\mathbf{P}}_{k-j}^{\mathbf{x}\mathbf{z}} = \tilde{\mathbf{P}}_{k-j} \mathbf{H}_{k-j}^T$  from Eq. (8.15), we obtain

$$\begin{aligned} \hat{\mathbf{P}}_k = & \tilde{\mathbf{P}}_k - \sum_{j=0}^{N_d} \hat{\alpha}_j \tilde{\mathbf{P}}_{k-j} \mathbf{H}_{k-j}^T \mathbf{K}^T - \mathbf{K} \sum_{j=0}^{N_d} \hat{\alpha}_j \mathbf{H}_{k-j} \tilde{\mathbf{P}}_{k-j} + \mathbf{K} \sum_{j=0}^{N_d} \left[ (P_{\alpha_j} + \hat{\alpha}_j^2) \right. \\ & \times \left. \left( \mathbf{H}_{k-j} \tilde{\mathbf{P}}_{k-j} \mathbf{H}_{k-j}^T + \mathbf{R}_{k-j} \right) + P_{\alpha_j} h(\tilde{\mathbf{x}}_{k-j}) h^T(\tilde{\mathbf{x}}_{k-j}) \right] \mathbf{K}^T. \end{aligned} \quad (8.32)$$

After adding and subtracting  $\sum_{j=1}^{N_d} \tilde{\mathbf{P}}_{k-j}$  on the right side of the above equation, it can be arranged as

$$\begin{aligned} \hat{\mathbf{P}}_k = & \sum_{j=0}^{N_d} (\mathbf{I} - \hat{\alpha}_j \mathbf{K} \mathbf{H}_{k-j}) \tilde{\mathbf{P}}_{k-j} (\mathbf{I} - \hat{\alpha}_j \mathbf{K} \mathbf{H}_{k-j})^T + \mathbf{K} \sum_{j=0}^{N_d} \left[ (P_{\alpha_j} + \hat{\alpha}_j^2) \right. \\ & \times \left. \left( \mathbf{H}_{k-j} \tilde{\mathbf{P}}_{k-j} \mathbf{H}_{k-j}^T + \mathbf{R}_{k-j} \right) + P_{\alpha_j} h(\tilde{\mathbf{x}}_{k-j}) h^T(\tilde{\mathbf{x}}_{k-j}) \right] \mathbf{K}^T - \sum_{j=1}^{N_d} \tilde{\mathbf{P}}_{k-j}. \end{aligned} \quad (8.33)$$

As discussed previously,  $\mathbf{H}_{k-j} \tilde{\mathbf{P}}_{k-j} \mathbf{H}_{k-j}^T$  and  $h(\tilde{\mathbf{x}}_{k-j}) h^T(\tilde{\mathbf{x}}_{k-j})$  are positive semidefinite, while  $\tilde{\mathbf{P}}_{k-j}$  and  $\mathbf{R}_{k-j}$  are positive definite due to being diagonal matrices with positive diagonal elements. Thus, it follows [195]

$$\mathbf{K} \sum_{j=0}^{N_d} \left[ (P_{\alpha_j} + \hat{\alpha}_j^2) \left( \mathbf{H}_{k-j} \tilde{\mathbf{P}}_{k-j} \mathbf{H}_{k-j}^T + \mathbf{R}_{k-j} \right) + P_{\alpha_j} h(\tilde{\mathbf{x}}_{k-j}) h^T(\tilde{\mathbf{x}}_{k-j}) \right] \mathbf{K}^T \geq 0 \quad (8.34)$$

and

$$\sum_{j=1}^{N_d} (\mathbf{I} - \hat{\alpha}_j \mathbf{K} \mathbf{H}_{k-j}) \tilde{\mathbf{P}}_{k-j} (\mathbf{I} - \hat{\alpha}_j \mathbf{K} \mathbf{H}_{k-j})^T \geq 0, \quad (8.35)$$



which further concludes that

$$\hat{\mathbf{P}}_k \geq (\mathbf{I} - \hat{\alpha}_0 \mathbf{K} \mathbf{H}_k) \tilde{\mathbf{P}}_k (\mathbf{I} - \hat{\alpha}_0 \mathbf{K} \mathbf{H}_k)^T - \sum_{j=1}^{N_d} \tilde{\mathbf{P}}_{k-j}. \quad (8.36)$$

Substituting  $\tilde{\mathbf{P}}_k = \mathbf{F}_{k-1} \hat{\mathbf{P}}_{k-1} \mathbf{F}_{k-1}^T + \mathbf{Q}_k$  from Eq. (8.14) and  $-\sum_{j=1}^{N_d} \tilde{\mathbf{P}}_{k-j} \geq -N_d \rho_2 \mathbf{I}$  from the bounds of  $\tilde{\mathbf{P}}_k$  (Eq. (8.23)), the above inequality can be expressed as

$$\begin{aligned} \hat{\mathbf{P}}_k \geq & (\mathbf{I} - \hat{\alpha}_0 \mathbf{K} \mathbf{H}_k) \mathbf{F}_{k-1} \hat{\mathbf{P}}_{k-1} \left\{ \mathbf{I} + \hat{\mathbf{P}}_{k-1}^{-1} \mathbf{F}_{k-1}^{-1} [\mathbf{Q}_k - N_d \rho_2 (\mathbf{I} - \hat{\alpha}_0 \mathbf{K} \mathbf{H}_k)^{-1} \right. \\ & \left. \times (\mathbf{I} - \hat{\alpha}_0 \mathbf{K} \mathbf{H}_k)^{-T}] \mathbf{F}_{k-1}^{-T} \right\} \mathbf{F}_{k-1}^T (\mathbf{I} - \hat{\alpha}_0 \mathbf{K} \mathbf{H}_k)^T. \end{aligned} \quad (8.37)$$

Multiplying  $\mathbf{F}_{k-1}^{-1} (\mathbf{I} - \hat{\alpha}_0 \mathbf{K} \mathbf{H}_k)^{-1}$  and  $(\mathbf{I} - \hat{\alpha}_0 \mathbf{K} \mathbf{H}_k)^{-T} \mathbf{F}_{k-1}^{-T}$  on the both sides of the above inequality gives

$$\begin{aligned} \mathbf{F}_{k-1}^{-1} (\mathbf{I} - \hat{\alpha}_0 \mathbf{K} \mathbf{H}_k)^{-1} \hat{\mathbf{P}}_k (\mathbf{I} - \hat{\alpha}_0 \mathbf{K} \mathbf{H}_k)^{-T} \mathbf{F}_{k-1}^{-T} \geq & \hat{\mathbf{P}}_{k-1} \left\{ \mathbf{I} + \hat{\mathbf{P}}_{k-1}^{-1} \mathbf{F}_{k-1}^{-1} \right. \\ & \left. \times [\mathbf{Q}_k - N_d \rho_2 (\mathbf{I} - \hat{\alpha}_0 \mathbf{K} \mathbf{H}_k)^{-1} (\mathbf{I} - \hat{\alpha}_0 \mathbf{K} \mathbf{H}_k)^{-T}] \mathbf{F}_{k-1}^{-T} \right\}. \end{aligned} \quad (8.38)$$

We now use the bounds of  $\hat{\mathbf{P}}_k$ ,  $\mathbf{F}_k$ , and  $\mathbf{Q}_k$  from inequality (8.23), and subsequently, apply the inverse operator. Thus, we obtain

$$\mathbf{F}_{k-1}^T (\mathbf{I} - \hat{\alpha}_0 \mathbf{K} \mathbf{H}_k)^T \hat{\mathbf{P}}_k^{-1} (\mathbf{I} - \hat{\alpha}_0 \mathbf{K} \mathbf{H}_k) \mathbf{F}_{k-1} \leq \left( 1 + \frac{1}{\rho_2 a^2} (q - \delta_1^2 N_d \rho_2) \right)^{-1} \hat{\mathbf{P}}_{k-1}^{-1}, \quad (8.39)$$

where  $\delta_1 = \Omega^l((\mathbf{I} - \hat{\alpha}_0 \mathbf{K} \mathbf{H}_k)^{-1})$ . With  $q/(\delta_1^2 N_d \rho_2) > 1$ , the following holds

$$0 < \left( 1 + \frac{q - \delta_1^2 N_d \rho_2}{\rho_2 a^2} \right)^{-1} < 1. \quad (8.40)$$

Let us now define  $\gamma = (q - \delta_1^2 N_d \rho_2)/(\rho_2 a^2 + q - \delta_1^2 N_d \rho_2)$ , concluding

$$0 < 1 - \gamma = \left( 1 + \frac{q - \delta_1^2 N_d \rho_2}{\rho_2 a^2} \right)^{-1} < 1. \quad (8.41)$$

For the above-defined  $1 - \gamma$  and  $\mathbf{j}_k$  given in Eq. (8.22), Eq. (8.39) deduces Eq. (8.29).  $\square$

We now prove the exponential stability of the EKF-S using the results of the two preceding lemmas. Recalling the previous discussions, the exponential stability

of EKF\_S requires that its estimation error, *i.e.*,  $\hat{\mathbf{e}}_k$  given in Eq. (8.21), remains exponentially bounded in mean square. We prove the boundedness of  $\hat{\mathbf{e}}_k$  in the subsequent theorem.

**Theorem 8.1.** Considering that the inequalities given in Eq. (8.23) hold true, for the ordinary EKF parameters given through Eqs. (8.14) and (8.15),  $\hat{\mathbf{e}}_k$  given in Eq. (8.21) approximately remains exponentially bounded in mean square, *i.e.*,

$$\mathbb{E}[\|\hat{\mathbf{e}}_k\|^2] \leq \kappa' \mathbb{E}[\|\hat{\mathbf{e}}_0\|^2] \theta^k + \sigma' \quad \forall k \in \{1, 2, \dots\}. \quad (8.42)$$

*Proof.* As stated earlier, the exponential boundedness of  $\hat{\mathbf{e}}_k$  requires that there exists a scalar-valued stochastic process  $\mathbb{V}(\hat{\mathbf{e}}_k)$ , satisfying Eqs. (8.11) and (8.12). We choose  $\mathbb{V}(\hat{\mathbf{e}}_k) = \hat{\mathbf{e}}_k^T \hat{\mathbf{P}}_k^{-1} \hat{\mathbf{e}}_k$ , which is rewritten by substituting  $\hat{\mathbf{e}}_k = \mathbf{j}_k \hat{\mathbf{e}}_{k-1} + \mathbf{i}_k + \mathbf{m}_k + \mathbf{n}_k$  from Eq. (8.21) as

$$\begin{aligned} \mathbb{V}(\hat{\mathbf{e}}_k) = & \hat{\mathbf{e}}_{k-1}^T \mathbf{j}_k^T \hat{\mathbf{P}}_k^{-1} \mathbf{j}_k \hat{\mathbf{e}}_{k-1} + \mathbf{m}_k^T \hat{\mathbf{P}}_k^{-1} (2\mathbf{j}_k \hat{\mathbf{e}}_{k-1} + \mathbf{m}_k) + 2\mathbf{i}_k^T \hat{\mathbf{P}}_k^{-1} \\ & \times (\mathbf{j}_k \hat{\mathbf{e}}_{k-1} + \mathbf{m}_k + \mathbf{n}_k) + \mathbf{i}_k^T \hat{\mathbf{P}}_k^{-1} \mathbf{i}_k + 2\mathbf{n}_k^T \hat{\mathbf{P}}_k^{-1} (\mathbf{j}_k \hat{\mathbf{e}}_{k-1} + \mathbf{m}_k) + \mathbf{n}_k^T \hat{\mathbf{P}}_k^{-1} \mathbf{n}_k. \end{aligned} \quad (8.43)$$

As  $\mathbb{V}(\hat{\mathbf{e}}_k)$  is scalar, which follows  $\mathbb{V}(\hat{\mathbf{e}}_k) = \|\mathbb{V}(\hat{\mathbf{e}}_k)\|$ . Subsequently, applying the norm-operator and using its property, the bounds for individual terms (comprising vectors and matrices) on right side of the above equation are obtained as

$$\left\{ \begin{array}{l} \|\mathbf{m}_k^T \hat{\mathbf{P}}_k^{-1} (2\mathbf{j}_k \hat{\mathbf{e}}_{k-1} + \mathbf{m}_k)\| \leq g_1 \\ \|\mathbf{i}_k^T \hat{\mathbf{P}}_k^{-1} \mathbf{i}_k\| \leq g_2 \\ \|2\mathbf{n}_k^T \hat{\mathbf{P}}_k^{-1} (\mathbf{j}_k \hat{\mathbf{e}}_{k-1} + \mathbf{m}_k)\| \leq g_3 \\ \|\mathbf{n}_k^T \hat{\mathbf{P}}_k^{-1} \mathbf{n}_k\| \leq g_4, \end{array} \right. \quad (8.44)$$

where  $g_1, g_2, g_3$ , and  $g_4$  are constants, which can be obtained in terms of  $\eta, \nu, c_1, c_2, a, c, \rho_1, \rho_2, \epsilon', h, q, q', r, r', \hat{\alpha}_j$ , and  $P_{a_j}$ .

Let us now adopt the following steps

- Extending Lemma 8.2 gives  $\hat{\mathbf{e}}_{k-1}^T \mathbf{j}_k^T \hat{\mathbf{P}}_k^{-1} \mathbf{j}_k \hat{\mathbf{e}}_{k-1} \leq (1 - \gamma)V(\hat{\mathbf{e}}_{k-1})$ .
- Substitute  $g_1, g_2, g_3, g_4$ , and  $\hat{\mathbf{e}}_{k-1}^T \mathbf{j}_k^T \hat{\mathbf{P}}_k^{-1} \mathbf{j}_k \hat{\mathbf{e}}_{k-1}$  from the above discussion, and

subsequently take the expectation operator.

- The expression of  $\mathbf{i}_k$  defined in Eq. (8.22) concludes that  $\mathbb{E}[2\mathbf{i}_k^T \hat{\mathbf{P}}_k^{-1}(\mathbf{j}_k \hat{\mathbf{e}}_k + \mathbf{m}_k + \mathbf{n}_k)] = 0$ , as  $\mathbf{i}_k$  comprises mean-zero noise terms  $\boldsymbol{\eta}_k$  and  $\boldsymbol{\nu}_k$ .

From the above discussion, we can rewrite Eq. (8.43) as

$$\mathbb{E}[\mathbb{V}(\hat{\mathbf{e}}_k)|\hat{\mathbf{e}}_{k-1}] - \mathbb{V}(\hat{\mathbf{e}}_{k-1}) \leq g_1 + g_2 + g_3 + g_4 - \gamma \mathbb{V}(\hat{\mathbf{e}}_{k-1}). \quad (8.45)$$

Defining  $g_1 + g_2 + g_3 + g_4 = \rho$ , and subsequently choosing  $g_1, g_2, g_3$ , and  $g_4$  such that  $\mathbb{V}(\hat{\mathbf{e}}_{k-1}) \geq \rho/\gamma$  satisfies, the above equation further (approximately) satisfies Eq. (8.12) (the second criterion).

Let us now consider the inequality of the error covariance matrix  $\hat{\mathbf{P}}_k$  presented in Eq. (8.23). We first apply the inverse operator and then multiply  $\hat{\mathbf{e}}_k^T$  and  $\hat{\mathbf{e}}_k$ . Subsequently, we get

$$\frac{1}{\rho_2} \|\hat{\mathbf{e}}_k\|^2 \leq \mathbb{V}(\hat{\mathbf{e}}_k) \leq \frac{1}{\rho_1} \|\hat{\mathbf{e}}_k\|^2. \quad (8.46)$$

Please note that with  $1/\rho_2 = \phi_1$  and  $1/\rho_1 = \phi_2$ , the above equation is the same as Eq. (8.11) (the first criterion).

It can be observed that Eqs. (8.45) and (8.46) collectively satisfy the two necessary conditions of stability presented through Eqs. (8.11) and (8.12). Thus, we can conclude that, for the bounds presented in Eq. (8.23), the estimation error of the EKF\_S remains exponentially bounded in the mean square, which concludes the stability of EKF\_S.  $\square$

## 8.2 Summary

This chapter studied the stochastic stability of the modified Gaussian filter for stochastically composed current and past measurements (GFSCM). The EKF-based (EKF\_S) formulation of the GFSCM was considered to for this purpose. The author proved that the estimation error of the EKF\_S remains exponentially bounded in mean square, if the system, filter, and noise parameters are bounded by a set of predefined conditions. Firstly, a dynamic model of the estimation error was formulated, and subsequently, it was shown to follow exponential boundedness for some

conditions.

It is worth mentioning that the author has also carried out stability analysis for other Gaussian filters developed in the thesis. The stability analysis for these filters also follow steps similar to those presented in this chapter, although various expressions and bounds are different from the ones presented in this chapter. The reason is that the measurement models for these filters differ as they incorporate irregularities of different forms. Therefore, the discussions on these filters were eliminated from this thesis for brevity.





# Chapter 9

## Gaussian Kernel Quadrature Kalman Filter

### 9.1 Introduction

The solutions to practical nonlinear filtering problems are divided into two broad categories: Gaussian filters [11, 15] and particle filters (PF) [197, 198]. In general, the Gaussian filters are computationally efficient and fast but less accurate [15]. However, the particle filters are computationally inefficient and slow but are more accurate [15]. Similar to various variants of the Gaussian filters [9, 10, 27, 28, 49, 62, 64, 68, 69] (discussed in Chapter 2), some popular versions of the PF appear in the filtering literature [197, 199–201].

The particle filters' computational inefficacy is mostly intolerable and the Gaussian filters become a common choice for practical applications. However, the current technological era of computational devices is witnessing remarkable developments and offering low-cost efficient computational devices. Subsequently, the computational capacity is often excessive for the general Gaussian filters [9, 26–28, 57, 61, 69], though inadequate for the particle filters. Thus, the practitioners may be benefited if an advanced Gaussian filter is developed, which can utilize the excessive computational capacity to improve the accuracy. Alternatively, an advanced Gaussian filter is desired that can provide a trade-off between the general Gaussian filters and particle filters in terms of the computational demand and accuracy. An inadequate trade-off is currently achieved by a class of Gaussian filters itself, named quadra-

ture rule based filters [11, 15], such as the quadrature Kalman filter (QKF) [28], sparse-grid quadrature Kalman filter (SQKF) [68], and adaptive sparse-grid quadrature Kalman filter (ASQKF) [69]. Their computational demand is higher than the general Gaussian filters, such as the EKF [10], UKF [26], CKF [9], and their extensions [9, 26–28, 57, 61, 69], although they improve the accuracy considerably. On the other hand, their computational burden is usually lesser than the particle filters, but the accuracy is also relatively poorer. Thus, improving the quadrature rule-based filters' accuracy without increasing the computational burden can provide an even better trade-off.

The Gaussian filters, including the quadrature rule based filters, witness intractable integrals. These integrals are numerically approximated using deterministic sets of sample points and weights [11, 15]. Different Gaussian filters, as mentioned previously [9, 26–28], apply different numerical approximation methods. Subsequently, their accuracy and computational cost depend on the accuracy and computational cost of corresponding numerical approximation methods. For general Gaussian filters, such as the UKF, CKF and their extensions, the numerical approximation is mostly based on unscented transformation [26] and spherical-cubature rules [9, 27, 57]. These methods are computationally efficient but give poor accuracy. Subsequently, the corresponding Gaussian filters are computationally efficient but offer poor accuracy. On the other hand, the quadrature rule based filters, such as the QKF, SQKF, ASQKF, *etc.*, utilize univariate Gauss-Hermite quadrature rule [202] for numerical approximation, which is highly accurate. Moreover, they apply an additional methodology to extend the univariate quadrature rule in multivariate domain, which increases the computational burden for higher dimensional systems.

The QKF utilizes the product rule for multivariate extension of the univariate quadrature rule. It results in an exponentially increasing computational burden with the increasing system dimension. The SQKF replaced the product rule with the Smolyak rule [203], which reduces the computational burden though it remains higher than the general Gaussian filters. The ASQKF further reduces the computational burden by replacing the product rule and Smolyak rule with an adaptive sparse-grid method [204]. However, it ambiguously fixes some filter parameters based on the system models. Another extension of the QKF, named multiple



QKF [205, 206], applied state partitioning to reduce the computational burden. However, it ignored the inter-state correlation, which harms accuracy.

As discussed above, the existing quadrature rule-based filters apply the univariate Gauss-Hermite quadrature rule for numerical approximation. However, Karvonen *et al.* [207] recently introduced a relatively advanced quadrature rule, named the Gaussian kernel quadrature rule. They proved that the numerical approximation for this advanced quadrature rule exponentially converges with the increasing number of quadrature points. Subsequently, it outperforms the ordinary Gauss-Hermite quadrature rule. They also proved that the numerical stability of the sample points and weights of this advanced quadrature rule is better than the ordinary Gauss-Hermite quadrature rule. To this end, it should be mentioned that the quadrature rules, including the Gaussian kernel quadrature rule, are accurate for a relatively higher-order of polynomials compared to the other numerical approximation techniques used in the filtering literature. Therefore, the Gaussian kernel quadrature rule outperforms the Gauss-Hermite quadrature rule as well as the other numerical approximation techniques used in the filtering literature. With this motivation, this chapter develops a new quadrature rule based filter, named Gaussian kernel quadrature Kalman filter (GKQKF), which replaces the univariate Gauss-Hermite quadrature rule with the Gaussian kernel quadrature rule [207]. The proposed GKQKF outperforms the existing Gaussian filters, such as the UKF, CKF, and QKF.

It should be mentioned that the Gaussian kernel quadrature rule is univariate and the GKQKF requires an additional methodology for extending the univariate rule in multivariate domain. Interestingly, any of the previously mentioned methodologies, such as the product rule, Smolyak rule and adaptive sparse-grid method, can be used for this purpose. This chapter explicitly implements the product rule as it is analytically convenient and easy to understand. However, a practitioner may choose to implement the Smolyak rule and adaptive sparse-grid method to reduce the computational burden. The proposed GKQKF is implemented for three simulation problems and the results are compared with the existing Gaussian filters, such as the UKF, CKF, CQKF, HDCKF, and QKF. The simulation results validate the improved accuracy of the proposed GKQKF.

From the above discussion, the contributions of this chapter can be summarized

as follows.

- It integrates the newly introduced Gaussian kernel quadrature rule in the traditional Gaussian filtering structure.
- The Gaussian kernel quadrature rule is originally univariate. The chapter extends the univariate quadrature rule for multivariate systems using the product rule.
- Finally, it develops a new Bayesian approximation filtering technique for multivariate systems under the Gaussian filtering design methodology.

## 9.2 Gaussian Kernel Quadrature Kalman Filter

The GKQKF is a development under the quadrature rule based filtering to improve the estimation accuracy without harming the computational demand, as compared to its existing quadrature filter counterparts. Recalling the previous discussions, the quadrature rule based filters follow the Gaussian filtering strategy. Please refer to [11, 15] for a detailed discussion on the Gaussian filtering strategy. It should be mentioned that [15] and [11] review the existing Gaussian filters that are developed by embedding various numerical approximation methods in the Gaussian filtering methodology. This chapter develops a new Gaussian filter, the GKQKF, by embedding a new numerical approximation method, named the Gaussian kernel quadrature rule, in the same Gaussian filtering methodology. Alternatively, we can say that the GKQKF introduces new sets of deterministic quadrature points and associated weights for numerically approximating the intractable integrals that appear during the filtering. The Gaussian kernel quadrature rule is more accurate than the numerical approximation methods used by the existing Gaussian filters. Following the discussion in the previous section, the accuracy of a Gaussian filter is commanded by the numerical approximation accuracy. Therefore, from the above discussion, it is conclusive that the accuracy of the proposed GKQKF should be improved in comparison to the existing Gaussian filters.

As discussed in Chapter 1 (Section 1.1.2), the Gaussian filtering is an analytical simplification of the Bayesian framework, where the PDFs are approximated

as Gaussian. Subsequently, they are characterized by their respective mean and covariance. The computation of mean and covariance involves intractable integrals of a general form (Eq. (1.22)), given as

$$I^n(g(\mathbf{x})) = \int_{\mathbb{R}^n} g(\mathbf{x}) \mathcal{N}(\boldsymbol{\mu}, \boldsymbol{\Sigma}) d\mathbf{x}. \quad (9.1)$$

where  $\mathbf{x}$  is a Gaussian random variable with mean  $\boldsymbol{\mu}$  and covariance  $\boldsymbol{\Sigma}$ ,  $g : \mathbb{R}^n \rightarrow \mathbb{R}^n$  is a general nonlinear function,  $\mathcal{N}$  denotes the Gaussian distribution and  $I^n : H \rightarrow H$  represents the Gaussian weighted integration of  $g(\mathbf{x})$  for some functional space  $H$ . In the later parts of this chapter, the notation  $I^n : H \rightarrow H$  will be used in a broader sense and accordingly the functional space  $H$  may be considered to be changing. For example,  $I^n(\mathbf{x})$  will denote  $I^n(\mathbf{x}) = \int_{\mathbb{R}^n} \mathbf{x} \mathcal{N}(\mathbf{x}; \boldsymbol{\mu}, \boldsymbol{\Sigma}) d\mathbf{x}$ . Similar representation may be used for univariate cases, such as for  $x \in \mathbb{R}$  that leads to  $I^1 : \mathbb{R} \rightarrow \mathbb{R}$ . Some more related notations will be introduced wherever required.

Recalling the discussion that the Gaussian kernel quadrature rule is univariate though the desired intractable integral  $I^n(g(\mathbf{x}))$  (Eq. (9.1)) is multivariate. This chapter implements the product rule for extending the univariate quadrature rule in multivariate domain. The remaining part of this section initially introduces the GKQKF's numerical approximation strategy (for approximating  $I^n(g(\mathbf{x}))$ ) with respect to standard Gaussian, *i.e.*,  $\mathcal{N}(\mathbf{x}; \mathbf{0}_{n \times 1}, \mathbf{I}_n)$ , where  $\mathbf{I}_n$  denotes unity matrix. Subsequently,  $I^n(g(\mathbf{x}))$  is simplified as

$$I_0^n(g(\mathbf{x})) = \int_{\mathbb{R}^n} g(\mathbf{x}) \mathcal{N}(\mathbf{x}; \mathbf{0}_{n \times 1}, \mathbf{I}_n) d\mathbf{x}. \quad (9.2)$$

The same numerical approximation strategy can be easily extended for the general Gaussian, *i.e.*,  $\mathcal{N}(\mathbf{x}; \boldsymbol{\mu}, \boldsymbol{\Sigma})$  (discussed in latter part of this section).

As the Gaussian kernel quadrature rule is univariate, it approximates a simplified form of  $I_0^n(g(\mathbf{x}))$  for  $n = 1$ , given as

$$I_0^1(f(x)) = \frac{1}{\sqrt{2\pi}} \int_{\mathbb{R}} f(x) e^{-\frac{x^2}{2}} dx, \quad (9.3)$$

where  $x \in \mathbb{R}$  as a univariate random variable.

This section initially introduces the Gaussian kernel quadrature rule for approx-

imating  $I_0^1(g(x))$  (Eq. (9.3)). Then, it discusses the product rule for extending the same approximation technique for  $I_0^n(g(\mathbf{x}))$  (Eq. (9.2)). Finally, it extends the same approximation strategy for the desired multivariate integral  $I^n(g(\mathbf{x}))$  (Eq. (9.1)).

The Gaussian kernel quadrature rule extends the Gauss-Hermite quadrature points and weights itself to generate the new sets of univariate quadrature points and weights. Therefore, explicit knowledge of generating the Gauss-Hermite quadrature points and weights is a prerequisite for the Gaussian kernel quadrature rule. Thus, this chapter first introduces the Gauss-Hermite quadrature rule and then proceeds to the Gaussian kernel quadrature rule.

### 9.2.1 Univariate Gauss-Hermite Quadrature Rule for Approximating $I_0^1(g(x))$

Let us denote  $\bar{Q}^1(I_0^1)$  as a univariate quadrature rule that approximates the univariate intractable integral  $I_0^1(g(x))$ . Let us consider that  $\bar{Q}^1(I_0^1)$  generates  $N_c$  number of univariate quadrature points and associated weights, denoted as  $\boldsymbol{\xi} = \{\xi_1, \xi_2, \dots, \xi_{N_c}\}$  and  $\boldsymbol{\omega} = \{\omega_1, \omega_2, \dots, \omega_{N_c}\}$ , respectively, *i.e.*,

$$I_0^1(g(x)) \approx \bar{Q}^1(I_0^1) := \sum_{j=0}^{N_c} \omega_j f(\xi_j). \quad (9.4)$$

It should be mentioned that different quadrature rules generate different sets of  $\boldsymbol{\xi}$  and  $\boldsymbol{\omega}$ . In the later parts of this chapter, the notations of  $\boldsymbol{\xi}$  and  $\boldsymbol{\omega}$  will be modified with appropriate superscripts for representing different quadrature rules.

**Definition 9.1.** *The quadrature rule  $\bar{Q}^1(I_0^1)$  for approximating  $I_0^1(g(x))$  is referred to as Gauss-Hermite quadrature rule if the univariate quadrature points  $\boldsymbol{\xi}^{GH} = \{\xi_1^{GH}, \xi_2^{GH}, \dots, \xi_{N_c}^{GH}\}$  are roots of the Hermite polynomials [208, 209]. Subsequently, the weights  $\boldsymbol{\omega}^{GH} = \{\omega_1^{GH}, \omega_2^{GH}, \dots, \omega_{N_c}^{GH}\}$  may be obtained by solving moment equations (discussed in the latter part of this section).*

The direct computation of Hermite polynomials' roots, *i.e.*, the univariate Gauss-Hermite quadrature points, is computationally challenging. Therefore, some approximated techniques are developed and commonly used in the filtering literature to

compute  $\boldsymbol{\xi}^{GH} = \{\xi_1^{GH}, \xi_2^{GH}, \dots, \xi_{N_c}^{GH}\}$  and  $\boldsymbol{\omega}^{GH} = \{\omega_1^{GH}, \omega_2^{GH}, \dots, \omega_{N_c}^{GH}\}$ . Two popular methods are the moment matching method [68] and Golub's method [28, 69].

### 9.2.2 Univariate Gaussian Kernel Quadrature Rule for Approximating $I_0^1(g(x))$

This quadrature rule is based on the Gaussian Kernel.

**Definition 9.2.** For given  $x \in \mathbb{R}$  and  $y \in \mathbb{R}$ , the Gaussian kernel  $\kappa(x, y)$  is defined as

$$\kappa(x, y) := e^{-(x-y)^2/2\sigma^2}, \quad (9.5)$$

where  $\sigma > 0$  is called kernel bandwidth.

**Definition 9.3.** For a given set of quadrature points  $\boldsymbol{\xi}^{GK} = \{\xi_1^{GK}, \xi_2^{GK}, \dots, \xi_{N_c}^{GK}\}$ , the quadrature rule  $\bar{Q}^1(I_0^1)$  for approximating  $I_0^1(g(x))$ , i.e.,

$$I_0^1(g(x)) = \frac{1}{\sqrt{2\pi}} \int_{\mathbb{R}} g(x) e^{-\frac{x^2}{2}} dx \approx \sum_{j=0}^{N_c} \omega_j^{GK} f(\xi_j^{GK}), \quad (9.6)$$

is called Gaussian kernel quadrature rule if the weights  $\boldsymbol{\omega}^{GK} = \{\omega_1^{GK}, \omega_2^{GK}, \dots, \omega_{N_c}^{GK}\}$  are obtained from the Gaussian kernel  $\kappa(x, y)$  by solving the linear relation

$$\boldsymbol{\kappa} \boldsymbol{\omega}^{GK} = \boldsymbol{\kappa}_I, \quad (9.7)$$

where  $\boldsymbol{\kappa}$  and  $\boldsymbol{\kappa}_I$  denote  $[\boldsymbol{\kappa}]_{ij} := \kappa(\xi_i^{GK}, \xi_j^{GK})$  and  $[\boldsymbol{\kappa}_I]_i := \int_{\mathbb{R}} \kappa(\xi_i^{GK}, \xi) dI_0^1(\xi^{GK})$ , respectively,  $\forall i \in \{1, 2, \dots, N_c\}$  and  $j \in \{1, 2, \dots, N_c\}$ .

The proposed GKQKF computes the univariate Gaussian kernel quadrature points  $\boldsymbol{\xi}^{GK} = \{\xi_1^{GK}, \xi_2^{GK}, \dots, \xi_{N_c}^{GK}\}$  as a scaled form of the univariate Gauss-Hermite quadrature points  $\boldsymbol{\xi}^{GH} = \{\xi_1^{GH}, \xi_2^{GH}, \dots, \xi_{N_c}^{GH}\}$ . Any moment matching and Galub's methods can be used for computing  $\boldsymbol{\xi}^{GH} = \{\xi_1^{GH}, \xi_2^{GH}, \dots, \xi_{N_c}^{GH}\}$ . The specific selection of  $\boldsymbol{\xi}^{GK}$  in terms of  $\boldsymbol{\xi}^{GH}$ , i.e., the selection of the specific scaling factor, is discussed in the later part of this section. It will be shown that  $\boldsymbol{\omega}^{GK} = \{\omega_1^{GK}, \omega_2^{GK}, \dots, \omega_{N_c}^{GK}\}$ , to be obtained as solutions of Eq. (9.7), can also be derived in terms of  $\boldsymbol{\omega}^{GH} = \{\omega_1^{GH}, \omega_2^{GH}, \dots, \omega_{N_c}^{GH}\}$ . Before proceeding to the specific

selection and derivation of  $\xi^{GK}$  and  $\omega^{GK}$  in terms of  $\xi^{GH}$  and  $\omega^{GH}$ , respectively, let us define a few mathematical parameters and quantities.

**Definition 9.4.** *Let us define a Gaussian probability measure  $\mu_\alpha$  with zero mean and variance  $1/2\alpha^2$ , i.e.,*

$$d\mu_\alpha(x) := \frac{\alpha}{\sqrt{\pi}} e^{-\alpha^2 x^2} dx. \quad (9.8)$$

**Definition 9.5.** *The  $i^{th}$  order probabilistic Hermite polynomials are defined as [208, 209]*

$$H_i(x) := (-1)^i e^{x^2/2} \frac{d^i}{dx^i} e^{-x^2/2}. \quad (9.9)$$

Let us define the following variables:  $\varepsilon = \frac{1}{\sqrt{2}\sigma}$ ,  $\beta = \left(1 + \left(\frac{2\varepsilon}{\alpha}\right)^2\right)^{1/4}$  and  $\delta^2 = \frac{\alpha^2}{2}(\beta^2 - 1)$ .

The general form of the Gaussian kernel quadrature rule is defined with respect to the Gaussian measure  $d\mu_\alpha(x)$  with mean zero and covariance  $1/2\alpha^2$ . It should be mentioned that our desired integral  $I_0^1(g(x))$  is concerned with zero mean and unity covariance, which is satisfied for  $\alpha = 1/\sqrt{2}$ . From Eqs. (9.6) and (9.8), we can conclude that  $\mu_{1/\sqrt{2}}(x) = I_0^1(x)$  for  $\alpha = 1/\sqrt{2}$ . Thus, in the remaining part of this chapter, the use of  $\mu_\alpha(x)$  will be avoided to overcome the unnecessary burden of a new variable. However, the parameter  $\alpha$  will be used to abide by the original structure of the Gaussian kernel quadrature rule. To understand the significance of  $\alpha$ , it becomes necessary to define  $d\mu_\alpha(x)$  even as it is not useful for the remaining parts of this chapter.

Our derivation of weights  $\omega^{GK} = \{\omega_1^{GK}, \omega_2^{GK}, \dots, \omega_{N_c}^{GK}\}$  is based on eigenvalues and eigenfunctions of the Gaussian kernel  $\kappa(x, y)$  (Eq. (9.5)). If  $\lambda_i^\alpha$  and  $\varphi_i^\alpha(x)$  denote the  $i^{th}$  eigenvalue and eigenfunction of  $\kappa(x, y)$ , respectively, then [208]

$$\begin{cases} \lambda_i^\alpha = \sqrt{\frac{\alpha^2}{\alpha^2 + \delta^2 + \varepsilon^2}} \left( \frac{\varepsilon^2}{\alpha^2 + \delta^2 + \varepsilon^2} \right)^i \\ \varphi_i^\alpha(x) = \sqrt{\frac{\beta}{i!}} e^{-\delta^2 x^2} H_i(\sqrt{2}\alpha\beta x). \end{cases} \quad (9.10)$$

Before proceeding forward to derive  $\omega^{GK} = \{\omega_1^{GK}, \omega_2^{GK}, \dots, \omega_{N_c}^{GK}\}$ , let us extend our analysis on  $\varphi_i^\alpha(x)$  further.

**Proposition 9.1.** The eigenfunctions of  $\kappa(x, y)$ , i.e.,  $\varphi_i^\alpha(x) \forall i \in \{1, 2, \dots\}$ , satisfy

$$\begin{cases} I_0^1(\varphi_{2l+1}^\alpha(x)) = 0 \\ I_0^1(\varphi_{2l}^\alpha(x)) = \sqrt{\frac{\beta}{1+2\delta^2}} \frac{\sqrt{(2l)!}}{2^l l!} \left( \frac{2\alpha^2 \beta^2}{1+2\delta^2} - 1 \right)^l. \end{cases} \quad (9.11)$$

The notation  $l$  is used to pick the odd and even values of  $i$ , i.e.,  $\varphi_{2l+1}^\alpha(x)$  and  $\varphi_{2l}^\alpha(x)$  represent the odd and even order eigenfunctions of  $\kappa(x, y)$ , respectively. Please note that  $\varphi_{2l+1}^\alpha(x)$  and  $\varphi_{2l}^\alpha(x)$  are determined from  $\varphi_i^\alpha(x) \forall i \in \{1, 2, \dots\}$  (Eq. (9.10)) for  $i = 2l + 1$  and  $i = 2l$ , respectively.

*Proof.* For  $I_0^1(g(x))$ ,  $H_i(x)$ , and  $\varphi_i^\alpha(x)$  given in Eqs. (9.6), (9.9), and (9.10), respectively, we get

$$I_0^1(\varphi_{2l+1}^\alpha(x)) = \frac{1}{\sqrt{2\pi}} \times \int_{\mathbb{R}} \left( \sqrt{\frac{\beta}{(2l+1)!}} e^{-\delta^2 x^2} H_{2l+1}(\sqrt{2\alpha\beta}x) e^{-\frac{x^2}{2}} \right) dx.$$

It should be mentioned that the Hermite polynomials,  $H_i(x) \forall i \in \{1, 2, \dots\}$ , are odd functions for all odd  $i$ . Thus, the above equation gives  $I_0^1(\varphi_{2l+1}^\alpha(x)) = 0$ . It proves that the first part of Eq. (9.11) holds true.

To prove the second part of Eq. (9.11), i.e., to derive  $I_0^1(\varphi_{2l}^\alpha(x))$ , let us represent  $H_i(x)$  for even  $i$ , such as  $i = 2l$ , in explicit form of Hermite polynomials, given as

$$H_{2l}(x) = \frac{(2l)!}{2^l} \sum_{j=0}^l \frac{(-1)^{l-j}}{(2j)!(l-j)!} (\sqrt{2}x)^{2j}. \quad (9.12)$$

From Eq. (9.10), the even order eigenfunction, i.e.,  $\varphi_{2l}^\alpha(x)$  can be expressed as

$$\varphi_{2l}^\alpha(x) = \sqrt{\frac{\beta}{(2l)!}} e^{-\delta^2 x^2} H_{2l}(2\alpha\beta x). \quad (9.13)$$

Let us expand the above equation by substituting  $H_{2l}(2\alpha\beta x)$  from Eq. (9.12). Subsequently, substituting the expanded  $\varphi_{2l}^\alpha(x)$  in  $I_0^1(\varphi_{2l}^\alpha(x)) = 1/\sqrt{2\pi} \int_{\mathbb{R}} \varphi_{2l}^\alpha(x) e^{-x^2/2} dx$  (obtained from Eq. (9.3)), we can write

$$I_0^1(\varphi_{2l}^\alpha(x)) = \sqrt{\frac{\beta}{(2l)!}} \frac{(2l)!}{2^l} \sum_{j=0}^l \left( \frac{(-1)^{l-j} (2\alpha\beta)^{2j}}{(2j)!(l-j)!} \frac{1}{\sqrt{2\pi}} \int_{\mathbb{R}} x^{2j} e^{-(\delta^2 + \frac{1}{2})x^2} dx \right). \quad (9.14)$$

Applying the Gaussian moment formula in the integral part of the above equation, we obtain [207]

$$\frac{1}{\sqrt{2\pi}} \int_{\mathbb{R}} x^{2j} e^{-(\delta^2 + \frac{1}{2})x^2} dx = \frac{(2j)!}{2^j j! (1 + 2\delta^2)^{j+1/2}}. \quad (9.15)$$

Substituting this into Eq. (9.14), after some rearrangements, we get

$$I_0^1(\varphi_{2l}^\alpha(x)) = \sqrt{\frac{\beta}{1 + 2\delta^2}} \frac{\sqrt{(2l)!}}{2^l} \sum_{j=0}^l \left( \frac{(-1)^{l-j}}{j!(l-j)!} \left( \frac{2\alpha^2\beta^2}{1 + 2\delta^2} \right)^j \right). \quad (9.16)$$

Following the representation  $\binom{l}{j} = l!/(j!(l-j)!)$ , we further simplify the above equation as

$$I_0^1(\varphi_{2l}^\alpha(x)) = \sqrt{\frac{\beta}{1 + 2\delta^2}} \frac{\sqrt{(2l)!}}{2^l l!} \sum_{j=0}^l \binom{l}{j} \left( \frac{2\alpha^2\beta^2}{1 + 2\delta^2} \right)^j (-1)^{l-j}.$$

Finally, applying the Binomial theorem to the summands in the above equation, we obtain  $I_0^1(\varphi_{2l}^\alpha(x))$  in the form of Eq. (9.11). It concludes that the second part of Eq. (9.11) also holds true.  $\square$

We can now derive the Gaussian kernel quadrature points and weights.

**Proposition 9.2.** The univariate Gaussian kernel quadrature points and weights, *i.e.*,  $\boldsymbol{\xi}^{GK} = \{\xi_1^{GK}, \xi_2^{GK}, \dots, \xi_{N_c}^{GK}\}$  and  $\boldsymbol{\omega}^{GK} = \{\omega_1^{GK}, \omega_2^{GK}, \dots, \omega_{N_c}^{GK}\}$ , as functions of the univariate Gauss-Hermite quadrature points and weights, *i.e.*,  $\boldsymbol{\xi}^{GH} = \{\xi_1^{GH}, \xi_2^{GH}, \dots, \xi_{N_c}^{GH}\}$  and  $\boldsymbol{\omega}^{GH} = \{\omega_1^{GH}, \omega_2^{GH}, \dots, \omega_{N_c}^{GH}\}$ , can be given as

$$\xi_j^{GK} = \frac{1}{\sqrt{2\alpha}\beta} \xi_j^{GH} \quad (9.17)$$

and

$$\omega_j^{GK} = \sqrt{\frac{1}{1 + 2\delta^2}} \omega_j^{GH} e^{\delta^2(\xi_j^{GK})^2} \left[ \sum_{l=0}^{\lfloor (N_c-1)/2 \rfloor} \frac{1}{2^l l!} \left( \frac{2\alpha^2\beta^2}{1 + 2\delta^2} - 1 \right)^l H_{2l}(\xi_j^{GH}) \right], \quad (9.18)$$

where  $j \in \{1, 2, \dots, N_c\}$ .

*Proof.* Recalling the Definition 9.3, the weights  $\boldsymbol{\omega}^{GK} = \{\omega_1^{GK}, \omega_2^{GK}, \dots, \omega_{N_c}^{GK}\}$  are



solutions of Eq. (9.7), which gives

$$\boldsymbol{\omega}^{GK} = (\boldsymbol{\kappa})^{-1} \kappa_I. \quad (9.19)$$

It should be mentioned that  $\boldsymbol{\kappa}$  and  $\kappa_I$  can be represented in terms of the Gaussian kernel  $\kappa(\xi_i^{GK}, \xi_j^{GK})$ . Moreover, as  $\boldsymbol{\kappa}$  is defined in terms of Gaussian kernels, it is of full rank and inherently invertible, given that the quadrature points are distinct. It should be mentioned that if two or more quadrature points are overlapping, then we can replace them with a single quadrature point that has a weight same as the sum of the weights of all overlapping quadrature points. Thus, the distinct behavior of the quadrature points is maintained and the invertibility of  $\boldsymbol{\kappa}$  remains ensured. As  $\boldsymbol{\kappa}$  is invertible, Eq. (9.19) is always defined.

Following the discussions in [207], the eigendecomposition of  $\kappa(\xi_i^{GK}, \xi_j^{GK})$  gives

$$\kappa(\xi_i^{GK}, \xi_j^{GK}) = \sum_{i=0}^{\infty} \lambda_i^\alpha \varphi_i^\alpha(\xi_i^{GK}) \varphi_i^\alpha(\xi_j^{GK}). \quad (9.20)$$

To derive the Gaussian kernel quadrature rule for  $N_c$  number of univariate quadrature points, *i.e.*,  $\boldsymbol{\xi}^{GK} = \{\xi_1^{GK}, \xi_2^{GK}, \dots, \xi_{N_c}^{GK}\}$  and  $\boldsymbol{\omega}^{GK} = \{\omega_1^{GK}, \omega_2^{GK}, \dots, \omega_{N_c}^{GK}\}$ , we truncate the summation in Eq. (9.20) up to  $N_c$  terms. At this end, let us define  $N_c$ -dimensional  $\psi$ ,  $\bar{\varphi}$  and  $\Lambda$  such that  $\psi_{ij} = \varphi_{j-1}^\alpha(\xi_i^{GK})$ ,  $\bar{\varphi}_i = I_0^1(\varphi_{i-1}^\alpha)$  and  $\Lambda_{ii} = \lambda_i^\alpha$  ( $\Lambda_{ij} = 0 \forall i \neq j$ )  $\forall i \in \{1, 2, \dots, N_c\}$  and  $j \in \{1, 2, \dots, N_c\}$ . Subsequently, recalling the definitions of  $\boldsymbol{\kappa}$  and  $\kappa_I$ , we can write  $\boldsymbol{\kappa} = (\psi \Lambda \psi^T)$  and  $\kappa_I = \psi \Lambda \bar{\varphi}$ . Substituting  $\boldsymbol{\kappa}$  and  $\kappa_I$  in Eq. (9.19), we get

$$\boldsymbol{\omega}^{GK} = (\psi \Lambda \psi^T)^{-1} \psi \Lambda \bar{\varphi} = (\psi^T)^{-1} \bar{\varphi}. \quad (9.21)$$

We can represent  $\psi$  in terms of a matrix  $V$  and a diagonal matrix  $E$ , as  $\psi = \sqrt{\beta} E^{-1} V$ , where  $E_{ii} = e^{(\delta \xi_i^{GK})^2}$  and

$$V_{ij} = \frac{1}{\sqrt{(j-1)!}} H_{j-1}(\sqrt{2\alpha\beta} \xi_i^{GK}).$$

Substituting  $\psi = \sqrt{\beta}E^{-1}V$  in Eq. (9.21), we get

$$\omega^{GK} = \frac{1}{\sqrt{\beta}}E(V^{-1})^T\bar{\varphi}. \quad (9.22)$$

Consider that the Gaussian kernel quadrature points  $\xi^{GK} = \{\xi_1^{GK}, \xi_2^{GK}, \dots, \xi_{N_c}^{GK}\}$  are obtained by scaling the conventional Gauss-Hermite quadrature points  $\xi^{GH} = \{\xi_1^{GH}, \xi_2^{GH}, \dots, \xi_{N_c}^{GH}\}$ , as

$$\xi_j^{GK} = \frac{1}{\sqrt{2\alpha\beta}}\xi_j^{GH}. \quad (9.23)$$

At this end, let us adopt the following statements directly from [207].

- Let us denote  $\xi = \{\xi_1, \xi_2, \dots, \xi_{N_c}\}$  and  $\omega = \{\omega_1, \omega_2, \dots, \omega_{N_c}\}$  as sets of univariate points and weights, respectively for a quadrature rule  $\bar{Q}^1(I)$ , where  $I$  represents a Gaussian weighted integration, such as  $I_0^1$ . Let us consider  $O_0(x), O_1(x), \dots, O_{N_c-1}(x)$  are  $L^2(V)$ -orthogonal polynomials and  $\varrho_{ij} = \sum_{l=0}^{N_c-1} O_l(\xi_i)O_l(\xi_j)$ . Then,  $\varrho$  is a diagonal matrix and  $\omega_i = 1/\varrho_{ii}$ .
- For a specific selection of  $\xi^{GK} = \{\xi_1^{GK}, \xi_2^{GK}, \dots, \xi_{N_c}^{GK}\}$ , as in Eq. (9.23), the matrix  $V$  is a Vandermonde matrix of normalized Hermite polynomials. Moreover,  $VV^T$  is the matrix  $\varrho$  in the above statement with the polynomials  $O_0(x), O_1(x), \dots, O_{N_c-1}(x)$  replaced by Hermite polynomials  $H_0(x), H_1(x), \dots, H_{N_c-1}(x)$ .

In conclusion to these statements, we can write

$$(VV^T)^{-1} = \bar{\omega}^{GH} \implies (V^T)^{-1} = \bar{\omega}^{GH}V,$$

where  $\bar{\omega}^{GH}$  is a diagonal matrix with  $\bar{\omega}_{ii}^{GH} = \omega_i^{GH}$ . Substituting  $(V^T)^{-1}$  in Eq. (9.22), we get

$$\omega^{GK} = \frac{1}{\sqrt{\beta}}E\bar{\omega}^{GH}V\bar{\varphi}.$$

It should be mentioned that  $E$  and  $\bar{\omega}^{GH}$  are diagonal matrices. Thus, the  $i^{th}$ -element of  $\omega^{GK}$ , i.e.,  $\omega_i^{GK}$ , can be given as

$$\omega_i^{GK} = \frac{1}{\sqrt{\beta}}E_{ii}\bar{\omega}_{ii}^{GH} \sum_{j=1}^{N_c} V_{ij}\bar{\varphi}_j.$$

From the definition of  $E$ ,  $\bar{\omega}^{GH}$ ,  $V$ , and  $\bar{\varphi}$ , we get

$$\omega_i^{GK} = \frac{1}{\sqrt{\beta}} e^{(\delta \xi_i^{GK})^2} \omega_i^{GH} \left[ \sum_{j=0}^{N_c-1} \frac{1}{\sqrt{j!}} H_j(\sqrt{2\alpha\beta} \xi_i^{GK}) I_0^1(\varphi_j^\alpha(\xi_i^{GK})) \right].$$

From Eq. (9.23), we can substitute  $\sqrt{2\alpha\beta} \xi_i^{GK} = \xi_i^{GH}$ . Moreover, from Proposition 9.1,  $I_0^1(\varphi_j^\alpha(\xi_i^{GK}))$  is nonzero only if  $j$  is even. Thus, considering only even  $j$  and substituting  $I_0^1(\varphi_j^\alpha(\xi_i^{GK}))$  for even  $j$  from Eq. (9.11), we get

$$\omega_i^{GK} = \frac{1}{\sqrt{\beta}} e^{(\delta \xi_i^{GK})^2} \omega_i^{GH} \sum_{l=0}^{\lfloor (N_c-1/2) \rfloor} \frac{1}{\sqrt{(2l)!}} H_{2l}(\xi_i^{GH}) \left[ \sqrt{\frac{\beta}{1+2\delta^2}} \frac{\sqrt{(2l)!}}{2^l l!} \left( \frac{2\alpha^2 \beta^2}{1+2\delta^2} - 1 \right)^l \right].$$

Simplifying further, we can express  $\omega_i^{GK}$  in the form of Eq. (9.18). Please note that  $\omega_i^{GK}$  is derived for  $\xi_i^{GK}$  given in Eq. (9.23), which is same as Eq. (9.17).  $\square$

We can substitute  $\xi_i = \xi_i^{GK}$  and  $\omega_i = \omega_i^{GK}$  in Eq. (9.6) to approximate the desired univariate integral  $I_0^1(g(x))$  using the univariate Gaussian kernel quadrature rule. As discussed in [207], the univariate Gaussian kernel quadrature rule is defined for all values of kernel bandwidth  $\sigma$ . However, a very large  $\sigma$  may lead to numerical ill-conditioning. Moreover, [207] stated, without giving any proof, that  $\omega_i^{GK}$  approaches to  $\omega_i^{GH}$  for large  $\sigma$ . In consequence of this discussion, a small value of  $\sigma$  is recommended for all practical implementations of the proposed GKQKF. To this end, it should be mentioned that [207] studied the improved accuracy of the univariate Gaussian kernel quadrature rule for  $\sigma$  up to 4.

From Eqs. (9.17) and (9.18), it is conclusive that  $\boldsymbol{\xi}^{GK} = \{\xi_1^{GK}, \xi_2^{GK}, \dots, \xi_{N_c}^{GK}\}$  and  $\boldsymbol{\omega}^{GK} = \{\omega_1^{GK}, \omega_2^{GK}, \dots, \omega_{N_c}^{GK}\}$  are scaled versions of the traditionally used  $\boldsymbol{\xi}^{GH} = \{\xi_1^{GH}, \xi_2^{GH}, \dots, \xi_{N_c}^{GH}\}$  and  $\boldsymbol{\omega}^{GH} = \{\omega_1^{GH}, \omega_2^{GH}, \dots, \omega_{N_c}^{GH}\}$ , respectively. However, as discussed in the introduction section,  $\boldsymbol{\xi}^{GK}$  and  $\boldsymbol{\omega}^{GK}$  provide better accuracy and numerical stability than  $\boldsymbol{\xi}^{GH}$  and  $\boldsymbol{\omega}^{GH}$ .

### 9.2.3 Multivariate Extension of Gaussian Kernel Quadrature Rule

The Gaussian kernel quadrature rule is univariate and cannot be used for approximating the desired multivariate integral  $I_0^n(g(\mathbf{x}))$  (Eq. (9.2)). However, several

methodologies are available in the literature to extend a univariate quadrature rule for approximating multivariate integrals. Some of the popular methods among them are the product rule [28], Smolyak rule [68, 203], and adaptive sparse-grid method [69] in the order of decreasing computational burden. This chapter adopts the product rule due to its simple structure, even though it is computationally most inefficient. Nevertheless, the practitioners may choose to replace it with the Smolyak rule or adaptive sparse-grid method to reduce the computational burden.

With  $\xi_i^{GK}$  and  $\omega_i^{GK} (\forall i \in \{1, 2, \dots, N_c\})$  being the univariate Gaussian kernel quadrature points and weights, respectively, the product rule approximates  $I_0^n(g(\mathbf{x}))$  as

$$I_0^n(g(\mathbf{x})) \approx \sum_{i_1=1}^{N_{s1}} \cdots \sum_{i_n=1}^{N_{s1}} f\left([\xi_{i_1}^{GK}, \dots, \xi_{i_n}^{GK}]^T\right) \omega_{i_1}^{GK} \cdots \omega_{i_n}^{GK}.$$

Subsequently, the multivariate integral  $I^n(g(\mathbf{x}))$  for general Gaussian  $\mathcal{N}(\mathbf{x}; \boldsymbol{\mu}, \boldsymbol{\Sigma})$  can be approximated as

$$I^n(g(\mathbf{x})) \approx \sum_{i_1=1}^{N_{s1}} \cdots \sum_{i_n=1}^{N_{s1}} f(\hat{\mathbf{x}} + \mathbf{S} [\xi_{i_1}^{GK}, \dots, \xi_{i_n}^{GK}]^T) \omega_{i_1}^{GK} \cdots \omega_{i_n}^{GK},$$

where  $\mathbf{S}\mathbf{S}^T = \boldsymbol{\Sigma}$ .

We can now denote the  $i^{th}$  multivariate Gaussian kernel quadrature points and weights as  $\boldsymbol{\xi}_i^{GK} = [\xi_{i_1}^{GK}, \xi_{i_2}^{GK}, \dots, \xi_{i_n}^{GK}]^T$  and  $\boldsymbol{\omega}_i^{GK} = \omega_{i_1}^{GK} \omega_{i_2}^{GK} \cdots \omega_{i_n}^{GK}$ , respectively, where  $i_1, i_2, \dots, i_n \in \{1, 2, \dots, N_c\}$  and  $i \in \{1, 2, \dots, (N_c)^n\}$ . Subsequently, a simplified representation for approximating  $I^n(g(\mathbf{x}))$  can be given as

$$I^n(g(\mathbf{x})) \approx \sum_{j=1}^{N_s} \boldsymbol{\omega}_j^{GK} f(\boldsymbol{\mu} + \mathbf{S}\boldsymbol{\xi}_j^{GK}), \quad (9.24)$$

where  $N_{gk} = (N_c)^n$  is the number of multivariate quadrature points. It should be mentioned that the multivariate quadrature rules are accurate for polynomials  $x_1^{l_1} x_2^{l_2} \cdots x_n^{l_n}$  with  $0 < l_j < N_c \forall j \in \{1, 2, \dots, n\}$ .

We can integrate the numerical approximation strategy of Eq. (9.24) with the Gaussian filtering strategy to formulate the filtering algorithm of the proposed GKQKF. It should be mentioned that it follows the same filtering structure [11, 15]

used for the generalized quadrature rule based filtering. However, it replaces the traditional quadrature points and weights by  $\xi^{GK}$  and  $\omega^{GK}$ , respectively. A pseudo-code for generating  $\xi^{GK}$  and  $\omega^{GK}$  is given in Algorithm 9.1. The pseudo-code considers the Golub's method of generating the univariate Gauss-Hermite univariate quadrature points and weights, *i.e.*,  $\xi^{GH}$  and  $\omega^{GH}$ .

---

**Algorithm 9.1** Pseudo-code for computing  $\xi_i^{GK}$  and  $\omega_i^{GK}$

---

**Input:** Number of univariate quadrature points and system dimension:  $N_c$  and  $n$

**Output:**  $\xi^{GK}$  and  $\mathbf{W}^{GK}$

- 1: Formulate  $\Xi$  as  $\Xi_{j,j} = 0 \forall j \in \{1, 2, \dots, N_c\}$  and  $\Xi_{i,i+1} = \sqrt{i/2} \forall i \in \{1, 2, \dots, N_c - 1\}$ .
  - 2: Determine eigenvalues and eigenvectors of  $\Xi$ :  $\Psi_i$  and  $(v_i)_1 \forall i \in \{1, 2, \dots, N_c\}$ .
  - 3: Determine  $\xi_i^{GH} = \sqrt{2}\Psi_i$  and  $\omega_i^{GH} = (v_i)_1^2 \forall i \in \{1, 2, \dots, N_c\}$ .
  - 4: Determine  $\xi_i^{GK}$  and  $\omega_i^{GK}$  using Eqs. (9.17) and (9.18), respectively.
  - 5: Determine the multivariate Gaussian kernel quadrature points and weights as  $\xi_i^{GK} = [\xi_{i_1}^{GK}, \xi_{i_2}^{GK}, \dots, \xi_{i_n}^{GK}]^T$  and  $\omega_i^{GK} = \omega_{i_1}^{GK} \omega_{i_2}^{GK} \dots \omega_{i_n}^{GK}$ , where  $i_j \in \{1, 2, \dots, N_{s_1}\} \forall j \in \{1, 2, \dots, n\}$  and  $i \in \{1, 2, \dots, (N_c)^n\}$ .
  - 6: **return**
  - 7:  $\xi_i^{GK}$  and  $\omega_i^{GK} \forall i \in \{1, 2, \dots, (N_c)^n\}$ .
- 

**Remark 9.1.** *The GKQKF is developed under the quadrature rule based filtering, which is the most accurate class of Gaussian filters.*

**Remark 9.2.** *For an  $n$ -dimensional system, the proposed GKQKF requires  $(N_c)^n$  number of multivariate quadrature points, the same as the QKF.*

**Remark 9.3.** *The proposed GKQKF uses the product rule, leading to exponentially increasing computational cost with increasing dimension.*

**Remark 9.4.** *Although the computational burden of the proposed GKQKF increases with the increasing dimension, it remains similar to the QKF. Moreover, it can be further reduced and achieved similar to the other computationally efficient quadrature filters, such as the SQKF and ASQKF, by replacing the product rule with the Smolyak rule and adaptive sparse-grid method, respectively.*

**Remark 9.5.** *In the current era of efficient computing devices, the computational burden of the quadrature rule based filters is becoming tolerable for a wide range of practical problems. Subsequently, their demand is rising due to the high accuracy, specifically for crucial applications (e.g., defense systems). Thus, the proposed*

*GKQKF is a potential solution for the practical scenarios where high accuracy is demanded and high computing power is available.*

The following discussion compares the GKQKF with the other existing Gaussian filters.

- The CKF, probably the most popular Gaussian filter, uses the third-degree spherical-cubature rule of numerical approximation, which is accurate for up to third-order polynomials only. On the other hand, the quadrature rule based filters, such as the proposed GKQKF, use quadrature rules of numerical approximation that are accurate for higher-order polynomials. Thus, the quadrature rule based filters, including the proposed GKQKF, outperform the CKF.
- The higher-order variants of the CKF, such as the CQKF and HDCKF, use relatively advanced numerical approximation techniques, which are accurate for comparatively higher-order polynomials. However, their accuracy has been observed to be saturating as the order of polynomials increases. Subsequently, they have been reported in literature [11, 15] to underperform the quadrature rule based filters, such as the QKF. Consequently, they underperform the proposed GKQKF as well.
- As discussed in the introduction section, the Gaussian kernel quadrature rule, used by the proposed GKQKF, is more accurate than the ordinary Gauss-Hermite quadrature rule, used by the QKF. Therefore, the proposed GKQKF outperforms the QKF. Moreover, the existing variants of the QKF, such as the SQKF and ASQKF, improve only the computational demand without improving the accuracy. Consequently, the proposed GKQKF outperforms these variants as well.
- The computational demand of the GKQKF is higher than the CKF and its variants, such as the CQKF and HDCQKF. Therefore, the GKQKF is expected to replace the CKF and its variants if high accuracy is essential and a high computational budget is available. Such examples frequently appear in defense applications and clinical biomedical tools.

- The computational demand of the proposed GKQKF is similar to the QKF. However, it is higher than various variants of the QKF, such as the SQKF and ASQKF. It should be mentioned that the SQKF and ASQKF reduce the computational demand by replacing the product rule with other computationally efficient methods of extending the univariate quadrature rules in multivariate domain, such as the Smolyak rule [203] and the adaptive sparse-grid method [69]. Thankfully, these rules can be applied with the proposed GKQKF also to reduce its computational demand.

Summarizing the above discussions, the proposed GKQKF outperforms the existing quadrature rule-based filters, as it utilizes univariate Gaussian kernel quadrature rule, which is more accurate than its counterparts used in the existing quadrature rule based filters. As the quadrature rule based filters are most accurate Gaussian filters, we can further state that the proposed GKQKF outperforms all the existing Gaussian filters. The increased computational burden of the proposed GKQKF in comparison to the UKF and CKF may not be of major concern, as the efficacy of the computational tools has increased manyfold since the development of the UKF and CKF. Thus, the proposed GKQKF can be the most appropriate choice for a wide range of the practical applications. We observe a widespread literature, including [59, 60], utilizing the quadrature rule based filters in practical applications. The proposed GKQKF can straightforwardly replace the existing quadrature rule based Gaussian filters in these applications.

Although the quadrature rule based Gaussian filters outperform other existing Gaussian filters, they didn't initially attract a huge research. However, the practitioners often prefer them over the other Gaussian filters due to their improved accuracy. In the beginning, their high computational demand was anticipated as the possible reason for the lack of interest from the researchers. However, the growth of the literature is still slow, irrespective of huge improvement in the efficacy of the contemporary computational devices, which are good enough even for implementing the computationally highly demanding particle filters. In this regard, we believe the non-triviality of the quadrature rules as the reasons for the lack of interest from the researchers. This chapter takes this challenge and introduces a new quadrature rule, *i.e.*, the Gaussian kernel quadrature rule. We describe the Gaussian kernel

quadrature rule in a simplified way, making the implementation convenient for the practitioners.

## 9.3 Simulation and Results

In this section, we simulate a numerical integral approximation problem and two real-life nonlinear filtering problems. The numerical integral approximation problem validates the improved numerical approximation accuracy of the Gaussian Kernel quadrature rule compared to the other numerical approximation methods used by the popular Gaussian filters, such as the UKF, CKF, CQKF, HDCKF, and QKF. On the other hand, the real-life filtering problems validate the improved accuracy of the proposed GKQKF compared to the existing popular Gaussian filters, such as the UKF, CKF, CQKF, HDCKF, and QKF. The UKF is implemented with its parameter  $\kappa = 1$  for the two nonlinear filtering problems. The QKF and GKQKF are implemented with 6-point univariate quadrature rules.

The generation of the univariate quadrature points and weights for the proposed GKQKF requires several parameters, such as  $\sigma$ ,  $\alpha$ ,  $\beta$ ,  $\epsilon$ , and  $\delta$ . Following the discussion towards the end of Section 9.2.2, we can conveniently consider  $\sigma$  up to 4, although the proposed GKQKF is applicable for any value of  $\sigma$ . Following the same, the simulation is performed for  $\sigma = 1$ . Moreover, from the discussion in Section 9.2.2, we must choose  $\alpha = 1/\sqrt{2}$ , as the proposed GKQKF is concerned with the Gaussian distribution. Subsequently, the other required parameters can be obtained as  $\epsilon = \frac{1}{\sqrt{2}\sigma}$ ,  $\beta = \left(1 + \left(\frac{2\epsilon}{\alpha}\right)^2\right)^{1/4}$  and  $\delta^2 = \frac{\alpha^2}{2}(\beta^2 - 1)$ , as discussed in Section 9.2.2. The filtering problems' analysis is based on root mean square error (RMSE).

### 9.3.1 Problem 1: Numerical Approximation of Intractable Integral

The integral considered for the numerical approximation is

$$I(g) = \int_{\mathbb{R}^n} \cos(\|\mathbf{x}\|_2) \mathcal{N}(\mathbf{x}; \mathbf{0}_{n \times 1}, \mathbf{I}_n) d\mathbf{x}, \quad (9.25)$$



where  $\|\mathbf{x}\|_2$  denotes the second norm of  $\mathbf{x} \in \mathbb{R}^n$ . The simulation is performed for  $n = 4$  and  $n = 6$ . The exact solutions of the integral for  $n = 4$  and  $n = 6$  are  $I(g) = 0.5(1 - 2\sqrt{2}D_w(1/\sqrt{2}))$  and  $I(g) = -3D_w(1/\sqrt{2})/(2\sqrt{2})$ , respectively, where  $D_w$  denotes the Dawson function given as  $D_w(x) := e^{-x^2} \int_0^x e^{y^2} dy$ . Subsequently,  $I(g)$  is approximately equal to -0.224778459007077 and -0.543583844255307 for  $n = 4$  and  $n = 6$ , respectively. These values will be considered as true values for validation.

Let us consider the following abbreviations and notations for different numerical approximation methods.  $UT_\kappa$  denotes the unscented transformation rule with the parameter  $\kappa$ , which is used by the UKF. SC represents the third-degree spherical cubature rule used by the CKF. CQ stands for the cubature quadrature rule used by the CQKF. HSC represents the higher-degree spherical cubature rule used by the HDCKF.  $GHQ_{N_c}$  denotes  $N_c$ -point Gauss-Hermite quadrature rule supported by the product rule, as the QKF uses it. Finally,  $GKQ_{N_c}$  denotes the  $N_c$ -point Gaussian kernel quadrature rule supported by the product rule, as the proposed GKQKF uses it.

The approximated values of  $I(f)$  and % errors obtained for different numerical approximation techniques are provided in Table 9.1 for  $n = 4$  and  $n = 6$ . The table concludes that the error is lowest for the Gaussian kernel quadrature rule. Subsequently, the resulting filter GKQKF is expected to outperform all the existing Gaussian filters, such as the UKF, CKF, and QKF.

### 9.3.2 Problem 2: Sinusoidal Growth Model

The dynamic state space model for this filtering problem follows the state-space model presented by Eqs. (4.17) and (4.18) in Chapter 4.

The simulation is performed for  $n = 2$ . The initial true and estimated states are taken as  $\mathbf{x}_0 = [1, 2]^T$  and  $\hat{\mathbf{x}}_{0|0} = [3, 4]^T$ , respectively. The initial error covariance is considered as  $\mathbf{P}_{0|0} = \mathbf{I}_n$ . The simulation is performed for two problem scenarios, defined by varying the noises, as

- Scenario 1:  $\mathbf{Q}_{ij} = 0.5 \forall i = j$  and 0.05 otherwise and  $\mathbf{R} = 1$ .
- Scenario 2:  $\mathbf{Q}_{ij} = 2.5 \forall i = j$  and 0.25 otherwise and  $\mathbf{R} = 5$ .

Table 9.1:  $I(f)$  with  $n = \{4, 6\}$ : Numerically approximated values and % error obtained from different numerical approximation techniques used in the filtering literature.

Rules	n = 4		n = 6	
	Approximated value	% Error	Approximated value	% Error
UT <sub>1</sub>	-0.293818301165733	30.714616	-0.611058914949911	12.413001
UT <sub>2</sub>	-0.179937153166595	19.949111	-0.463522346094386	14.728454
UT <sub>3</sub>	-0.074039276633274	67.061222	-0.326661664400297	39.905928
SC	-0.416146836547142	85.136439	-0.769905729749893	41.635138
CQ	-0.227952368853859	-1.412016	-0.549220926370814	-1.037021
HSC	-0.179937153166595	19.949111	-0.463522346094386	14.728454
GHQ <sub>3</sub>	-0.203505307617691	9.464052	-0.516177282395964	5.041827
GHQ <sub>4</sub>	-0.226372242270946	0.709046	-0.545713521963565	0.391784
GHQ <sub>5</sub>	-0.224687273190453	0.040566	-0.543459260335630	0.022918
GHQ <sub>6</sub>	-0.224782686910015	0.001881	-0.543589707702025	0.001078
GKQ <sub>3</sub>	-0.209138184525495	6.958084	-0.522984078045846	3.789620
GKQ <sub>4</sub>	-0.225640090592589	0.383324	-0.544760796005950	0.216517
GKQ <sub>5</sub>	-0.224746811029037	0.014079	-0.543539604404307	0.008138
GKQ <sub>6</sub>	-0.224779238737018	0.000346	-0.543584954470293	0.000204

It should be mentioned that the noise covariances are simply increased five times in the second scenario.

Figs. 9.1 and 9.2 show the RMSE plots for the two scenarios obtained for 200 Monte-Carlo simulations. The RMSE plots are shown for the proposed GKQKF and the popular Gaussian filters, such as the UKF, CKF, CQKF, HDCKF, and QKF. The figures conclude that the RMSE is the lowest for the proposed GKQKF. It further concludes that the accuracy of the proposed GKQKF is highest among all the Gaussian filters. The relative computational times of the UKF, CKF, CQKF, HDCKF, QKF, and GKQKF are obtained as 1.07, 1, 1.67, 1.94, 6.26, and 6.01, respectively. Thus, the computational time of the proposed GKQKF is observed similar to the QKF. It concludes that the accuracy of the quadrature rule based filtering could be improved without increasing the computational cost.

## 9.4 Summary

This chapter introduces an advanced nonlinear Gaussian filter, named as GKQKF in its abbreviated form, to improve the accuracy. The proposed GKQKF utilizes univariate Gaussian kernel quadrature rule of numerical approximation in the Gaussian

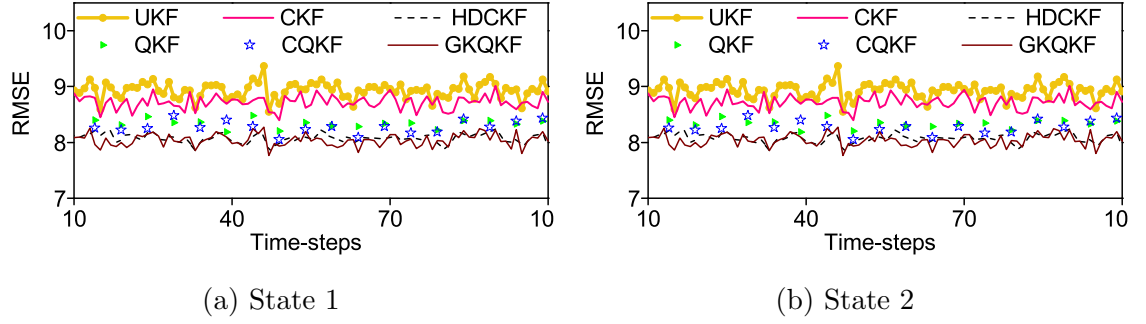


Figure 9.1: Problem 2: Comparison of RMSE plots of the proposed GKQKF with the UKF, CKF, CQKF, HDCKF, and QKF for Scenario 1.

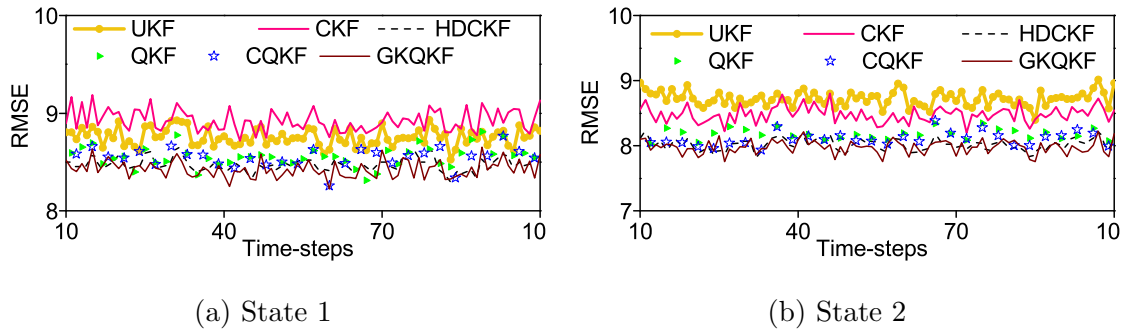


Figure 9.2: Problem 2: Comparison of RMSE plots of the proposed GKQKF with the UKF, CKF, CQKF, HDCKF, and QKF for Scenario 2.

filtering structure. The Gaussian kernel quadrature rule is relatively more accurate than the traditionally used numerical approximation methods in the filtering literature, which is the reason for the improved accuracy of the proposed GKQKF. In dealing with multivariate systems, the proposed GFQKF utilizes product rule for extending the univariate Gaussian kernel quadrature rule into multivariate domain. The improved accuracy of the proposed GFQKF is validated through simulation results in comparison to various existing Gaussian filters such as the UKF, CKF, CQKF, HDCKF, and QKF.

The Gaussian filtering literature, interestingly, consist of a variety of alternatives, which can be used in different practical applications. For example, the UKF and CKF are computationally efficient alternatives. Moreover, if the available computational budget is slightly higher, we can use the CQKF and HDCKF to further improve the accuracy. Furthermore, if a high accuracy is demanded and large computational budget is available, the quadrature rule based filters, such as the QKF and the proposed GKQKF, can be preferred. As the proposed GKQKF outper-

forms the QKF, it may be probably the most likely choice for accomplishing the high accuracy demands.

The recent decades have witnessed significant developments in efficient computational tools. Consequently, in the recent years, the quadrature rule based filters broadly replaced their computationally efficient counterparts, such as the UKF, CKF, and others, in practical applications. As the proposed GKQKF outperforms even the existing quadrature rule based filters, it can broadly replace the existing Gaussian filters if sufficient computational budget is available. Nevertheless, for lower dimensional systems, the computational demand of the proposed GKQKF is as small as its computationally efficient counterparts.





# Chapter 10

## Conclusions and Future Works

The Kalman filter and its nonlinear variants, the Gaussian filter, are extensively used mathematical tools in various fields, including target tracking, power systems, financial modeling, and biomedical diagnosis. Despite their widespread use, there is a notable absence in the literature of a robust filtering method capable of accurately estimating the dynamic state of systems in diverse practical environments. This limitation is primarily due to the significant performance degradation of existing Gaussian filters when faced with irregularities such as delayed and missing measurements. Although the various Gaussian filters are reasonably accurate, their effectiveness are greatly reduced in the presence of these irregularities. While there are some extensions of nonlinear Gaussian filters that can insignificantly address these irregularities, they are typically inadequate for dealing with real-world problems. Following this, the key motivation of this thesis is to develop advanced filtering algorithms capable of dealing with irregularities of delayed and missing measurements.

### **10.1 Performance gain of the proposed methods in terms of accuracy and computational demand**

The author now summarizes the performance gain of various methods discussed through Chapters 3 to 9 by presenting the relative accuracy and relative computa-

tional demand. These metrics are defined as follows

$$\text{Relative accuracy} = \frac{\text{Mean RMSE of the proposed filter}}{\text{Mean RMSE of the filter}}$$

$$\text{Relative computational times } (T_r) = \frac{\text{Computational time of the filter}}{\text{Computational time of the proposed filter}}$$

Table 10.1: **Chapter 3:** Relative accuracy and computational time comparison of the proposed method (EKF\_M) and the competitive filters. The proposed EKF\_M is considered as reference.

Filters	EKF_M	EKF	UKF	CKF	CQKF	RFM	RDF	KFM
Relative accuracy	1	0.15	0.15	0.16	0.21	0.24	0.26	0.3
$T_r$	1	0.87	3.92	4.31	10.02	2.11	2.32	1.44

Table 10.2: **Chapter 4:** Relative accuracy and computational time comparison between the traditional Gaussian filters and their extensions under the proposed method. The CKF-based extension of the proposed method *i.e.*, CKFS is considered as the reference.

Filters	CKF	CKFS	CQKF	CQKFS	GHF	GHFS
Relative accuracy	0.69	1	0.84	1.06	0.84	1.10
$T_r$	0.96	1	2.20	2.22	3.70	2.93

Table 10.3: **Chapter 5:** Relative accuracy and computational time comparison between the proposed CKF\_RD\_PD and competitive filters CKF\_1D, CKF\_RD, and MLCKF. The proposed method CKF\_RD\_PD is considered as the reference.

Filters	CKF_RD_PD	CKF_1D	CKF_RD	MLCKF
Relative accuracy	1	0.72	0.53	0.85
$T_r$	1	0.8	0.79	2.04

## 10.2 Conclusions

- A comprehensive discussion on delayed and missing measurements was presented. The discussion covered reasons triggering these irregularities and a detailed literature review on the existing developments to handle these irregularities.



Table 10.4: **Chapter 6:** Relative accuracy and computational time comparison between the traditional Gaussian filters CKF, CQKF, and GHF and their extensions under the proposed methodology. The CKF-based extension of the proposed method *i.e.*, CKF\_S is considered as the reference.

Filters	CKF_S	CKF	CQKF_S	CQKF	GHF_S	GHF
Relative accuracy	1	0.79	1.04	0.8	1.04	0.81
$T_r$	1	0.97	1.87	1.58	2.10	1.84

Table 10.5: **Chapter 7:** Relative accuracy and computational time comparison between the proposed MDCKF and competitive filters CKF, MEKF, CKF\_RD, and MLCKF. The proposed method MDCKF is considered as the reference.

Filters	MDCKF	CKF	MEKF	CKF_RD	MLCKF
Relative accuracy	1	0.3	0.15	0.54	0.4
$T_r$	1	0.3	0.94	0.99	1.90

Table 10.6: **Chapter 9:** Relative accuracy and computational time comparison between the existing Gaussian filters and proposed Gaussian filter GKQKF. The GKQKF is considered as reference.

Filters	GKQKF	UKF	CKF	CQKF	HDCKF	QKF
Relative accuracy	1	0.02	0.004	0.26	0.19	0.04
$T_r$	1	0.17	0.16	0.28	0.32	1.04

- The issue of missing measurements was addressed for systems with small measurement processing time. To achieve this, the extended Kalman filter was re-structured using a modified measurement model that accounted for potential missing measurements. The effectiveness of the newly developed method was evaluated on individual sinusoids identification problem (Table 10.1), which also included high-frequency sinusoids.
- To address a wider class of problems, a generalized Gaussian filtering was developed. It modeled the missing measurement possibilities by using Bernoulli random variables and subsequently, re-derived the typical measurement model. Then, a new filtering method is designed by re-deriving the traditional Gaussian filtering method for the reformulated measurement model. The newly developed method used the last available measurement if the measurement at any time-step was lost. The performance was validated by considering the CKF-, CQKF-, and GHF-based extensions of the proposed method (Table

10.2).

- To reduce the number of delay probabilities requirement and relax an ambiguous selection of the delay's upper bound, a generalized Gaussian filter (CKF\_RD\_PD) was presented. The CKF\_RD\_PD used Poisson random variable to incorporate the possibilities of delays in the measurement model. The CKF\_RD\_PD demonstrate improved performance over the existing delay filters (Table 10.3).
- A new irregularity was identified and subsequently, a generalized Gaussian filter (GFSCM) was proposed to address the concerned irregularity. Under this irregularity, the actual measurement was stochastically composed of present and previous measurements. Table 10.4 summarizes the efficacy of the GFSCM to handle the concerned irregularity.
- The simultaneous presence of delayed and missing measurements was addressed. Such measurement irregularity was dealt with by incorporating the possibilities of jointly occurring delayed and missing measurements into a modified measurement model, through different sets of Bernoulli random variables. Subsequently, the Gaussian filter was re-derived for the new measurement model. Table 10.5 concludes the improved performance of the proposed method over traditional Gaussian filters.
- The stochastic stability of all the developed filters was analyzed. However, for the sake of brevity, this thesis only presented the stochastic stability results for the GFSCM, considering the EKF-based formulation.
- An advanced Gaussian filter (GKQKF), which used a more accurate quadrature rule for numerically approximating the intractable integrals, was proposed. The GKQKF shown improved estimation accuracy over the existing quadrature-rule based Gaussian filtering counterparts (Table 10.6).

### 10.3 Future Works

Based on the contributions of the thesis, the following discussions highlight some possible future research directions

- The contributions in Chapters 3 and 4 addressed the missing measurement phenomenon with known probability. A future extension of these contributions may be about addressing the missing measurements with unknown or time-varying probabilities.
- The contribution in Chapter 5 for handling the delayed measurements considers that the average delay probability is known, which can be extended for unknown average delay.
- Chapter 6 address a new kind of irregularity which stems from the delay occurrence in different channels. This can possibly be extended to consider the missing measurements phenomenon as well.
- Chapter 7 addressed the simultaneous presence of delayed and missing measurements. This contribution can be extended for addressing more measurement irregularities such as cyber-attack.
- For performing stochastic stability analysis, various system, noise, and filter-related bounds were assumed in Chapter 8. A possible study is performing the same with less assumptions.
- Chapter 9 presented a more accurate version of the Gaussian filter (GKQKF), using a more accurate numerical integration method to approximate intractable integrals. The GKQKF can be further re-derived to handle different measurement irregularities.

# References

- [1] Y. Bar-Shalom, X. R. Li, and T. Kirubarajan, *Estimation with applications to tracking and navigation: theory algorithms and software*. John Wiley & Sons, 2004.
- [2] Z. Zhang, K. Fu, X. Sun, and W. Ren, “Multiple target tracking based on multiple hypotheses tracking and modified ensemble Kalman filter in multi-sensor fusion,” *Sensors*, vol. 19, no. 14, p. 3118, 2019.
- [3] A. K. Singh, M. V. Rebec, and A. Haidar, “Kalman-based calibration algorithm for agamatrix continuous glucose monitoring system,” *IEEE Transactions on Control Systems Technology*, vol. 29, no. 3, pp. 1257–1267, 2020.
- [4] S. Huang, K. K. Tan, and T. H. Lee, “Fault diagnosis and fault-tolerant control in linear drives using the Kalman filter,” *IEEE Transactions on Industrial Electronics*, vol. 59, no. 11, pp. 4285–4292, 2012.
- [5] M. Dhanya and A. Chandrasekar, “Improved rainfall simulation by assimilating Oceansat-2 surface winds using ensemble Kalman filter for a heavy rainfall event over south India,” *IEEE Transactions on Geoscience and Remote Sensing*, vol. 52, no. 12, pp. 7721–7726, 2014.
- [6] Z. A. Sadik, P. M. Date, and G. Mitra, “Forecasting crude oil futures prices using global macroeconomic news sentiment,” *IMA Journal of Management Mathematics*, vol. 31, no. 2, pp. 191–215, 2020.
- [7] G. Marion, L. Hadley, V. Isham, D. Mollison, J. Panovska-Griffiths, L. Pellis, G. S. Tomba, F. Scarabel, B. Swallow, P. Trapman, *et al.*, “Modelling: understanding pandemics and how to control them,” *Epidemics*, vol. 39, p. 100588, 2022.

- [8] H. Fang, N. Tian, Y. Wang, M. Zhou, and M. A. Haile, “Nonlinear Bayesian estimation: From Kalman filtering to a broader horizon,” *IEEE/CAA Journal of Automatica Sinica*, vol. 5, no. 2, pp. 401–417, 2018.
- [9] I. Arasaratnam and S. Haykin, “Cubature Kalman filters,” *IEEE Transactions on Automatic Control*, vol. 54, no. 6, pp. 1254–1269, 2009.
- [10] B. D. Anderson and J. B. Moore, *Optimal filtering*. Courier Corporation, 2012.
- [11] A. K. Singh, “Major development under Gaussian filtering since unscented Kalman filter,” *IEEE/CAA Journal of Automatica Sinica*, vol. 7, no. 5, pp. 1308–1325, 2020.
- [12] R. E. Kalman, “A new approach to linear filtering and prediction problems,” 1960.
- [13] R. G. Brown, P. Y. Hwang, *et al.*, *Introduction to random signals and applied Kalman filtering*, vol. 3. Wiley New York, 1992.
- [14] M. Huber, *Nonlinear Gaussian Filtering: Theory, Algorithms, and Applications*, vol. 19. KIT Scientific Publishing, 2015.
- [15] S. Bhaumik and P. Date, *Nonlinear estimation: methods and applications with deterministic Sample Points*. CRC Press, 2019.
- [16] J. L. Purohit and S. C. Patwardhan, “Development of iterative extended Kalman filter for DAE system,” *IFAC-PapersOnLine*, vol. 51, no. 1, pp. 691–696, 2018.
- [17] L. Duan, X. Zhang, Z. Jiang, Q. Gong, Y. Wang, and X. Ao, “State of charge estimation of lithium-ion batteries based on second-order adaptive extended kalman filter with correspondence analysis,” *Energy*, p. 128159, 2023.
- [18] M. Athans, R. Wishner, and A. Bertolini, “Suboptimal state estimation for continuous-time nonlinear systems from discrete noisy measurements,” *IEEE Transactions on Automatic Control*, vol. 13, no. 5, pp. 504–514, 1968.
- [19] C. M. Kellett and P. Braun, *Introduction to Nonlinear Control: Stability, Control Design, and Estimation*. Princeton University Press, 2023.

- [20] H.-D. Chiang, “Lyapunov stability and stability regions of nonlinear dynamical systems,” 2011.
- [21] X. Mao, *Exponential stability of stochastic differential equations*. Marcel Dekker, 1994.
- [22] R. Has’minskii, “Necessary and sufficient conditions for the asymptotic stability of linear stochastic systems,” *Theory Probability Appl.*, vol. 12, pp. 144–147, 1967.
- [23] T. Morozan, “On the stability of stochastic discrete systems,” in *Control theory and topics in functional analysis*, 1976.
- [24] B. Xu, P. Zhang, H. Wen, and X. Wu, “Stochastic stability and performance analysis of cubature Kalman filter,” *Neurocomputing*, vol. 186, pp. 218–227, 2016.
- [25] G. Y. Kulikov and M. V. Kulikova, “Stability analysis of extended, cubature and unscented Kalman filters for estimating stiff continuous–discrete stochastic systems,” *Automatica*, vol. 90, pp. 91–97, 2018.
- [26] S. J. Julier and J. K. Uhlmann, “New extension of the Kalman filter to nonlinear systems,” in *Signal processing, sensor fusion, and target recognition VI*, vol. 3068, pp. 182–193, Spie, 1997.
- [27] S. Bhaumik and Swati, “Cubature quadrature Kalman filter,” *IET Signal Processing*, vol. 7, no. 7, pp. 533–541, 2013.
- [28] I. Arasaratnam, S. Haykin, and R. J. Elliott, “Discrete-time nonlinear filtering algorithms using gauss–hermite quadrature,” *Proceedings of the IEEE*, vol. 95, no. 5, pp. 953–977, 2007.
- [29] A. K. Naik, G. Kumar, P. K. Upadhyay, P. Date, and A. K. Singh, “Gaussian filtering for simultaneously occurring delayed and missing measurements,” *IEEE Access*, vol. 10, pp. 100746–100762, 2022.
- [30] A. Farina, D. Benvenuti, and B. Ristic, “A comparative study of the Benes filtering problem,” *Signal Processing*, vol. 82, no. 2, pp. 133–147, 2002.

- [31] T. Gao, J. Duan, J. Qiu, and W. Ma, “Robust forecasting-aided state estimation of power system based on extended Kalman filter with adaptive kernel risk-sensitive loss,” *International Journal of Electrical Power & Energy Systems*, vol. 147, p. 108809, 2023.
- [32] S. Kavitha, P. Mula, M. Kamat, S. Nirmala, and J. G. Manathara, “Extended Kalman filter-based precise orbit estimation of LEO satellites using GPS range measurements,” *IFAC-PapersOnLine*, vol. 55, no. 1, pp. 235–240, 2022.
- [33] X. Zhu, B. Gao, Y. Zhong, C. Gu, and K.-S. Choi, “Extended Kalman filter based on stochastic epidemiological model for COVID-19 modelling,” *Computers in Biology and Medicine*, vol. 137, p. 104810, 2021.
- [34] Y. Jia, L. Brancato, M. Giglio, and F. Cadini, “Temperature enhanced early detection of internal short circuits in lithium-ion batteries using an extended Kalman filter,” *Journal of Power Sources*, vol. 591, p. 233874, 2024.
- [35] L. Duan, X. Zhang, Z. Jiang, Q. Gong, Y. Wang, and X. Ao, “State of charge estimation of lithium-ion batteries based on second-order adaptive extended kalman filter with correspondence analysis,” *Energy*, vol. 280, p. 128159, 2023.
- [36] M. Majji, J. L. Junkins, and J. D. Turner, “A high order method for estimation of dynamic systems,” *The Journal of the Astronautical Sciences*, vol. 56, no. 3, pp. 401–440, 2008.
- [37] C. Zhang, J. Qin, C. Yan, Y. Shi, Y. Wang, and M. Li, “Towards invariant extended Kalman filter-based resilient distributed state estimation for moving robots over mobile sensor networks under deception attacks,” *Automatica*, vol. 159, p. 111408, 2024.
- [38] J. Li, S. Zhang, H. Yang, Z. Jiang, and X. Bai, “A fast continuous self-calibration method for FOG rotational inertial navigation system based on invariant extended Kalman filter,” *IEEE Sensors Journal*, vol. 23, no. 3, pp. 2456–2469, 2022.
- [39] Z. He, Y. Li, Y. Sun, S. Zhao, C. Lin, C. Pan, and L. Wang, “State-of-

- charge estimation of lithium ion batteries based on adaptive iterative extended Kalman filter,” *Journal of Energy Storage*, vol. 39, p. 102593, 2021.
- [40] Y. Tao and S. S.-T. Yau, “Outlier-robust iterative extended kalman filtering,” *IEEE Signal Processing Letters*, 2023.
- [41] S. Swain and B. Subudhi, “Grid synchronization of a PV system with power quality disturbances using unscented Kalman filtering,” *IEEE Transactions on Sustainable Energy*, vol. 10, no. 3, pp. 1240–1247, 2018.
- [42] B. Cole and G. Schamberg, “Unscented Kalman filter for long-distance vessel tracking in geodetic coordinates,” *Applied Ocean Research*, vol. 124, p. 103205, 2022.
- [43] C. Uysal, A. Onat, and T. Filik, “Non-contact respiratory rate estimation in real-time with modified joint unscented Kalman filter,” *IEEE Access*, vol. 8, pp. 99445–99457, 2020.
- [44] H. B. Khamseh, S. Ghorbani, and F. Janabi-Sharifi, “Unscented Kalman filter state estimation for manipulating unmanned aerial vehicles,” *Aerospace Science and Technology*, vol. 92, pp. 446–463, 2019.
- [45] C. Liu, P. Shui, and S. Li, “Unscented extended Kalman filter for target tracking,” *Journal of Systems Engineering and Electronics*, vol. 22, no. 2, pp. 188–192, 2011.
- [46] A. Rouhani and A. Abur, “Constrained iterated unscented Kalman filter for dynamic state and parameter estimation,” *IEEE Transactions on Power Systems*, vol. 33, no. 3, pp. 2404–2414, 2017.
- [47] R. Zhan and J. Wan, “Iterated unscented Kalman filter for passive target tracking,” *IEEE Transactions on Aerospace and Electronic Systems*, vol. 43, no. 3, pp. 1155–1163, 2007.
- [48] L. Chang, B. Hu, A. Li, and F. Qin, “Transformed unscented Kalman filter,” *IEEE Transactions on Automatic Control*, vol. 58, no. 1, pp. 252–257, 2012.



- [49] R. Van Der Merwe and E. A. Wan, “The square-root unscented Kalman filter for state and parameter-estimation,” in *2001 IEEE international conference on acoustics, speech, and signal processing. Proceedings (Cat. No. 01CH37221)*, vol. 6, pp. 3461–3464, IEEE, 2001.
- [50] O. Straka, J. Duník, and M. Šimandl, “Unscented Kalman filter with advanced adaptation of scaling parameter,” *Automatica*, vol. 50, no. 10, pp. 2657–2664, 2014.
- [51] H.-H. Tang, K. Zhang, B. Wang, X.-j. Zu, Y.-Y. Li, W.-W. Feng, X. Jiang, P. Chen, and Q.-A. Li, “Early bearing fault diagnosis for imbalanced data in offshore wind turbine using improved deep learning based on scaled minimum unscented kalman filter,” *Ocean Engineering*, vol. 300, p. 117392, 2024.
- [52] X.-S. Trinh, D. Ngoduy, M. Keyvan-Ekbatani, and B. Robertson, “Incremental unscented Kalman filter for real-time traffic estimation on motorways using multi-source data,” *Transportmetrica A: Transport Science*, vol. 18, no. 3, pp. 1127–1153, 2022.
- [53] J. Bittler and P. A. Bhounsule, “Hybrid unscented Kalman filter: Application to the simplest walker,” *IFAC-PapersOnLine*, vol. 56, no. 3, pp. 55–60, 2023.
- [54] J. Luo, J. Peng, and H. He, “Lithium-ion battery SOC estimation study based on cubature Kalman filter,” *Energy Procedia*, vol. 158, pp. 3421–3426, 2019.
- [55] R. V. Garcia, P. C. P. M. Pardal, H. K. Kuga, and M. Zanardi, “Nonlinear filtering for sequential spacecraft attitude estimation with real data: Cubature Kalman filter, unscented Kalman filter and extended Kalman filter,” *Advances in Space Research*, vol. 63, no. 2, pp. 1038–1050, 2019.
- [56] A. Sharma, S. C. Srivastava, and S. Chakrabarti, “A cubature Kalman filter based power system dynamic state estimator,” *IEEE Transactions on Instrumentation and Measurement*, vol. 66, no. 8, pp. 2036–2045, 2017.
- [57] B. Jia, M. Xin, and Y. Cheng, “High-degree cubature Kalman filter,” *Automatica*, vol. 49, no. 2, pp. 510–518, 2013.

- [58] A. K. Singh and S. Bhaumik, “Higher degree cubature quadrature Kalman filter,” *International Journal of Control, Automation and Systems*, vol. 13, pp. 1097–1105, 2015.
- [59] H. Wang, W. Zhang, J. Zuo, and H. Wang, “Generalized cubature quadrature Kalman filters: derivations and extensions,” *Journal of Systems Engineering and Electronics*, vol. 28, no. 3, pp. 556–562, 2017.
- [60] A. K. Singh and S. Bhaumik, “Tracking of low earth orbit satellite using cubature quadrature Kalman filter,” in *2014 IEEE International Symposium on Signal Processing and Information Technology (ISSPIT)*, pp. 000114–000118, IEEE, 2014.
- [61] H. Benzerrouk, A. Nebylov, and H. Salhi, “Quadrotor UAV state estimation based on high-degree cubature Kalman filter,” *IFAC-PapersOnLine*, vol. 49, no. 17, pp. 349–354, 2016.
- [62] J. Shen, Z. Zhang, S. Shen, Y. Zhang, Z. Chen, and Y. Liu, “Accurate state of temperature estimation for lithium-ion batteries based on square root cubature Kalman filter,” *Applied Thermal Engineering*, vol. 242, p. 122452, 2024.
- [63] S. Bhaumik and Swati, “Square-root cubature-quadrature Kalman filter,” *Asian Journal of Control*, vol. 16, no. 2, pp. 617–622, 2014.
- [64] M. Kiani and S. H. Pourtakdoust, “Adaptive square-root cubature–quadrature Kalman particle filter via KLD-sampling for orbit determination,” *Aerospace Science and Technology*, vol. 46, pp. 159–167, 2015.
- [65] G. Y. Kulikov and M. V. Kulikova, “Square-root high-degree cubature Kalman filters for state estimation in nonlinear continuous-discrete stochastic systems,” *European Journal of Control*, vol. 59, pp. 58–68, 2021.
- [66] A. K. Singh and S. Bhaumik, “Transformed cubature quadrature Kalman filter,” *IET Signal Processing*, vol. 11, no. 9, pp. 1095–1103, 2017.
- [67] J. Mu and Y.-l. Cai, “Iterated cubature Kalman filter and its application,” in *2011 IEEE International Conference on Cyber Technology in Automation, Control, and Intelligent Systems*, pp. 33–37, IEEE, 2011.

- [68] B. Jia, M. Xin, and Y. Cheng, “Sparse-grid quadrature nonlinear filtering,” *Automatica*, vol. 48, no. 2, pp. 327–341, 2012.
- [69] A. K. Singh, R. Radhakrishnan, S. Bhaumik, and P. Date, “Adaptive sparse-grid Gauss–Hermite filter,” *Journal of Computational and Applied Mathematics*, vol. 342, pp. 305–316, 2018.
- [70] N. Adurthi, P. Singla, and T. Singh, “Conjugate unscented transformation: Applications to estimation and control,” *Journal of Dynamic Systems, Measurement, and Control*, vol. 140, no. 3, p. 030907, 2018.
- [71] N. Adurthi and P. Singla, “Conjugate unscented transformation-based approach for accurate conjunction analysis,” *Journal of Guidance, Control, and Dynamics*, vol. 38, no. 9, pp. 1642–1658, 2015.
- [72] R. Madankan, P. Singla, T. Singh, and P. D. Scott, “Polynomial-chaos-based Bayesian approach for state and parameter estimations,” *Journal of Guidance, Control, and Dynamics*, vol. 36, no. 4, pp. 1058–1074, 2013.
- [73] C. S. Raghavendra, K. M. Sivalingam, and T. Znati, *Wireless sensor networks*. Springer, 2006.
- [74] W. K. Seah and D. Harrison, “Rare-events sensing and event-powered wireless sensor networks,” *Wireless Sensor Systems for Extreme Environments: Space, Underwater, Underground and Industrial*, pp. 83–110, 2017.
- [75] J. Zheng, L. Xu, Q. Hu, and L. Xie, *Control Over Communication Networks: Modeling, Analysis, and Design of Networked Control Systems and Multi-agent Systems Over Imperfect Communication Channels*. John Wiley & Sons, 2023.
- [76] J. Du, M. Hu, and W. Zhang, “Missing data problem in the monitoring system: A review,” *IEEE Sensors Journal*, vol. 20, no. 23, pp. 13984–13998, 2020.
- [77] C. Lv, Q. Wang, W. Yan, and Y. Shen, “Energy-balanced compressive data gathering in wireless sensor networks,” *Journal of Network and Computer Applications*, vol. 61, pp. 102–114, 2016.

- [78] D. F. Heitjan and D. B. Rubin, “Ignorability and coarse data,” *The annals of statistics*, pp. 2244–2253, 1991.
- [79] H. Zheng, F. Yang, X. Tian, X. Gan, X. Wang, and S. Xiao, “Data gathering with compressive sensing in wireless sensor networks: A random walk based approach,” *IEEE Transactions on Parallel and Distributed Systems*, vol. 26, no. 1, pp. 35–44, 2014.
- [80] Z. Huanan, X. Suping, and W. Jiannan, “Security and application of wireless sensor network,” *Procedia Computer Science*, vol. 183, pp. 486–492, 2021.
- [81] M. C. Dacier, S. Dietrich, F. Kargl, H. König, *et al.*, “Network attack detection and defense: security challenges and opportunities of software-defined networking,” in *Dagstuhl Seminar*, vol. 16361, p. 6, 2016.
- [82] Z. Xiaoyan, W. Houjun, and D. Zhijian, “Wireless sensor networks based on compressed sensing,” in *2010 3rd International Conference on Computer Science and Information Technology*, vol. 9, pp. 90–92, IEEE, 2010.
- [83] M. Prabha, S. S. Darly, and B. J. Rabi, “A novel approach of hierarchical compressive sensing in wireless sensor network using block tri-diagonal matrix clustering,” *Computer Communications*, vol. 168, pp. 54–64, 2021.
- [84] H. M. Faridani, “Performance of Kalman filter with missing measurements,” *Automatica*, vol. 22, no. 1, pp. 117–120, 1986.
- [85] Y. Shi and H. Fang, “Kalman filter-based identification for systems with randomly missing measurements in a network environment,” *International Journal of Control*, vol. 83, no. 3, pp. 538–551, 2010.
- [86] Y. Shi, H. Fang, and M. Yan, “Kalman filter-based adaptive control for networked systems with unknown parameters and randomly missing outputs,” *International Journal of Robust and Nonlinear Control*, vol. 19, no. 18, pp. 1976–1992, 2009.
- [87] L. Hu, Z. Wang, I. Rahman, and X. Liu, “A constrained optimization approach to dynamic state estimation for power systems including PMU and missing

- measurements,” *IEEE Transactions on Control Systems Technology*, vol. 24, no. 2, pp. 703–710, 2015.
- [88] A. F. Molisch, “Technical challenges of wireless communications,” 2011.
- [89] J.-W. Lee and S.-C. Park, “Artificial neural network-based data recovery system for the time series of tide stations,” *Journal of Coastal Research*, vol. 32, no. 1, pp. 213–224, 2016.
- [90] J. Shao, W. Meng, and G. Sun, “Evaluation of missing value imputation methods for wireless soil datasets,” *Personal and Ubiquitous Computing*, vol. 21, pp. 113–123, 2017.
- [91] L. Labonte, A. Abedi, and P. Shankar, “Feedback control challenges with wireless networks in extreme environments,” *Wireless Sensor Systems for Extreme Environments: Space, Underwater, Underground and Industrial*, pp. 21–44, 2017.
- [92] J. Chen, Q. Zhu, and Y. Liu, “Modified Kalman filtering based multi-step-length gradient iterative algorithm for ARX models with random missing outputs,” *Automatica*, vol. 118, p. 109034, 2020.
- [93] L. Hu, Z. Wang, I. Rahman, and X. Liu, “A constrained optimization approach to dynamic state estimation for power systems including PMU and missing measurements,” *IEEE Transactions on Control Systems Technology*, vol. 24, no. 2, pp. 703–710, 2015.
- [94] C. Genes, I. Esnaola, S. M. Perlaza, L. F. Ochoa, and D. Coca, “Robust recovery of missing data in electricity distribution systems,” *IEEE Transactions on Smart Grid*, vol. 10, no. 4, pp. 4057–4067, 2018.
- [95] C. M. Hernandez, J. A. Isaza-Hurtado, and S. Rivadeneria, “Towards blood glucose and insulin estimation using off-line data and missing information,” in *2021 IEEE 5th Colombian Conference on Automatic Control (CCAC)*, pp. 145–150, IEEE, 2021.

- [96] A. S. Nejad, R. Alaiz-Rodríguez, G. D. McCarthy, B. Kelleher, A. Grey, and A. Parnell, “SERT: a transformer based model for multivariate temporal sensor data with missing values for environmental monitoring,” *Computers & Geosciences*, vol. 188, p. 105601, 2024.
- [97] W. Yao and S. Shu-Li, “Recursive distributed fusion estimation for multi-sensor systems with missing measurements, multiple random transmission delays and packet losses,” *Signal Processing*, vol. 204, p. 108829, 2023.
- [98] J. Hu, J. Li, Y. Kao, and D. Chen, “Optimal distributed filtering for nonlinear saturated systems with random access protocol and missing measurements: The uncertain probabilities case,” *Applied Mathematics and Computation*, vol. 418, p. 126844, 2022.
- [99] C. Lu, W. Feng, W. Li, Y. Zhang, and Y. Guo, “An adaptive IMM filter for jump Markov systems with inaccurate noise covariances in the presence of missing measurements,” *Digital signal processing*, vol. 127, p. 103529, 2022.
- [100] L. Zha, R. Liao, J. Liu, J. Cao, and X. Xie, “Dynamic event-triggered security control of cyber-physical systems against missing measurements and cyber-attacks,” *Neurocomputing*, vol. 500, pp. 405–412, 2022.
- [101] M. Chaubey, L. K. Singh, and M. Gupta, “Measurement of missing video frames in npp control room monitoring system using Kalman filter,” *Nuclear Engineering and Technology*, vol. 55, no. 1, pp. 37–44, 2023.
- [102] Z. Peng, C. Pan, S. Yang, G. Wen, and T. Huang, “Resilient filter for state of charge and parameter co-estimation with missing measurement,” *IEEE Transactions on Industrial Informatics*, 2022.
- [103] W. Qian, S. Guo, Y. Zhao, X. Xu, and S. Fei, “Distributed resilient state estimation for nonlinear systems with randomly occurring communication delays and missing measurements,” *International Journal of Adaptive Control and Signal Processing*, vol. 36, no. 2, pp. 315–333, 2022.
- [104] X. Wang and E. E. Yaz, “Second-order fault tolerant extended Kalman fil-

- ter for discrete time nonlinear systems,” *IEEE Transactions on Automatic Control*, vol. 64, no. 12, pp. 5086–5093, 2019.
- [105] H. Chen, E. Tian, and L. Wang, “State-of-charge estimation of lithium-ion batteries subject to random sensor data unavailability: a recursive filtering approach,” *IEEE Transactions on Industrial Electronics*, vol. 69, no. 5, pp. 5175–5184, 2021.
- [106] I. Mohammed, S. J. Geetha, S. S. Shinde, K. Rajawat, and S. Chakrabarti, “Modified re-iterated Kalman filter for handling delayed and lost measurements in power system state estimation,” *IEEE Sensors Journal*, vol. 20, no. 7, pp. 3946–3955, 2019.
- [107] J. Hu, Z. Wang, G.-P. Liu, H. Zhang, and R. Navaratne, “A prediction-based approach to distributed filtering with missing measurements and communication delays through sensor networks,” *IEEE Transactions on Systems, Man, and Cybernetics: Systems*, vol. 51, no. 11, pp. 7063–7074, 2020.
- [108] N. Vatanski, J.-P. Georges, C. Aubrun, E. Rondeau, and S.-L. Jämsä-Jounela, “Networked control with delay measurement and estimation,” *Control Engineering Practice*, vol. 17, no. 2, pp. 231–244, 2009.
- [109] S. Chandrasekaran, V. Varadan, S. V. Krishnan, F. Dörfler, and M. H. Mamduhi, “Distributed state estimation for linear time-varying systems with sensor network delays,” in *2023 European Control Conference (ECC)*, pp. 1–6, IEEE, 2023.
- [110] W. Zeng, J. Cote, X. Chen, Y.-A. Kim, W. Wei, K. Suh, B. Wang, and Z. J. Shi, “Delay monitoring for wireless sensor networks: An architecture using air sniffers,” *Ad hoc networks*, vol. 13, pp. 549–559, 2014.
- [111] G. Fornaro, N. D’Agostino, R. Giuliani, C. Noviello, D. Reale, and S. Verde, “Assimilation of GPS-derived atmospheric propagation delay in DInSAR data processing,” *IEEE journal of selected topics in applied Earth observations and remote sensing*, vol. 8, no. 2, pp. 784–799, 2014.

- [112] S. M. Blair, M. H. Syed, A. J. Roscoe, G. M. Burt, and J.-P. Braun, “Measurement and analysis of PMU reporting latency for smart grid protection and control applications,” *IEEE Access*, vol. 7, pp. 48689–48698, 2019.
- [113] R. Moose and T. Dailey, “Adaptive underwater target tracking using passive multipath time-delay measurements,” *IEEE transactions on acoustics, speech, and signal processing*, vol. 33, no. 4, pp. 778–787, 1985.
- [114] R. Priemer and A. Vacroux, “Estimation in linear discrete systems with multiple time delays,” *IEEE Transactions on Automatic Control*, vol. 14, no. 4, pp. 384–387, 1969.
- [115] G. C. Goodwin, J. C. Agüero, and A. Feuer, “State estimation for systems having random measurement delays using errors in variables,” *IFAC Proceedings Volumes*, vol. 35, no. 1, pp. 385–390, 2002.
- [116] V. N. Phat and A. V. Savkin, “Robust state estimation for a class of uncertain time-delay systems,” *Systems & control letters*, vol. 47, no. 3, pp. 237–245, 2002.
- [117] H.-q. Wang, H.-s. Zhang, and G.-R. Duan, “State estimate schemes for descriptor systems with multi-time delayed measurements,” *IFAC Proceedings Volumes*, vol. 38, no. 1, pp. 315–320, 2005.
- [118] X. Lu, H. Zhang, W. Wang, and K.-L. Teo, “Kalman filtering for multiple time-delay systems,” *Automatica*, vol. 41, no. 8, pp. 1455–1461, 2005.
- [119] M. Pohjola and H. Koivo, “Measurement delay estimation for Kalman filter in networked control systems,” *IFAC Proceedings Volumes*, vol. 41, no. 2, pp. 4192–4197, 2008.
- [120] L. Baramov, D. Pachner, and V. Havlena, “Kalman filter for systems with communication delay,” *IFAC Proceedings Volumes*, vol. 42, no. 20, pp. 310–315, 2009.
- [121] A. Hermoso-Carazo and J. Linares-Pérez, “Extended and unscented filtering algorithms using one-step randomly delayed observations,” *Applied Mathematics and Computation*, vol. 190, no. 2, pp. 1375–1393, 2007.



- [122] A. Hermoso-Carazo and J. Linares-Pérez, “Unscented filtering algorithm using two-step randomly delayed observations in nonlinear systems,” *Applied Mathematical Modelling*, vol. 33, no. 9, pp. 3705–3717, 2009.
- [123] A. K. Singh, P. Date, and S. Bhaumik, “New algorithm for continuous-discrete filtering with randomly delayed measurements,” *IET Control Theory and Applications*, vol. 10, no. 17, pp. 2298–2305, 2016.
- [124] X. Wang, Y. Liang, Q. Pan, and C. Zhao, “Gaussian filter for nonlinear systems with one-step randomly delayed measurements,” *Automatica*, vol. 49, no. 4, pp. 976–986, 2013.
- [125] A. K. Singh, P. Date, and S. Bhaumik, “A modified Bayesian filter for randomly delayed measurements,” *IEEE Transactions on Automatic Control*, vol. 62, no. 1, pp. 419–424, 2016.
- [126] R. Esmzad and R. M. Esfanjani, “Bayesian filter for nonlinear systems with randomly delayed and lost measurements,” *Automatica*, vol. 107, pp. 36–42, 2019.
- [127] Z. Wang, Y. Huang, Y. Zhang, G. Jia, and J. Chambers, “An improved Kalman filter with adaptive estimate of latency probability,” *IEEE Transactions on Circuits and Systems II: Express Briefs*, vol. 67, no. 10, pp. 2259–2263, 2019.
- [128] Y. Tong, Z. Zheng, W. Fan, Q. Li, and Z. Liu, “An improved unscented Kalman filter for nonlinear systems with one-step randomly delayed measurement and unknown latency probability,” *Digital Signal Processing*, vol. 121, p. 103324, 2022.
- [129] L. Zhao, R. Wang, J. Wang, T. Yu, and A. Su, “Nonlinear state estimation with delayed measurements using data fusion technique and cubature Kalman filter for chemical processes,” *Chemical Engineering Research and Design*, vol. 141, pp. 502–515, 2019.
- [130] L. Zhao, J. Wang, T. Yu, K. Chen, and T. Liu, “Nonlinear state estimation for fermentation process using cubature kalman filter to incorporate delayed

- measurements,” *Chinese Journal of Chemical Engineering*, vol. 23, no. 11, pp. 1801–1810, 2015.
- [131] J. Chen, J. He, G. Wang, and B. Peng, “A maritime multi-target tracking method with non-Gaussian measurement noises based on joint probabilistic data association,” *IEEE Transactions on Instrumentation and Measurement*, 2025.
- [132] A. C. Varghese, A. Pal, and G. Dasarathy, “Transmission line parameter estimation under non-Gaussian measurement noise,” *IEEE Transactions on Power Systems*, vol. 38, no. 4, pp. 3147–3162, 2022.
- [133] B. Chen, X. Liu, H. Zhao, and J. C. Principe, “Maximum correntropy kalman filter,” *Automatica*, vol. 76, pp. 70–77, 2017.
- [134] Y. Wang, S. Fu, and F. Wang, “Improved maximum correntropy criterion kalman filter with adaptive behaviors for INS/UWB fusion positioning algorithm,” *Alexandria Engineering Journal*, vol. 109, pp. 702–714, 2024.
- [135] G. Wang, X. Fan, J. Zhao, C. Yang, L. Ma, and W. Dai, “Iterated maximum mixture correntropy Kalman filter and its applications in tracking and navigation,” *IEEE Sensors Journal*, 2024.
- [136] B. Chen, L. Dang, Y. Gu, N. Zheng, and J. C. Príncipe, “Minimum error entropy Kalman filter,” *IEEE Transactions on Systems, Man, and Cybernetics: Systems*, vol. 51, no. 9, pp. 5819–5829, 2019.
- [137] J. He, G. Wang, Z. Feng, S. Zhong, P. Zhang, and B. Peng, “Distributed generalized minimum error entropy unscented Kalman filter under hybrid attacks without prior knowledge,” *IEEE Transactions on Instrumentation and Measurement*, 2025.
- [138] C. Chen, Q. Zhang, W. Liao, F. Zhu, M. Li, and H. Wu, “State of charge estimation for lithium-ion batteries using an adaptive cubature Kalman filter based on improved generalized minimum error entropy criterion,” *Green Energy and Intelligent Transportation*, p. 100292, 2025.

- [139] G. Terejanu, P. Singla, T. Singh, and P. D. Scott, “Adaptive Gaussian sum filter for nonlinear Bayesian estimation,” *IEEE Transactions on Automatic Control*, vol. 56, no. 9, pp. 2151–2156, 2011.
- [140] G. Terejanu, P. Singla, T. Singh, and P. D. Scott, “Uncertainty propagation for nonlinear dynamic systems using Gaussian mixture models,” *Journal of guidance, control, and dynamics*, vol. 31, no. 6, pp. 1623–1633, 2008.
- [141] A. A. Syed, Q. Sun, and H. Foroosh, “Frequency estimation of sinusoids from nonuniform samples,” *Signal Processing*, vol. 129, pp. 67–81, 2016.
- [142] A. Abutaleb, “The estimation of the instantaneous amplitudes of sum of sinusoids with unknown frequencies and phases: The martingale approach,” *Signal Processing*, vol. 93, no. 4, pp. 811–817, 2013.
- [143] J. Reddy, P. K. Dash, R. Samantaray, and A. K. Moharana, “Fast tracking of power quality disturbance signals using an optimized unscented filter,” *IEEE Transactions on Instrumentation and Measurement*, vol. 58, no. 12, pp. 3943–3952, 2009.
- [144] P. K. Ray and B. Subudhi, “Ensemble-Kalman-filter-based power system harmonic estimation,” *IEEE Transactions on Instrumentation and Measurement*, vol. 61, no. 12, pp. 3216–3224, 2012.
- [145] P. Dash and R. Mallick, “Accurate tracking of harmonic signals in VSC-HVDC systems using PSO based unscented transformation,” *International Journal of Electrical Power & Energy Systems*, vol. 33, no. 7, pp. 1315–1325, 2011.
- [146] D. Alves and R. Coelho, “An adaptive algorithm for real-time multi-tone estimation and frequency tracking of non-stationary signals,” *IEEE Transactions on Nuclear Science*, vol. 58, no. 4, pp. 1582–1587, 2011.
- [147] M. Niedźwiecki and P. Kaczmarek, “Estimation and tracking of complex-valued quasi-periodically varying systems,” *Automatica*, vol. 41, no. 9, pp. 1503–1516, 2005.

- [148] J. Bian, J. Xing, J. Liu, Z. Li, and H. Li, “An adaptive and computationally efficient algorithm for parameters estimation of superimposed exponential signals with observations missing randomly,” *Digit Signal Processing*, vol. 48, pp. 148–162, 2016.
- [149] S. Yang and Q. Zhao, “Real-time frequency estimation for sinusoidal signals with application to robust fault detection,” *International Journal of Adaptive Control and Signal Processing*, vol. 27, no. 5, pp. 386–399, 2013.
- [150] S.-W. Chen, W. Panton, and R. Gilmore, “Effects of nonlinear distortion on CDMA communication systems,” *IEEE Transactions on Microwave Theory and Techniques*, vol. 44, no. 12, pp. 2743–2750, 1996.
- [151] L. Cristaldi and A. Ferrero, “Harmonic power flow analysis for the measurement of the electric power quality,” *IEEE Transactions on Instrumentation and Measurement*, vol. 44, no. 3, pp. 683–685, 1995.
- [152] M. W. Arun, N. Yoganandan, B. D. Stemper, and F. A. Pintar, “A methodology to condition distorted acoustic emission signals to identify fracture timing from human cadaver spine impact tests,” *Journal of the Mechanical Behavior of Biomedical Materials*, vol. 40, pp. 156–160, 2014.
- [153] P. M. Djuric, M. Vemula, and M. F. Bugallo, “Target tracking by particle filtering in binary sensor networks,” *IEEE Transactions on Signal Processing*, vol. 56, no. 6, pp. 2229–2238, 2008.
- [154] S. Suranthiran and S. Jayasuriya, “Recovery of signals distorted by sensor non-linearity,” *Journal of Dynamic Systems, Measurement, and Control*, vol. 126, no. 4, pp. 848–859, 2004.
- [155] R. C. Williamson, B. James, B. D. Anderson, and P. J. Kootsookos, “Threshold effects in multiharmonic maximum likelihood frequency estimation,” *Signal Processing*, vol. 37, no. 3, pp. 309–331, 1994.
- [156] D. Starer and A. Nehorai, “Newton algorithms for conditional and unconditional maximum likelihood estimation of the parameters of exponential signals

- in noise,” *IEEE Transactions on Signal Processing*, vol. 40, no. 6, pp. 1528–1534, 1992.
- [157] M. T. Kilani and J. F. Chicharo, “A constrained notch Fourier transform,” *IEEE Transactions on Signal Processing*, vol. 43, no. 9, pp. 2058–2067, 1995.
- [158] S. Djukanović and V. Popović-Bugarin, “Efficient and accurate detection and frequency estimation of multiple sinusoids,” *IEEE Access*, vol. 7, pp. 1118–1125, 2018.
- [159] L. Fan and G. Qi, “Frequency estimator of sinusoid based on interpolation of three DFT spectral lines,” *Signal Processing*, vol. 144, pp. 52–60, 2018.
- [160] L. Fan, G. Qi, J. Liu, J. Jin, L. Liu, and J. Xing, “Frequency estimator of sinusoid by interpolated DFT method based on maximum sidelobe decay windows,” *Signal Processing*, vol. 186, p. 108125, 2021.
- [161] G. Sharma and V. Reddy, “A DFT based alternating projection algorithm for parameter estimation of superimposed complex sinusoids,” *Signal Processing*, vol. 37, no. 1, pp. 73–85, 1994.
- [162] H. Hajimolahoseini, R. Amirfattahi, H. Soltanian-Zadeh, and S. Gazor, “Instantaneous fundamental frequency estimation of non-stationary periodic signals using non-linear recursive filters,” *IET Signal Processing*, vol. 9, no. 2, pp. 143–153, 2015.
- [163] A. Serbes, “Fast and efficient sinusoidal frequency estimation by using the DFT coefficients,” *IEEE Transactions on Communications*, vol. 67, no. 3, pp. 2333–2342, 2018.
- [164] B. F. La Scala and R. R. Bitmead, “Design of an extended Kalman filter frequency tracker,” *IEEE Transactions on Signal Processing*, vol. 44, no. 3, pp. 739–742, 1996.
- [165] E. J. Knobbe and B. Buckingham, “The extended Kalman filter for continuous glucose monitoring,” *Diabetes Technology & Therapeutics*, vol. 7, no. 1, pp. 15–27, 2005.

- [166] A. K. Singh, S. Bhaumik, and P. Date, “Quadrature filters for one-step randomly delayed measurements,” *Applied Mathematical Modelling*, vol. 40, no. 19-20, pp. 8296–8308, 2016.
- [167] R. Ramaswami, K. Sivarajan, and G. Sasaki, *Optical networks: a practical perspective*. Morgan Kaufmann, 2009.
- [168] P. Harremoës, “Binomial and Poisson distributions as maximum entropy distributions,” *IEEE Transactions on Information Theory*, vol. 47, no. 5, pp. 2039–2041, 2001.
- [169] E. Ghahremani and I. Kamwa, “Online state estimation of a synchronous generator using unscented Kalman filter from phasor measurements units,” *IEEE Transactions on Energy Conversion*, vol. 26, no. 4, pp. 1099–1108, 2011.
- [170] C. Wang, J. Shen, P. Vijayakumar, and B. B. Gupta, “Attribute-based secure data aggregation for isolated IoT-enabled maritime transportation systems,” *IEEE Transactions on Intelligent Transportation Systems*, vol. 24, no. 2, pp. 2608–2617, 2021.
- [171] R. Sameni, “Mathematical modeling of epidemic diseases; a case study of the COVID-19 coronavirus,” *arXiv preprint arXiv:2003.11371*, 2020.
- [172] P. Radanliev, D. De Roure, and R. Walton, “Data mining and analysis of scientific research data records on Covid-19 mortality, immunity, and vaccine development-in the first wave of the Covid-19 pandemic,” *Diabetology & Metabolic Syndrome*, vol. 14, no. 5, pp. 1121–1132, 2020.
- [173] H. Fischer, *A history of the central limit theorem: from classical to modern probability theory*, vol. 4. Springer, 2011.
- [174] G. Kumar, A. K. Naik, R. B. Pachori, and A. K. Singh, “Improved Gaussian filtering for handling concurrent delayed and missing measurements,” *Asian Journal of Control*.
- [175] G. Kumar, S. K. Nanda, A. K. Verma, V. Bhatia, and A. K. Singh, “Nonlinear Gaussian filtering with network-induced delay in measurements,” *IEEE Trans-*

- actions on Aerospace and Electronic Systems*, vol. 58, no. 6, pp. 5974–5981, 2022.
- [176] S. K. Nanda, G. Kumar, V. Bhatia, and A. K. Singh, “Kalman-based compartmental estimation for COVID-19 pandemic using advanced epidemic model,” *Biomedical Signal Processing and Control*, vol. 84, p. 104727, 2023.
- [177] J. Liang, Z. Wang, and X. Liu, “State estimation for coupled uncertain stochastic networks with missing measurements and time-varying delays: the discrete-time case,” *IEEE Transactions on Neural Networks and Learning Systems*, vol. 20, no. 5, pp. 781–793, 2009.
- [178] K. J. Uribe-Murcia, Y. S. Shmaliy, C. K. Ahn, and S. Zhao, “Unbiased FIR filtering for time-stamped discretely delayed and missing data,” *IEEE Transactions on Automatic Control*, vol. 65, no. 5, pp. 2155–2162, 2019.
- [179] M. Moayed, Y. K. Foo, and Y. C. Soh, “Adaptive Kalman filtering in networked systems with random sensor delays, multiple packet dropouts and missing measurements,” *IEEE Transactions on Signal Processing*, vol. 58, no. 3, pp. 1577–1588, 2009.
- [180] C. Ran and Z. Deng, “Robust fusion Kalman estimators for networked mixed uncertain systems with random one-step measurement delays, missing measurements, multiplicative noises and uncertain noise variances,” *Information Sciences*, vol. 534, pp. 27–52, 2020.
- [181] L. Xu, K. Ma, W. Li, Y. Liu, and F. E. Alsaadi, “Particle filtering for networked nonlinear systems subject to random one-step sensor delay and missing measurements,” *Neurocomputing*, vol. 275, pp. 2162–2169, 2018.
- [182] J. Hu, J. Li, Y. Kao, and D. Chen, “Optimal distributed filtering for nonlinear saturated systems with random access protocol and missing measurements: The uncertain probabilities case,” *Applied Mathematics and Computation*, vol. 418, p. 126844, 2022.
- [183] N. Modalavalasa, G. S. B. Rao, K. S. Prasad, L. Ganesh, and M. Kumar, “A new method of target tracking by EKF using bearing and elevation measure-

- ments for underwater environment,” *Rob. Auton. Syst.*, vol. 74, pp. 221–228, 2015.
- [184] J. Hu, Z. Wang, H. Gao, and L. K. Stergioulas, “Extended Kalman filtering with stochastic nonlinearities and multiple missing measurements,” *Automatica*, vol. 48, no. 9, pp. 2007–2015, 2012.
- [185] V. Saini, D. Bhattacharyya, D. Purdy, J. Parker, and C. Boohaker, “Non-linear state estimation of a power plant superheater by using the extended Kalman filter for differential algebraic equation systems,” *Applied Thermal Engineering*, p. 123471, 2024.
- [186] Z. Chen *et al.*, “Bayesian filtering: From Kalman filters to particle filters, and beyond,” *Statistics*, vol. 182, no. 1, pp. 1–69, 2003.
- [187] T. Karvonen, S. Bonnabel, E. Moulines, and S. Sarkka, “On stability of a class of filters for nonlinear stochastic systems,” *SIAM Journal on Control and Optimization*, vol. 58, no. 4, pp. 2023–2049, 2020.
- [188] A. Lederer, A. J. O. Conejo, K. A. Maier, W. Xiao, J. Umlauft, and S. Hirche, “Gaussian process-based real-time learning for safety critical applications,” in *International Conference on Machine Learning*, pp. 6055–6064, PMLR, 2021.
- [189] K. Rapp and P.-O. Nyman, “Stability properties of the discrete-time extended Kalman filter,” *IFAC Proceedings Volumes*, vol. 37, no. 13, pp. 1377–1382, 2004.
- [190] L. Özbek, E. K. Babacan, and M. Efe, “Stochastic stability of the discrete-time constrained extended Kalman filter,” *Turkish Journal of Electrical Engineering and Computer Sciences*, vol. 18, no. 2, pp. 211–224, 2010.
- [191] K. Reif, S. Gunther, E. Yaz, and R. Unbehauen, “Stochastic stability of the discrete-time extended Kalman filter,” *IEEE Transactions on Automatic control*, vol. 44, no. 4, pp. 714–728, 1999.
- [192] A. Daid, E. Busvelle, and M. Aidene, “On the convergence of the unscented Kalman filter,” *European journal of control*, vol. 57, pp. 125–134, 2021.



- [193] S. Kluge, K. Reif, and M. Brokate, “Stochastic stability of the extended Kalman filter with intermittent observations,” *IEEE Transactions on Automatic Control*, vol. 55, no. 2, pp. 514–518, 2010.
- [194] L. Li and Y. Xia, “Stochastic stability of the unscented Kalman filter with intermittent observations,” *Automatica*, vol. 48, no. 5, pp. 978–981, 2012.
- [195] K. Reif, S. Gunther, E. Yaz, and R. Unbehauen, “Stochastic stability of the discrete-time extended Kalman filter,” *IEEE Transactions on Automatic Control*, vol. 44, no. 4, pp. 714–728, 1999.
- [196] R. A. Horn and C. R. Johnson, *Matrix analysis*. Cambridge university press, 2012.
- [197] N. J. Gordon, D. J. Salmond, and A. F. Smith, “Novel approach to nonlinear/non-gaussian bayesian state estimation,” in *IEE proceedings F (radar and signal processing)*, vol. 140, pp. 107–113, IET, 1993.
- [198] M. S. Arulampalam, S. Maskell, N. Gordon, and T. Clapp, “A tutorial on particle filters for online nonlinear/non-Gaussian Bayesian tracking,” *IEEE Trans. Sig. Proc.*, vol. 50, no. 2, pp. 174–188, 2002.
- [199] A. Doucet, N. De Freitas, and N. Gordon, “An introduction to equential Monte Carlo methods,” in *Sequential Monte Carlo methods in practice*, pp. 3–14, Springer, 2001.
- [200] R. Van Der Merwe, A. Doucet, N. De Freitas, and E. Wan, “The unscented particle filter,” *Advances in Neural Information Processing Systems*, vol. 13, pp. 584–590, 2000.
- [201] F. Sun and L.-J. Tang, “Cubature particle filter,” *Journal of Systems Engineering and Electronics*, vol. 33, no. 11, pp. 2554–2557, 2011.
- [202] W. H. Press, S. A. Teukolsky, W. T. Vetterling, and B. P. Flannery, “Numerical recipes in c,” 1988.

- [203] S. A. Smolyak, “Quadrature and interpolation formulas for tensor products of certain classes of functions,” in *Doklady Akademii Nauk*, vol. 148, pp. 1042–1045, Russian Academy of Sciences, 1963.
- [204] T. Gerstner and M. Griebel, “Dimension–adaptive tensor–product quadrature,” *Computing*, vol. 71, no. 1, pp. 65–87, 2003.
- [205] P. Closas, C. Fernandez-Prades, and J. Vila-Valls, “Multiple quadrature Kalman filtering,” *IEEE Transactions on Signal Processing*, vol. 60, no. 12, pp. 6125–6137, 2012.
- [206] R. Radhakrishnan, A. K. Singh, S. Bhaumik, and N. K. Tomar, “Multiple sparse-grid Gauss–Hermite filtering,” *Applied Mathematical Modelling*, vol. 40, no. 7-8, pp. 4441–4450, 2016.
- [207] T. Karvonen and S. Särkkä, “Gaussian kernel quadrature at scaled Gauss–Hermite nodes,” *BIT Numerical Mathematics*, vol. 59, no. 4, pp. 877–902, 2019.
- [208] S. S. Bonan and D. S. Clark, “Estimates of the Hermite and the Freud polynomials,” *Journal of Computational and Applied Mathematics*, vol. 63, no. 2, pp. 210–224, 1990.
- [209] Y. Ku and M. Drubin, “Network synthesis using Legendre and Hermite polynomials,” *Journal of the Franklin Institute*, vol. 273, no. 2, pp. 138–157, 1962.